

UNIVERSIDADE ESTADUAL DE MARINGÁ
CENTRO DE CIÊNCIAS BIOLÓGICAS
PROGRAMA DE PÓS-GRADUAÇÃO EM CIÊNCIAS BIOLÓGICAS
ÁREA DE CONCENTRAÇÃO EM BIOLOGIA CELULAR E MOLECULAR

DYONI MATIAS DE OLIVEIRA

**UNRAVELING THE GRASS CELL WALL STRUCTURE AND
THE COMPOSITIONAL SHIFTS UNDERLYING SALT STRESS**

MARINGÁ
PARANÁ – BRASIL
2020

UNIVERSIDADE ESTADUAL DE MARINGÁ
CENTRO DE CIÊNCIAS BIOLÓGICAS
PROGRAMA DE PÓS-GRADUAÇÃO EM CIÊNCIAS BIOLÓGICAS
ÁREA DE CONCENTRAÇÃO EM BIOLOGIA CELULAR E MOLECULAR

DYONI MATIAS DE OLIVEIRA

**UNRAVELING THE GRASS CELL WALL STRUCTURE AND
THE COMPOSITIONAL SHIFTS UNDERLYING SALT STRESS**

Tese apresentada ao Programa de Pós-Graduação em Ciências Biológicas (área de concentração - Biologia Celular e Molecular) da Universidade Estadual de Maringá para a obtenção do grau de Doutor em Ciências Biológicas.

Orientador: Wanderley Dantas dos Santos

MARINGÁ
PARANÁ – BRASIL

2020

Dados Internacionais de Catalogação-na-Publicação (CIP)
(Biblioteca Central - UEM, Maringá - PR, Brasil)

O48u

Oliveira, Dyoni Matias de

Unraveling the grass cell wall structure and the compositional shifts underlying salt stress / Dyoni Matias de Oliveira. -- Maringá, PR, 2020.
168 f.: il. color., figs., tabs.

Orientador: Prof. Dr. Wanderley Dantas dos Santos.

Tese (Doutorado) - Universidade Estadual de Maringá, Centro de Ciências Biológicas, Departamento de Bioquímica, Programa de Pós-Graduação em Ciências Biológicas (Biologia Celular), 2020.

1. Ácido ferúlico. 2. Estresse salino. 3. Lignificação. 4. Gramíneas - Parede celular. 5. Xilano. I. Santos, Wanderley Dantas dos, orient. II. Universidade Estadual de Maringá. Centro de Ciências Biológicas. Departamento de Bioquímica. Programa de Pós-Graduação em Ciências Biológicas (Biologia Celular). III. Título.

CDD 23.ed. 572

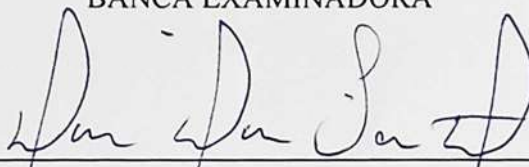
DYONI MATIAS DE OLIVEIRA

UNRAVELING THE GRASS CELL WALL STRUCTURE AND
THE COMPOSITIONAL SHIFTS UNDERLYING SALT STRESS

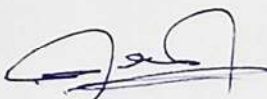
Tese apresentada ao Programa de Pós-Graduação em Ciências Biológicas (área de concentração – Biologia Celular e Molecular) da Universidade Estadual de Maringá para a obtenção do título de Doutor em Ciências Biológicas.

Aprovado em: 19 de Fevereiro de 2020.

BANCA EXAMINADORA



Prof. Dr. Wanderley Dantas dos Santos (Presidente)
Universidade Estadual de Maringá – UEM



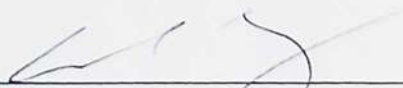
Prof. Dr. Osvaldo Ferrarese-Filho
Universidade Estadual de Maringá – UEM



Prof. Dra. Emy Luiza Ishii Iwamoto
Universidade Estadual de Maringá – UEM



Prof. Dr. Wagner Rodrigo de Souza
Universidade Federal do ABC – UFABC



Prof. André Luis Ferraz
Universidade de São Paulo – USP

BIOGRAFIA

Dyoni M. de Oliveira nasceu em Marialva, Paraná (1989). Depois de se graduar em Ciências Biológicas pela Universidade Estadual de Maringá (2013), obteve o grau de mestre em Biologia Celular e Molecular pela Universidade Estadual de Maringá (2016), onde investigou o papel da lignina e compostos fenólicos ligados a parede celular na recalcitrância da biomassa lignocelulósica de gramíneas forrageiras para a produção de bioetanol. Atualmente está concluindo o doutorado (2016–2020) pelo mesmo Programa de Pós-Graduação, trabalhando com bioquímica de plantas sob a supervisão do professor Wanderley D. dos Santos. Em 2017, realizou estágio na Embrapa Agroenergia em Brasília, com caracterização química da parede celular de plantas de *Setaria viridis* transgênicas, sob a supervisão de Hugo B. C. Molinari. De 2018 a 2019, realizou o doutorado sanduíche com Simon McQueen-Mason e Leonardo Gomez na *University of York*, York, Inglaterra, onde trabalhou com caracterização de polissacarídeos de parede celular de milho (*Zea mays*) crescidos em condição de estresse salino.

Buscando compreender a organização e a dinâmica das paredes celulares, desenvolveu seus conhecimentos em diferentes aspectos da biossíntese, estrutura e degradação da parede celular de gramíneas, focando principalmente no mecanismo de adição de ácido ferúlico ao arabinoxilano, processo chamado de feruloilação. Seus estudos culminaram em descobertas e publicações de artigos científicos em revistas científicas internacionais. Pensando na pouco compreendida relação entre a tolerância das plantas a salinidade com a formação de paredes celulares e o padrão de deposição de lignina, investigou como a salinidade afeta a composição e o metabolismo da parede celular de gramíneas. Desta forma, como parte majoritária do doutorado, realizou um estudo aprofundado das mudanças na composição da parede celular sob estresse salino em plântulas e plantas de milho.

Este estudo do metabolismo de parede celular em resposta ao estresse salino recebeu duas premiações. Em 2017, o resumo intitulado '*Salt stress modulates the lignin metabolism and feruloylation in maize*' foi premiado como melhor pôster apresentado durante a 46ª Reunião Anual da Sociedade Brasileira de Bioquímica e Biologia Molecular (SBBq). Em 2019, o doutorando foi finalista do 23º Prêmio Jovem Talento em Ciências da Vida, a mais conceituada premiação na área de Ciências da Vida da América do Sul, que é promovida pela SBBq juntamente com a GE Healthcare Brasil. A seleção considerou o desempenho acadêmico do candidato e as descobertas apresentadas no resumo intitulado '*Salt stress modulates the dynamics, structure and architecture of plant cell walls*'.

AGRADECIMENTOS

Agradeço ao Conselho Nacional de Desenvolvimento Científico e Tecnológico (CNPq) pelo financiamento e concessão da bolsa de doutorado (GM/GD – 141076/2016-0) e a Coordenação de Aperfeiçoamento de Pessoal de Nível Superior (CAPES) pela concessão da bolsa de doutorado sanduíche no exterior (PDSE – 88881.188627/2018-01).

A minha esposa, Thatiane R. Mota, que também é companheira de trabalho e parceira científica, por toda a ajuda ao longo do doutorado, paciência, companheirismo e apoio em todas as decisões. Obrigado por ‘acender’ a fagulha da curiosidade científica em mim!

Aos meus pais, Áurea M. F. de Oliveira e Jacó A. de Oliveira, pelo apoio nas minhas decisões, por todo o esforço que proporcionou minha conquista de conhecimento e por serem exemplos de vida e perseverança.

Aos meus irmãos, Dyozepe e Dyulie, pela amizade e confiança depositadas em mim.

Ao professor Dr. Wanderley D. dos Santos, que me orientou ao longo dos últimos anos, a todas as oportunidades, aos valiosos ensinamentos, discussões e supervisão para o desenvolvimento da tese.

Ao professor Dr. Osvaldo Ferrarese-Filho (idealizador do Laboratório de Bioquímica de Plantas – BIOPLAN) e Dr. Rogério Marchiosi, pelas discussões, revisões de trabalhos científicos e apoio para seguir na carreira científica.

Ao professor Dr. Simon J. McQueen-Mason e Dr. Leonardo D. Gomes, da *University of York* (York, Inglaterra, UK), pela oportunidade de realizar o doutorado sanduíche no CNAP (*Centre of Novel Agricultural Products*) e discussões científicas.

Ao Dr. Hugo B. C. Molinari, da Embrapa Agroenergia (Brasília, DF), pela oportunidade de realizar o estágio no Laboratório de Genética e Biotecnologia de Plantas.

Aos colegas do laboratório BIOPLAN (ou que outrora fizeram parte), Guilherme H.G. de Almeida, Fábio V. Salatta, Renata C. Sinzker e Érica P. Hoshino, que me auxiliaram e contribuíram para o desenvolvimento dos trabalhos que compõem a tese.

Aos funcionários do BIOPLAN, Aparecida M. Dantas, Antônio N. Silva e Fabiano R. Assis pelo apoio técnico.

A Rachael Simister pelo auxílio e colaboração durante as atividades no CNAP.

A todos os pesquisadores de diferentes universidades que figuram como coautores dos trabalhos, que colaboraram com análises experimentais, discussões científicas e participação durante o processo de escrita dos artigos científicos.

Meus sinceros agradecimentos.

ÍNDICE

Biografia.....	04
Agradecimentos.....	05
Apresentação	09
Resumo geral.....	11
General abstract.....	12
Chapter 1. Phenolic compounds in plants: implications for bioenergy	13
Abstract.....	14
1. Introduction.....	15
2. Lignin emergence and composition.....	15
3. Lignin biosynthesis	17
4. Roles of core and noncore lignin in the cell wall architecture.....	18
5. The role of BAHD acyl-CoA transferases in GAX feruloylation	20
6. Soluble phenolic compounds' impact on production of cellulosic ethanol	22
Future perspectives	23
References.....	25
Chapter 2. Modulation of cellulase activity by lignin-related compounds	29
Abstract.....	30
1. Introduction.....	31
2. Material and methods	32
2.1. Materials	32
2.2. Determination of cellulase activity.....	32
2.3. FTIR and Raman spectroscopy	33
2.4. Enzymatic hydrolysis	33
3. Results and discussion	33
3.1. Screening inhibition of crystalline cellulose saccharification by LRCs.....	34
3.2. Modulations of cellulase activity according to the concentration of LRCs	35
3.3. Modulation of cellulase activity by LRCs over-time	36
4. Conclusions.....	37
References.....	39
Supporting material.....	41
Chapter 3. Feruloyl esterases: biocatalysts to overcome biomass recalcitrance and for the production of bioactive compounds	42
Abstract.....	43
1. Introduction.....	44
2. Ferulic acid: a polyvalent molecule	45
2.1. Ferulic acid in plant cell walls and biomass recalcitrance	47
2.2. Pharmaceutical potential of ferulic acid and derivatives.....	48
3. Classification of feruloyl esterases and genome analysis	49
4. Biochemical properties of microbial FAEs	52

5.	Heterologous expression of FAEs by microbial systems and protein engineering	58
6.	Three-dimensional structures.....	60
7.	Identification of glycosylation sites.....	62
8.	Releasing FA and FA dehydromers from plant cell walls.....	66
9.	Synergism between FAEs and hemicellulases.....	67
10.	Immobilization and influence of organic co-solvents on the FAE activity	70
11.	Synthesis of esters-products by esterification activity.....	72
12.	Future perspectives	74
13.	Conclusion	74
	References	76

Chapter 4. Feruloyl esterase activity and its role in regulating the feruloylation of maize cell walls..... 88

	Abstract.....	89
1.	Introduction.....	90
2.	Material and methods.....	92
	2.1. Preparation and purification of methyl ferulate	92
	2.2. Plant material.....	92
	2.3. Protein extraction and ZmFAE activity.....	92
	2.4. HPLC analysis	92
	2.5. Determination of cell wall ester-linked ferulic acid.....	93
	2.6. Statistical analysis	93
3.	Results and discussion	93
	3.1. A standard method for protein extraction, reaction condition, and HPLC separation for FAE activity.....	93
	3.2. Potential role of ZmFAE in controlling the feruloylation of arabinoxylan.....	95
	Conclusions.....	100
	References.....	101

Chapter 5. Designing xylan for improved sustainable biofuel production 104

1.	Background.....	105
2.	Tailoring xylan structure.....	106
	Future perspectives	108
	References.....	109

Chapter 6. Cell wall remodeling under salt stress: Insights into changes in polysaccharides, feruloylation, lignification and phenolic metabolism 110

	Abstract.....	111
	Significance statement	111
1.	Introduction.....	112
2.	Material and methods.....	114
	2.1. Plant materials and growth conditions	114
	2.2. Alcohol insoluble residue preparation.....	114
	2.3. ATR-FTIR spectroscopy	115

2.4.	Matrix monosaccharide compositional analysis and crystalline cellulose content ..	115
2.5.	Sequential extraction and analysis of xylan	115
2.6.	Xylan analysis by size-exclusion chromatography coupled to multi-angle light-scattering (SEC-MALS)	116
2.7.	Enzymatic hydrolysis of xylan and polysaccharide analysis by carbohydrate gel electrophoresis (PACE).....	116
2.8.	Determination of total cell wall ester-linked hydroxycinnamates.....	116
2.9.	Determination of hydroxycinnamate conjugates released by mild acidolysis	117
2.10.	Quantitative real-time PCR	117
2.11.	Enzymatic assays.....	117
2.12.	Metabolic profiling.....	118
2.13.	Determination of lignin content and composition.....	119
2.14.	Cell wall characterization by two-dimensional NMR.....	119
2.15.	Statistical analysis	119
3.	Results.....	120
3.1.	Salt stress induces changes in plant growth and cell wall polysaccharides	120
3.2.	Salt-stressed roots exhibit reduced arabinoxylan content	122
3.3.	Salinity modulates cell wall-esterified FA and <i>pCA</i>	124
3.4.	Salt stress induces the biosynthesis and accumulation of ferulic acid	126
3.5.	Phenolic profile changes following salt exposure.....	128
3.6.	Salt stress increases lignin content and incorporation of S-units	130
4.	Discussion.....	132
	References.....	141
	Supporting information.....	147
	Addendum. Ten simple rules for developing a successful research proposal in Brazil....	157
	Introduction.....	158
	Rule 1. Define the problem clearly	158
	Rule 2. Formulate falsifiable hypotheses and include preliminary data.....	159
	Rule 3. Establish clear objectives	160
	Rule 4. Estimate the duration and requirements of experimental procedures carefully..	160
	Rule 5. Explain the methodologies for the goal, to demonstrate that you can carry out the research	161
	Rule 6. Clearly define the tasks, people in charge, and costs in your research proposal.....	162
	Rule 7. Preventing the unpredictable: establish a flexible schedule.....	162
	Rule 8. Justify the benefits your research will provide.....	163
	Rule 9. Write a good title and abstract.....	163
	Rule 10. Organize a logical structure and make the text more readable.....	164
	References.....	166
	Appendix.	167

APRESENTAÇÃO

Esta tese de doutorado é composta por seis capítulos e um adendo, sendo cinco artigos científicos, um capítulo de livro e um editorial. Em consonância com as regras do Programa de Pós-Graduação em Ciências Biológicas (PBC), os capítulos foram redigidos de acordo com as normas de publicação dos periódicos nos quais os respectivos artigos foram submetidos e publicados, divergindo apenas no posicionamento das figuras e tabelas ao longo do texto.

O **capítulo 1** da tese, publicado na forma de capítulo de livro intitulado '*Phenolic compounds in plants: implications for bioenergy*', discute o papel de compostos fenólicos na sacarificação da biomassa lignocelulósica. Como continuação deste projeto, foi desenvolvido o artigo de pesquisa intitulado '*Modulation of cellulase activity by lignin-related compounds*' que é apresentado no **capítulo 2**, no qual é relatado que compostos fenólicos relacionados a lignina, como o ácido siríngico e ácido ferúlico (FA), são ativadores de celulasas e aumentam em até 110% a conversão de celulose microcristalina em glicose. A ativação de celulasas por ácidos fenólicos desponta como uma potencial ferramenta biotecnológica para o processamento de biomassa lignocelulósica para bioenergia e biorrefinaria.

O outro projeto desenvolvido durante o doutorado, que é apresentado no **capítulo 3**, foi realizado o estudo teórico publicado na forma de revisão bibliográfica intitulado '*Feruloyl esterases: biocatalysts to overcome biomass recalcitrance and for the production of bioactive compounds*'. Neste artigo é apresentado várias estratégias para a aplicação biotecnológica de feruloil esterases (FAEs), que são enzimas capazes de liberar o FA da parede celular, destacando aspectos bioquímicos para melhorar a produção de açúcares a partir da biomassa vegetal e para a produção de compostos bioativos. Durante a extensiva revisão bibliográfica, foi identificado que a grande maioria dos estudos relatam FAEs de origem bacteriana e fúngica, com poucos trabalhos mostrando a atividade FAE em plantas. Apesar da importância do FA para as paredes celulares de gramíneas e do seu papel em resposta ao estresse abiótico e biótico, a função bioquímica das FAEs em plantas permanece incerta. Desta forma, buscamos desenvolver uma metodologia para a determinação da atividade FAE em milho e compreender o papel desta enzima durante o estresse osmótico, resultando no **capítulo 4** '*Feruloyl esterase activity and its role in regulating the feruloylation of maize cell walls*'.

Visando aprofundar no estudo da parede celular de gramíneas, o **capítulo 5** '*Designing xylan for improved sustainable biofuel production*' discute os recentes avanços na biossíntese de xilano e modificação por adição de FA, componentes essenciais para a arquitetura e

metabolismo da parede celular de gramíneas. Pesquisas que visam elucidar os genes necessários para a biossíntese de xilano e como as mudanças nesses genes influenciam o desenvolvimento das plantas foram impulsionadas pelo potencial da biomassa lignocelulósica como fonte de energia renovável. Como projeto principal de doutorado, foi realizado um estudo aprofundado sobre as mudanças composicionais das paredes celulares de plântulas e plantas de milho em resposta à salinidade, que resultou no **capítulo 6** '*Cell wall remodeling under salt stress: Insights into changes in polysaccharides, feruloylation, lignification, and phenolic metabolism in maize*'. Adicionalmente, por meio da análise de expressão gênica, atividade de enzimas e abordagem metabolômica, foi verificada a alteração na biossíntese e abundância de FA e seus derivados em resposta à salinidade. Este estudo fornece uma melhor compreensão de como as plantas lidam com um ambiente salino modulando a composição e a estrutura de suas paredes celulares.

Por último, o artigo de divulgação científica '*Ten Simple Rules for Developing a Successful Research Proposal in Brazil*' foi publicado na forma de Editorial e adicionado à tese como um **adendo**. Além das orientações oferecidas nos sites das próprias agências de fomento e materiais científicos já disponíveis, este editorial sumariza e lista alguns dos principais aspectos que os jovens pesquisadores podem levar em conta na hora de elaborar uma proposta de pesquisa no Brasil.

RESUMO GERAL

As gramíneas representam as culturas mais importantes do mundo, fornecendo a maioria das calorias consumidas diariamente pelos seres humanos. Além disso, as paredes celulares das gramíneas são uma fonte abundante de energia renovável porque os polissacarídeos podem ser convertidos em combustíveis líquidos e a despolimerização da lignina pode resultar em uma ampla gama de produtos químicos de alto valor agregado. Enquanto as funções gerais das paredes celulares das gramíneas e eudicotiledôneas são semelhantes, elas diferem consideravelmente nos tipos e abundâncias relativas de polissacarídeos não-celulósicos, na reticulação dos polissacarídeos e abundância de compostos fenólicos. A principal característica distintiva das paredes celulares das gramíneas é a presença de quantidades significativas de dois hidroxycinamatos, ferulato (FA) e *p*-coumarato (*p*CA), esterificados aos resíduos arabinofuranosil da cadeia xilano, formando o arabinoxilano (AX). A feruloilação do AX pode atuar como ligações cruzadas entre as cadeias do AX entre si ou entre o AX e a lignina, resultando em um complexo altamente recalcitrante de lignina-hidroxycinamato-carboidrato. Como este arranjo complexo e recalcitrante dos polímeros da parede celular fornece integridade mecânica e estrutural a cada célula, é um desafio extrair os polissacarídeos ligados na parede celular para aplicações industriais. Portanto, esta tese foi amplamente focada na obtenção de uma visão abrangente da estrutura da parede celular de gramíneas, das mudanças de composição subjacentes ao estresse salino e do mecanismo de feruloilação. Resumidamente, as principais descobertas que apresento nesta tese foram: (1) uma base conceitual de diferentes compostos fenólicos intrínsecos as paredes celulares de gramíneas e como esses componentes podem afetar a sacarificação da biomassa lignocelulósica; (2) um conjunto de dados experimentais revelando que os compostos fenólicos alteram a conversão de celulose microcristalina por celulasas; (3) uma avaliação crítica das feruloil esterases como biocatalisadores versáteis para superar a recalcitrância de biomassa e para a produção de compostos bioativos; (4) um método para a determinação da atividade da feruloil esterase em milho e seu papel potencial para a feruloilação das paredes celulares de gramíneas; (5) uma discussão teórica dos recentes avanços na biossíntese de xilano e como a estrutura modificada do xilano pode levar a uma maior sacarificação da biomassa; (6) e um estudo aprofundado de como o estresse salino afeta a estrutura da parede celular de plântulas e plantas de milho, determinando os polissacarídeos, lignina e a feruloilação, investigando os genes e as enzimas relacionadas à biossíntese de ferulato e a abundância de metabólitos fenólicos expressos diferencialmente durante a exposição a salinidade.

PALAVRAS-CHAVES: Ácido ferúlico; Estresse abiótico; Estresse salino; Lignificação; Parede celular; Xilano.

GENERAL ABSTRACT

Grasses represent the most important crops worldwide, providing the majority of calories consumed daily by humans. Furthermore, grass cell walls are an abundant source of renewable energy because the polysaccharides can be converted into liquid fuels, and the depolymerization of lignin can result in a broad array of value-added chemicals. Whereas the overall functions of cell walls of grasses and eudicots are similar, they differ considerably in the types and relative abundance of non-cellulosic polysaccharides, cross-linking of the polysaccharides, and abundance of phenolic compounds. The major distinguishing feature of grass cell walls is the presence of significant quantities of two hydroxycinnamates, ferulate (FA) and *p*-coumarate (*p*CA), ester-linked to the arabinofuranosyl residues of xylan chain, assembling the arabinoxylan (AX). Feruloylation of AX may act as cross-links between AX chains to each other or between AX to lignin, resulting in a highly recalcitrant lignin–hydroxycinnamate–carbohydrate complex. As the complex and recalcitrant arrangement of cell wall polymers provides mechanical and structural integrity to each cell, it is challenging to extract the polysaccharides locked up into cell wall for industrial applications. Therefore, this thesis was largely focused on obtaining a comprehensive picture of the grass cell wall structure, the compositional shifts underlying salt stress, and the mechanism of feruloylation. Briefly, the main findings I deliver in this thesis were: (1) the conceptual basis of different phenolic compounds intrinsic to grass cell walls and how these components may affect biomass saccharification; (2) a dataset experimental data revealing that phenolic compounds alter the conversion of microcrystalline cellulose by cellulases; (3) a critical assessment into feruloyl esterases as versatile biocatalysts to overcome biomass recalcitrance and for the production of bioactive compounds; (4) a method for the determination of feruloyl esterase activity in maize and its potential role for the feruloylation of grass cell walls; (5) a theoretical discussion of recent advances into xylan biosynthesis and how tailored xylan structure can lead to improved biomass saccharification; (6) and an in-depth study of how salt stress affects the cell wall structure of maize seedlings and plants, determining the polysaccharides, lignin and feruloylation, investigating the genes and enzymes related to ferulate biosynthesis, and the abundance of phenolic metabolites differentially expressed upon salinity.

KEYWORDS: Abiotic stress; Cell wall; Ferulic acid; Feruloylation; Lignification; Salt stress; Xylan.

CHAPTER 1

Phenolic Compounds in Plants: Implications for Bioenergy

Dyoni M. Oliveira¹, Aline Finger-Teixeira², Denis L. de Freitas¹, Gabriela E. Barreto¹, Rogério B. de Lima¹, Anderson Ricardo Soares¹, Osvaldo Ferrarese-Filho¹, Rogério Marchiosi¹, Wanderley D. dos Santos^{1*}

¹ Department of Biochemistry, State University of Maringá, PR, Brazil

² Department of Biology, Federal Institute of Paraná, Paranavaí, PR, Brazil

* Corresponding author

Wanderley D. dos Santos

E-mail: wdsantos@uem.br

Type of chapter:

Book chapter

Book title:

Advances of Basic Science for Second Generation
Bioethanol from Sugarcane

Editors:

M.S. Buckeridge, A.P. De Souza

Publisher:

Springer International Publishing

Date of publication:

March 2017

DOI:

10.1007/978-3-319-49826-3_4

Abstract

Lignin is a copolymer of three main hydroxycinnamyl alcohols identified as *p*-hydroxyphenyl (H), guaiacyl (G), and syringyl (S) units. The highly condensed matrix (core lignin) may also be associated with low-molecular-weight phenolics such as the hydroxycinnamates, *p*-coumarate and ferulate, dubbed noncore lignins. Lignin confers hydrophobicity, mechanical and chemical strength for plant tissues, providing a barrier against the attack of microbial pathogens and herbivores. The content and composition of lignin are strongly affected by biotic and abiotic stresses. Besides core and noncore lignin, free phenolic compounds perform a relevant activity in response to plant stresses. The toxicity of allelochemicals is partially due to their ability to bind and inhibit enzyme activities. The presence of lignin imposes a physical barrier to the action of enzymes in saccharification of plant cell wall polysaccharides for the production of cellulosic ethanol. The presence of endogenous phenolic compounds as well as pretreatments to degrade lignin, in turn, release phenolic compounds that adsorb and inhibit the activity of cellulases, xylanases, and accessory enzymes during biomass saccharification. This chapter provides basic information into phenolic compounds of interest to support the sustainable use of plant biomass as raw material for the production of biofuels, discussing the main approaches ongoing to reduce their negative impact in biomass saccharification.

Keywords: Lignin, Phenylpropanoids, Allelopathy, Plant defense, Plant stress.

1. Introduction

The use of lignocellulosic biomass as a renewable energy source can provide a significant contribution for the development of a sustainable industrial society. Lignocellulose consists mainly of polysaccharides and structural phenylpropanoids. Lignin and hydroxycinnamates such as ferulate and *p*-coumarate (noncore lignin) are critical components of supporting tissues, and they also perform an essential role in plant defense against plant predators. The roles of noncore lignin are particularly relevant in grasses, which are the primary sources of biomass for production of biofuels.

Just as these compounds inhibit the action of enzymes from pathogens and herbivores, they also reduce the saccharification efficiency of lignocellulosic biomass, currently considered an essential step in the production of second-generation ethanol (E2G). Therefore, a significant effort has been devoted to reduce the production of these compounds in a controlled manner, as well as efficiently remove them postharvest to improve saccharification. Thus, a basic knowledge of structural phenylpropanoids is a fundamental requirement for physiologists, biochemistries, and engineers interested in the research and development of technologies for E2G production.

In this chapter, we attempt to meet this demand by introducing the major chemical characteristics, metabolic pathways, and biological roles of core and noncore lignin. Also, the chapter presents a brief, but clarifying review of the current research aimed at producing more friendly raw materials for the production of E2G.

2. Lignin emergence and composition

Plant cell wall consists mainly of cellulose, a polysaccharide formed by polymerization of β -glucopyranose molecules. Associated with cellulose, other polysaccharides occur as hemicelluloses and pectins. Once cell growth and elongation cease, some cells can deposit lignin monomers, which are *in muro* polymerized conferring mechanical and chemical resistance to the wall. The emergence of vascular plants, about 400 million years ago, allowed plant kingdom to conquer the continental environment (Weng and Chapple, 2010). Lignin is responsible for the tensile strength that enabled plants to transport water from the roots to the leaves, and sustains large stems and high canopies. Lignin further provides resistance against the attack of pathogens and herbivores reducing the access of enzymes to the wall polysaccharides and the cell content. Therefore, lignin is of great industrial importance either for providing resistance and quality for woods and papers or for hindering the production of cellulose, forage digestibility, and production of E2G (dos Santos *et al.*, 2014). Besides the

production of several carbohydrate polymers, wall biosynthesis ended up integrating phenylpropanoid metabolism into the synthesis of lignin, leading to the establishment of a Glycomic Code (Buckeridge and De Souza, 2014).

Angiosperms synthesize lignin by polymerizing the three main monolignols: *p*-coumaryl alcohol, coniferyl alcohol, and sinapyl alcohol (Moreira-Vilar *et al.*, 2014). Once polymerized, the monomeric composition is identified as *p*-hydroxyphenyl (H unit), guaiacyl (G unit), and syringyl (S unit). These monomers are irregularly linked by a variety of ether linkages, the most common being the arylglycerol- β -aryl bond (β -O-4), but many other linkages are present (**Fig. 1**).

The composition of lignin varies according to the type of cell and plant. Softwoods (gymnosperms or conifers) present by 27–33% of lignin made mainly by G units (*c.* 90%). Hardwoods (angiosperms) have by 18 to 25% of lignin, with similar amounts of units G and S and only a small amount of H units. In turn, grasses, as sugarcane bagasse, may present similar contents of H, G, and S units (Moreira-Vilar *et al.*, 2014).

Lignin is insoluble in most organic solvents, so its isolation is difficult. When there is a separation, the molecular structure is generally compromised. Although it is not possible to extract the lignin without degrading it, it is estimated that the molecular weight is in the range of 1,000 – 20,000 units. Fragments of isolated lignin present dark color and are easily oxidized due to its high aromatic content. They are relatively stable in acidic solutions and soluble in hot aqueous bases.

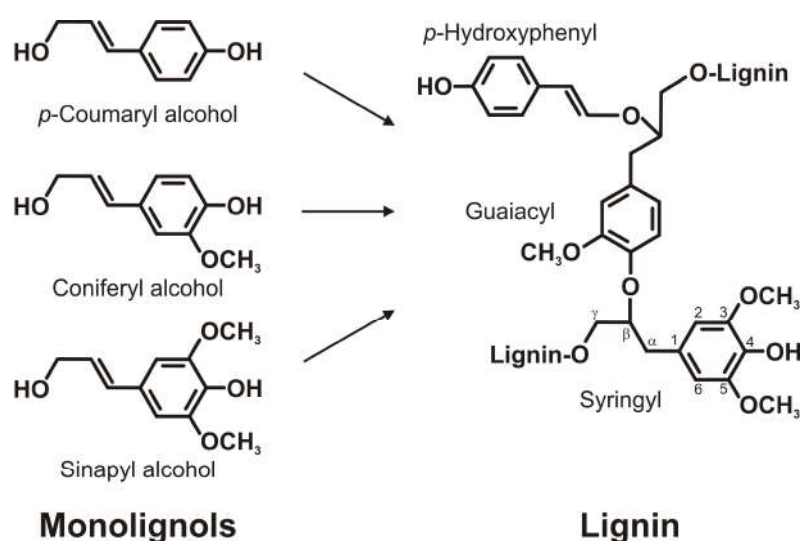


Figure 1. Monolignols and lignin fragment showing the main linkage β -O-4. The origin of the monomeric units may be inferred by the substituent functions of the aromatic rings.

3. Lignin biosynthesis

Both core and noncore lignin components are produced in the phenylpropanoid pathway. This secondary metabolism begins with the activity of phenylalanine-ammonia lyase (PAL) on phenylalanine producing cinnamic acid and ammonia. The action of the cinnamate 4-hydroxylase (C4H) on cinnamate releases *p*-coumaric acid, the first phenolic compound to be produced in the biosynthetic route. In grasses, PAL enzyme is also active on tyrosine receiving the alternative name of tyrosine-ammonia lyase (TAL). It catalyzes the conversion of tyrosine directly in *p*-coumaric acid. The activation of *p*-coumaric acid with coenzyme A by 4-coumarate coenzyme A ligase (4-CL) releases the *p*-coumaroyl-CoA ester, which can follow two different routes. The action of cinnamoyl-CoA reductase (CCR) produces *p*-coumaraldehyde, which is substrate to cinnamyl alcohol dehydrogenase (CAD). The enzyme produces *p*-coumaroyl alcohol, the simplest monolignol.

The *p*-coumaroyl-CoA thioester is also substrate for hydroxycinnamate-CoA transferase (HCT), which substitutes the thioesterification with coenzyme A to an esterification with shikimic or quinic acids. The esterification with shikimic or quinic acids, produced in the primary metabolism, is thought to perform a role in the regulation of the pathway. The *p*-coumaroyl shikimate/quinic acid is the substrate for coumarate 3'-hydroxylase (C3'H) that catalyzes the biosynthesis of caffeoyl ester. The enzyme HCT promotes the transesterification of caffeoyl shikimate/quinic acid to produce caffeoyl-CoA, the precursor of caffeic acid by the action of the enzyme caffeoyl shikimate/quinic acid esterase (CSE) and feruloyl-CoA by the action of the enzyme caffeoyl-CoA *O*-methyl transferase (CCoAOMT). Caffeic acid can generate ferulic acid by the action of caffeate *O*-methyl transferase (COMT). The enzyme CCR catalyzes the reductive cleavage of feruloyl-CoA producing coniferaldehyde. The activity of coniferaldehyde dehydrogenase (CALDH) on coniferaldehyde also produces ferulic acid (**Fig. 2**, right). The enzyme CCR is also active on *p*-coumaroyl-CoA, releasing *p*-coumaraldehyde. Cinnamyl alcohol dehydrogenase then reduces the coniferaldehyde to coniferyl alcohol monolignol, the most abundant component of lignin.

The enzyme ferulate 5-hydroxylase catalyzes the hydroxylation of coniferaldehyde to give rise to 5-hydroxyconiferaldehyde, another substrate of COMT, which in this case produces sinapaldehyde. Once again, CAD reduces the sinapaldehyde to sinapyl alcohol monolignol. At least some plants present a reductase specific for sinapaldehyde, therefore named SAD (**Fig. 2**).

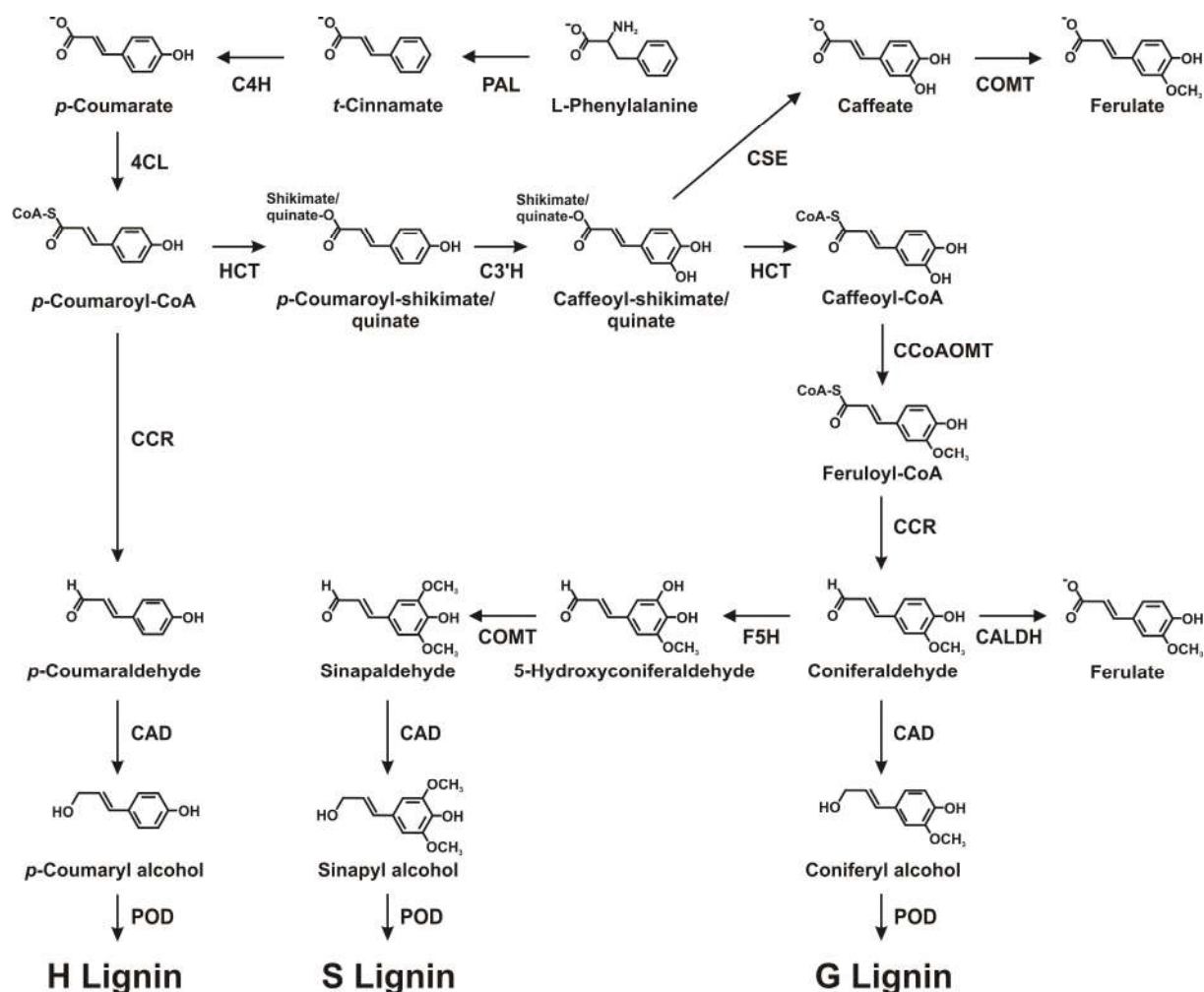


Figure 2. Simplified phenylpropanoid pathway responsible for the biosynthesis of core and noncore lignin precursors (see text for detailed description of the enzymes acronyms – arrows).

4. Roles of core and noncore lignin in the cell wall architecture

Lignocellulosic biomass is largely made up of the secondary cell walls with relevant differences in the proportion of their constituents among plant species and tissues (Carpita *et al.*, 2001). Cellulose, the main component of the cell wall, is a homopolysaccharide consisting of a long and linear chain of $\beta(1 \rightarrow 4)$ -linked glucose units. Each cellulose molecule is tightly bound to other molecules by means of multiple hydrogen bonds producing insoluble, rigid, and crystalline microfibrils (Carpita and McCann, 2000). The presence of hemicelluloses with distinct physical and chemical properties avoids celluloses microfibrils to collapse to produce macrofibrils. The richer topology of these components frequently branched hemicelluloses allows them to link only occasionally with cellulose microfibrils. Intermittent pattern of free and bound regions from hemicellulose with cellulose results in the cross-linking of microfibrils (Carpita, 1996). The overall architectures of cell walls consist of a network of cellulose fibers surrounded by a matrix of noncellulosic polysaccharides. Besides hemicelluloses, cell walls

present pectins, a complex group of heteropolysaccharides branched with acidic sugars as glucuronic and galacturonic acids, with a capacity of adsorbing high amounts of water. These polysaccharides form a gel, which is involved in cell-cell adhesion, pore sizing, pH control, and cation trapping (Buckeridge *et al.*, 2010).

Primary cell walls can be divided into two broad categories: types I and II. Type I is found in dicots, non-commelinoid angiosperms (*e.g.*, aroids, alismatids, and lilioids) and gymnosperms. Type I cell walls consist of cellulose fibers encased in a network of xyloglucan (XyG), pectin, and structural proteins. XyG is composed of a glucose backbone branched with xylose which in turn may be substituted with galactose and fucose (Carpita and Gibeaut, 1993). Type II cell walls, found only in commelinoid monocotyledons (*e.g.*, grasses, sedges, rushes, and gingers), are composed of cellulose fibers encased in a glucuronoarabinoxylan (GAX) matrix. Those GAX may be highly branched with hydroxycinnamates, such as ferulic acid (FA), while lignin can present a high content of *p*-coumaric acids. In addition, the cell walls of grasses and some related families in Poales, such as sugarcane, contain significant quantities of mixed-linkage β -glucans (Carpita and Gibeaut, 1993; Vogel, 2008). The most relevant characteristic of type II cell walls is the abundance of GAX. It is composed of a core chain of xylan branched with arabinose and glucuronic acid, with the arabinose residues esterified with feruloyl residues. Type II cell walls have a low content of pectin and structural proteins.

Produced in the phenylpropanoid pathway together with monolignols (**Fig. 2**), FA and feruloyl esters are polymerized oxidatively by the action of peroxidases. The reaction produces dehydrodimers such as 5-5'-dehydrodiferulic acid, 8-*O*-4'-dehydrodiferulic acid, and 8-5'-dehydrodiferulic acid, along with higher oligomers. In grasses, FA might branch GAX to produce FA-GAX, a polysaccharide believed to occur only in these species and perform a set of distinguished structural and physiological roles in their cell walls (Carpita *et al.*, 2001; dos Santos *et al.*, 2008a). Ferulic acid occurs in higher concentrations in type II cell walls of commelinoids, *e.g.*, maize grain (*Zea mays*) 20.66 mg g⁻¹cell wall, sugarcane (*Saccharum officinarum*) 8.0 to 17.0 3.51 mg g⁻¹, barley (*Hordeum vulgare*) 3.51 mg g⁻¹, and perennial ryegrass (*Lolium perenne*) 6.03 mg g⁻¹. However, it might also occur in high concentration in type I cell walls of “core” Caryophyllales as beetroot (*Beta vulgaris*) 6.93 mg g⁻¹. In non-commelinoid monocots and dicots, FA occurs in much lower concentrations: *e.g.*, asparagus (*Asparagus officinalis*) 0.078–0.096 mg g⁻¹ and onion (*Allium cepa*) 0.007 mg g⁻¹ (Harris and Trethewey, 2010).

Secondary cell walls contain lignin that is deposited inside of the primary cell walls. Secondary cell walls are prominent features of xylem, fibers, and sclerenchyma cell. This rigid

structure of cell wall is a frontline barrier against microorganisms and pathogens. Beyond being hard to digest, lignin fractions adsorb hydrolytic proteins reducing the access of enzymes to the polysaccharides (Huang *et al.*, 2011). In mature cells, lignin forms a highly hydrophobic matrix of C–C and C–O–C-linked phenylpropanoids, mainly coniferyl, sinapyl, and *p*-coumaroyl alcohols. Respective residues in lignin are named G, S, and H units. The amount of lignin, as well as its monomeric composition, is ontogenetic-tissue-species dependent. Lignin confers high hydrophobicity and mechanical resistance to cell walls required by xylem vessels to perform the capillary transport of water and for fibers support the massive habit of trees (Pedersen *et al.*, 2005; Zobiolo *et al.*, 2010). In lignified secondary cell walls, the FA ester linked to GAX is a nucleation site for lignin polymerization through ether bounds, anchoring lignin to polysaccharide moiety (Renger and Steinhart, 2000; Carpita *et al.*, 2001).

5. The role of BAHD acyl-CoA transferases in GAX feruloylation

Using bioinformatics approach, Mitchell *et al.* (2007) compared expressed sequence tags (ESTs) from an orthologous group of grasses and dicots to identify clades where genes are differentially expressed in grasses. One of the clades showing the greatest bias in gene expression was within the BAHD acyl-CoA transferase gene family (also referred as PFAM PF02458 family). BAHD family is named after the first four characterized members: benzylalcohol *O*-acetyltransferase from *Clarkia breweri* (**BEAT**); anthocyanin *O*-hydroxycinnamoyl transferases from *Petunia*, *Senecio*, *Gentiana*, *Perilla*, and *Lavandula* (**AHCTs**); anthranilate *N*-hydroxycinnamoyl/benzoyltransferase from *Dianthus caryophyllus* (**HCBT**); and deacetylvindoline 4-*O*-acetyltransferase from *Catharanthus roseus* (**DAT**). BAHD proteins are predicted to be cytosolic based on the protein sequences, and this is the localization for all known members of the family (D’Auria, 2006).

The predicted role of BAHD proteins is supported by experiments using RNAi in rice, resulting in significant decrease (–19%) in cell wall-bound FA residues (Piston *et al.*, 2010). In another study, rice lines with one BAHD gene upregulated increased the amount of *p*-coumaroyl ester linked to GAX (Bartley *et al.*, 2013). These studies provide circumstantial support for the hypothesis that BAHD genes are responsible for GAX feruloylation, although a definitive evidence is still lacking. Putative genes within a grass-specific clade of the BAHD acyl-CoA transferase superfamily have been identified as being responsible for the ester linkage of FA to GAX. The mechanism about which FA is esterified into GAX is not elucidated, and genes and enzymes responsible for feruloylation of GAX are still unknown. There are two possible potential mechanisms leading to arabinoxylan feruloylation (**Fig. 3**). In the first, GAX

may be synthesized in the Golgi apparatus and then feruloylated, by feruloyl transferase, using feruloyl-CoA transported from cytosol as an FA donor (Buanafina, 2009; Molinari *et al.*, 2013). The second putative mechanism involves a cytosolic BAHD acyl-CoA transferase responsible for the feruloylation of UDP-arabinosyl to form FA-Ara-UDP, which can be the substrate for the GAX feruloylation. In this mechanism, it is suggested that a glycosyltransferase, present in Golgi lumen, introduces the ferulate-arabinosyl (FA-Ara) into the nascent GAX chain with feruloyl-CoA acting as a donor substrate. The last steps in both mechanisms occur in the Golgi apparatus, and the feruloylated glucuronoarabinoxylan (FA-GAX) can be oxidatively coupled, forming dehydroferulic acid dimers. FA-GAX and their coupled derivatives are transported into cell wall by the Golgi secretion (Buanafina, 2009; Anders *et al.*, 2012; Burton and Fincher, 2012).

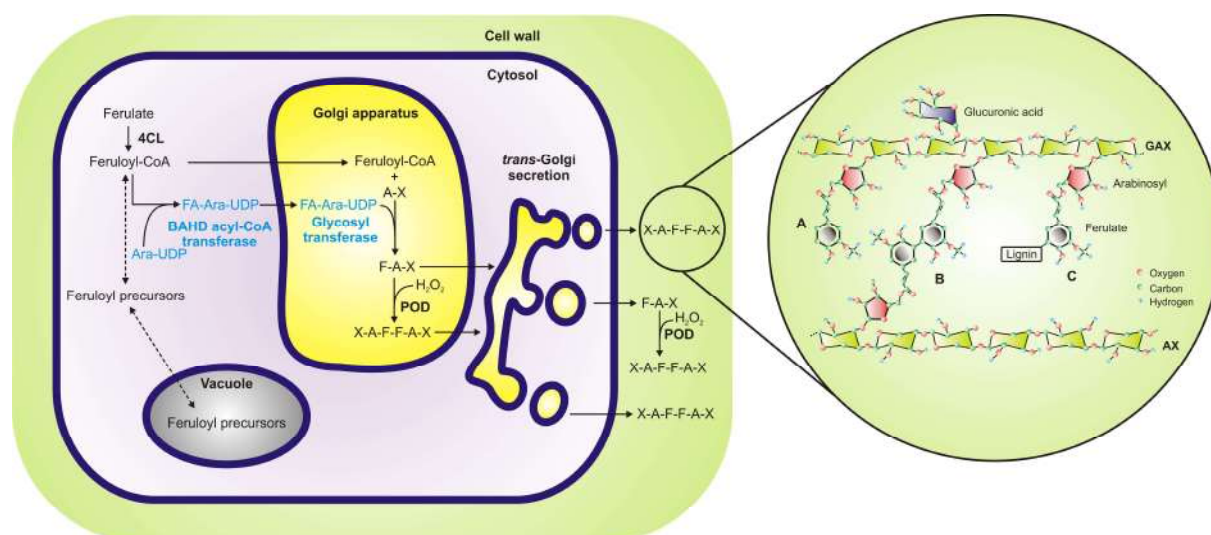


Figure 3. Routes for GAX feruloylation. *Blue text* shows putative pathways for feruloylation based on cytosolic location of BAHD proteins implicated in feruloylation. *A* arabinosyl, *FA* feruloyl group, *F-A-X* feruloylated arabinosyl, *POD* peroxidase, *Ara-UDP* UDP-arabinofuranose, *X* xylan polymer. *Right:* Schematic representation of FA-GAX and FA-GAX cross-linked by dehydrodiferulic acid.

Esterification models involving transport of FA from RE pathway have been partially discarded. [^{14}C]Feruloylated polysaccharides were observed both in protoplasm and apoplast when wheat roots were incubated with *trans*-[^{14}C]cinnamic acid or L-[1- ^{14}C]arabinose. The appearance of [^{14}C]feruloylated polysaccharides occurred even in the presence of the lactone antibiotic brefeldin A, which is used to suppress the transport between RE and Golgi apparatus (Mastrangelo *et al.*, 2009). The apoplastic polymerization among FA residues esterified to GAX has been related to cessation of cell wall growth and defense-related mechanisms. Feruloyl residues can polymerize after oxidation by peroxidases (Santos *et al.*, 2008b; Oliveira *et al.*,

2014). Oxidative coupling of polysaccharides through ester-linked feruloyl groups might occur both within the protoplast in the Golgi apparatus (dos Santos *et al.*, 2008b; Mastrangelo *et al.*, 2009; Umezawa, 2009) and after their secretion into the apoplast. This process is catalyzed by multiple cell wall bounds and putative Golgi-resident isoperoxidases, which use hydrogen peroxide as a substrate in a mechanism similar to that of lignin polymerization (Fry, 1986; Hatfield *et al.*, 1999; Lindsay and Fry, 2008).

6. Soluble phenolic compounds' impact on production of cellulosic ethanol

Unlike animals, plants lack specialized immune cells and immunological memory. However, each plant cell has developed the capability of sensing pathogens and mounting immune responses. Plant lineages have developed effective mechanisms to resist to almost all infectious agents in their environment (Jones and Dangl, 2006; Sticher *et al.*, 1997; Thakur and Sohal, 2013). The biosynthetic routes of phenolic metabolism derive from primary metabolism, and there is increasing evidence that duplications of essential genes of primary metabolism have been an important basis for gene recruitment in secondary metabolism. In the course of evolution, these duplicated genes have acquired new functions and have been optimized and diversified for their roles in new pathways (Dixon and Steele, 1999). Lignin precursors themselves might exert a toxic effect on pathogens (Moura *et al.*, 2010). In spite of the protective functions of the cinnamic acid and their hydroxylated derivatives against oxidative stress, plants themselves are not very tolerant to cinnamic acid itself. It acts as an ionophore, carrying protons from the apoplast to the protoplast through cell wall (Weng *et al.*, 2010). In addition, cinnamic acid and hydroxycinnamates are enzyme inhibitors (Baziramakenga *et al.*, 1995). The excess of cinnamic acid induces a strong electrolyte leakage, impairing plant nutrition and starting defensive reactions (dos Santos *et al.*, 2008a). To top it off, cinnamic acid and derivatives show antiauxin activity that severely affects the plant growth (Baziramakenga *et al.*, 1995; Salvador *et al.*, 2013). Many plants exude these toxic phenols affecting the growth and development of plant competitors unable to cope with the presence of the toxic compound (Einhellig, 2004; dos Santos *et al.*, 2014).

For the efficient saccharification of cell wall is required a set of enzymes, such as cellulases, hemicellulases, and accessory enzymes. They act synergistically in the hydrolysis of cell wall polysaccharides. The presence of soluble phenolic compounds stored in vacuoles and apoplast and released by pretreatments affects severely the activity of enzymes used to hydrolyze the cell wall polysaccharides (Bhat and Bhat, 1997; Eriksson *et al.*, 2002). Indeed, the presence of phenolic compounds appears to be the strongest cause of the reduction in the

activity of cellulases (Ximenes *et al.*, 2010; Vohra *et al.*, 1980). Delignification procedures promote digestibility of cellulose by enhancing the accessibility of cellulases to cellulose and by reducing the adsorption of enzymes to lignin (Ko *et al.*, 2014). However, by-products of lignin degradation can also inhibit the enzymatic hydrolysis of cellulose and reduce the production of fermentable sugars.

Although understanding the inhibition of enzymatic hydrolysis by phenolic compounds is critical to the development of techniques to promote the efficiency of bioconversion of lignocellulose (Qin *et al.*, 2016), our knowledge about the inhibition of cellulases by phenolics is still limited. Pan (2008) investigated the inhibitory effects caused by phenolic compounds and found that the presence of phenolic hydroxyl groups is critical to their inhibitory activity. The authors observed that phenolic hydroxyl groups could be correlated with the intensity of their inhibitory effect on cellulases. Their data suggested that the interference of phenolic hydroxyl groups on the enzyme activity is more important than the steric effect and nonspecific adsorption of cellulase to lignin. Yun *et al.* (2014) determined the kinetics of vanillin inhibition on the cellulase, verifying that vanillin presents competitive and reversible inhibition with the enzyme and that its aldehyde and phenolic hydroxyl groups are responsible for the inhibitory effect. More recently, Qin *et al.* (2016) found that different degrees of inhibition by phenolic compounds are related to the presence of different functional groups. This study suggests that apart from the hydroxyls, the presence of methoxyl groups in the aryl groups and the level of oxidation of the carbonyl groups increase the degree of inhibition of phenolic compounds on cellulases.

Futures perspectives

Phenolic compounds are important components in plant ecological interactions. They protect the plant from biologic, chemical, and physical attacks limiting accessibility of pathogens, herbivores, and industries to their valuable biomass. The main strategies to circumvent the negative impact of phenolic compounds on saccharification are the genetic control of the production of phenylpropanoid (Vanholme *et al.*, 2010). Chen and Dixon (2007) downregulated the genes for C4H, HCT, C3'H, F5H, CCoAOMT, or COMT in alfalfa revealing that lines suppressed in C4H, HCT, and C3'H present the lowest lignin level (<50%) and almost twice the enzymatic saccharification efficiencies. In turn, alfalfa lines suppressed in COMT, CCoAOMT, and F5H produced little effect on lignin content and digestibility efficiencies. Li *et al.* (2008) reported that the impact of downregulation of genes codifying for the first enzymes of the phenylpropanoid pathway (PAL, C4H, HCT, and C3'H; **Fig. 2**) strongly reduced lignin content

and biomass (Chen and Dixon, 2007; Li *et al.*, 2008; Poovaiah *et al.*, 2014). In contrast, downregulation of F5H or COMT reduced the lignin S:G ratio, but has a smaller effect on lignin content or digestibility (Li *et al.*, 2008). Whereas strong reductions in lignin content lead to an unavoidable reduction in biomass production, Jung and Phillips (2010) demonstrated a putative mutation in maize seedling that reduces the content of feruloyl esters and ether cross-linking in the cell wall and increases the biomass digestibility without affecting plant growth and yield.

In addition to the genetic approach, new types of pretreatments have been developed to get rid of phenolic compounds before or during their production enzyme digestion. Our group has been developing an *in vivo* ‘pretreatment’ that we named physiological engineering in which we apply specific inhibitors of phenylpropanoid enzymes in order to control the production of specific phenylpropanoids as ferulic and *p*-coumaric acids without reducing other relevance for production of biomass. The preliminary results suggest that a small reduction in hydroxycinnamate content can strongly enhance the digestibility of grasses as maize and sugarcane (dos Santos *et al.*, 2008a, b; Ita, 2012; Salvador *et al.*, 2013; Parizotto, 2012; Ferro, 2014). Another related approach under development consists in inducing plants to produce chemically modified lignin. At least five types of these designed lignins have been proposed: (1) lignins with a lower degree of polymerization, (2) lignins that are less hydrophobic, (3) lignins with fewer bonds to structural carbohydrates, (4) lignins containing chemically labile bonds, and (5) lignins designed to harbor value-added chemical moieties (Mottiar *et al.*, 2016). Although most of results of this approach were obtained in *in vitro* assays (Tobimatsu *et al.*, 2008, 2012; Lan *et al.*, 2015) there are evidences that plants transformed to overproduce a specific phenolic compound (Stewart *et al.*, 2009; Wilkerson *et al.*, 2014) or feed with phenolic compounds incorporate them in the lignin structure (dos Santos *et al.*, 2008a, b; Salvador *et al.*, 2013; Lima *et al.*, 2013). Designer lignin has the potential to revolutionize the field both by providing plants and/or agronomical treatments to produce friendly lignocellulose and by using plant metabolism as biofactories to produce value-added phenolics from crude matter.

Acknowledgments

D.M.O. gratefully acknowledge the doctoral scholarship granted by Brazilian National Council for Scientific and Technological Development (CNPq).

Competing Interests

The authors have declared that no competing interests exist.

References

- Anders N, Wilkinson MD, Lovegrove A, Freeman J, Tryfona T, Pellny TK, Weimar T, Mortimer JC, Stott K, Baker JM, Defoin-Platel M, Shewry PR, Dupree P, Mitchell RAC (2012) Glycosyl transferase in family 61 mediate arabinofuranosyl transfer onto xylan in grasses. *PNAS* 109(3):989–993.
- Bartley LE, Peck ML, Kim SR, Ebert B, Manisseri C, Chiniquy DM, Sykes R, Gao L, Rautengarten C, Vega-Sanchez ME, Benke PI, Canlas PE, Cao P, Brewer S, Lin F, Smith WL, Zhang X, Keasling JD, Jentoff RE, Foster SB, Zhou J, Ziebell A, An G, Scheller HV, Ronald PC (2013) Overexpression of a BAHD acyltransferase, OsAt10, alters rice cell wall hydroxycinnamic acid content and saccharification. *Plant Physiol* 161(4):1615–1633.
- Baziramakenga R, Leroux GD, Simard RR (1995) Effects of benzoic and cinnamic acids on membrane permeability of soybean roots. *J Chem Ecol* 21:1271–1285.
- Bhat MK, Bhat S (1997) Cellulose degrading enzymes and their potential industrial applications. *Biotechnol Adv* 15(3–4):583–620.
- Buanafina M (2009) Feruloylation in grasses: current and future perspectives. *Mol Plant* 2:861–872.
- Buckeridge MS, De Souza AP (2014) Breaking the “glycomic code” of cell wall polysaccharides may improve second-generation bioenergy production from biomass. *Bioenergy Res* 7:1065–1073.
- Buckeridge M, dos Santos WD, Souza A (2010) Routes for cellulosic ethanol. In: Sugarcane bioethanol, R&D for productivity and sustainability. C. LAB, Blucher.
- Burton RA, Fincher GB (2012) Current challenges in cell wall biology in the cereals and grasses. *Front Plant Sci* 3:130.
- Carpita N (1996) Structure and biogenesis of the cell walls of grasses. *Annu Rev Plant Physiol Plant Mol Biol* 47:445–476.
- Carpita N, Gibeaut D (1993) Structural models of primary cell walls in flowering plants: consistency of molecular structure with the physical properties of the walls during growth. *Plant J* 3:1–30.
- Carpita N, McCann M (2000) The cell wall. In: Buchanan B, Jones R (eds) *Biochemistry and molecular biology of plants*. American Society of Plant Physiologists, Rockville.
- Carpita NC, Defernez M, Findlay K, Wells B, Shoue DA, Catchpole G, Wilson RH, McCann MC (2001) Cell wall architecture of the elongating maize coleoptile. *Plant Physiol* 127(2):551–565.
- Chen F, Dixon R (2007) Lignin modification improves fermentable sugar yields for biofuel production. *Nat Biotechnol* 25:759–761.
- D’Auria JC (2006) Acyltransferase in plants: a good time to be BAHD. *Curr Opin Plant Biol* 9:331–340.
- de Oliveira DM, Finger-Teixeira A, Mota TR, Salvador VH, Moreira-Vilar FC, Molinari HBC, Mitchell RAC, Marchiosi R, Ferrarese-Filho O, dos Santos WD (2014) Ferulic acid: a key component in grass lignocellulose recalcitrance to hydrolysis. *Plant Biotechnol J* 13:1224–1232.

- Dixon RA, Steele CL (1999) Flavonoids and isoflavonoids: a gold mine for metabolic engineering. *Trends Plant Sci* 4(10):394–400.
- dos Santos WD, Ferrarese MLL, Nakamura CV, Mourão KSM, Mangolin CA, Ferrarese-Filho O (2008a) Soybean (*Glycine max*) root lignification induced by ferulic acid. The possible mode of action. *J Chem Ecol* 34:120–1241.
- dos Santos WD, Ferrarese MLL, Ferrarese-Filho O (2008b) Ferulic acid: an allelochemical troublemaker. *Funct Plant Sci Biotechnol* 2:47–55.
- dos Santos WD, Marchiosi R, Vilar FCM, Lima RB, Soares AR, Parizotto AV, Oliveira DM, Ferrarese-Filho O (2014) Polyvalent lignin: recent approaches in determination and applications. In: Lu F (ed) *Structural analysis, applications in biomaterials and ecological significance*, Biochemistry research trends. Nova, New York, 419 p.
- Einhellig FA (2004) Mode of allelochemical action of phenolic. In: Macias FA et al (eds) *Allelopathy: chemistry and mode of action of allelochemicals*. CRC Press, Boca Raton, pp 217–238.
- Eriksson T, Karlsson J, Tjerneld F (2002) A model explaining declining rate in hydrolysis of lignocellulose substrates with cellobiohydrolase I (cel7A) and endoglucanase I (cel7B) of *Trichoderma reesei*. *Appl Biochem Biotechnol* 101(1):41–60.
- Ferro AP (2014) Parede Celular de cana-de-açúcar: enzimas da via de fenilpropenoides e a biossíntese de lignina. Tese de Doutorado em Ciências Biológicas (Biologia Celular) – Universidade Estadual de Maringá.
- Fry S (1986) Cross-Linking of matrix polymers in the growing cell walls of angiosperms. *Annu Rev Plant Physiol* 37:165–186.
- Harris P, Trethewey J (2010) The distribution of ester-linked ferulic acid in the cell walls of angiosperms. *Phytochem Rev* 9:19–33.
- Hatfield R, Ralph J, Grabber J (1999) Cell wall cross-linking by ferulates and diferulates in grasses. *J Sci Food Agric* 79:403–407.
- Huang R, Su R, Qi W, He Z (2011) Bioconversion of lignocellulose into bioethanol process intensification and mechanism research. *Bioenergy Res* 4:225–245.
- Ita AG (2012) Efeito do ácido metilenodioxícínâmico sobre a recalcitrância do bagaço à digestão enzimática de diferentes cultivares de cana-de-açúcar. Tese de Mestrado em Agronomia. Universidade Estadual de Maringá.
- Jones JD, Dangl JL (2006) The plant immune system. *Nature* 444:323–329.
- Jung H, Phillips R (2010) Putative seedling ferulate ester (sfe) maize mutant: morphology, biomass yield, and stover cell wall composition and rumen degradability. *Crop Sci* 50:403–418.
- Ko JK, Ximenes E, Kim Y, Ladisch MR (2014) Adsorption of enzyme onto lignins of liquid hot water pretreated hardwoods. *Biotechnol Bioeng* 112(3):447–456.
- Lan W, Lu F, Regner M, Zhu Y, Rencoret J, Ralph SA, Zakai UI, Morreel K, Boerjan W, Ralph J (2015) Tricin, a flavonoid monomer in monocot lignification. *Plant Physiol* 167:1284–1295.
- Li X, Weng J-K, Chapple C (2008) Improvement of biomass through lignin modification. *Plant J* 54:569–581.

- Lima RB, Salvador VH, dos Santos WD, Bubna GA, Finger-Teixeira A, Marchiosi R, Ferrarese MLL, Ferrarese-Filho O (2013) Enhanced lignin monomer production caused by cinnamic acid and its hydroxylated derivatives inhibits soybean root growth. *PLoS One* 8:e80542.
- Lindsay S, Fry S (2008) Control of diferulate formation in dicotyledonous and gramineous cell-suspension cultures. *Planta* 227:439–452.
- Mastrangelo LI, Lenucci MS, Piro G, Dalessandro G (2009) Evidence for intra and extra-protoplasmic feruloylation and cross-linking in wheat seedling roots. *Planta* 229:343–355.
- Mitchell R, Dupree P, Shewry P (2007) Novel bioinformatics approach identifies candidate genes for the synthesis and feruloylation of arabinoxylan. *Plant Physiol* 144:43–53.
- Molinari HBC, Pellny TK, Freeman J, Shewry PR, Mitchell RAC (2013) Grass cell wall feruloylation: distribution of bound ferulate and candidate gene expression in *Brachypodium distachyon*. *Front Plant Sci* 4(50):1–10
- Moreira-Vilar FC, Siqueira-Soares RC, Finger-Teixeira A, Oliveira DM, Ferro AP, Rocha GJ, Ferrarese MLL, dos Santos WD, Ferrarese-Filho O (2014) The acetyl bromide method is faster, simpler and presents best recovery of lignin in different herbaceous tissues than Klason and Thioglycolic acid methods. *PLoS One* 9(10):1–7.
- Mottiar Y, Vanholme R, Boerjan W, Ralph J, Mansfield SD (2016) Designer lignins: harnessing the plasticity of lignification. *Curr Opin Biotechnol* 37:190–200.
- Moura JCMS, Bonine CAV, De Oliveira FVJ, Dornelas MC, Mazzafera P (2010) Abiotic and biotic stresses and changes in the lignin content and composition in plants. *J Integr Plant Biol* 52:360–376.
- Pan X (2008) Role of functional groups in lignin inhibition of enzymatic hydrolysis of cellulose to glucose. *J Biobased Mater Bioenergy* 2:25–32.
- Parizotto AV (2012) Cafeato *O*-metiltransferase de milho (*Zea mays* L.): Estrutura da enzima, prospecção de inibidores e recalcitrância da parede celular. Tese de Doutorado em Ciências Biológicas (Biologia Celular). Universidade Estadual de Maringá.
- Pedersen J, Vogel K, Funnell D (2005) Impact of Reduced Lignin on Plant Fitness. *Crop Sci* 45:812.
- Piston F, Uauy C, Fu L, Langston J, Labavitch J, Dubcovsky J (2010) Down-regulation of four putative arabinoxylan feruloyl transferase genes from family PF02458 reduces ester-linked ferulate content in rice cell walls. *Planta* 231:677–691.
- Poovaiah CR, Nageswara-Rao M, Soneji JR, Baxter HL, Stewart CNJR (2014) Altered lignin biosynthesis using biotechnology to improve lignocellulosic biofuel feedstocks. *Plant Biotechnol J* 12(9):1163–1173.
- Qin L, Li WC, Liu L, Zhu JQ, Li X, Li BZ, Yuan YJ (2016) Inhibition of lignin-derived phenolics compounds to cellulose. *Biotechnol Biofuels* 9:70.
- Renger A, Steinhart H (2000) Ferulic acid dehydrodimers as structural elements in cereal dietary fiber. *Eur Food Res Technol* 211:422–428.
- Salvador VH, Lima RB, dos Santos WD, Soares AR, Böhm PAF, Marchiosi R, Ferrase MLL, Ferrarese-Filho O (2013) Cinnamic Acid Increases Lignin Production and Inhibits Soybean Root Growth. *PLoS One* 8:e69105.

- Stewart JJ, Akiyama T, Chapple CC, Ralph J, Mansfield SD (2009) The effects on lignin structure of overexpression of ferulate 5-hydroxylase in hybrid poplar. *Plant Physiol* 150:621–635.
- Sticher L, Mauch-Mani B, Métraux JP (1997) Systemic acquired resistance. *Annu Rev Phytopathol* 35:235–270.
- Thakur M, Sohal BS (2013) Role of elicitors in inducing resistance in plants against pathogen infection: a review. *ISRN Biochem Article ID 762412*, 10 p.
- Tobimatsu Y, Takano T, Kamitakahara H, Nakatsubo F (2008) Studies on the dehydrogenative polymerizations (DHPs) of monolignol β -glycosides: Part 4. Horseradish peroxidase-catalyzed copolymerization of isoconiferin and isosyringin. *Holzforschung* 62:495–500.
- Tobimatsu Y, Elumalai S, Grabber JH, Davidson CL, Pan X, Ralph J (2012) Hydroxycinnamate conjugates as potential monolignol replacements: *in vitro* lignification and cell wall studies with rosmarinic acid. *ChemSusChem* 5:676–686.
- Umezawa T (2009) The cinnamate/monolignol pathway. *Phytochem Rev* 9:1–17.
- Vanholme R, Ralph J, Akiyama T, Lu F, Pazo JR, Kim H, Christensen JH, Van Reusel B, Storme V, De Rycke R et al (2010) Engineering traditional monolignols out of lignin by concomitant up-regulation of F5H1 and down-regulation of COMT in *Arabidopsis*. *Plant J* 64:885–897.
- Vogel J (2008) Unique aspects of the grass cell wall. *Curr Opin Plant Biol* 11:301–307.
- Vohra RM, Shirsot CK, Dhawan S, Gupta KG (1980) Effect of lignin and some of its components on the production and activity of cellulase(s) by *Trichoderma reesei*. *Biotechnol Bioeng* 22:1497–1500.
- Weng J-K, Chapple C (2010) The origin and evolution of lignin biosynthesis. *New Phytol* 87:273–285.
- Weng J-K, Akiyama T, Bonawitz ND, Li X, Ralph J et al (2010) Convergent evolution of syringyl lignin biosynthesis via distinct pathways in the lycophyte *Selaginella* and flowering plants. *Plant Cell* 22:1033–1045.
- Wilkerson CG, Mansfield SD, Lu F, Withers S, Park J-Y, Karlen SD, Gonzales-Vigil E, Padmakshan D, Unda F, Rencoret J, Ralph J (2014) Monolignol ferulate transferase introduces chemically labile linkages into the lignin backbone. *Science* 344:90–93.
- Ximenes E, Kim Y, Mosier N, Dien B, Ladisch M (2010) Inhibition of cellulases by phenols. *Enzyme Microb Technol* 46:170–176.
- Yun L, Benkun Q, Yinhua W (2014) Inhibitory effect of vanillin on cellulose activity in hydrolysis of cellulosic biomass. *Bioresour Technol* 167:324–330.
- Zobiolo L, dos Santos WD, Bonini E, Ferrarese-Filho O, Kremer R, Oliveira-Júnior R (2010) Lignin: from nature to industry. In: Paterson R (ed) *Lignin: properties and applications in Biotechnology and bioenergy*. Hauppauge, New York, pp 419–436.

CHAPTER 2

Modulation of Cellulase Activity by Lignin-Related Compounds

Dyoni M. Oliveira*, Érica P. Hoshino, Thatiane R. Mota, Rogério Marchiosi, Osvaldo Ferrarese-Filho, Wanderley D. dos Santos*

Department of Biochemistry, State University of Maringá, Maringá, PR, Brazil

*** Corresponding author**

Dyoni M. Oliveira

Wanderley D. dos Santos

E-mail: dyonioliveira@gmail.com; wdsantos@uem.br

Type of chapter:	Short communication
Journal:	Bioresource Technology Reports
Volume/issue, pages:	10, 100390
Date of publication:	June 2020
DOI:	10.1016/j.biteb.2020.100390

Abstract

Pretreatment of lignocellulosic biomass generates a wide variety of lignin-related compounds (LRCs) derived from lignin depolymerization, which inhibit the enzymatic saccharification. Here, the effects of different LRCs were evaluated on cellulase activity for the hydrolysis of microcrystalline cellulose. Maximum activation of 110% on microcrystalline cellulose conversion by cellulases was observed with 30 mM syringic acid, whereas 20 mM ferulic acid increased it by 68%. Conversely, maximum inhibition of 40% was observed with 50 mM syringaldehyde. Furthermore, all phenolic acids had their maximum stimulatory effects on cellulase activity before the first 4 h of enzymatic hydrolysis, while syringaldehyde had the maximum inhibition after 12 h of hydrolysis. Activation of cellulases by phenolic acids emerges as a potential tool for lignocellulosic biomass processing for bioenergy and biorefinery.

Keywords: Benzoic acids; Cellulase; Cellulose; Ferulic acid; Syringic acid.

1. Introduction

Lignocellulosic biomass is highly abundant and low-cost renewable feedstock for the production of bioethanol and commodity chemicals (Bomble *et al.*, 2017; Oliveira *et al.*, 2019). Lignocellulose is mainly composed of cellulose, hemicellulose, lignin, and low levels of phenolic compounds and pectin. While cellulose and hemicellulose polysaccharides can be depolymerized into fermentable sugars by cellulases and hemicellulases, lignin plays a negative role in biomass saccharification reducing its efficiency (Mota *et al.*, 2018; Zhang *et al.*, 2019; Oliveira *et al.*, 2020). Lignin is an aromatic heteropolymer composed mainly of the three canonical monolignols: *p*-hydroxyphenyl (H), guaiacyl (G) and syringyl (S), which are polymerized primarily in plant cell walls by aryl ether and diaryl ether bonds (Vanholme *et al.*, 2010). Given the complex structure of lignocellulosic biomass and the presence of lignin polymer, the enzymatic hydrolysis is considered the rate-limiting step for bioethanol production, leading to increased downstream operating costs (Yu *et al.*, 2014; Qin *et al.*, 2016; Ponnusamy *et al.*, 2019).

Several pretreatments have been employed to reduce the biomass recalcitrance conferred by the presence of lignin and the complex arrangement of cell wall polymers. More in particular, pretreatments modify the chemical and physical properties of lignocellulose and increase the enzymatic saccharification efficiency (Gao *et al.*, 2019; Mota *et al.*, 2019). Furthermore, many novel methods have been developed to optimize novel routes for lignocellulose pretreatment, lignin depolymerization and valorization (Banu *et al.*, 2019; Ponnusamy *et al.*, 2019). Despite the advantages, pretreatments commonly generate by-products from the degradation of polysaccharides and lignin, which inhibit cellulase and hemicellulase activity, reducing the production of fermentable sugars. The content and types of enzyme inhibitors formed during pretreatments depend on the biomass composition, the type of pretreatment and the reactive conditions (Ximenes *et al.*, 2010; Kim *et al.*, 2011; Zhao and Chen, 2014).

Lignin depolymerization processes result in heterogeneous mixtures of lignin-related compounds (LRCs) such as vanillin, syringaldehyde, ferulic acid, 4-coumaric acid, which create a challenge to overcome the enzyme inhibition during saccharification (Qin *et al.*, 2016). The LRCs present higher inhibitory effect for cellulases than soluble sugars, furfurals and simple organic acids, because LRCs may cause protein precipitation and irreversible inhibition (Ximenes *et al.*, 2010; Zhao and Chen, 2014). The understanding of how LRCs change cellulase activity is fundamental for the development of approaches to improve the cellulose

conversion (Qin *et al.*, 2016). However, knowledge about cellulase inhibition by phenolic compounds is still limited.

Some studies have contributed significantly to the advancement of knowledge about the structure-activity relationship of LRCs for cellulase activity. Further evidence is given by inhibition of exoglucanases, endoglucanases and β -glucosidase by vanillin, syringaldehyde, cinnamic acid, tannic acid, and benzoic acids (Ximenes *et al.*, 2010; Ximenes *et al.*, 2011). Li and coworkers (2014) determined the inhibition kinetics of vanillin on cellulase activity and suggested that it has reversible and non-competitive inhibition on cellulase, and aldehyde and hydroxyl groups confer the inhibitory effect. More recently, Qin and coworkers (2016) suggested that the degree of inhibition caused by different LRCs varies with the presence of distinct functional groups. Taken together, these studies suggest that the presence of methoxyl, carbonyl or carboxyl groups promote different degree of inhibition of phenolic compounds on cellulases. Here, pure microcrystalline cellulose was used as the substrate to avoid the interference of any LRC during enzymatic hydrolysis by a commercial cellulase. We evaluated the impact of eight different LRCs of common existence in hydrolysates from lignin depolymerization on cellulase activity. Fundamental insights are constructive to understand the mechanism of cellulase stimulation and inhibition by LRCs and how to improve the enzymatic hydrolysis of lignocellulosic biomass.

2. Material and methods

2.1. Materials

Microcrystalline cellulose type 20 (Sigmacell cellulose, particle size 20 μm , Sigma-Aldrich, St. Louis, USA) was used as the cellulosic substrate. The commercial cellulase NS22086 containing exoglucanase, endoglucanase and β -glucosidase was kindly provided by Novozymes (Araucaria, Brazil). 4-Hydroxybenzaldehyde, vanillin, syringaldehyde, 4-hydroxybenzoic acid, vanillic acid, syringic acid, 4-coumaric acid and ferulic acid were purchased from Sigma-Aldrich (St. Louis, USA).

2.2. Determination of cellulase activity

Cellulase activity was measured by colorimetric assay using carboxymethyl cellulose as the substrate (Oliveira *et al.*, 2020). The reaction mixture containing 50 μl of substrate 1% (w/v) in 0.05 M sodium acetate buffer pH 5.0 and 50 μl enzyme solution was incubated at 50 $^{\circ}\text{C}$ for 30 min. The reaction was stopped by adding 100 μl of 3,5-dinitrosalicylic acid (DNS) and

immediate boiling for 5 min (Miller, 1959) and the reducing sugars were determined at 540 nm, using glucose as standard. The cellulase activity was determined as 711.33 U ml⁻¹.

2.3. FTIR and Raman spectroscopy

The analysis by Fourier transform infrared (FTIR) and Raman spectroscopies were performed as previously described (Oliveira *et al.*, 2020). FTIR experiment was performed with a Bruker Vertex 70 FTIR spectrometer equipped with an attenuated total reflectance accessory. The scanning ranged from 1,800 to 800 cm⁻¹, with the resolution of two cm⁻¹ and 128 scans per sample. Raman experiments were carried out with a MultiRAM FT-Raman Spectrometer (Bruker, Billerica, MA, USA). An Nd:YAG laser was used for excitation at 1,064 nm. The resolution was set to two cm⁻¹ and recorded 128 scans per sample, scanning from 1,800 to 800 cm⁻¹. FTIR and Raman experiments were carried out in triplicates.

2.4. Enzymatic hydrolysis

The enzymatic hydrolysis was performed using the commercial cellulase Novozymes NS22086. The reaction mixtures contained 15 mg of microcrystalline cellulose, 10 U ml⁻¹ cellulase, 0.02% sodium azide (v/v) to inhibit microbial contamination, LRC prepared in sodium acetate buffer, and 50 mM sodium acetate buffer pH 5.0 at 50 °C in a final volume of 1 ml (Oliveira *et al.*, 2016). Mixtures were incubated at 50 °C and sampled for analysis at different time points. The supernatant from samples was collected by centrifugation (12,000×g, 5 min) and the quantitation of the reducing sugars was determined by the DNS method at 540 nm (Miller, 1959).

3. Results and discussion

The microcrystalline cellulose was first analyzed using Fourier transform infrared (FTIR) and Raman spectroscopies to verify the presence of LRCs as contaminants. FTIR and Raman spectra of microcrystalline cellulose revealed the absence of peaks between 1,510 – 1,630 cm⁻¹ corresponding to C=C stretching and aromatic skeletal vibrations of aromatic rings assigned to lignin and LRCs (Oliveira *et al.*, 2020), indicating the absence of aromatic compounds (**Fig. S1**). Thereafter, the subsequent experiments were performed using microcrystalline cellulose as the substrate for cellulase activity, making easier to figure out the origin of enzyme inhibition or stimulation rather than using more complex lignified lignocellulosic biomass.

3.1. Screening inhibition of crystalline cellulose saccharification by LRCs

The modulation of cellulase activity was investigated with the application of different LRCs at 30 mM for the release of reducing sugars from microcrystalline cellulose (**Fig. 1**). Notably, the phenolic aldehydes strongly inhibited the cellulose conversion. Cellulase inhibition increased as the adjunction of methoxyl group at the aromatic ring, as observed in 4-hydroxybenzaldehyde (−22%), vanillin (−28%), and syringaldehyde (−42%). The absence of methoxyl group in 4-hydroxybenzaldehyde allowed the lower cellulase inhibition in comparison with vanillin, a monomethoxylated aldehyde, and syringaldehyde, a dimethoxylated aldehyde. By contrast, the benzoic acids, 4-hydroxybenzoic acid, vanillic acid and syringic acid stimulated the cellulase activity by 12% to 44%, whereas the ferulic acid, a hydroxycinnamic acid, increased by 26% the enzyme activity. No significant difference was observed in cellulase activity upon 4-coumaric acid incubation. The data showed that hydroxybenzaldehydes are inhibitory to cellulose conversion by cellulases, with syringaldehyde being the most inhibitory.

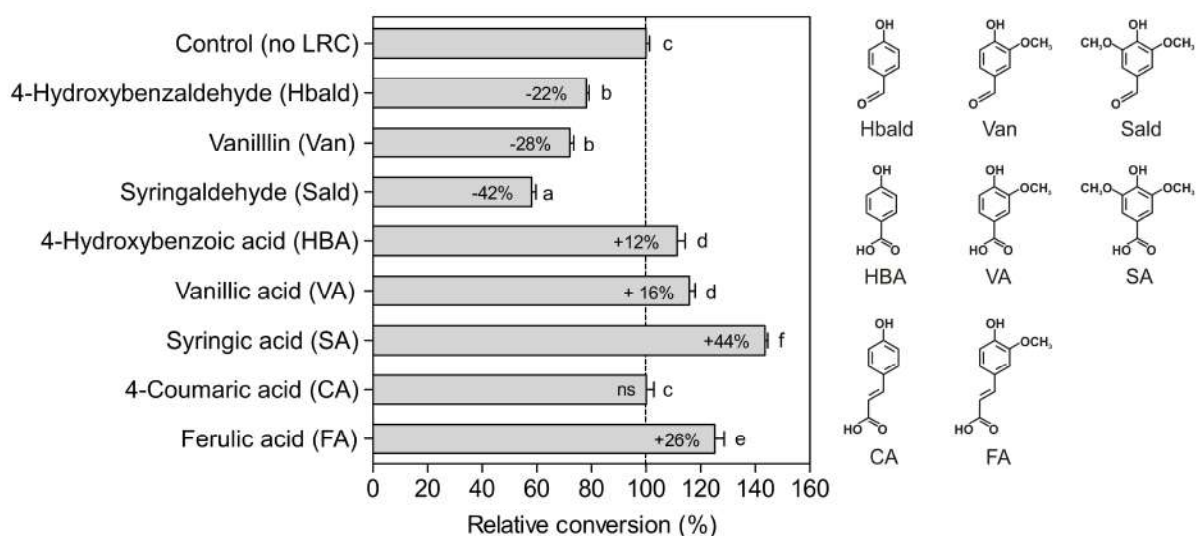


Figure 1. Effects of different lignin-related compounds (LRCs) on cellulase activity. Mean values \pm SEM ($n = 4-5$) marked with different letters are significantly different ($P \leq 0.05$, Tukey test).

Previous reports have suggested that cellulase inhibition by phenolic aldehydes or activation by phenolic acids are correlated with the functional carbonyl and carboxyl groups (Zhao and Chen, 2014; Qin *et al.*, 2016). According to our data, the presence of the carbonyl group, found in phenolic aldehydes, led to the inhibitory effects of 4-hydroxybenzaldehyde, vanillin and syringaldehyde. The chemical structures of 4-hydroxybenzaldehyde and 4-hydroxybenzoic acid (**Fig. 2**) are structurally different only in the functional group and,

therefore, it is likely that the presence of the carbonyl group allowed the inhibitory effect. In contrast, phenolic acids strongly improved cellulase activity. Although the nature of this stimulus is not fully understood, phenolic compounds present potent antioxidant properties, with ability to entrap unpaired electrons (free radicals), stopping free radical chain reactions (Paiva *et al.*, 2013; de Oliveira *et al.*, 2015). Therefore, further studies are required for full elucidation of the molecular mechanism responsible for the stimulus of cellulase activity observed in the presence of phenolic compounds. Furthermore, hydrophobic interactions are thought to play an important role in the adsorption of cellulases and related enzymes to lignocellulose (Berlin *et al.*, 2006). Accordingly, our assays suggest that the degree of hydrophobicity, due to the phenolic ring methoxylations, increased the inhibitory effect of phenolic aldehydes and the stimulatory effect of phenolic acids.

3.2. Modulations of cellulase activity according to the concentration of LRCs

Because syringic and ferulic acids and syringaldehyde presented the most prominent modulations on cellulase activity, we further investigated their effects on cellulose conversion catalyzed by the commercial cellulase. Maximum activation of 110% on cellulase activity was observed with 30 mM syringic acid, whereas 20 mM ferulic acid increased it by 68%. Maximum inhibition of 40% was found with 50 mM syringaldehyde (Fig. 3). Notably, at 50 mM ferulic and syringic acids stimulated cellulase activity but to a lesser extent than at 20–30 mM, respectively.

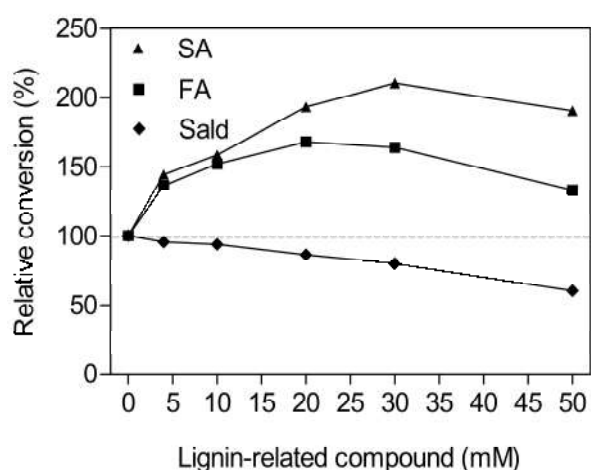


Figure 2. Modulation of cellulose hydrolysis by cellulase in different concentrations (0–50 mM) of lignin-related compounds. (▲) Syringic acid, SA; (■) ferulic acid, FA; (◆) syringaldehyde, Sald. Mean values \pm SEM ($n = 4-5$).

Previously, Zhao and Chen (2014) proposed that phenolic acids at low concentrations could form a hydrophobic layer on the protein surface, leading to a higher hydrophobicity of cellulase surface and more interaction sites with crystalline cellulose through van der Waals forces and aromatic ring polarization. However, at high concentrations of phenolic acids, the

hydrophobicity of the cellulase surface can increase, leading to high protein interaction to each other followed by precipitation, resulting in the inhibitory effect of the enzymes (Kim *et al.*, 2011; Zhao and Chen, 2014).

3.3. Modulation of cellulase activity by LRCs over-time

In order to evaluate the maximum inhibitory or stimulatory effect of LRCs (at 30 mM) on cellulase activity at different hydrolysis times, microcrystalline cellulose was hydrolyzed for 96 h and the releasable reducing sugars were determined at different reaction times (**Fig. 4a**). Next, to determine the effect of individual reaction time for cellulose conversion, it was calculated the enzymatic hydrolysis rate that is the amount of reducing sugar released from microcrystalline cellulose by cellulase at the specific time point (**Fig. 4b**). The results indicated that LRCs differentially modulated the cellulose conversion and hydrolysis rate. Maximum inhibition of ~50% and lowest hydrolysis rate were observed with syringaldehyde between 12 h to 96 h of enzymatic hydrolysis, while cellulose conversion was inhibited by 13% to 43% between 2 h to 8 h of hydrolysis, respectively. In contrast, incubation with syringic acid had the maximum stimulation and highest hydrolysis rate of 129% at 2 h of hydrolysis and 75% at 4 h. Similarly, ferulic acid increased the cellulose conversion by 70% at 2 h and 51% at 4 h. It is important to note that both the phenolic acids had their maximum stimulatory effects before the first 4 h of hydrolysis, while syringaldehyde had the maximum inhibition after 12 h of hydrolysis times.

For maximum cellulose depolymerization, a degrading system requires at least three related activities, acting synergistically for cellulose hydrolysis (Binod *et al.*, 2019). Exoglucanases release cellobiose from the reducing and nonreducing ends of cellulose chains, whereas endoglucanases randomly hydrolyze internal glycosidic bonds reducing cellulose length, and β -glucosidases split off cellobiose and cello-oligomers to glucose (Segato *et al.*, 2014; Segato *et al.*, 2017; Mota *et al.*, 2018). Therefore, considering that syringic and ferulic acids showed higher stimulatory effects at the first 4 h of enzymatic hydrolysis, it is likely that these compounds act primarily on exoglucanases and endoglucanases, during the initial steps of crystalline cellulose depolymerization. In contrast, syringaldehyde might act more effectively inhibiting β -glucosidases during cellobiose breakdown.

The data suggest that inhibitory and stimulatory effects of LRCs on cellulase activity exhibit different features underlying the chemical nature inherent to each compound. Although there is a clear correlation between the structure of LRCs and their effects on cellulase activity, further studies are required to clarify the mechanism of action of these compounds. The results

indicate that cellulose hydrolysis by cellulases was significantly improved by benzoic acids and ferulic acid, a hydroxycinnamic acid, whereas hydroxybenzaldehydes are efficient inhibitors for cellulases.

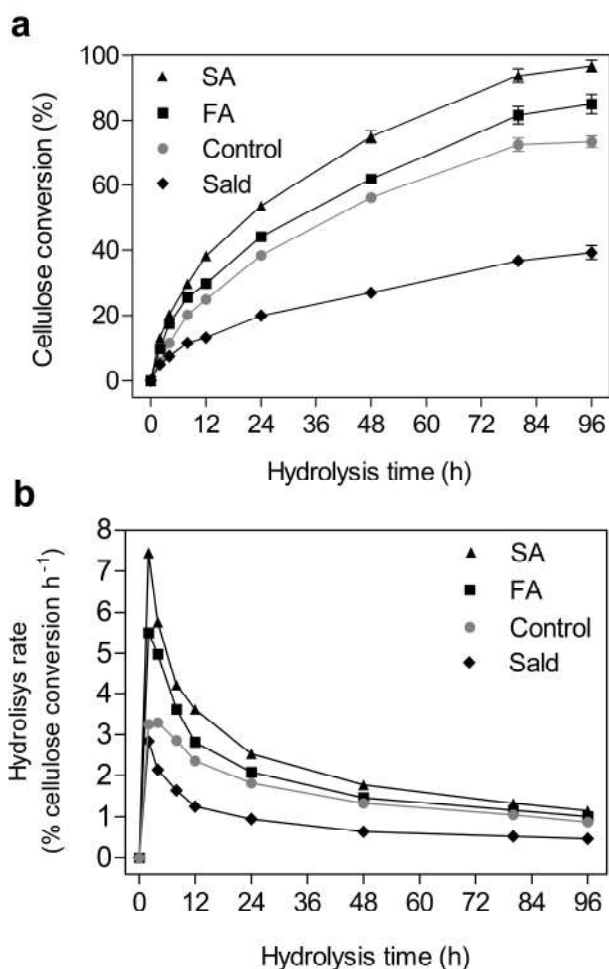


Figure 3. Effects of lignin-related compounds on cellulose hydrolysis by cellulase in different hydrolysis times (0–96 h). (●) Control; (▲) 30 mM syringic acid, SA; (■) 30 mM ferulic acid, FA; (◆) 30 mM syringaldehyde, Sald. Mean values \pm SEM ($n = 4-5$).

Future investigations may center in reducing the interference of phenolic aldehydes in cellulase activity, performing biomass saccharification over shorter times to decrease the enzyme inhibition. In addition, it could be explored the application of chemical, microbial or enzymatic conversion of phenolic aldehydes to inactive forms. Alternative strategies may focus on the optimization of biomass pretreatments to generate specific LRCs with positive effects to cellulases. Moreover, the activation of cellulases by phenolic acids can be a potential tool for the processing of lignocellulosic biomass for bioenergy and biorefinery.

4. Conclusions

The present study demonstrated the contrasting effects of LRCs at different concentrations and hydrolysis times on cellulose conversion by a commercial cellulase. The presence of carbonyl group in phenolic aldehydes plays a fundamental role in inhibitory action

on cellulase activity. Conversely, the carboxyl group seems to have an activating effect for cellulases. Together, the results reveal that the stimulatory effect conferred by syringic and ferulic acids on cellulase activity may be considered for the improvement of lignocellulosic biomass saccharification for bioethanol production.

Acknowledgements

D.M.O. and T.R.M. gratefully acknowledge the doctoral scholarship granted by Brazilian National Council for Scientific and Technological Development (CNPq) and Coordination of Enhancement of Higher Education Personnel (CAPES). R.M. and O.F.F. are research fellows granted by CNPq.

Conflict of interests

The authors declare that they have no competing interests.

References

- Banu, J.R., Kavitha, S., Yukesh Kannah, R., Poornima Devi, T., Gunasekaran, M., Kim, S.-H., Kumar, G. 2019. A review on biopolymer production via lignin valorization. *Bioresour. Technol.*, **290**, 121790.
- Berlin, A., Balakshin, M., Gilkes, N., Kadla, J., Maximenko, V., Kubo, S., Saddler, J. 2006. Inhibition of cellulase, xylanase and beta-glucosidase activities by softwood lignin preparations. *J. Biotechnol.*, **125**(2), 198-209.
- Binod, P., Gnansounou, E., Sindhu, R., Pandey, A. 2019. Enzymes for second generation biofuels: Recent developments and future perspectives. *Biores. Technol. Rep.*, **5**, 317-325.
- Bomble, Y.J., Lin, C.Y., Amore, A., Wei, H., Holwerda, E.K., Ciesielski, P.N., Donohoe, B.S., Decker, S.R., Lynd, L.R., Himmel, M.E. 2017. Lignocellulose deconstruction in the biosphere. *Curr. Opin. Chem. Biol.*, **41**, 61-70.
- de Oliveira, D.M., Finger-Teixeira, A., Mota, T.R., Salvador, V.H., Moreira-Vilar, F.C., Molinari, H.B., Mitchell, R.A., Marchiosi, R., Ferrarese-Filho, O., dos Santos, W.D. 2015. Ferulic acid: a key component in grass lignocellulose recalcitrance to hydrolysis. *Plant Biotechnol. J.*, **13**(9), 1224-1232.
- Gao, J., Xin, S., Wang, L., Lei, Y., Ji, H., Liu, S. 2019. Effect of ionic liquid/inorganic salt/water pretreatment on the composition, structure and enzymatic hydrolysis of rice straw. *Biores. Technol. Rep.*, **5**, 355-358.
- Kim, Y., Ximenes, E., Mosier, N.S., Ladisch, M.R. 2011. Soluble inhibitors/deactivators of cellulase enzymes from lignocellulosic biomass. *Enzym. Microb. Technol.*, **48**(4-5), 408-415.
- Li, Y., Qi, B., Wan, Y. 2014. Inhibitory effect of vanillin on cellulase activity in hydrolysis of cellulosic biomass. *Bioresour. Technol.*, **167**, 324-30.
- Miller, G.L. 1959. Use of dinitrosalicylic acid reagent for determination of reducing sugar. *Anal. Chem.*, **31**(3), 426-428.
- Mota, T.R., Oliveira, D.M., Marchiosi, R., Ferrarese-Filho, O., dos Santos, W.D. 2018. Plant cell wall composition and enzymatic deconstruction. *AIMS Bioeng.*, **5**(1), 63-77.
- Mota, T.R., Oliveira, D.M., Morais, G.R., Marchiosi, R., Buckeridge, M.S., Ferrarese-Filho, O., dos Santos, W.D. 2019. Hydrogen peroxide-acetic acid pretreatment increases the saccharification and enzyme adsorption on lignocellulose. *Ind. Crop. Prod.*, **140**, 111657.
- Oliveira, D.M., Mota, T.R., Grandis, A., de Morais, G.R., de Lucas, R.C., Polizeli, M.L.T.M., Marchiosi, R., Buckeridge, M.S., Ferrarese-Filho, O., dos Santos, W.D. 2020. Lignin plays a key role in determining biomass recalcitrance in forage grasses. *Renew. Energy*, **147**, 2206-2217.
- Oliveira, D.M., Mota, T.R., Oliva, B., Segato, F., Marchiosi, R., Ferrarese-Filho, O., Faulds, C.B., Dos Santos, W.D. 2019. Feruloyl esterases: Biocatalysts to overcome biomass recalcitrance and for the production of bioactive compounds. *Bioresour. Technol.*, **278**, 408-423.
- Oliveira, D.M., Salvador, V.H., Mota, T.R., Finger-Teixeira, A., Almeida, R.F., Paixão, D.A.A., de Souza, A.P., Buckeridge, M.S., Marchiosi, R., Ferrarese-Filho, O., Squina,

- F.M., dos Santos, W.D. 2016. Feruloyl esterase from *Aspergillus clavatus* improves xylan hydrolysis of sugarcane bagasse. *AIMS Bioeng.*, **4**(1), 1-11.
- Paiva, L.B.d., Goldbeck, R., Santos, W.D.d., Squina, F.M. 2013. Ferulic acid and derivatives: molecules with potential application in the pharmaceutical field. *Braz. J. Pharm. Sci.*, **49**, 395-411.
- Ponnusamy, V.K., Nguyen, D.D., Dharmaraja, J., Shobana, S., Banu, J.R., Saratale, R.G., Chang, S.W., Kumar, G. 2019. A review on lignin structure, pretreatments, fermentation reactions and biorefinery potential. *Bioresour. Technol.*, **271**, 462-472.
- Qin, L., Li, W.C., Liu, L., Zhu, J.Q., Li, X., Li, B.Z., Yuan, Y.J. 2016. Inhibition of lignin-derived phenolic compounds to cellulase. *Biotechnol. Biofuels*, **9**, 70.
- Segato, F., Damásio, A.R.L., Lucas, R.C., Squina, F.M., Prade, R.A. 2014. Genomics review of holocellulose deconstruction by Aspergilli. *Microbiol. Mol. Biol. Rev.*, **78**.
- Segato, F., Dias, B., Berto, G.L., de Oliveira, D.M., De Souza, F.H.M., Citadini, A.P., Murakami, M.T., Damasio, A.R.L., Squina, F.M., Polikarpov, I. 2017. Cloning, heterologous expression and biochemical characterization of a non-specific endoglucanase family 12 from *Aspergillus terreus* NIH2624. *Biochim. Biophys. Acta, Proteins Proteomics*, **1865**(4), 395-403.
- Vanholme, R., Demedts, B., Morreel, K., Ralph, J., Boerjan, W. 2010. Lignin biosynthesis and structure. *Plant Physiol.*, **153**(3), 895-905.
- Ximenes, E., Kim, Y., Mosier, N., Dien, B., Ladisch, M. 2011. Deactivation of cellulases by phenols. *Enzym. Microb. Technol.*, **48**(1), 54-60.
- Ximenes, E., Kim, Y., Mosier, N., Dien, B., Ladisch, M. 2010. Inhibition of cellulases by phenols. *Enzym. Microb. Technol.*, **46**(3-4), 170-176.
- Yu, Z., Gwak, K.-S., Treasure, T., Jameel, H., Chang, H.-m., Park, S. 2014. Effect of lignin chemistry on the enzymatic hydrolysis of woody biomass. *ChemSusChem*, **7**(7), 1942-1950.
- Zhang, L., Loh, K.-C., Zhang, J. 2019. Enhanced biogas production from anaerobic digestion of solid organic wastes: Current status and prospects. *Biores. Technol. Rep.*, **5**, 280-296.
- Zhao, J., Chen, H. 2014. Stimulation of cellulases by small phenolic compounds in pretreated stover. *J. Agric. Food Chem.*, **62**(14), 3223-3229.

Supporting Material

Chapter 2. Modulation of Cellulase Activity by Lignin-Related Compounds

Dyoni M. Oliveira*, Érica P. Hoshino, Thatiane R. Mota, Rogério Marchiosi, Osvaldo Ferrarese-Filho, Wanderley D. dos Santos*

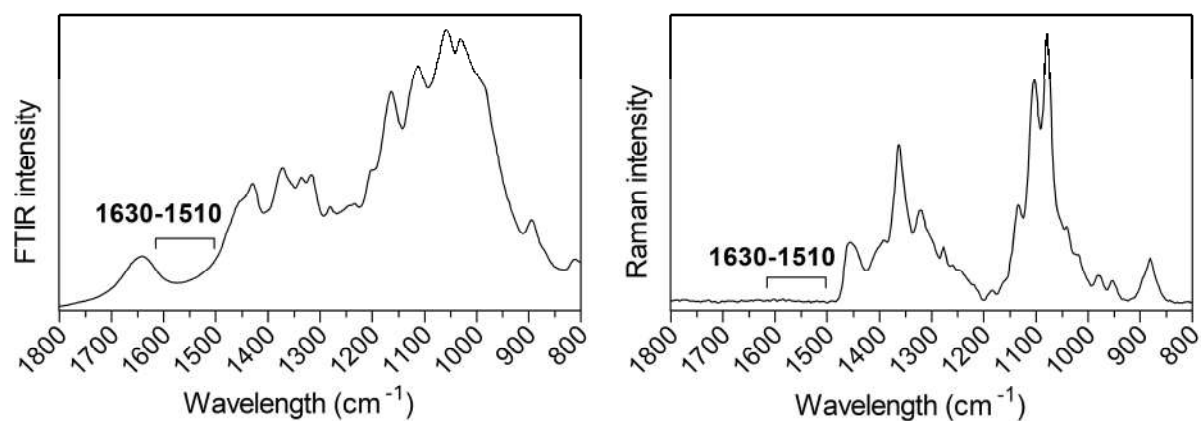


Figure S1. FTIR and Raman spectra of microcrystalline cellulose indicating the absence of peaks at 1,510–1,630 cm⁻¹ corresponding to C=C stretching and aromatic skeletal vibrations of aromatic rings. Bands are assigned as previously described by Oliveira et al. (2020).

CHAPTER 3

Feruloyl Esterases: Biocatalysts to Overcome Biomass Recalcitrance and for the Production of Bioactive Compounds

Dyoni M. Oliveira^{1a*}, Thatiane R. Mota^{1a}, Bianca Oliva², Fernando Segato², Rogério Marchiosi¹, Osvaldo Ferrarese-Filho¹, Craig B. Faulds³, Wanderley D. dos Santos^{1*}

¹ Department of Biochemistry, State University of Maringá, PR, Brazil

² Department of Biotechnology, Engineering School of Lorena, University of São Paulo, Lorena, São Paulo, Brazil

³ Aix-Marseille Université, INRA UMR 1163 Biodiversité et Biotechnologie Fongiques (BBF), 13009 Marseille, France

^a The authors contributed equally

*** Corresponding author**

Dyoni M. Oliveira

Wanderley D. dos Santos

E-mail: dyonioliveira@gmail.com; wdsantos@uem.br

Type of chapter:	Review article
Journal:	Bioresource Technology
Impact factor:	6.669
Volume/issue, pages:	278, 408-423
Date of publication:	April 2019
DOI:	10.1016/j.biortech.2019.01.064

Abstract

Ferulic acid and its hydroxycinnamate derivatives represent one of the most abundant forms of low molecular weight phenolic compounds in plant biomass. Feruloyl esterases are part of a microorganism's plant cell wall-degrading enzymatic arsenal responsible for cleaving insoluble wall-bound hydroxycinnamates and soluble cytosolic conjugates. Stimulated by industrial requirements, accelerating scientific discoveries and knowledge transfer, continuous improvement efforts have been made to identify, create and repurposed biocatalysts dedicated to plant biomass conversion and biosynthesis of high-added value molecules. Here we review the basic knowledge and recent advances in biotechnological characteristics and the gene content encoding for feruloyl esterases. Information about several enzymes is systematically organized according to their function, biochemical properties, substrate specificity, and biotechnological applications. This review contributes to further structural, functional, and biotechnological R&D both for obtaining hydroxycinnamates from agricultural by-products as well as for lignocellulose biomass treatments aiming for production of bioethanol and other derivatives of industrial interest.

Keywords: Biorefinery; Carbohydrate esterases; Cell wall; Genome mining; Lignocellulose; Saccharification.

1. Introduction

Feruloyl esterases (FAE; EC 3.1.1.73) are a subclass of carboxylic acid esterases with the capacity to release ferulic acid (FA) and other hydroxycinnamic acids from plant cell walls, plant cytoplasm and synthetic substrates. FAEs are found in bacteria, fungi and plants, with many biotechnological applications, such as: obtaining FA from agricultural by-product wastes and subsequent bioconversion to high added value aromatic compounds, biological delignification of non-woody plants for the paper industry, enzymatic hydrolysis for bioethanol production, improving the digestion of forage plants for ruminants, and as biosynthetic tools to catalyze esterification and transesterification of esters of hydroxycinnamic acids (Furuya *et al.*, 2017; Gopalan *et al.*, 2015; Oliveira *et al.*, 2017).

Ferulic acid (FA) has applications as a food preservative due to its antioxidant and antimicrobial properties; as a therapeutic agent, including anti-inflammatory, antibacterial, antidiabetic and neuroprotective effects; and as a sun protective factor. FA and its derivatives are able to neutralize free radicals, protecting cell membranes and DNA (Paiva *et al.*, 2013). It is also a precursor for synthesis of flavor compounds, such as vanillin and 4-vinyl guaiacol; the microbial biotransformation of FA to vanillin (a major food industry aroma) has been extensively investigated (Furuya *et al.*, 2017). FA is an important factor for lignocellulosic biomass recalcitrance, cross-linking the cell wall polymers. Therefore, the application of FAEs for lignocellulosic biomass deconstruction has a key role in decreasing the biomass recalcitrance to hydrolysis, wherefore lignocellulosic biomass is the most abundant renewable raw material in nature and has the potential to produce biofuels on a scale large enough to replace oil in the mid-term (Linh *et al.*, 2017; Mota *et al.*, 2018).

Biomass recalcitrance is mainly derived from the plant cell wall composition and architecture and it is conferred by different interactions among its components, requiring additional energy inputs for their disruption attack (McCann and Carpita, 2015). The complex architecture of lignocellulose provides a barrier to convert cellulose into fermentable sugars, due to the several factors such as, cellulose crystallinity, accessibility and polymerization, the organization of cellulose microfibrils, hemicellulose polymerization and substitution pattern, lignin content and composition, and the occlusion of the cell wall by lignin-hydroxycinnamate-hemicellulose cross-linking (McCann and Carpita, 2015).

This research review describes the current fundamental knowledge and recent advances in comprehensive mining about biotechnological and biochemical characteristics. Information about several enzymes is systematically organized according to their function, kinetics, biochemical properties, and substrate specificity. We believe that this mapping of FAEs and

their substrate relationship may be a powerful instrument for further functional, biochemical and structural evaluation, as well as biotechnological applications of FAEs to the obtainment of hydroxycinnamic acids from agricultural by-products and improved saccharification of lignocellulosic biomass.

2. Ferulic acid: a polyvalent molecule

2.1. Ferulic acid in plant cell walls and biomass recalcitrance

Ferulic acid is a hydroxycinnamic acid with the systematic name (3-methoxy-4-hydroxy)-3-phenyl-2-propenoic acid or 3-methoxy-4-hydroxy-cinnamic acid (**Fig. 1A**). Produced via the phenylpropanoid pathway, FA and its ester of CoA, FA-CoA, can be seen both as intermediary metabolites towards the formation of monolignols during lignin biosynthesis and as final products of the pathway (Oliveira *et al.*, 2015). Like monolignols and other phenolic compounds, FA presents a polyenic (conjugated) structure that allows the molecule to stabilize a free radical (non-paired electron) produced by UV-light, respiratory chain, peroxidases and other metabolic activities (Bento-Silva *et al.*, 2018). As the ΔG for releasing a free radical is positive, phenylpropanoids stop free radical chain reactions by conserving the radical resonating among their chemical linkages. For this reason, it works as a sunscreen and antioxidant in plants and pharmaceutical products (dos Santos *et al.*, 2008). In plant cell walls, FA plays a key role in inter- and intra-polymer cross-linkage. It may also be covalently linked to lignin through the ether or ester bonds and esterified to polysaccharides (Terrett and Dupree, 2019).

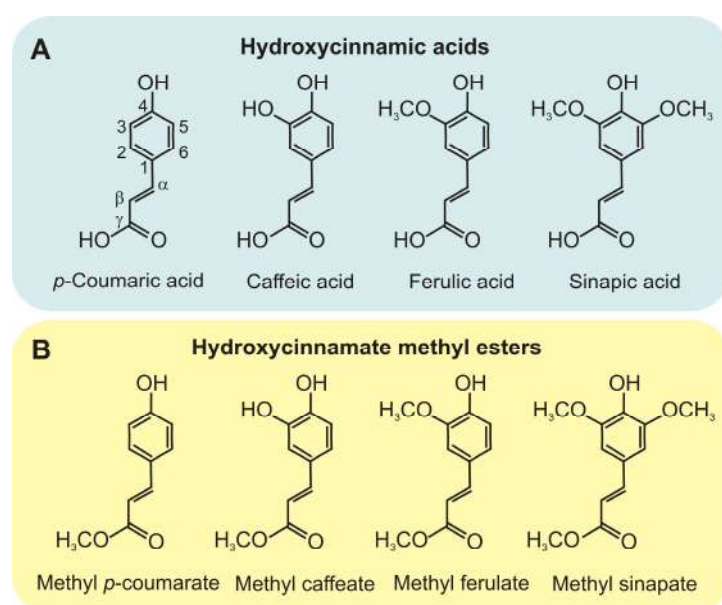


Figure 1. Chemical structures of hydroxycinnamic acids (A) and hydroxycinnamate methyl esters (B).

In commelinid monocots — a group of angiosperms including grasses, palms, bromeliads, gingers, and ‘core’ Caryophyllales — ester-linked FA occurs in the cell wall at different and high concentrations (>3.5 mg g⁻¹ cell wall) according to the specie, organ and tissue, as summarized in **Table 1**.

Table 1. Amount of ferulic acid in different biomass sources.

Group	Species, family	Organ or tissue	Concentration of FA (mg g ⁻¹)	Reference	
Commelinid monocots	Maize (<i>Zea mays</i>), Poaceae	Grain	20.66	(Hartley and Haverkamp, 1984)	
		Bran	26.1 to 33.0	(Zhao and Moghadasian, 2008)	
		Stem	6.27	(Hartley and Haverkamp, 1984)	
		Leaf blade	3.86	(Hartley and Haverkamp, 1984)	
		Perennial ryegrass (<i>Lolium perenne</i>), Poaceae	Shoot	6.03	(Hartley and Haverkamp, 1984)
		Sugarcane (<i>Saccharum officinarum</i>), Poaceae	Culm bagasse	8.0 to 17.0	(Masarin <i>et al.</i> , 2011)
		Barley (<i>Hordeum vulgare</i>), Poaceae	Stem	3.51	(Hartley and Haverkamp, 1984)
		Rice (<i>Oryza sativa</i>), Poaceae	Grain	0.091 to 0.143	(Zhao and Moghadasian, 2008)
		Nile grass (<i>Cyperus papyrus</i>), Cyperaceae	Stem	3.18	(Karlen <i>et al.</i> , 2018)
		Ginger lily (<i>Hedychium gardnerianum</i>), Zingiberaceae	Stem	3.43	(Karlen <i>et al.</i> , 2018)
		Pineapple (<i>Ananas comosus</i>), Bromeliaceae	Fruit core	6.84	(Karlen <i>et al.</i> , 2018)
		Tassel cord Rush (<i>Baloskion tetraphyllum</i>), Restionaceae	Stem	2.27	(Karlen <i>et al.</i> , 2018)
		Blue ginger (<i>Dichorisandra thysiflora</i>), Commelinaceae	Stem	1.07	(Karlen <i>et al.</i> , 2018)
		Canary island date palm (<i>Phoenix canariensis</i>), Arecaceae	Leaf	0.17	(Karlen <i>et al.</i> , 2018)
Non-commelinid plants	Onion (<i>Allium cepa</i>), Alliaceae	Bulb	0.007	(Zhao and Moghadasian, 2008)	
	Beetroot (<i>Beta vulgaris</i>), Amaranthaceae	Root	6.93	(Waldron <i>et al.</i> , 1999)	
	Sugarbeet (<i>Beta vulgaris</i>), Amaranthaceae	Root	4.59	(Waldron <i>et al.</i> , 1999)	
	Spinach (<i>Spinacia oleraceae</i>), Amaranthaceae	–	0.074	(Mattila and Hellström, 2007)	
	Soybean (<i>Glycine max</i>), Fabaceae	–	0.12	(Mattila and Hellström, 2007)	
	White cabbage (<i>Brassica oleraceae</i>), Brassicaceae	–	0.0027	(Mattila and Hellström, 2007)	
	Broccoli (<i>Brassica oleraceae</i>), Brassicaceae	–	0.041	(Mattila and Hellström, 2007)	
	Tomato (<i>Lycopersicum esculentum</i>), Solanaceae	–	0.0029	(Mattila and Hellström, 2007)	

–, not defined or not mentioned.

In the primary cell walls of commelinid monocots, including grasses, FA is esterified in the C-5 hydroxyl group of the arabinosyl residue of the arabinoxylan (β -1,4-linked xylopyranosyl backbone) and is more abundant than other groups (Oliveira *et al.*, 2015). FA ester-linked to the arabinosyl residue of arabinoxylan is able to ether-link with lignin or dimerize with other FA-arabinoxylan, cross-linking these cell wall polymers. Such cross-

linkages can block the attack of hydrolases, reducing enzymatic hydrolysis efficiency (Oliveira *et al.*, 2015). The production of FA cross-linkages is catalyzed by specific peroxidases that act on FA and FA esters to produce dehydrodimers (e.g. 5-5' and 8-O-4'-dehydrodiferulic acid) cross-linking vicinal arabinoxylan (**Fig. 2**) (Hatfield and Ralph, 1999).

Lignin polymer and feruloylation of plant tissues imposes a barrier to efficient cell wall conversion and negatively impacts digestibility (Ponnusamy *et al.*, 2019). Feruloylation of arabinoxylan is important not only because it leads to cross-linked arabinoxylan in grasses, but also because ferulate may act as a nucleating site for the formation of lignin, and hence linking arabinoxylans to lignin by forming a lignin–ferulate–arabinoxylan complex (Oliveira *et al.*, 2015; Terrett and Dupree, 2019).

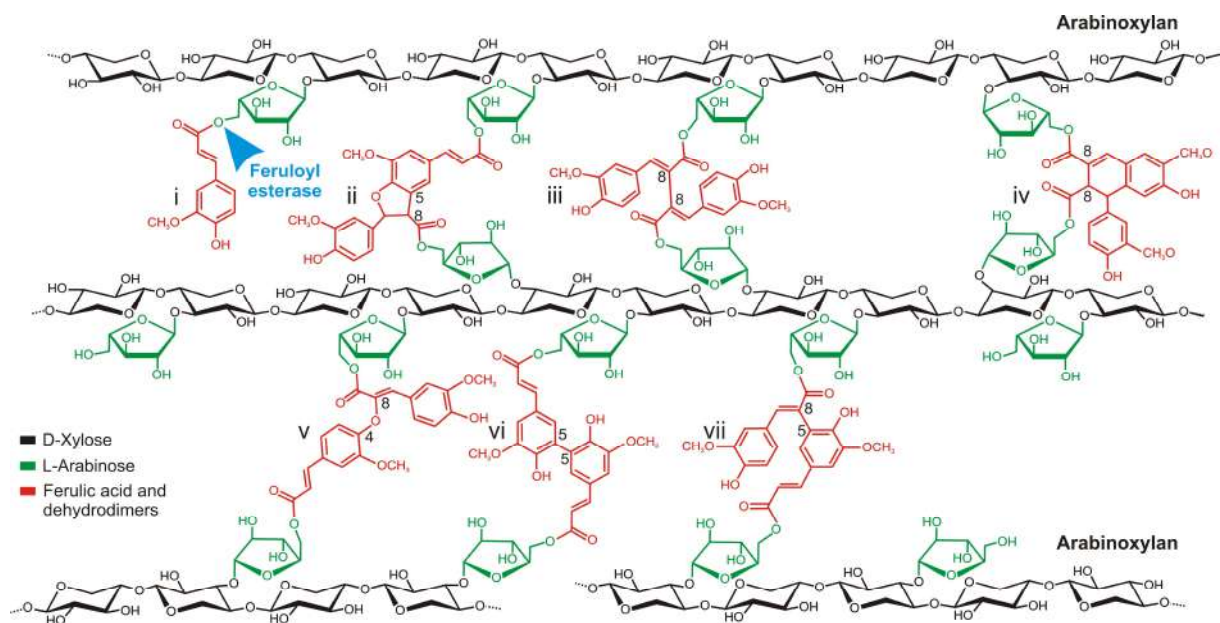


Figure 2. Schematic representation of arabinoxylan ester-linked with FA and FA dehydrodimers. i) FA esterified to arabinosyl residue and the site of action of FAE, ii) 8-5' diFA benzofuran form, iii) 8-8' diFA, iv) 8-8' diFA aryltetralin form, v) 8-O-4' diFA, vi) 5-5' diFA, and vii) 8-5' diFA.

Cross-linking of grass cell wall components, especially through FA and diFA esterified to arabinoxylan affects many cell wall properties, such as adherence, extensibility, accessibility and biodegradability. An additional consequence of diFA cross-linkages of arabinoxylan is the increase of recalcitrance with consequent reduction of digestibility of cell wall polysaccharides by glycosyl hydrolases, a limitation for biomass conversion to bioethanol (Oliveira *et al.*, 2015; Perez-Boada *et al.*, 2014).

2.2. Pharmaceutical potential of ferulic acid and derivatives

The therapeutic effect and efficacy of FA are dependent on some properties such as physiological concentration and pharmacokinetics. Generally, in a given meal, people ingest from 180 to 165 mg of FA, which is present in its conjugated and free forms, having low toxicity to the organism and showing a broad variety of biomedical properties: anti-carcinogenic, antioxidant, anti-allergic, anti-inflammatory, antiviral, antimicrobial, and cholesterol-lowering, among others. For that reason, FA is a popular food additive in some countries (Srinivasan *et al.*, 2007).

Due to the observed properties, an extensive study of biological functions and related activities of FA has demonstrated its protective effects against tumor necrosis factor (TNF) and its antimicrobial activities with effects against yeasts and bacteria (Borges *et al.*, 2013). FA has been investigated as an adjunct administered in cancer chemotherapy due to its capacity to enhance natural immune defenses and gastrointestinal tract movement, protecting the organism against side effects (abdominal discomfort), which limit the treatment (Badary *et al.*, 2006). In addition, the increase of intestinal motility promoted by FA inhibits some intestinal disorders and can act synergistically with antibiotics in the treatment of pathogenic microorganisms such as *Escherichia coli*, *Helicobacter pylori*, *Pseudomonas aeruginosa*, *Staphylococcus aureus* and *Lysteria monocytogenes*.

The phytochemical-antibiotic combination assays showed a synergistic effect when applied in consort with streptomycin against both pathogenic Gram-negative and Gram-positive bacteria by changing cell morphology and membrane permeability (Shi *et al.*, 2016). FA has mixed antioxidant and pro-oxidant capacities, inducing apoptosis mechanisms in parasites. As an important function, microfilaricidal activity induced by FA culminates in apoptosis and alteration in key antioxidant components, such as glutathione, glutathione S-transferase and superoxide dismutase (Saini *et al.*, 2012). The administration of FA in Wistar rats via intragastric intubation increases protection against lipid peroxidation and decreases the DNA damage due to the improvement in antioxidant performance (Paiva *et al.*, 2013; Sompong *et al.*, 2017).

FA exhibits anti-inflammatory properties, decreasing the levels of compounds produced by macrophages. Diabetic rats supplemented with FA showed a reduction in blood glucose and thiobarbituric acid-reactive substances, and also increases the action of superoxide dismutase and catalase. These results are correlated with the antioxidant capacity of FA, which interacts synergistically with some drugs used in the treatment of diabetes (Nankar *et al.*, 2017). An important function of FA was observed as protective, showing therapeutic action on

nephropathy and protective effects in organs such as the brain, kidney, pancreas, intestine and liver by reducing inflammation and oxidative stress (Ren *et al.*, 2017). Additional work has demonstrated that FA increases the levels of monoamine neurotransmitter in the brain and promotes vasodilatation that can be beneficial for the treatment of mood disorders (Chen *et al.*, 2015).

In food science, FA has much utilization due to its intrinsic characteristics in the cell wall together with insolubility of compounds, and can be used in cereal dietary fibers. FA dehydrodimers may be used against *Fusarium graminearum*, a fungus accountable for disease in maize. Besides that, FA shows activity that inhibits the growth of microorganisms and acts as a natural compound that preserves foods, so it has very diversified uses, including preserving oranges, stabilizing soybean oil, inhibiting the oxidation of biscuits, and increasing the viscosity of polysaccharides to obtain gels, and it can be incorporated into materials used to produce drug packages (Silva and Batista, 2017).

3. Classification of feruloyl esterases and genome analysis

Currently, the known FAEs are classified into the Carbohydrate Esterase Family 1 (CE1) within the Carbohydrate-Active Enzymes database (CAZy – www.cazy.org), in accordance with its amino acid sequences and mode of action (Lombard *et al.*, 2014). Different classification systems have been proposed for FAEs. In this article, we reviewed and explained the different methods used to classify FAEs.

The Crepin's classification system is based in the correlation between previously determined biochemical and functional characteristics and sequence similarities (Crepin *et al.*, 2004). According to Crepin's classification, FAEs can be classified by amino acid sequences similarities into A, B, C, D and a putative E types, and this similarity also correlated with their specificity for synthetic substrates containing hydroxycinnamic methyl esters (methyl ferulate – MFA, methyl *p*-coumarate – MpCA, methyl caffeate – MCA, and methyl sinapate – MSA, **Fig. 1B**), ability to release FA dehydrodimers (especially, 5,5'-diFA, **Fig. 2**) from esterified substrates, and amino acid sequence homology, which also indicates the evolutionary relationship among the microbial FAEs. However, this classification system presents some disadvantages because it is based at the time (2004) on a very small number of confirmed FAEs and sequences. The information of specificity of the enzymes was acquired with different methodologies with natural or synthetic substrates, and unrelated enzymes are part of the same group – *e.g.* PeFaeA from *Pleurotus eryngii* and AnFaeA from *A. niger*.

According to Crepin's classification, the phylogenetic analysis also suggests that some microbial FAEs do not belong to any kind of type in the previous four classifications. To date, these enzymes are predominantly bacterial in origin, suggesting that fungal and bacterial FAEs are encoded different from each other. Therefore, these enzymes are classified in the putative type E sub-class. This fifth sub-class comprises *Orpinomyces* sp. OspFaeA, *Clostridium thermocellum* XynZ, *Ruminococcus* sp. RspXyn1, *R. flavefaciens* RfXynE and *R. albus* RaXynB. Nevertheless, members of this sub-class may only be identified based on their primary amino acid sequence identity. No further correlation could be established due to the lack of comparable enzyme activity data (Crepin *et al.*, 2004). This classification has been used by other researchers in characterizing their FAES. For example, the cinnamoyl esterase from *L. acidophilus* F46 is classified into the putative type E, indicating that the functional classification of the microbial FAE based on fungal origin is not enough to describe it according to Crepin's classification (Kim and Baik, 2015).

As a further refinement for FAEs classification, Benoit and coworkers provided an elegant system based on the phylogenic analysis of known fungal genomic sequences expanding the comprehension of known FAEs (Benoit *et al.*, 2008). Based on Benoit's classification system, seven subfamilies (SF 1 to 7) of candidate FAEs were identified in many fungal genomes, containing three biochemically characterized types of FAEs (types A, B and C), excluding those esterases classified previously as type D and all bacterial FAEs. Members of the genus *Aspergillus* are present in the subfamily 1, 3, 4, 5, 6 and 7. Subfamily 7 is restricted to FAEs genes from *A. niger*, *A. oryzae* and *A. terreus* based on the primary dataset these authors had access to. The same is almost true for subfamily 1 that contains FAE genes from *A. fumigatus*, *A. niger*, *A. oryzae* and *A. nidulans*. However, this subfamily also includes the FAE gene from *Talaromyces stipitatus* as a member and is closely related to subfamily 2, while subfamily 7 is very distant from all the other subfamilies.

Udatha and coworkers extended the classification of FAEs further by proposing a novel classification system, grouping for the first time FAEs from three kingdoms – fungi, bacteria and plant. The classification resulted in 12 distinct families, which have the capability of acting on a large range of substrates for cleaving ester bonds and synthesizing high-added value molecules through esterification and transesterification reactions (Udatha *et al.*, 2011). In this classification system, 365 putative FAE-related sequences of fungi, bacteria and plant origin were collected and clustered into distinct groups based on amino acid composition, protein secondary structure, and physicochemical composition descriptors derived from the respective amino acid sequence. The 12 proposed families were validated applying a combination of

prediction tools with experimental data. Unfortunately with this, FAEs share a high sequence identity with other serine proteases, such as acetyl esterases, proteases and lipases, and so a sequence-based only classification is difficult to predict without corresponding biochemical data confirming that these sequences correspond to actual FAEs.

Recently, the groups of de Vries and Hildén have proposed another classification for fungal FAEs considering both phylogeny and substrate specificity (Dilokpimol *et al.*, 2016). In this latest classification, 13 sub-families are proposed together with an unclassified group, demonstrating the limitations in grouping both bacterial and fungal FAEs together. However, according to this classification, only some FAEs from sub-families 5 and 6 are grouped in CE1 family of CAZy database (Udatha *et al.*, 2011). More recently, the same research groups performed a phylogenetic analysis that divided fungal FAEs members of CE1 family into five subfamilies, this upgrade in the last classification system was able with the identification and characterization of a novel AtFaeD from *A. terreus* (Dilokpimol *et al.*, 2016).

With the expansion of microbial genome sequencing, it has been revealed that organisms contain a multiplicity of putative enzyme-encoding genes. Multiple predicted FAE-encoding genes have thus far been identified in fungi, which will allow more FAEs to be heterologously expressed and characterized soon. While some fungi, such as *Trichoderma reesei*, do not contain FAE-encoding sequences (Martinez *et al.*, 2008), other species in the *Trichoderma* genus do contain putative FAEs in their genome (Dilokpimol *et al.*, 2016). Thirteen predicted FAEs were identified in the genome of *A. oryzae* belonging to six subfamilies of the Udatha's classification. These sequences were subsequently modeled for structural analysis and three sequences cloned and expressed in *Pichia pastoris* (a system well-disposed for esterase expression), and their substrate specificity was determined. Furthermore, 37 putative FAEs were identified in the basidiomycetes *Moniliophthora roreri*, *Auricularia subglabra* and *Agaricus bisporus* var *bisporus*, and predicted genes encoding FAE were identified in the genomes of several ascomycetes such as *A. flavus* with 16 genes, 29 in *A. niger*, 16 in *Chaetomium globosum*, and 11 in *Fusarium graminearum* (Dilokpimol *et al.*, 2016). As these authors pointed out, however, a genome sequence prediction is not always accurate, as pseudogenes and non-FAE related enzymes, such as tannases, acetyl esterases, and others, could be included. Similarly, gene cloning followed by protein expression and characterization are essential to determine the ability of a microbe to produce multiple FAEs. More recently, Dilokpimol and coworkers confirmed the ability of the genome mining strategy to identify eligible candidates for fungal FAE encoding genes for related biotechnological applications, by

demonstrating that 20 out of 27 putative fungal FAEs possessed esterase activity (Dilokpimol *et al.*, 2018).

4. Biochemical properties of microbial FAEs

Since their first identification in the 1980s and purification in 1991 (Faulds and Williamson, 1991), more than 80 FAEs with different molecular masses, substrate preferences, isoelectric points, and optimum reaction conditions have been characterized from microbial sources. Microbial FAEs from different sources present a broad range of biochemical properties and kinetic values, as summarized in **Table 2**. The biochemical characteristics of FAEs show significant variation in molecular weight (18.5 – 210 kDa), isoelectric points (3.0 – 9.9), optimum pH (3.0 – 10.0) and temperature (20 – 75 °C). Based on the biochemical properties of characterized FAEs (**Table 2**), we organized the data for molecular mass, optimum temperature, pH and isoelectric point for better understanding and to contribute to further functional studies (**Fig. 3**). According to relative frequencies and medians, FAEs frequently have a molecular mass of 36 kDa (**Fig. 3A**), optimum temperature at 50 °C (**Fig. 3B**), and pH at 6.5 (**Fig. 3C**), and they have acidic *pI* values suggesting a high proportion of negative amino acids (**Fig. 3D**).

FAEs display a common fundamental mechanism having at their active site a catalytic triad consisting of a serine (Ser), a histidine (His) and a carboxylic acid, mainly aspartic acid (Asp) or glutamic acid. In the classical catalytic triad, the protonation states or the net charges of Asp and His residues are very important for maintaining the activity of FAEs (Udatha *et al.*, 2012). In this sense, the FAE-catalyzed reaction is very similar to the hydrolytic action of serine proteases, lipases and other esterases, involving a covalent acyl-enzyme intermediate (Uraji *et al.*, 2018). As we presented in **Fig. 3C**, FAEs are optimally active at pH 6.5, suggesting a clear importance of pH dependence by FAEs, His acts as a general acid-base catalyst, and Asp neutralizes the charge that forms on His during the catalytic process (Udatha *et al.*, 2012).

As described above, each FAE has its own specificity, releasing specific hydroxycinnamic acids such as FA, *p*-coumaric, sinapic or caffeic acids from their esters. Several methods have been developed for FAE activity determination with natural and synthetic substrates (Ramos-de-la-Peña and Contreras-Esquivel, 2016).

Table 2. Biochemical properties and kinetic values of microbial FAEs.

Microorganism	Enzyme	MW (kDa)	pI	pH opt	T opt (°C)	T sta (°C)	K _m (mM)	k _{cat} (s ⁻¹)	k _{cat} /K _m (s ⁻¹ mM ⁻¹)	Substrate	Reference
<i>Actinomyces</i> sp.	ActOFaeI	32	–	6.5	30	40	2.79	278.18	99.61	MCA	(Hunt <i>et al.</i> , 2016)
<i>Aspergillus awamori</i>	AwFaeA	35	4.2	5.5	55	50	1.38	–	–	MFA	(Fazary <i>et al.</i> , 2010)
<i>Aspergillus clavatus</i>	AcFae	28.4	–	7.0	30	–	–	–	–	–	(Damásio <i>et al.</i> , 2013)
<i>Aspergillus flavus</i>	AfFaeA	40	–	6.0	58	–	0.44 0.31 0.26	2.21 0.27 0.90	5.02 0.88 3.47	MFA MpCA MSA MCA	(Zhang <i>et al.</i> , 2013)
<i>Aspergillus nidulans</i>	AN1772.2	130	4.6	7.0	45	45	0.248 0.659	– –	– –	MFA MpCA	(Shin and Chen, 2007)
<i>Aspergillus niger</i>	Fae-I	63	3.0	–	–	–	1.21 0.15	– –	– –	MFA MpCA	(Faulds and Williamson, 1993; Wong, 2006)
	Fae-II	29	3.6	–	–	–	1.11 0.47	– –	– –	MFA MpCA	(Faulds and Williamson, 1993)
	AnFaeA	36-31	3.3	5.0	55-60	–	2.08 1.44	70.74 84.95	91.0 3.53	MFA MSA	(Faulds and Williamson, 1994); (Wu <i>et al.</i> , 2017)
	AnFaeB	75	4.9	6.0	50	50	–	–	–	–	(de Vries <i>et al.</i> , 2002); (Levasseur <i>et al.</i> , 2004)
	AnFaeC	30	4.8	7.0	50	45	–	–	–	–	(Dilokpimol <i>et al.</i> , 2017)
<i>Aspergillus oryzae</i>	AoFaeA	37	4.9	5.0	50	50	0.81	–	–	MFA	(Zeng <i>et al.</i> , 2014)
	AoFaeB	61	–	6.0	55	55	0.14 0.022 0.104	– – –	– – –	MFA MpCA MCA	(Koseki <i>et al.</i> , 2009)
	AoFaeC	75	–	6.0	55	60	0.10 0.058 0.091	– – –	– – –	MFA MpCA MCA	(Koseki <i>et al.</i> , 2009)
<i>Aspergillus terreus</i>	AtFaeA	35	–	5.0	50	–	0.61 0.38 0.29 ND	2.59 0.31 4.68 ND	4.25 0.81 16.14 ND	MFA MpCA MSA MCA	(Zhang <i>et al.</i> , 2015)
	AtFaeD	43	4.34	7.0	50	37	–	–	–	–	(de Vries <i>et al.</i> , 1997)
	AtFAE-1	76	–	5.0	50	55	0.08	1.32	16.58	MpCA	(de Vries <i>et al.</i> , 1997)
	AtFAE-2	23	–	5.0	40	55	0.07	1.27	18.14	MpCA	(de Vries <i>et al.</i> , 1997)
	AtFAE-3	36	–	5.0	40	55	0.07	1.32	18.89	MpCA	(de Vries <i>et al.</i> , 1997)

Table 2. (continued)											
<i>Aspergillus tubingensis</i>	AtFaeA	36	3.3	5.0	60	–	–	–	–	–	(de Vries <i>et al.</i> , 1997)
<i>Aspergillus usamii</i>	AuFaeA	36	4.3	5.0	45	45	4.64	–	–	MFA	(Gong <i>et al.</i> , 2013)
<i>Aureobasidium pullulans</i>	ApFae	210	6.5	6.7	60	60	0.050	15.3	304.78	MFA	(Rumbold <i>et al.</i> , 2003)
							0.010	31.1	2,933.96	MpCA	
							0.137	23.7	172.99	MSA	
							0.098	30.0	306.12	MCA	
<i>Auricularia auricula-judae</i>	EstBC	36	3.2	6.5	61-66	–	0.04	1.4	38	MFA	(Haase-Aschoff <i>et al.</i> , 2013)
<i>Butyrivibrio proteoclasticus</i>	Est1E	31.6 ¹	–	–	–	–	0.19	23.0	121.05	pNA	(Goldstone <i>et al.</i> , 2010)
							0.24	24.0	100.0	pNB	
<i>Cellvibrio japonicus</i>	CjFae1B	61	–	6.5	35-40	40	–	–	–	–	(McClendon <i>et al.</i> , 2011)
<i>Cellulosilyticum ruminicola</i> H1	FaeI	58	5.59	6.0-7.0	40	50	4.78	8.46	1.77	MFA	(Li <i>et al.</i> , 2011)
							2.50	2.34	0.94	MCA	
	13.76	7.78	0.57	MpCA							
	FaeII	31.5	6.02	8.0	35	45	0.36	645.9	1,794.2	MFA	
							0.16	232.7	1,454.4	MCA	
	FaeIII	42	4.98	9.0	40	50	0.51	310.5	608.8	MpCA	
							0.03	2,130.9	71.029	MFA	
							1.06	330.9	312.1	MCA	
							1.26	538.6	427.4	MpCA	
							0.98	–	–	MFA	
<i>Chaetomium sp.</i> CQ31	Fae	29.6	–	7.5	60	50	–	–	–	–	(Yang <i>et al.</i> , 2013)
<i>Chrysosporium lucknowense</i>	Fae1	29	5.5	6.5	45	–	–	–	–	–	(Kühnel <i>et al.</i> , 2012)
	Fae2	36	5.2	7.5	40	–	–	–	–	–	
	FaeB2	33	6.0	8.0	65	–	–	–	–	–	
<i>Clostridium thermocellum</i>	XynZ	45	5.8	6.0	60	70	5.0	–	–	FAXXX	(Blum <i>et al.</i> , 2000)
<i>Erwinia chrysanthemi</i>	FaeD	35	–	7.5	–	–	–	–	–	–	(Hassan and Hugouvieux-Cotte-Pattat, 2011)
	FaeT	35	–	7.5	–	–	–	–	–	–	
<i>Fusarium oxysporum</i>	FoFaeA/FaeII	27	9.9	7.0	45	45	0.58	0.65	1.13	MFA	(Topakas <i>et al.</i> , 2003)
							0.68	0.21	0.31	MpCA	
							0.29	1.94	6.70	MSA	
							0.81	0.13	0.16	MCA	
	FoFaeB/FaeI	31	9.5	7.0	55	30	0.60	6.85	11.41	MFA	
							0.20	19.88	99.44	MpCA	
							1.12	0.46	0.416	MSA	
						0.26	5.91	22.75	MCA		

Table 2. (continued)											
<i>Fusarium proliferatum</i>	FpFae	31	–	6.5–7.5	50	50	0.146	–	–	MFA	(Shin and Chen, 2006)
							0.263	–	–	MpCA	
							0.196	–	–	MCA	
<i>Lactarius hatsudake</i>	LhFae	55	–	4.0	30	–	0.54	–	–	MFA	(Wang <i>et al.</i> , 2016)
<i>Lactobacillus acidophilus</i>	FaeLac	29-36	5.6	6.5-7.5	–	–	–	–	–	–	(Xu <i>et al.</i> , 2017)
<i>Lactobacillus amylovorus</i>	FaeLam	29	–	8.0	45-50	50	–	–	–	–	(Xu <i>et al.</i> , 2017)
<i>Lactobacillus farciminis</i>	FaeLfa	29	–	7.0	45-50	50	–	–	–	–	(Xu <i>et al.</i> , 2017)
<i>Lactobacillus fermentum</i>	FaeLfe	29	–	6.5-7.0	37-50	50	–	–	–	–	(Xu <i>et al.</i> , 2017)
<i>Lactobacillus plantarum</i>	Lp_0796	28	–	7.0	–	30	–	–	–	–	(Esteban-Torres <i>et al.</i> , 2013)
<i>Myceliophthora thermophila</i>	MtFaeB	33	3.1	6.0	55-60	50	0.71	3.30	4.64	MFA	(Topakas <i>et al.</i> , 2004)
							0.09	5.47	60.77	MpCA	
							0.21	4.56	21.74	MCA	
	MtFaeC	23	3.5	6.0	55	60	1.64	2.60	1.58	MFA	(Topakas <i>et al.</i> , 2005)
							0.59	0.53	0.90	MpCA	
							0.57	0.40	0.70	MSA	
NcFae-I	35	8.26	6.0	55	–	0.14	0.13	0.95	MCA	(Crepin <i>et al.</i> , 2003a)	
						0.25	5.24	21	MFA		
						0.021	12.19	580	MpCA		
<i>Panus giganteus</i>	PgFae	61	–	4.0	40	40	0.36	–	–	–	(Wang <i>et al.</i> , 2014)
<i>Penicillium expansum</i>	PeFae	65	–	5.6	37	–	2.6	–	–	MFA	(Donaghy and McKay, 2003)
<i>Penicillium piceum</i>	PpFae	56	–	3.0	70	60	–	–	–	–	(Gao <i>et al.</i> , 2016)
<i>Pleurotus eryngii</i>	PeFaeA	67	5.2	5.0	50	40	0.145	0.85	5.85	MFA	(Nieter <i>et al.</i> , 2014)
							0.44	3.41	7.75	FAX	
<i>Pleurotus sapidus</i>	PsEst1	55	5.7	6.0	50	–	1.95	–	11.2	MFA	(Linke <i>et al.</i> , 2013)
<i>Schizophyllum commune</i>	ScFaeD1	63	–	7.5	45	45	0.159	51.0	319.2	MFA	(Nieter <i>et al.</i> , 2016)
							0.151	105.1	696.3	MpCA	
							0.123	38.4	310.6	MCA	
	ScFaeD2	54	–	7.5	45	45	0.146	54.7	372.6	MFA	
							0.137	91.4	666.2	MpCA	
							0.123	34.1	275.1	MCA	
<i>Sorangium cellulosum</i>	ScFae1	35	5.07	7.0	–	45	0.74	8.3	11.21	MFA	(Wu <i>et al.</i> , 2012)
							0.43	9.6	22.32	MSA	
							0.22	8.2	37.27	MFA	
	ScFae2	34	4.67	6.0-8.0	–	55	0.18	6.5	36.11	MSA	

Table 2. (continued)																					
<i>Streptomyces sp.</i>	R18	38	–	7.5	50	45	4.99	–	–	MFA	(Uraji <i>et al.</i> , 2014)										
							4.31	–	–	MpCA											
							3.31	–	–	MCA											
	R43	52	–	7.0	40	40	9.39	–	–	MSA											
							4.41	–	–	MFA											
							3.00	–	–	MpCA											
SoFae	29	7.9	5.5	30	-	2.61	–	–	MCA												
						0.54	–	–	MSA												
						1.86	–	–	MFA												
<i>Streptomyces werraensis</i>	SwFaeD	48	–	7.5	40	45	0.23	1.98	8.73	MFA	(Schulz <i>et al.</i> , 2018)										
							0.12	0.89	7.67	MSA											
<i>Talaromyces stipitatus</i>	TsFaeA	35	3.5	–	–	–	–	–	–	–	(Garcia-Conesa <i>et al.</i> , 2004); (Crepin <i>et al.</i> , 2003b)										
	TsFaeB	35	5.3	–	–	–	–	–	–	–											
	TsFaeC	65	4.6	6.0-7.0	60	–	0.04	9.65	323.0	MFA											
<i>Talaromyces wortmanni</i>	Fae125	40	5.6	–	–	–	–	–	–	–	(Antonopoulou <i>et al.</i> , 2019)										
												Fae7262	43	5.2	–	–	–	–	–	–	
												Fae68	58.8	4.9	–	–	–	–	–	–	–
												Tan410	55	4.7	7.0	35	40	–	–	–	–
² Cotton soil metagenomics	Tvms10	18.6	–	7.0	35	40	–	–	–	–	(Yao <i>et al.</i> , 2013)										
												Tvmz2a	31.2	–	8.0	38	40	–	–	–	–
² Fecal samples of <i>Rusa unicolor</i> and <i>Equus burchelli</i>	RuFae2	29	8.5	7.0	50	50	–	–	–	–	(Wong <i>et al.</i> , 2013)										

¹Dimeric protein. ²Metagenomic analysis. FAXX: *O*-[5-*O*-(transferuloyl)- α -L-arabinofuranosyl]-(1 \rightarrow 3)-*O*- β -D-xylopyranosyl-(1 \rightarrow 4)-D-xylopyranose; FAXXX: *O*- β -D-xylopyranosyl-(1 \rightarrow 4)-*O*-[5-*O*-(trans-feruloyl)- α -L-arabinofuranosyl-(1 \rightarrow 3)]-*O*- β -D-xylopyranosyl-(1 \rightarrow 4)-D-xylopyranose; MCA: methyl caffeate; MFA: methyl ferulate; MpCA: methyl *p*-coumarate; MSA: methyl sinapate; ND, not detected; pNA: *p*-Nitrophenyl acetate; pNB: *p*-Nitrophenyl butyrate; pNF: *p*-Nitrophenyl ferulate; –, not detected or not mentioned.

Numerous model substrates including methyl and ethyl esters of hydroxycinnamates have been evaluated as monoferuloylated 4-nitrophenyl glycosides and natural substrates such as FAX (2-*O*-[5-*O*-(*trans*-feruloyl)- β -L-arabinofuranosyl]-D-xylopyranose) and FAXX (*O*-[5-*O*-(*trans*-feruloyl)- α -L-arabinofuranosyl]-(1 \rightarrow 3)-*O*- β -D-xylopyranosyl-(1 \rightarrow 4)-D-xylopyranose) (Hunt *et al.*, 2017; Topakas *et al.*, 2012a).

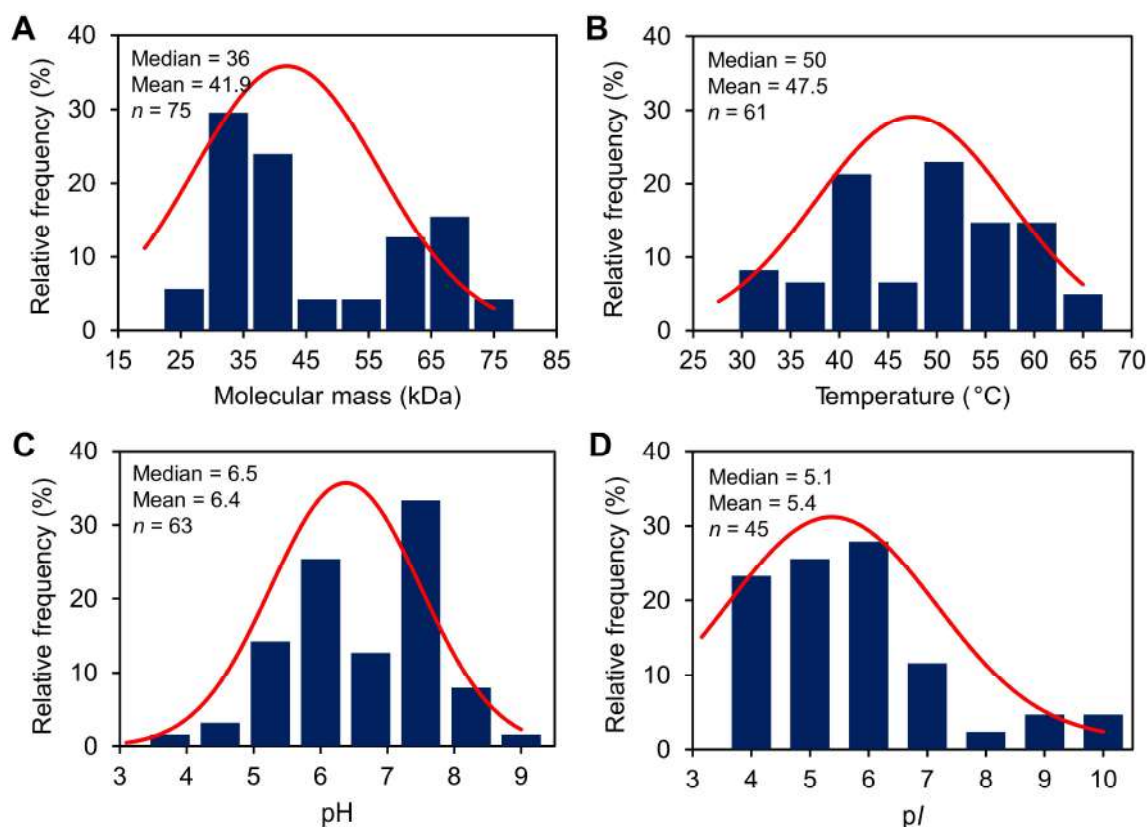


Figure 3. Histogram and normal distribution of biochemical properties of microbial FAEs. Frequencies of molecular masses (kDa for monomers) (A), optimum temperature (B), optimum pH (C), and isoelectric point (D). Outlier values presented in Table 2 were excluded of analysis. *n* is the number of characterized enzymes used for the calculations.

The kinetic values, K_m , k_{cat} and k_{cat}/K_m (Table 2) are affected by structural differences in the substrate, such as: (1) the type of substitutions on the phenolic ring, as hydroxyl or methoxyl groups; (2) the number of substitutions on the phenolic ring; (3) the distance between the ester bond and the phenolic ring; (4) the presence or absence of unsaturation in the aliphatic chain; and (5) the number of sugar residues linked to the phenolic acid (Hunt *et al.*, 2017).

An important proof-of-principle demonstrated that FAEs can hydrolyze nonpolar ferulic acid esters (Schär *et al.*, 2016). A systematic evaluation of the activity of FAEs from different classes (AnFaeA, MtFaeB, CtFae and RoFae) on nonpolar *n*-alkyl ferulates was carried out to evaluate if microbial FAEs are capable of hydrolyzing naturally occurring *n*-alkyl ferulates. A

decrease in K_m and k_{cat} is correlated with decreased substrate polarity for FAEs. This led to the conclusion that for FAEs, nonpolar ferulic acid esters such as long-chain *n*-alkyl ferulates are very poor substrates.

5. Heterologous expression of FAEs by microbial systems and protein engineering

Most well characterized FAEs have been cloned and expressed in heterologous hosts in order to a) make them suitable for industrial applications by increasing their thermal stability, protease resistance, and pH stability; b) understand structure-function relationships; c) delineate the role of particular amino acid residues; d) increase production; and e) purify enzymes in single step with high yield and specific activity (for example, an *E. coli* based expression system is suitable for protein engineering and high-throughput structural analysis) (Zhang *et al.*, 2012; Zhang and Wu, 2011). Previous studies have predominantly focused on AnFaeA isolated from *A. niger*. The enzyme has been cloned and successfully expressed in *E. coli*, *P. pastoris*, and *A. niger* expression systems.

Increasing the repertoire of cloned FAEs, Wu and colleagues performed studies with two FAEs from the myxobacterium *Sorangium cellulosum*, ScFae1 and ScFae2, which were cloned into a pSD80 vector and expressed in *E. coli* as a soluble fraction, followed by three purification steps (DEAE, Butyl-S and Superdex 75 column) (Wu *et al.*, 2012). Wong and coworkers isolated the FAE gene from microflora of a cow's rumen (RuFae2), cloned into *E. coli* and expressed in active form (Wong *et al.*, 2013). The enzyme RuFae2 had the amino acid sequence closely related to the primary structures of bacterial FAEs from *Prevotella oris* C735 (41.9% identity) and *L. johnsonii* (47% identity). The *E. coli* expression system has advantages and disadvantages. An example of the disadvantage using *E. coli* BL21 (DE3) cells, the cDNA of AcFae from *A. clavatus* was cloned into pET28a vector and overexpressed as an insoluble fraction (Damásio *et al.*, 2013). The inclusion bodies containing the protein had to be denatured and purified by affinity chromatography, and after the refolding, the extract was concentrated and the enzyme was purified by gel filtration chromatography, which resulted in a small fraction of purified enzyme showing activity. On the other hand, XynZ from *C. thermocellum* (containing domains corresponding to xylanase and FAE) was well-expressed in *E. coli* BL21 (DE3) as a soluble fraction and purified by two steps — first, immobilized metal ion affinity chromatography, followed by a size exclusion chromatography, which resulted in a high fraction of purified enzyme (Mandelli *et al.*, 2014).

Using a *P. pastoris* GS115 expression system, Yin and coworkers investigated the effects of disulfide bridges on the thermostability of AuFaeA from *A. usarii* introducing an

extra disulfide bridge to, or by eliminating each native disulfide bridge in, the protein sequence (Yin *et al.*, 2015a). The experimental results confirmed that the disulfide bridges contribute significantly to the thermostability of AuFaeA. This same group improved the thermostability of AuFaeA by iterative saturation mutagenesis of Ser33 and Asn92 (Yin *et al.*, 2015b). The study revealed that the best variant Ser33E/Asn92-4 produced a T_m value of 44.5 °C (39.8 °C in WT), the half-life of 198 min at 50 °C, corresponding to a 3.96-fold improvement compared to the wild-type. Further, the best Ser33 variant Ser33-6 was thermostable 32 min longer than wild-type at 50 °C with a half-life of 82 min.

The substrate specificity of FAE involves interaction between the substitutions on the phenolic ring of the hydroxycinnamates with the residues within the active site of FAEs. For AnFaeA, it was shown that the OH and OCH₃ of FA interact with the hydroxyl groups of Tyr80 (Faulds *et al.*, 2005). When the importance of the polar and aromatic residues in the active site of AnFaeA was investigated, it was shown that these residues are involved in binding, as measured by K_m , but also the specificity, as replacement of Tyr80 and Trp260 with smaller residues such as valine or serine resulted in a broadening of the substrate specificity of this esterase. Mutations in the lid/flap region of AwFaeA from *A. awamori*, especially a Tyr to Phe or Ile mutation, changed the hydrophobicity of the region and hence the substrate discrimination of this esterase towards long-acyl chain naphthyl esters, as has been found for lipases, as well as influencing its optimum pH (Koseki *et al.*, 2005). When a Phe to Ile mutation on a corresponding residue was constructed in a *Thermomyces lanuginosa* lipase, the enzyme obtained significant FAE activity, suggesting that the mutant adopted an open conformation to accommodate FA-type substrates into the active site in the aqueous phase (Andersen *et al.*, 2002).

Directed evolution was applied to improve the thermostability of AnFaeA (Zhang *et al.*, 2012) and the dimeric EstF27 from a soil metagenomics library (Cao *et al.*, 2015). Twelve residues in AnFaeA, four being surface exposed and eight being in the inner part of the enzyme, were identified after directed evolution to be beneficial to the thermostability of AnFaeA. After two rounds of directed evolution, the thermostability of the mutated EstF27 at 50 °C was improved over 3000-fold, and a 1.9-fold higher catalytic efficiency and a 2-fold improvement of FA release from wheat bran was obtained as a result of six amino acid substitutions, mainly associated with the dimer interface, leading to the formation of a new disulphide bond and a general increase in hydrophobicity of the protein.

The EstF27 isolated from a soil metagenomics library and overexpressed in *E. coli* displays low thermostability at temperatures higher than 50 °C but was able to release FA

efficiently from wheat bran (Sang *et al.*, 2011). Furthermore, EstF27 had its thermostability improved by two rounds of random mutagenesis (Cao *et al.*, 2015). The mutations promoted an increase in the optimal temperatures to 60 °C (mutant M4) and 65 °C (mutant M6), which correspond to 20 °C and 25 °C higher than that shown by the wild-type. In addition, the storage stability of wild-type and mutant M6 was also assessed. After storage at 25 °C for 150 days, the activity of M6 remained constant (100%), whereas only residual activity remained with the wild-type (21.2%). The kinetic values also increased; the k_{cat}/K_m value of M6 at its optimal temperature of 65 °C is about 1.9-fold higher than that of wild-type. High-throughput screening (HTS) was successfully applied for the generation of 30,000 mutants of MtFae1a from *M. thermophila*, followed with their screening for selecting the variants with higher activity than the wild-type enzyme (Varriale *et al.*, 2018)

6. Three-dimensional structures

Only a few crystal structures of FAEs have been solved to date, which makes our understanding of the residues involved in specific substrate interactions for the different classes of FAEs rather limited. Structural information is important if one decides to improve or change catalytic function for biotechnological applications. The structures of the two FAE modules of *C. thermocellum* XynY and XynZ were the first to be solved (Prates *et al.*, 2001; Schubot *et al.*, 2001), each displaying the canonical eight-strand α/β fold of lipases/esterases. This fold is also called the TIM-barrel and forms the active site cleft at the carboxy-terminal of the sheet. A lid, analogous to lipases, confines the active site cavity with a loop that confers plasticity to the substrate-binding site.

Some FAEs have sequences and structures related to lipases, showing the same serine active-site motif in a α/β -hydrolase fold, which consists of nine β -sheet core surrounded by five α -helices and two additional β -strands indicative of enzymes capable of hydrolyzing synthetic ferulate dehydrodimers (**Fig. 4A-C**). Many FAE models have been constructed based around sequence identity to lipases where crystal structure was unavailable. It is believed that a functional shift following a duplication event was responsible for the neofunctionalization of fungal FAEs from ancestral lipases (Levasseur *et al.*, 2006; McAuley *et al.*, 2004). On the other hand, unlike FAEs, lipases show two conformational states with an opened or closed active site, while FAEs have only the first configuration. **Fig. 4** shows the closed conformation in the structures of AnFaeA from *A. niger* with a lipase from *T. lanuginosa* in its open conformation linked with the respective substrates in the catalytic cleft (**Fig. 4D-F**). Lipases are lipolytic carboxyl ester hydrolases with the ability to hydrolyze water-insoluble esters, releasing long-

chain fatty acids, whereas esterases act on water-soluble esters bearing short-chain acyl residues (Romano *et al.*, 2015).

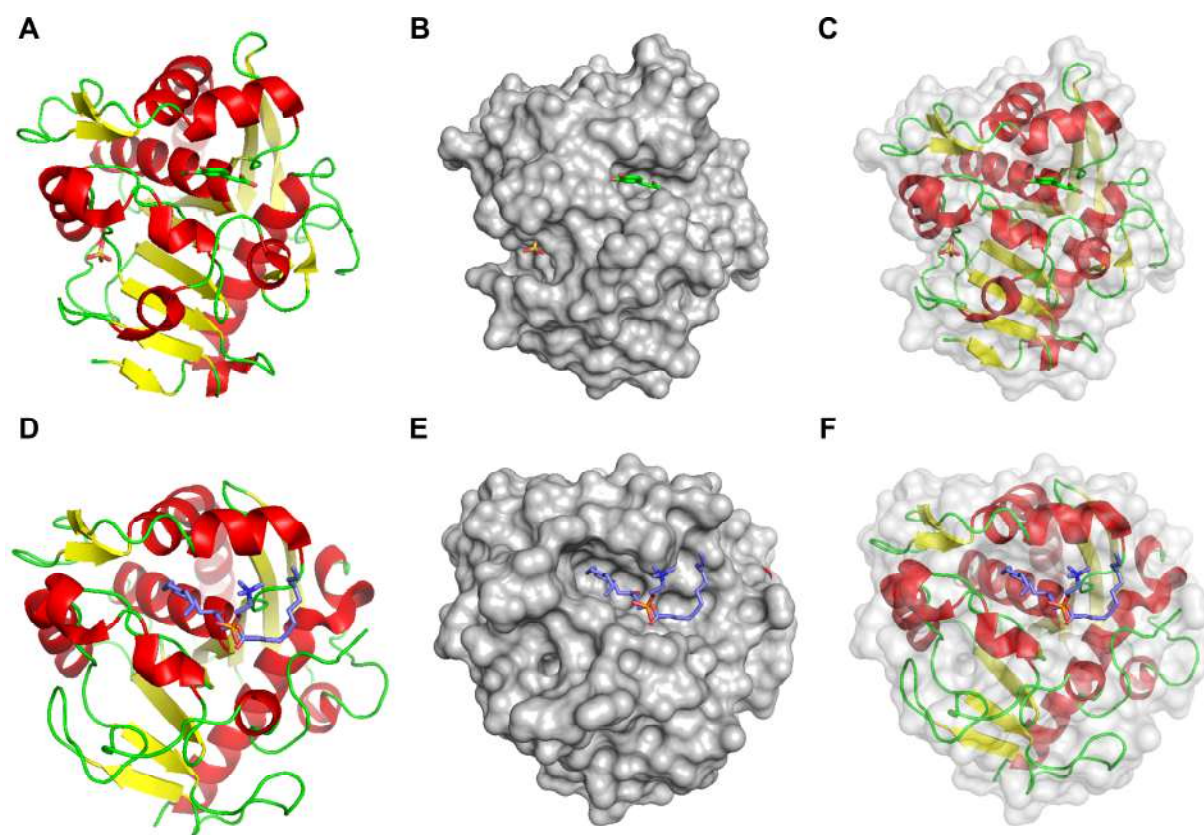


Figure 4. Crystallographic structures of AnFaeA from *Aspergillus niger* (PDB entry 1UZA) (A to C) and a lipase from *Thermomyces lanuginosa* (PDB entry 1EIN) (D to E). The catalytic cleft with the substrate from both AnFaeA and lipase, which is in the open configuration (B and E). Cleft depth from AnFaeA and lipase (C and F).

The classical catalytic triad at the core of the active sites of these two esterases and that of AnFaeA (Fig. 4) were identified in the hydrophobic binding pocket (Hermoso *et al.*, 2004; McAuley *et al.*, 2004; Uraji *et al.*, 2018). In addition, biochemical studies displayed the importance of the position of the ester-linkage and the length and composition of the sugar-sugar moieties esterified to FA in the catalytic performance of AnFaeA (Faulds *et al.*, 2005). To date, the carbohydrate part of the FA-arabinoxyloligosaccharides used in co-crystallization studies has never been visualized. This lack of visualization of the carbohydrates in the crystal structures suggests a loose interaction between the enzyme binding residues and the carbohydrate, perhaps reflecting the heterogeneity of the arabinoxylan polymers and a more specific, tight binding to the phenolic ring. Structural models of the MtFae1 were constructed, and this esterase resembled a lipase-type structure with a small cap-like domain over the active site, which is postulated to influence substrate specificity (Topakas *et al.*, 2012b). While MtFae1 resembles lipases, the structure of *A. oryzae* AoFaeB indicated that this esterase exists

as a dimer, contains a novel CS-D-HC motif at the catalytic site, and is more closely related to tannases than lipases (**Fig. 4**). Presenting a unique lid structure, such proteins display no significant structural similarities to any protein in the Protein Data Bank (Suzuki *et al.*, 2014).

The three-dimensional structure of AoFaeB from *A. oryzae* is composed of two regions that are identified as catalytic domains containing the Ser-His-Asp triad (**Fig. 5A dashed circle**) and the lid domain which covers the active site (**Fig. 5 blue region**) (Suzuki *et al.*, 2014). The lid domain contains a calcium ion coordinated by water and five amino acids (Asp272, Asp 275, Ala277, Asp 279 and Ile281), which are far from the active site and involved in lid domain stabilization (**solid circle in Fig. 5A**). The catalytic domain shows α/α -hydrolase fold, and in an interface between these domains and the lid domain, the active center of the AoFaeB, which is covered by the lid forming the substrate pocket of the enzyme (**Fig. 5B and D**).

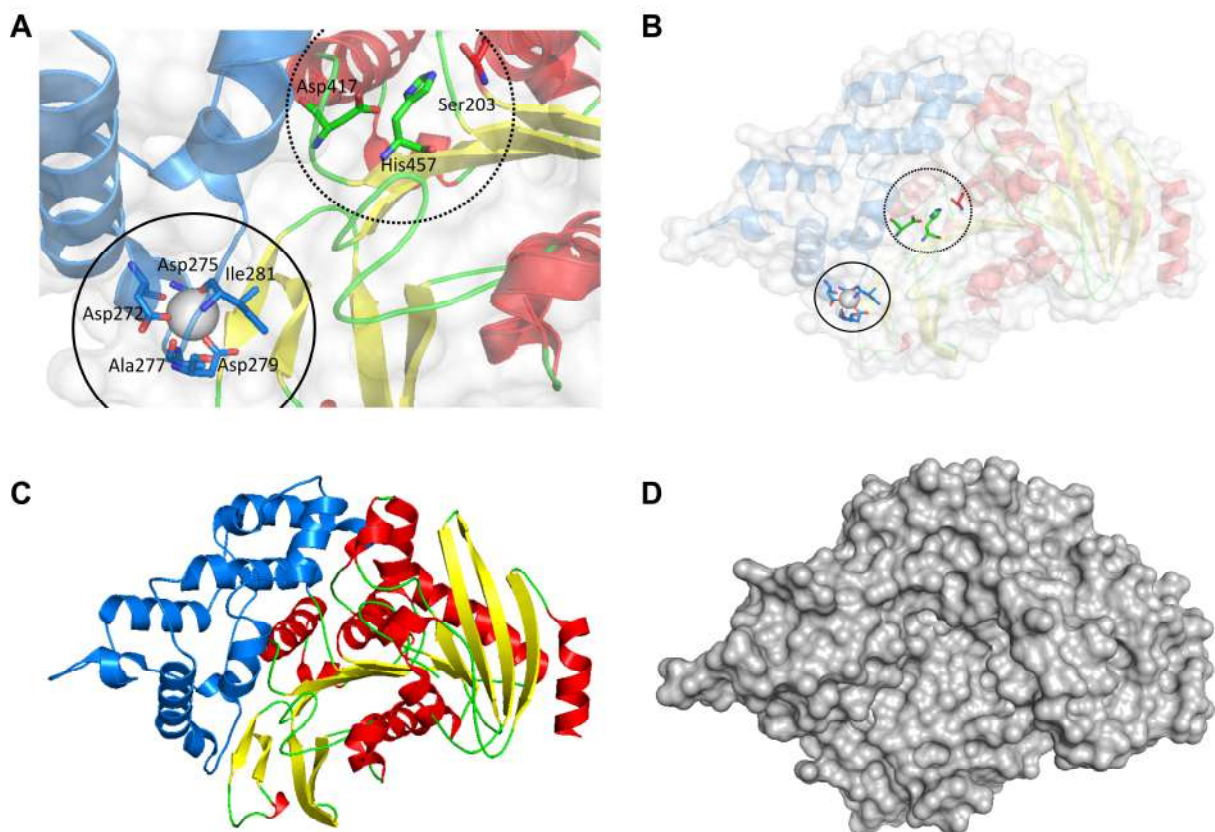


Figure 5. Structure of *Aspergillus oryzae* AoFaeB (PDB entry 3WMT). The active site with Ser203, His457 and Asp417 triad (dashed circle) and the calcium ion at the lid position (solid circle) (A). Monomer of AoFaeB, showing the lid and catalytic cleft position (B), cartoon representation (C) and molecular surface (D).

7. Identification of glycosylation sites

It is desirable that enzymes used in industrial processes resist non-physiological conditions such as extreme pH and temperature. Glycosylation has long been identified as a key point in the thermal stability of glycoproteins, representing a promising target for protein

engineering efforts. Glycosylation is a post-translational modification with biological functions in recognition, signaling and thermostability of enzymes. Secreted enzymes are often covalently *N*-linked and *O*-linked to glycosides at specific sites. *N*-glycosylation generally attaches a branched mannose or a single *N*-acetylglucosamine residue to the β -amide group of an asparagine residue, while *O*-glycosylation attaches the carbohydrate (generally one to three mannose residues) to the β -hydroxyl group of a serine or threonine residue (Zhang *et al.*, 2015).

In an investigation of the effect of glycosylation on protein mass, interestingly, *P. sapidus* PsEst1 presents a protein band in SDS-PAGE 10 kDa higher than the theoretical molecular mass, which was 59.4 kDa, as shown in **Table 3** (Kelle *et al.*, 2016). The amino acid sequence analysis of PsEst1 reveals four potential *N*-glycosylation sites that after being removed from the purified PsEst1 using endo- β -*N*-acetylglucosaminidase H, the deglycosylated enzyme presents 60 kDa by SDS-PAGE. AtFaeA from *A. terreus* has two potential *N*-glycosylation sites and 53 potential *O*-glycosylation sites, which is more than the 46 and 49 potential *O*-glycosylation sites of *A. flavus* AfFaeA and AnFaeA, respectively (Zhang *et al.*, 2015). SDS-PAGE protein bands of AtFaeA have around 40 and 37 kDa, and the purified protein treated with endo- β -*N*-acetylglucosaminidase H resulted in a major protein band of 35 kDa. The AnFaeA and *A. tubingensis* AtFaeA enzymes are very acidic proteins, showing a *pI* of 3.3 and molecular mass of 28 kDa for both proteins. However, the SDS-PAGE indicates an apparent molecular mass of 36 kDa, due to a high amount of glycosylation in its structure (de Vries *et al.*, 1997; Faulds and Williamson, 1994). The enzyme AnFaeB has 18 *N*-glycosylation sites and the electron-density maps in this region indicated no additional carbohydrate residues attached to the *N*-acetylglucosamine residue (de Vries *et al.*, 1997; McAuley *et al.*, 2004).

The *N*-glycosylation site in AnFaeA coupled with the high ratio of polar residues in this region stabilizes the 'lid' of the esterase in an open configuration, thus conferring an esterase character rather than an interfacial-active lipase activity (Hermoso *et al.*, 2004). This raises the question of the actual importance of glycosylation in the thermal stability of AnFaeA. The thermal stability of four molecular forms of AnFaeA – native, refolded, glycosylated, non-glycosylated – was evaluated, demonstrating that AnFaeA produced in *A. niger* (melting point temperature of 56 °C) is more heat resistant than AnFaeA produced in *E. coli* (melting point temperature of 52 °C) recovered by inclusion bodies and refolded without glycosylation (Benoit *et al.*, 2006a).

The crystallographic structure of AnFaeA in its native form revealed a fungal *N*-glycosylation pattern linked to Asn79. The mature protein NcFae-I of *N. crassa* contains a

molecular mass estimated by SDS-PAGE 6 kDa higher than the calculated molecular mass of 29.2 kDa, the *N*-glycosylation was confirmed by electrospray ionization-mass spectrometry, which revealed a molecular mass of 35.04 kDa (Crepin *et al.*, 2003a). AnFaeB and TsFaeC contain 521 and 530 amino acids and calculated molecular masses of 55.5 kDa and 55.34 kDa, respectively. Nevertheless, the native proteins are glycosylated, yielding proteins with molecular masses of 74 kDa and 65 kDa, respectively. Deglycosylated AnFaeB has a molecular mass of 60 kDa by SDS-PAGE analysis (Crepin *et al.*, 2003b; Garcia-Conesa *et al.*, 2004).

A study describing a novel feruloyl esterase from *A. niger*, AnFaeC, found that unlike AnFaeA and AnFaeB, it did not show a decrease in molecular mass after deglycosylation, maintaining the molecular weight of 30 kDa (Dilokpimol *et al.*, 2017). In contrast, the PpFaeA and PcFae-1 from *P. purpurogenum* and *P. chrysogenum*, respectively, showed slight reduction of molecular mass from 35 to 32 kDa for PpFaeA and from 62 to 60 kDa for PcFae-1 with the deglycosylation treatment (Oleas *et al.*, 2017; Sakamoto *et al.*, 2005). Zhang and coworkers (2013) and Topakas and coworkers (2012b) did not confirm the glycosylation of AfFaeA from *A. flavus* and MtFae1 from *M. thermophila*, but compared it with the theoretical molecular mass and suggested the enzymes may be glycosylated due to the potential N-glycosylation sites found out. This analysis was performed based on the presence of Asn–Xaa–Thr/Ser sequons, which are characterized as an oligosaccharide acceptor and a prerequisite for N-glycosylation. A great extent of glycosylation was observed in the studies of Rumbold *et al.* (2003) and Shin and Chen (2007) of feruloyl esterases AN1772.2 (from *A. nidulans*) and ApFae (from *A. pullulans*), respectively. The AN1772.2 glycosylated contained more than double the molecular mass of deglycosylated enzyme and the ApFae showed about 48% of glycosylation influence on the molecular mass value (**Table 3**).

The *A. oryzae* enzymes, AoFaeB and AoFaeC, have an apparent relative molecular mass of 61 and 75 kDa, respectively, on SDS-PAGE. After *N*-deglycosylation, both proteins had a relative molecular mass of 55 kDa, suggesting that both enzymes are *N*-glycosylated. Thirteen and ten potential *N*-glycosylation recognition sites are present in the AoFaeB and AoFaeC sequences, respectively (Koseki *et al.*, 2009).

Table 3. Comparison in protein glycosylation effects of heterologous expressed FAEs.

Organism	Protein	Expressed host	MW (kDa)		Glycosylation site		Optimum temperature (°C)		Reference
			Glycosylated	Non-glycosylated	O	N	Glycosylated	Non-glycosylated	
<i>Aureobasidium pullulans</i>	ApFae	-	210	110	-	-	60	-	(Rumbold <i>et al.</i> , 2003)
<i>Aspergillus nidulans</i>	AN1772.2	<i>S. cerevisiae</i>	130	56	-	6	45	-	(Shin and Chen, 2007)
<i>Aspergillus flavus</i>	AfFaeA	<i>P. pastoris</i>	40	28.164 [#]	-	2	58	-	(Zhang <i>et al.</i> , 2013)
<i>Aspergillus niger</i>	AnFaeA	<i>A. niger</i> ¹ and <i>E. coli</i> ²	30.246	28.552	-	1	55	50	(Benoit <i>et al.</i> , 2006)
<i>Aspergillus niger</i>	AnFaeB	<i>A. niger</i> CMICC 298302	74	60	-	18	-	-	(de Vries <i>et al.</i> , 2002)
<i>Aspergillus niger</i> N402	AnFaeC	<i>P. pastoris</i>	30	30	-	-	50	-	(Dilokpimol <i>et al.</i> , 2017)
<i>Aspergillus niger</i>	AnFaeD	<i>P. pastoris</i>	43	-	2	7	-	-	(Mäkelä <i>et al.</i> , 2018)
<i>Aspergillus oryzae</i>	AoFaeB	<i>P. pastoris</i>	61	55	-	13	-	-	(Koseki <i>et al.</i> , 2009)
<i>Aspergillus oryzae</i>	AoFaeC	<i>P. pastoris</i>	75	55	-	10	-	-	(Koseki <i>et al.</i> , 2009)
<i>Aspergillus terreus</i>	AtFaeA	<i>P. pastoris</i>	40 and 37	35	53	2	50	-	(Zhang <i>et al.</i> , 2015)
<i>Myceliophthora thermophila</i>	MtFae1	<i>P. pastoris</i>	39	32.303 [#]	-	3	50	-	(Topakas <i>et al.</i> , 2012)
<i>Neurospora crassa</i>	NcFae-I	<i>P. pastoris</i>	35.04	29.286 [#]	-	4	55	-	(Crepin <i>et al.</i> , 2003a)
<i>Penicillium purpurogenum</i>	PpFaeA	<i>P. pastoris</i>	35	32	-	-	48	-	(Oleas <i>et al.</i> , 2017)
<i>Pleurotus sapidus</i>	PsEst1	<i>P. pastoris</i>	70	60	1	3	50	-	(Kelle <i>et al.</i> , 2016)
<i>Talaromyces stipitatus</i>	TsFaeC	<i>P. pastoris</i>	66	55.340 [#]	-	-	60	-	(Crepin <i>et al.</i> , 2004)
<i>Talaromyces wortmannii</i>	Fae68	<i>M. thermophila</i> C1	58.8	-	11	10	-	-	(Antonopoulou <i>et al.</i> , 2018)
	Fae125		40	-	22	0	-	-	
	Fae7262		43	-	23	2	-	-	

¹ Glycosylated. ² Non-glycosylated. [#] Predicted molecular mass. * Tm (melting temperature). -, not detected or not mentioned.

Previously, Koseki and colleagues also reported that *N*-glycosylation is important for the thermostability and protein folding of the AwFaeA from *A. awamori*, similar to the results reported for an FAE of *A. niger* (Koseki *et al.*, 2006). *N*-linked glycosylation motif (Asn79-Tyr-Thr) was found in the sequence of FAEs from Aspergilli enzymes (Benoit *et al.*, 2006a). Understanding the role of *N*-linked oligosaccharides located in the flap region made it possible to clarify the biochemical properties of AwFaeA from *A. awamori* expressed in *P. pastoris*. The analysis of removed *N*-linked glycosylation recognition sites by site-directed mutagenesis demonstrated that Asn79 replaced with Ala79 or Gln79 had lower activity than glycosylated wild-type AwFaeA (Koseki *et al.*, 2006). Both mutant enzymes exhibited a significant decrease in hydrolysis rate and efficient catalysis. The wild type showed a K_m of 0.26 mM and k_{cat}/K_m of $588 \text{ s}^{-1} \text{ mM}^{-1}$, the mutant Ala79 values were K_m 0.66 mM and k_{cat}/K_m $145 \text{ s}^{-1} \text{ mM}^{-1}$, and mutant Gln79 values were K_m 0.28 mM and k_{cat}/K_m $73 \text{ s}^{-1} \text{ mM}^{-1}$. These data suggest that the glycan chains affect substrate discrimination and contribute to the stabilization of the flap in its open conformation in the wild-type Asn79.

8. Releasing FA and FA dehydrodimers from plant cell walls

Monomers and dimers of FA are important structural components of complex plant cell walls. FAEs were applied to release FA and diFA from numerous agro-industrial by-products, as wheat bran, maize bran, maize fiber, brewer's (or barley) spent grain, corn stalk, sugar beet pulp, coastal bermudagrass, oat hulls, sugarcane bagasse, jojoba meal, wheat straw, and elephant grass. The cleavage of a linear xylan backbone yields short feruloylated oligosaccharides (Oliveira *et al.*, 2016). Specific cell wall degrading enzymes such as xylanase are required to solubilize part of the cell wall structure by forming short feruloylated xylooligosaccharides. Then, FAE may act on these feruloylated compounds to release FA. In turn, the removal of FA residues from feruloylated xylooligosaccharides makes them again more accessible for further hydrolysis by xylanase and other degrading enzymes (Long *et al.*, 2018).

Faulds and coworkers were able to release hydroxycinnamic acids from brewers' spent grain by applying a *Humicola insolens* commercial enzyme cocktail containing FAE activity, the reaction releases of 76, 40, 71 and 73% of FA, *p*-coumaric, 5,5'-diFA and 8-*O*-4'-diFA, respectively, in comparison with the total released in alkali (TRA) (Faulds *et al.*, 2004). Benoit *et al.* (2006b) studied the ability of AnFaeA and AnFaeB to release hydroxycinnamic acids, such as FA, *p*-coumaric, and caffeic acids from coffee pulp, maize bran, apple marc and sugar beet pulp. AnFaeB releases 100% and 83% of caffeic acid from coffee pulp and apple

marc, respectively and 73% and 34% of *p*-coumaric acid, respectively, while AnFaeA does not show substantial effects on these biomasses. On the other hand, 40% of FA is released with AnFaeA compared to 8% with AnFaeB from autoclaved maize bran.

Some microbial FAEs release dehydrodimers and, therefore, can potentially break down xylan-lignin crosslinks. *P. fluorescens* PfXylD and AnFaeA, alone or in concert with a xylanase, release 5-5'-diFA and 8-*O*-4'-diFA from barley and wheat cell walls (See Fig. 2). AnFaeA is able to release 5-5'-diFA from brewers' spent grain and wheat bran (Faulds *et al.*, 2006). The type of xylanases used in synergy with FAEs affects the level and form of FA released. Glycoside hydrolase family 11 xylanases (GH11) are more efficient for releasing FA, whereas family 10 xylanases (GH10) are more effective at releasing diFA (Faulds *et al.*, 2006).

FaeLac from *Lactobacillus acidophilus* K1 hydrolyzes brewers' spent grain and releases different amounts of HCA, when compared with TRA: FA (2.1%), *p*-coumaric acid (2.9%), sinapic acid (2.8%), and caffeic acid (3.7%) (Szwajgier *et al.*, 2010). AcFae from *A. clavatus* is able to release FA and *p*-coumaric acid from sugarcane biomass and insoluble wheat arabinoxylan (Damásio *et al.*, 2013). The enzymatic hydrolysis of wheat arabinoxylan releases up to 85% of the alkaline extractable *p*-coumaric acid and 2-fold more FA than TRA, after 15 h of incubation. In turn, AcFae exhibited only 37% and 7% efficiency for releasing FA and *p*-coumaric acid from sugarcane bagasse, respectively. Cao *et al.* (2015) conducted a detailed study using EstF27 from the soil metagenomics library and EstF27 thermostable mutant to hydrolyze wheat bran for 10 h at 40 °C. The EstF27 was able to release 17.7% and the mutant 21.6% of the TRA from wheat bran. At 65 °C, the mutant released 36.8% of TRA FA but the EstF27 was completely denatured after 10 h.

9. Synergism between FAEs and hemicellulases

The maximum bioconversion of lignocellulosic material requires the action of efficient cellulolytic enzymes in synergy with hemicellulases and auxiliary enzymes. The utilization of hemicellulose sugars is essential for the efficient and cost-effective conversion of lignocellulosic biomass to biofuel (Braga *et al.*, 2014; Li *et al.*, 2014).

The degree of synergy or synergism measures the ability of two or more enzymes to cooperate in each other's action upon a substrate (Dyk and Pletschke, 2012). The synergism is also dependent on the properties of the substrate, the specific enzymes and other experimental conditions, such as enzyme loading in the reaction mixture (Jia *et al.*, 2015). FAEs exhibit strong synergistic relationships with endo-hydrolases and debranching enzymes, such as xylanases, arabinanases, galactanases, mannanases, polygalacturonases, and

rhamnogalacturonases (Mandalari *et al.*, 2008; Segato *et al.*, 2014; Xue *et al.*, 2017). FAEs have been employed to improve biomass degradation because they disrupt the lignin-cellulose-hemicellulose network, increasing the accessibility of cellulases and hemicellulases to their respective substrates (Debeire *et al.*, 2012).

FA is efficiently released from a wheat bran preparation by AnFaeA plus xylanase. AnFaeA released 24-fold more FA from wheat bran when xylanase is added in the incubation. AnFaeB released 1% FA from sugar-beet pulp, while the addition of arabinanase and arabinofuranosidase in the reaction mixture improved the release of FA to 12% (Kroon and Williamson, 1996). AnFaeA and AnFaeB are involved in the degradation of pectin and xylan substrates, but they have opposite preferences for these polysaccharides (de Vries *et al.*, 2002). AnFaeB is most active towards sugar-beet pectin, whereas AnFaeA is most active in wheat arabinoxylan, demonstrating a clear substrate specificity of AnFaeB for feruloylated pectin oligosaccharides. The incubation of AnFaeB with arabinofuranosidase and β -galactosidase (both enzymes from *A. niger*) increases the hydrolysis of sugar-beet pectin, though the concomitant incubation of AnFaeA and AnFaeB do not result in an increment in the amount of FA released compared with AnFaeB alone (de Vries *et al.*, 2002).

Topakas and coworkers observed the maximal release of FA (33% of TRA) from wheat bran, applying 0.4 U/g of *M. thermophila* MtFae with 500 U/g xylanase within 1 h of reaction time (Topakas *et al.*, 2004). *E. coli*-expressed *S. cellulosum* ScFae1 and ScFae2 were purified and applied in triticale bran hydrolysis. ScFae2 appeared to be more efficient releasing FA from triticale bran (Wu *et al.*, 2012). The experiments with 0.45 U/ml of ScFae2 incubated with 5.3 U/ml of *T. viride* xylanase demonstrated that 3 h of hydrolysis resulted in a release of 96% of FA from triticale bran. The application of blends of enzymes produced by the fungi *T. reesei* and *A. awamori* efficiently hydrolyzed steam-pretreated sugarcane bagasse (Gottschalk *et al.*, 2010). *A. awamori* produced FAE, which acts synergistically with cellulolytic–xylanolytic enzymes, enhancing the effectiveness of the cellulase and xylanase enzyme blends. Li *et al.* (2011) reported the production of three FAEs from *Cellulosilyticum ruminicola* H1, FaeI, FaeII and FaeIII. The addition of FaeI and FaeII to xylanase from *T. lanuginosus* increased 37% and 27%, respectively, the amount of reducing sugars released from maize cob in 6 h of incubation at 38 °C. Likewise, FaeI elevated cellulase activity by 17%, while FaeII and FaeIII reduced it by 34%. In turn, both cellulase and xylanase enhanced the activities of the three FAEs between 2 to 40%, displaying the highest degree of synergy (1.5) with FaeIII.

The addition of RuFae2 in reaction mixtures of endoxylanase GH10 from *Cellvibrio mixtus* increased 6.7-fold the release of FA from wheat bran and 2.7-fold from wheat-insoluble

arabinoxylan (Wong *et al.*, 2013). Zhang *et al.* (2015) conducted a thorough study using AtFaeA from *A. terreus* with xylanase from *A. niger* to hydrolyze different particle sizes (20, 40, 80, 100 mesh) of corn stalk and corncob for 1 h at 50 °C. The content of reducing sugars produced from corncob is about 2-fold higher than from corn stalk, and the production of them increased along with the particle size of corncob and corn stalk. Recently, our research group evaluated the synergistic effect of AcFae from *A. clavatus* and a commercial xylanase preparation on sugarcane bagasse hydrolysis at 30 °C for 24 h (Oliveira *et al.*, 2016). The treatment resulted in a significant increase in the amount of reducing sugars (1.97-fold) released from sugarcane bagasse, an agricultural residue containing a high concentration of FA. Although the treatment with AcFae plus xylanase released only 7.7% of TRA, the enzymes show a high degree of synergy, 5.1.

Evaluating the simultaneous cooperation of AnFaeA and xylanase GH11 (AnXyn11A) in hydrolyzing wheat bran for the co-production of FA and xylooligosaccharides, Wu and coworkers applied AnFaeA (100 U) and AnXyn11A (0 to 1000 U) simultaneously, and the FA released was greatly enhanced from 16.8% to 70% as the activity of AnXyn11A increased from 0 to 300 U, and xylooligosaccharide yield almost doubled in the optimum level of enzyme addition (Wu *et al.*, 2017). On the other hand, AnFaeC from *A. niger* in synergy with xylanase (*T. lanuginosus*) releases FA and *p*-coumaric acid from wheat arabinoxylan and wheat bran, but did not show cooperative effect with endopolygalacturonase, rhamnogalacturonan hydrolase and rhamnogalacturonan acetyl esterase (Dilokpimol *et al.*, 2017). The proof-of-principle was able to demonstrate the differential effect of sequential or co-incubation treatment with FAE and xylanase to release FA from lignocellulosic substrates. The releasing of FA from wheat arabinoxylan was 11-fold more efficient when the substrate was sequentially pre-treated with xylanase followed with AtFaeD than the enzymes co-incubated together (Mäkelä *et al.*, 2018). Besides, the production of xylooligosaccharides from wheat arabinoxylan was successfully improved by 27% to 30% with the treatment with AtFaeD from *A. terreus* and commercial xylanase.

Several groups are currently working to understand precisely why FAEs and debranching enzymes respond differently towards the feruloylated polysaccharides. This phenomenon indicates that FAE isoenzymes may target different substrates in a complementary manner, contributing to the efficient degradation of diverse plant biomass. Future investigations should therefore center upon more complex enzymatic cocktails, or mixtures of cocktails, that accurately reflect the complexity of plant cell walls.

10. Immobilization and influence of organic co-solvents on the FAE activity

In industry, immobilization is often employed to stabilize enzymes and facilitate their reuse, reducing costs. Immobilized enzymes can be used for the *de novo* synthesis of bioactive compounds and platform chemicals, and in the development of nanomaterials for biomedical applications. The immobilization of FAE has been studied for such applications. Monocomponent FAEs have been immobilized on magnetic Fe₃O₄ nanoparticles, leading to an increase in optimal temperature from 45 °C to 55 °C and temperature stability, retaining 52.4% of its initial activity for the release of FA from insoluble wheat bran after 5 cycles (He *et al.*, 2015). Supermagnetic Fe₃O₄@Au core-shell nanoparticles were used to immobilize a putative FAE, PhEst, with a 2-fold increase in activity compared to the free enzyme (Parracino *et al.*, 2011). It was proposed that such immobilized biocatalysts could be used for therapeutic as well as biosensor applications. Soybean peroxidase immobilized on silica-coated magnetic Fe₃O₄ nanoparticles removes 99% of FA from a reaction mix compared to only 57% obtained with the free peroxidase (Silva *et al.*, 2016). While this system was proposed for environmental remediation of effluents from wine distilleries, olive oil production and pulp and paper mills, phenolic acids cross-linked by peroxidases could also be used to generate new bioactive compounds, with higher potential than monomeric FA as antioxidants.

AnFaeA and feruloyl esterase-containing enzyme cocktails have been successfully immobilized as cross-linked enzyme aggregates (CLEAs) and used in the synthesis of alkyl hydroxycinnamates, compounds with application as antioxidants and inhibitors of LDL-oxidation (Vafiadi *et al.*, 2008a; Vafiadi *et al.*, 2008b). Immobilization of eight FAEs from *M. thermophila* and *T. wortmanni* using CLEA methodology demonstrated that conditions for immobilization have to be carefully designed individually for each enzyme, since the maximum activity and enzyme stability can vary in different FAE preparations (Zerva *et al.*, 2018). Mesoporous materials have been used as enzyme immobilization supports due to their large surface area, allowing high enzyme loading, their high mechanical stability, and the ability to adjust the pore size of the material to the dimensions of the enzyme of interest.

Immobilization of FoFaeC from *F. oxysporum* on a mesoporous silica support was shown to be correlated with the pH, with a one unit shift in the optimal transesterification pH (Thörn *et al.*, 2011; Thörn *et al.*, 2013). Accessibility to the active site of the FAE was influenced by the surface charge distribution around the active site pocket, indicating that the esterase can adopt different orientations within the silica pores, which are pH-dependent (Thörn *et al.*, 2013). Other factors can influence the interaction of FAEs with their proposed substrate, or can alter the specificity of the FAE. The physical adsorption stability of the esterase

can be affected by the hydrophobicity, crystallinity and surface charge of the material it is interacting with, whether it is an immobilization support or the lignocellulosic biomass itself. The adsorption of AnFaeA onto a charged surface was simulated and shown to be regulated by electrostatic forces between the protein and the surface, in a way that such interaction can be weakened or strengthened with buffer ionic strength (Liu *et al.*, 2015). A positively charged surface at low surface charge density and high ionic strength can maximize the control and utilization of an immobilized FAE.

The addition of organic co-solvents can expand the use of FAEs in lignocellulose deconstruction by altering the solubility of substrates or changing the solubility of lignocellulose components. A study by Faulds *et al.* (2011) demonstrated that low concentrations of DMSO (<20% v/v) enhanced and broadened the hydrolytic capacity of FAEs against model compounds, including acetylated compounds, possibly through an active site rearrangement. Ionic liquids (IL) can be used for both hydrolytic and synthetic reactions involving FAEs, but some FAEs have been shown to be more unstable in ILs than others (Zeuner *et al.*, 2011). Stability in ILs was linked to being both anion dependent and enzyme structure dependent, with the more lipase-like FAEs being more stable.

The immobilization of four FAEs, MtFaeA1, MtFaeA2, MtFaeB1, and MtFaeB2 from *M. thermophila*, was studied and optimized via physical adsorption onto various mesoporous silica particles with pore diameters varying from 6.6 nm to 10.9 nm (Hüttner *et al.*, 2017). Using crude enzyme preparations, enrichment of immobilized FAEs was observed in function on pore diameter and protein size. The immobilized enzymes were successfully used for the synthesis of butyl ferulate through transesterification of methyl ferulate with 1-butanol. Although the highest butyl ferulate yields are obtained with the free enzyme, the synthesis-to-hydrolysis ratio was higher when using immobilized enzymes. In addition, over 90% of the initial activity was observed in a reusability experiment after nine reaction cycles, each lasting 24 h. Rinsing with solvent to remove water from the immobilized enzymes further improved their activity. This study demonstrates the suitability of immobilized crude enzyme preparations in the development of biocatalysts for esterification reactions (Hüttner *et al.*, 2017).

The immobilization of a commercially available feruloyl esterase, E-FAERU, on mesoporous silica by physical adsorption results in lower transesterification efficiency, since the hydrolysis reaction is preferred by E-FAERU, regardless of whether it is free or immobilized (Bonzom *et al.*, 2018). This result demonstrates that enzyme immobilization is enzyme-specific and cannot be regarded as reflecting the general behavior of FAEs.

11. Synthesis of esters-products by esterification activity

Feruloyl esters and phenolic ester sugars have important biological functions, as antitumor, antimicrobial, antiviral and anti-inflammatory agents (Paiva *et al.*, 2013). FAEs may catalyze esterification and transesterification in non- or low-aqueous solvents to produce the esterified compounds with novel physicochemical characteristics, expanding their use in a variety of food and pharmaceutical applications (Nieter *et al.*, 2016). Esterification can be used to modify the physical properties of FA and various hydroxycinnamic acids, with widespread industrial potential due to their antioxidant properties. For industrial applications, transesterification reactions are more expensive and complicated than esterification reactions, since FA cannot be directly used as the donor in transesterification reactions. A major obstacle for application of FA in oil-based food processing and other corresponding industries is its low solubility and stability in hydrophobic media, to overcome this limitation, it has been reported that modification of FA through esterification with aliphatic alcohols or transesterification with triacylglycerols (Vafiadi *et al.*, 2008b). Current knowledge of biotechnological approaches for the biosynthesis of ferulate derivatives is summarized in **Fig. 6**.

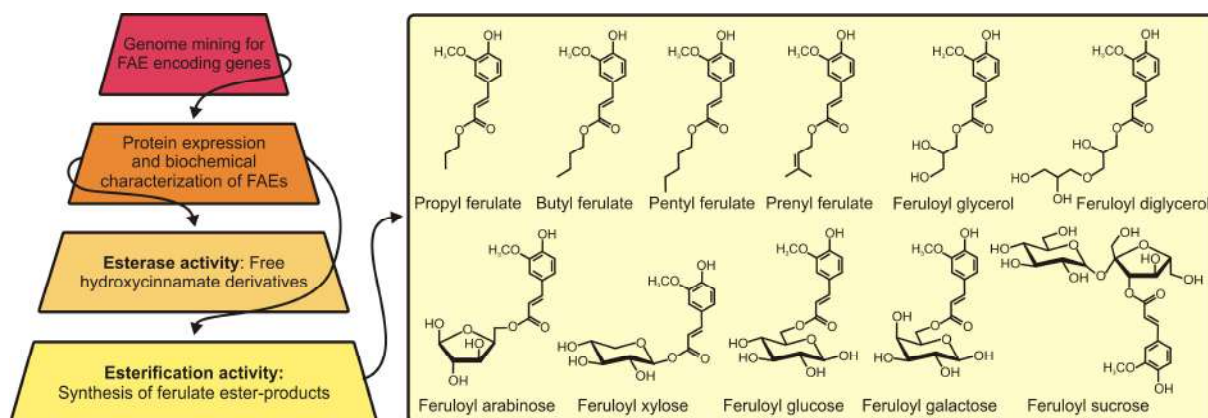


Figure 6. Biotechnological approaches for FAE production and applications affording feruloylated derivatives.

There has been remarkable progress in synthesizing many feruloylated compounds to improve the water solubility of FA by linking it to hydrophilic compounds, such as glycerol and sugars. In turn, the alteration of FA via esterification with aliphatic alcohols results in lipophilic byproducts (Kikugawa *et al.*, 2012; Kikugawa *et al.*, 2016). Feruloyl glycerols (FGs) consist of FA esterified to glycerol, a compound naturally found in plants, which present higher solubility in water than free FA. Natural derivatives of FA, FG present many biological functions as natural UV light filters and antioxidants in the chemical, food, and drug industries (Compton *et al.*, 2012). However, it has been reported that it is difficult to separate FGs from

natural raw materials since the contents of monoferuloyl glycerol (MFG) and diferuloyl glycerol (DFG) are lower than 0.1% (Sun and Chen, 2015). In comparison to chemical methods, enzymatic synthesis of FGs involves high catalytic efficiency in mild reaction conditions, low energy consumption and high enantioselectivity (Compton *et al.*, 2012).

An important proof-of-principle milestone was achieved with the synthesis of feruloylated L-arabinose by MtFaeC from *M. thermophila* (Topakas *et al.*, 2005), which is the first demonstration of enzymatic feruloylation of carbohydrates. In additional studies, FAEs have been used as synthetic tools for the esterification of hydroxycinnamic acids to polyols, mono- and oligosaccharides (Tsuchiyama *et al.*, 2006; Vafiadi *et al.*, 2007; Vafiadi *et al.*, 2006). Commercial enzyme preparations are able to perform transesterifications of FA to various glycoside esters, using FA esters as FA donors (Kelle *et al.*, 2016; Tsuchiyama *et al.*, 2006). AnFaeA is able to synthesize 1-glycerol ferulate in a mixture of 1% FA, 85% glycerol and 5% DMSO at pH 4.0, 50 °C for 30 min (Tsuchiyama *et al.*, 2006). Kikugawa and coworkers synthesized water-soluble FA derivatives by esterification of FA with diglycerol using FAE purified from a commercial enzyme preparation produced by *A. niger* (Kikugawa *et al.*, 2012). The major reaction product was determined to be γ -feruloyl- α,α' -diglycerol by NMR and electrospray ionization mass spectrometry analysis. Feruloyl diglycerol-1 is a sticky liquid whose water solubility (>980 mg/ml) is dramatically higher than that of FA (0.69 mg/ml).

Zeng and coworkers conducted a study using AoFaeA from *A. oryzae* expressed in *P. pastoris* to produce two feruloyl glycerol isomers, with the ester bond occurring at either the internal hydroxyl group of glycerol (2-FG) or at one of the terminal hydroxyl groups (1-FG) (Zeng *et al.*, 2014). The maximum esterification yield reached 60.3% at water content of 20%, the major product being 1-FG and the minor product being 2-FG. Est1 from *P. sapidus* was applied for transferuloylation of different monosaccharides (D-glucose, D-fructose, D-galactose) and disaccharides (D-sucrose, D-lactose, D-maltose) using methyl ferulate as a FA donor (Kelle *et al.*, 2016). Fortunately, there is a new development on this front. During transesterification with glucose, fructose and galactose, related substances were identified via LC-MS as the corresponding feruloylated saccharides. Five FAEs, MtFaeA1, MtFaeA2, MtFaeB1, and MtFaeB2 from *M. thermophila* C1 and MtFae1a from *M. thermophila* ATCC 42464, were tested for their ability to catalyze the transesterification of vinyl ferulate with prenol in detergentless microemulsions forming a novel feruloylated derivative, prenyl ferulate (Antonopoulou *et al.*, 2017). The wild-type and evolved variants of MtFae1a from *M. thermophila* were able to catalyze prenyl ferulate, prenyl caffeate, glyceryl caffeate, glyceryl

ferulate, n-butyl ferulate and 5-O-feruloyl-L-arabinose by transesterification using vinyl ferulate, vinyl caffeate, fatty alcohols and carbohydrates as acyl donors (Varriale *et al.*, 2018).

12. Future perspectives

In the plant cell wall, FA is an essential component cross-linking polysaccharides to lignin, increasing the cell wall's resistance to hydrolysis. FAE employment with accessory enzymes, as xylanases and arabinofuranosidases, improves lignocellulosic biomass conversion to biofuel, helping to achieve the goals set for cost-effective production of alternative and renewable fuels and chemicals. Future investigations should center upon more complex enzymatic cocktails containing FAE, or mixtures of cocktails, that accurately reflect the complexity of plant cell walls. Thereupon, recent concepts for producing FAEs in plants, via the carefully controlled expression of CAZymes in cell walls for the purpose of initiating or even completing digestion, could well hold such promise.

Even though most studies have produced and characterized FAEs, recent developments have highlighted exceptional potential in employing the genome mining strategy to discover novel FAE encoding genes, and heterologous expression and biochemical characterization allows for the unraveling of powerful FAEs with hitherto unknown properties. With the emergence of molecular approaches to selectively alter plant cell wall structure, hydroxycinnamate-derived materials and chemicals are expected to find increasingly extensive applications, opening up new paths for the fine chemical and fuel industries.

13. Conclusion

This review presents a critical assessment comparing various strategies for FAE valorization, highlighting the recent advances in the biochemical properties, biodiversity and biotechnological applications of FAEs. Evaluation of the recent scientific literature shows that FAEs are extensively applied for obtaining FA from agricultural by-products waste and subsequent bioconversion to high added-value aromatic compounds, and as biosynthetic tools to catalyze esterification and transesterification of esters of hydroxycinnamic acids. FA and derivatives released from lignocellulose are employed as pharmaceutical agents, as food chemicals, and in the fine chemical industry.

Acknowledgments

This work was supported by grants from the Conselho Nacional de Desenvolvimento Científico e Tecnológico (CNPq), Coordenação de Aperfeiçoamento de Pessoal de Nível

Superior (CAPES) and Fundação de Amparo à Pesquisa do Estado de São Paulo (FAPESP, contract numbers 2014/18714-2 and 2017/00525-0).

Conflict of interest

The authors have declared that no competing interests exist.

References

- Andersen, A., Svendsen, A., Vind, J., Lassen, S.F., Hjort, C., Borch, K., Patkar, S.A. 2002. Studies on ferulic acid esterase activity in fungal lipases and cutinases. *Colloids Surf. B Biointerfaces*, **26**(1), 47-55.
- Antonopoulou, I., Iancu, L., Jutten, P., Piechot, A., Rova, U., Christakopoulos, P. 2019. Screening of novel feruloyl esterases from *Talaromyces wortmannii* for the development of efficient and sustainable syntheses of feruloyl derivatives. *Enzyme. Microb. Technol.*, **120**, 124-135.
- Antonopoulou, I., Leonov, L., Jutten, P., Cerullo, G., Faraco, V., Papadopoulou, A., Kletsas, D., Ralli, M., Rova, U., Christakopoulos, P. 2017. Optimized synthesis of novel prenyl ferulate performed by feruloyl esterases from *Myceliophthora thermophila* in microemulsions. *Appl. Microbiol. Biotechnol.*, **101**(8), 3213-3226.
- Badary, O.A., Awad, A.S., Sherief, M.A., Hamada, F.M. 2006. In vitro and in vivo effects of ferulic acid on gastrointestinal motility: inhibition of cisplatin-induced delay in gastric emptying in rats. *World J. Gastroenterol.*, **12**(33), 5363-7.
- Benoit, I., Asther, M., Sulzenbacher, G., Record, E., Marmuse, L., Parsiegla, G., Gimbert, I., Asther, M., Bignon, C. 2006a. Respective importance of protein folding and glycosylation in the thermal stability of recombinant feruloyl esterase A. *FEBS Lett.*, **580**(25), 5815-21.
- Benoit, I., Danchin, E.G., Bleichrodt, R.J., de Vries, R.P. 2008. Biotechnological applications and potential of fungal feruloyl esterases based on prevalence, classification and biochemical diversity. *Biotechnol. Lett.*, **30**(3), 387-96.
- Benoit, I., Navarro, D., Marnet, N., Rakotomanomana, N., Lesage-Meessen, L., Sigoillot, J.-C., Asther, M., Asther, M. 2006b. Feruloyl esterases as a tool for the release of phenolic compounds from agro-industrial by-products. *Carbohydr. Res.*, **341**(11), 1820-1827.
- Bento-Silva, A., Patto, M.C.V., Bronze, M.R. 2018. Relevance, structure and analysis of ferulic acid in maize cell walls. *Food Chem.*, **246**, 360-378.
- Blum, D., Kataeva, I., Li, X., Ljungdahl, L. 2000. Feruloyl esterase activity of the *Clostridium thermocellum* cellulosome can be attributed to previously unknown domains of XynY and XynZ. *J. Bacteriol.*, **182**(5), 1346-51.
- Bonzom, C., Schild, L., Gustafsson, H., Olsson, L. 2018. Feruloyl esterase immobilization in mesoporous silica particles and characterization in hydrolysis and transesterification. *BMC Biochem.*, **19**(1), 1.
- Borges, A., Ferreira, C., Saavedra, M.J., Simões, M. 2013. Antibacterial activity and mode of action of ferulic and gallic acids against pathogenic bacteria. *Microb. Drug Resist.*, **19**(4), 256-65.
- Braga, C.M.P., Delabona, P.D.S., Lima, D., Paixão, D.A.A., Pradella, J., Farinas, C.S. 2014. Addition of feruloyl esterase and xylanase produced on-site improves sugarcane bagasse hydrolysis. *Bioresour. Technol.*, **170**, 316-324.
- Cao, L.C., Chen, R., Xie, W., Liu, Y.H. 2015. Enhancing the Thermostability of Feruloyl Esterase EstF27 by Directed Evolution and the Underlying Structural Basis. *J. Agric. Food Chem.*, **63**(37), 8225-33.

- Chandrasekharaiah, M., Thulasi, A., Vijayarani, K., Kumar, D.P., Santosh, S.S., Palanivel, C., Jose, V.L., Sampath, K.T. 2012. Expression and biochemical characterization of two novel feruloyl esterases derived from fecal samples of *Rusa unicolor* and *Equus burchelli*. *Gene*, **500**(1), 134-9.
- Chen, J., Lin, D., Zhang, C., Li, G., Zhang, N., Ruan, L., Yan, Q., Li, J., Yu, X., Xie, X., Pang, C., Cao, L., Pan, J., Xu, Y. 2015. Antidepressant-like effects of ferulic acid: involvement of serotonergic and norepinephrine systems. *Metab. Brain Dis.*, **30**(1), 129-36.
- Compton, D.L., Laszlo, J.A., Evans, K.O. 2012. Antioxidant properties of feruloyl glycerol derivatives. *Ind. Crops Prod.*, **36**(1), 217-221.
- Crepin, V., Faulds, C., Connerton, I. 2003a. A non-modular type B feruloyl esterase from *Neurospora crassa* exhibits concentration-dependent substrate inhibition. *Biochem. J.*, **370**(2), 417-27.
- Crepin, V., Faulds, C., Connerton, I. 2003b. Production and characterization of the *Talaromyces stipitatus* feruloyl esterase FAEC in *Pichia pastoris*: identification of the nucleophilic serine. *Protein Expr. Purif.*, **29**(2), 176-84.
- Crepin, V.F., Faulds, C.B., Connerton, I.F. 2004. Functional classification of the microbial feruloyl esterases. *Appl. Microbiol. Biotechnol.*, **63**(6), 647-52.
- Damásio, A.R.L., Braga, C.M.P., Brenelli, L.B., Citadini, A.P., Mandelli, F., Cota, J., de Almeida, R.F., Salvador, V.H., Paixao, D.A.A., Segato, F., Mercadante, A.Z., Neto, M.O., dos Santos, W.D., Squina, F.M. 2013. Biomass-to-bio-products application of feruloyl esterase from *Aspergillus clavatus*. *Appl. Microbiol. Biotechnol.*, **97**(15), 6759-67.
- de Oliveira, D.M., Finger-Teixeira, A., Mota, T.R., Salvador, V.H., Moreira-Vilar, F.C., Molinari, H.B., Mitchell, R.A., Marchiosi, R., Ferrarese-Filho, O., dos Santos, W.D. 2015. Ferulic acid: a key component in grass lignocellulose recalcitrance to hydrolysis. *Plant Biotechnol. J.*, **13**(9), 1224-1232.
- de Vries, R.P., Michelsen, B., Poulsen, C., Kroon, P., van den Heuvel, R., Faulds, C., Williamson, G., van den Hombergh, J., Visser, J. 1997. The *faeA* genes from *Aspergillus niger* and *Aspergillus tubingensis* encode ferulic acid esterases involved in degradation of complex cell wall polysaccharides. *Appl. Environ. Microbiol.*, **63**(12), 4638-4644.
- de Vries, R.P., vanKuyk, P.A., Kester, H.C.M., Visser, J. 2002. The *Aspergillus niger* *faeB* gene encodes a second feruloyl esterase involved in pectin and xylan degradation and is specifically induced in the presence of aromatic compounds. *Biochem. J.*, **363**, 377-86.
- Debeire, P., Khoune, P., Jeltsch, J.-M., Phalip, V. 2012. Product patterns of a feruloyl esterase from *Aspergillus nidulans* on large feruloyl-arabino-xylo-oligosaccharides from wheat bran. *Bioresour. Technol.*, **119**, 425-428.
- Dilokpimol, A., Mäkelä, M.R., Aguilar-Pontes, M.V., Benoit-Gelber, I., Hilden, K.S., de Vries, R.P. 2016. Diversity of fungal feruloyl esterases: updated phylogenetic classification, properties, and industrial applications. *Biotechnol. Biofuels*, **9**, 231.
- Dilokpimol, A., Mäkelä, M.R., Mansouri, S., Belova, O., Waterstraat, M., Bunzel, M., de Vries, R.P., Hilden, K.S. 2017. Expanding the feruloyl esterase gene family of *Aspergillus niger* by characterization of a feruloyl esterase, *FaeC*. *N. Biotechnol.*, **37**(Pt B), 200-209.

- Dilokpimol, A., Mäkelä, M.R., Varriale, S., Zhou, M., Cerullo, G., Gidijala, L., Hinkka, H., Bras, J.L.A., Jutten, P., Piechot, A., Verhaert, R., Hilden, K.S., Faraco, V., de Vries, R.P. 2018. Fungal feruloyl esterases: Functional validation of genome mining based enzyme discovery including uncharacterized subfamilies. *N. Biotechnol.*, **41**, 9-14.
- Donaghy, J., McKay, A.M. 2003. Purification and characterization of a feruloyl esterase from the fungus *Penicillium expansum*. *J. Appl. Microbiol.*, **83**(6), 718-726.
- dos Santos, W.D., Ferrarese, M.L.L., Ferrarese-Filho, O. 2008. Ferulic acid: an allelochemical troublemaker. *Funct. Plant Sci. Biotechnol.*, **2**, 47-55.
- Dyk, J.S.V., Pletschke, B.I. 2012. A review of lignocellulose bioconversion using enzymatic hydrolysis and synergistic cooperation between enzymes - factors affecting enzymes, conversion and synergy. *Biotechnol. Adv.*, **30**(6), 1458-80.
- Esteban-Torres, M., Reveron, I., Mancheno, J.M., de Las Rivas, B., Munoz, R. 2013. Characterization of a feruloyl esterase from *Lactobacillus plantarum*. *Appl. Environ. Microbiol.*, **79**(17), 5130-6.
- Faulds, C., Williamson, G. 1991. The purification and characterization of 4-hydroxy-3-methoxycinnamic (ferulic) acid esterase from *Streptomyces olivochromogenes*. *J. Gen. Microbiol.*, **137**(10), 2339-45.
- Faulds, C., Williamson, G. 1994. Purification and characterization of a ferulic acid esterase (FAE-III) from *Aspergillus niger*: Specificity for the phenolic moiety and binding to microcrystalline cellulose. *Microbiology*, **140**(4), 779-787.
- Faulds, C.B., Mandalari, G., Lo Curto, R.B., Bisignano, G., Christakopoulos, P., Waldron, K. 2006. Synergy between xylanases from glycoside hydrolase family 10 and family 11 and a feruloyl esterase in the release of phenolic acids from cereal arabinoxylan. *Appl. Microbiol. Biotechnol.*, **71**(5), 622-9.
- Faulds, C.B., Mandalari, G., LoCurto, R., Bisignano, G., Waldron, K.W. 2004. Arabinoxylan and mono- and dimeric ferulic acid release from brewer's grain and wheat bran by feruloyl esterases and glycosyl hydrolases from *Humicola insolens*. *Appl. Microbiol. Biotechnol.*, **64**(5), 644-50.
- Faulds, C.B., Molina, R., Gonzalez, R., Husband, F., Juge, N., Sanz-Aparicio, J., Hermoso, J.A. 2005. Probing the determinants of substrate specificity of a feruloyl esterase, AnFaeA, from *Aspergillus niger*. *FEBS J.*, **272**(17), 4362-71.
- Faulds, C.B., Perez-Boada, M., Martinez, A.T. 2011. Influence of organic co-solvents on the activity and substrate specificity of feruloyl esterases. *Bioresour. Technol.*, **102**(8), 4962-7.
- Faulds, C.B., Williamson, G. 1993. Ferulic acid esterase from *Aspergillus niger*: Purification and partial characterisation of two forms from a commercial source of pectinase. *Biotechnol. Appl. Biochem.*, **17**, 349-359.
- Fazary, A.E., Hamad, H.A., Lee, J.C., Koskei, T., Lee, C.K., Ju, Y.H. 2010. Expression of feruloyl esterase from *Aspergillus awamori* in *Escherichia coli*: Characterization and crystal studies of the recombinant enzyme. *Int. J. Biol. Macromol.*, **46**(4), 440-4.
- Furuya, T., Kuroiwa, M., Kino, K. 2017. Biotechnological production of vanillin using immobilized enzymes. *J. Biotechnol.*, **243**, 25-28.

- Gao, L., Wang, M., Chen, S., Zhang, D. 2016. Biochemical characterization of a novel feruloyl esterase from *Penicillium piceum* and its application in biomass bioconversion. *J. Mol. Catal., B Enzym.*, **133**, S388-S394.
- Garcia-Conesa, M., Crepin, V., Goldson, A., Williamson, G., Cummings, N., Connerton, I., Faulds, C., Kroon, P. 2004. The feruloyl esterase system of *Talaromyces stipitatus*: production of three discrete feruloyl esterases, including a novel enzyme, TsFaeC, with a broad substrate specificity. *J. Biotechnol.*, **108**(3), 227-41.
- Goldstone, D.C., Villas-Boas, S.G., Till, M., Kelly, W.J., Attwood, G.T., Arcus, V.L. 2010. Structural and functional characterization of a promiscuous feruloyl esterase (Est1E) from the rumen bacterium *Butyrivibrio proteoclasticus*. *Proteins*, **78**(6), 1457-69.
- Gong, Y.Y., Yin, X., Zhang, H.M., Wu, M.C., Tang, C.D., Wang, J.Q., Pang, Q.F. 2013. Cloning, expression of a feruloyl esterase from *Aspergillus usamii* E001 and its applicability in generating ferulic acid from wheat bran. *J. Ind. Microbiol. Biotechnol.*, **40**(12), 1433-41.
- Gopalan, N., Rodriguez-Duran, L.V., Saucedo-Castaneda, G., Nampoothiri, K.M. 2015. Review on technological and scientific aspects of feruloyl esterases: A versatile enzyme for biorefining of biomass. *Bioresour. Technol.*, **193**, 534-44.
- Gottschalk, L.M.F., Oliveira, R.A., Bon, E.P.S. 2010. Cellulases, xylanases, β -glucosidase and ferulic acid esterase produced by *Trichoderma* and *Aspergillus* act synergistically in the hydrolysis of sugarcane bagasse. *Biochem. Eng. J.*, **51**(1-2), 72-78.
- Haase-Aschoff, P., Linke, D., Berger, R.G. 2013. Detection of feruloyl- and cinnamoyl esterases from basidiomycetes in the presence of interfering laccase. *Bioresour. Technol.*, **130**, 231-8.
- Hartley, R.D., Haverkamp, J. 1984. Pyrolysis-mass spectrometry of the phenolic constituents of plant cell walls. *J. Sci. Food Agric.*, **35**(1), 14-20.
- Hassan, S., Hugouvieux-Cotte-Pattat, N. 2011. Identification of two feruloyl esterases in *Dickeya dadantii* 3937 and induction of the major feruloyl esterase and of pectate lyases by ferulic acid. *J. Bacteriol.*, **193**(4), 963-70.
- Hatfield, R.D., Ralph, J. 1999. Modelling the feasibility of intramolecular dehydro-diferulate formation in grass walls. *J. Sci. Food Agric.*, **79**, 425-427.
- He, F., Zhang, S., Liu, X. 2015. Immobilization of feruloyl esterases on magnetic nanoparticles and its potential in production of ferulic acid. *J. Biosci. Bioeng.*, **120**(3), 330-4.
- Hermoso, J.A., Sanz-Aparicio, J., Molina, R., Juge, N., Gonzalez, R., Faulds, C.B. 2004. The crystal structure of feruloyl esterase A from *Aspergillus niger* suggests evolutive functional convergence in feruloyl esterase family. *J. Mol. Biol.*, **338**(3), 495-506.
- Hunt, C.J., Antonopoulou, I., Tanksale, A., Rova, U., Christakopoulos, P., Haritos, V.S. 2017. Insights into substrate binding of ferulic acid esterases by arabinose and methyl hydroxycinnamate esters and molecular docking. *Sci. Rep.*, **7**(1), 17315.
- Hunt, C.J., Tanksale, A., Haritos, V.S. 2016. Biochemical characterization of a halotolerant feruloyl esterase from *Actinomyces* spp.: refolding and activity following thermal deactivation. *Appl. Microbiol. Biotechnol.*, **100**(4), 1777-87.

- Hüttner, S., Gomes, M.Z.V., Iancu, L., Palmqvist, A., Olsson, L. 2017. Immobilisation on mesoporous silica and solvent rinsing improve the transesterification abilities of feruloyl esterases from *Myceliophthora thermophila*. *Bioresour. Technol.*, **239**, 57-65.
- Jia, L., Gonçalves, G.A.L., Takasugi, Y., Mori, Y., Noda, S., Tanaka, T., Ichinose, H., Kamiya, N. 2015. Effect of pretreatment methods on the synergism of cellulase and xylanase during the hydrolysis of bagasse. *Bioresour. Technol.*, **185**, 158-164.
- Karlen, S.D., Free, H.C., Padmakshan, D., Smith, B.G., Ralph, J., Harris, P.J. 2018. Commelinid Monocotyledon Lignins are Acylated by *p*-Coumarate. *Plant Physiol.*, **177**, 513-521.
- Kelle, S., Nieter, A., Krings, U., Zelena, K., Linke, D., Berger, R.G. 2016. Heterologous production of a feruloyl esterase from *Pleurotus sapidus* synthesizing feruloyl-saccharide esters. *Biotechnol. Appl. Biochem.*, **63**(6), 852-862.
- Kikugawa, M., Tsuchiyama, M., Kai, K., Sakamoto, T. 2012. Synthesis of highly water-soluble feruloyl diglycerols by esterification of an *Aspergillus niger* feruloyl esterase. *Appl. Microbiol. Biotechnol.*, **95**(3), 615-22.
- Kikugawa, M., Tsutsuki, H., Ida, T., Nakajima, H., Ihara, H., Sakamoto, T. 2016. Water-soluble ferulic acid derivatives improve amyloid- β -induced neuronal cell death and dysmnnesia through inhibition of amyloid- β aggregation. *Biosci. Biotechnol. Biochem.*, **80**(3), 547-553.
- Kim, J.-H., Baik, S.-H. 2015. Properties of recombinant novel cinnamoyl esterase from *Lactobacillus acidophilus* F46 isolated from human intestinal bacterium. *J. Mol. Catal., B Enzym.*, **116**, 9-15.
- Koseki, T., Hori, A., Seki, S., Murayama, T., Shiono, Y. 2009. Characterization of two distinct feruloyl esterases, AoFaeB and AoFaeC, from *Aspergillus oryzae*. *Appl. Microbiol. Biotechnol.*, **83**(4), 689-96.
- Koseki, T., Takahashi, K., Fushinobu, S., Iefuji, H., Iwano, K., Hashizume, K., Matsuzawa, H. 2005. Mutational analysis of a feruloyl esterase from *Aspergillus awamori* involved in substrate discrimination and pH dependence. *Biochim. Biophys. Acta*, **1722**(2), 200-8.
- Koseki, T., Takahashi, K., Handa, T., Yamane, Y., Fushinobu, S., Hashizume, K. 2006. N-linked oligosaccharides of *Aspergillus awamori* feruloyl esterase are important for thermostability and catalysis. *Biosci. Biotechnol. Biochem.*, **70**(10), 2476-80.
- Kühnel, S., Pouvreau, L., Appeldoorn, M.M., Hinz, S.W., Schols, H.A., Gruppen, H. 2012. The ferulic acid esterases of *Chrysosporium lucknowense* C1: purification, characterization and their potential application in biorefinery. *Enzyme Microb. Technol.*, **50**(1), 77-85.
- Levasseur, A., Benoit, I., Asther, M., Asther, M., Record, E. 2004. Homologous expression of the feruloyl esterase B gene from *Aspergillus niger* and characterization of the recombinant enzyme. *Protein Expr. Purif.*, **37**(1), 126-33.
- Levasseur, A., Saloheimo, M., Navarro, D., Andberg, M., Monot, F., Nakari-Setälä, T., Asther, M., Record, E. 2006. Production of a chimeric enzyme tool associating the *Trichoderma reesei* swollenin with the *Aspergillus niger* feruloyl esterase A for release of ferulic acid. *Appl. Microbiol. Biotechnol.*, **73**(4), 872-80.

- Li, J., Cai, S., Luo, Y., Dong, X. 2011. Three feruloyl esterases in *Cellulosilyticum ruminicola* H1 act synergistically to hydrolyze esterified polysaccharides. *Appl. Environ. Microbiol.*, **77**(17), 6141-7.
- Li, J., Zhou, P., Liu, H., Xiong, C., Lin, J., Xiao, W., Gong, Y., Liu, Z. 2014. Synergism of cellulase, xylanase, and pectinase on hydrolyzing sugarcane bagasse resulting from different pretreatment technologies. *Bioresour. Technol.*, **155**, 258-265.
- Linh, T.N., Fujita, H., Sakoda, A. 2017. Release kinetics of esterified p-coumaric acid and ferulic acid from rice straw in mild alkaline solution. *Bioresour. Technol.*, **232**, 192-203.
- Linke, D., Matthes, R., Nimtz, M., Zorn, H., Bunzel, M., Berger, R.G. 2013. An esterase from the basidiomycete *Pleurotus sapidus* hydrolyzes feruloylated saccharides. *Appl. Microbiol. Biotechnol.*, **97**(16), 7241-51.
- Liu, J., Peng, C., Yu, G., Zhou, J. 2015. Molecular simulation study of feruloyl esterase adsorption on charged surfaces: effects of surface charge density and ionic strength. *Langmuir*, **31**(39), 10751-63.
- Lombard, V., Golaconda Ramulu, H., Drula, E., Coutinho, P.M., Henrissat, B. 2014. The carbohydrate-active enzymes database (CAZy) in 2013. *Nucleic Acids Res.*, **42**.
- Long, L., Zhao, H., Ding, D., Xu, M., Ding, S. 2018. Heterologous expression of two *Aspergillus niger* feruloyl esterases in *Trichoderma reesei* for the production of ferulic acid from wheat bran. *Bioprocess Biosyst. Eng.*, **41**(5), 593-601.
- Mäkelä, M.R., Dilokpimol, A., Koskela, S.M., Kuuskeri, J., de Vries, R.P., Hildén, K. 2018. Characterization of a feruloyl esterase from *Aspergillus terreus* facilitates the division of fungal enzymes from Carbohydrate Esterase family 1 of the carbohydrate-active enzymes (CAZy) database. *Microbial Biotechnol.*, **11**(5), 869-880.
- Mandalari, G., Bisignano, G., Lo Curto, R.B., Waldron, K.W., Faulds, C.B. 2008. Production of feruloyl esterases and xylanases by *Talaromyces stipitatus* and *Humicola grisea* var. *thermoidea* on industrial food processing by-products. *Bioresour. Technol.*, **99**(11), 5130-5133.
- Mandelli, F., Brenelli, L.B., Almeida, R.F., Goldbeck, R., Wolf, L.D., Hoffmam, Z.B., Ruller, R., Rocha, G.J.M., Mercadante, A.Z., Squina, F.M. 2014. Simultaneous production of xylooligosaccharides and antioxidant compounds from sugarcane bagasse via enzymatic hydrolysis. *Ind. Crops Prod.*, **52**, 770-775.
- Martinez, D., Berka, R.M., Henrissat, B., Saloheimo, M., Arvas, M., Baker, S.E., Chapman, J., Chertkov, O., Coutinho, P.M., Cullen, D., Danchin, E.G., Grigoriev, I.V., Harris, P., Jackson, M., Kubicek, C.P., Han, C.S., Ho, I., Larrondo, L.F., de Leon, A.L., Magnuson, J.K., Merino, S., Misra, M., Nelson, B., Putnam, N., Robbertse, B., Salamov, A.A., Schmoll, M., Terry, A., Thayer, N., Westerholm-Parvinen, A., Schoch, C.L., Yao, J., Barabote, R., Nelson, M.A., Detter, C., Bruce, D., Kuske, C.R., Xie, G., Richardson, P., Rokhsar, D.S., Lucas, S.M., Rubin, E.M., Dunn-Coleman, N., Ward, M., Brettin, T.S. 2008. Genome sequencing and analysis of the biomass-degrading fungus *Trichoderma reesei* (syn. *Hypocrea jecorina*). *Nat. Biotechnol.*, **26**(5), 553-60.

- Masarin, F., Gurpilhares, D.B., Baffa, D.C.F., Barbosa, M.H.P., Carvalho, W., Ferraz, A., Milagres, A.M.F. 2011. Chemical composition and enzymatic digestibility of sugarcane clones selected for varied lignin content. *Biotechnol. Biofuels*, **4**(1), 55.
- Mattila, P., Hellström, J., 2007. Phenolic acids in potatoes, vegetables, and some of their products. *J. Food Compost. Anal.*, **20**(3-4), 152-160.
- McAuley, K., Svendsen, A., Patkar, S., Wilson, K. 2004. Structure of a feruloyl esterase from *Aspergillus niger*. *Acta Crystallogr. D Biol. Crystallogr.*, **D60**, 878-87.
- McCann, M.C., Carpita, N.C. 2015. Biomass recalcitrance: a multi-scale, multi-factor, and conversion-specific property. *J Exp Bot*, **66**(14), 4109-18.
- McClendon, S.D., Shin, H.D., Chen, R.R. 2011. Novel bacterial ferulic acid esterase from *Cellvibrio japonicus* and its application in ferulic acid release and xylan hydrolysis. *Biotechnol. Lett.*, **33**(1), 47-54.
- Mota, T.R., Oliveira, D.M., Marchiosi, R., Ferrarese-Filho, O., dos Santos, W.D. 2018. Plant cell wall composition and enzymatic deconstruction. *AIMS Bioeng.*, **5**(1), 63-77.
- Moukoulis, M., Topakas, E., Christakopoulos, P. 2008. Cloning, characterization and functional expression of an alkalitolerant type C feruloyl esterase from *Fusarium oxysporum*. *Appl. Microbiol. Biotechnol.*, **79**(2), 245-254.
- Nankar, R., Prabhakar, P., M, D. 2017. Hybrid drug combination: Combination of ferulic acid and metformin as anti-diabetic therapy. *Phytomedicine*, **37**, 10-13.
- Nieter, A., Haase-Aschoff, P., Linke, D., Nimtz, M., Berger, R.G. 2014. A halotolerant type A feruloyl esterase from *Pleurotus eryngii*. *Fungal Biol.*, **118**(3), 348-57.
- Nieter, A., Kelle, S., Linke, D., Berger, R.G. 2016. Feruloyl esterases from *Schizophyllum commune* to treat food industry side-streams. *Bioresour. Technol.*, **220**, 38-46.
- Oleas, G., Callegari, E., Sepulveda, R., Eyzaguirre, J. 2017. Heterologous expression, purification and characterization of three novel esterases secreted by the lignocellulolytic fungus *Penicillium purpurogenum* when grown on sugar beet pulp. *Carbohydr. Res.*, **443-444**, 42-48.
- Oliveira, D.M., Finger-Teixeira, A., Freitas, D.L., Barreto, G.E., Lima, R.B., Soares, A.R., Ferrarese-Filho, O., Marchiosi, R., dos Santos, W.D. 2017. Phenolic Compounds in Plants: Implications for Bioenergy. in: *Advances of Basic Science for Second Generation Bioethanol from Sugarcane*, (Eds.) M.S. Buckeridge, A.P. de Souza, Springer International Publishing. Cham, pp. 39-52.
- Oliveira, D.M., Salvador, V.H., Mota, T.R., Finger-Teixeira, A., Almeida, R.F., Paixão, D.A.A., de Souza, A.P., Buckeridge, M.S., Marchiosi, R., Ferrarese-Filho, O., Squina, F.M., dos Santos, W.D. 2016. Feruloyl esterase from *Aspergillus clavatus* improves xylan hydrolysis of sugarcane bagasse. *AIMS Bioeng.*, **4**(1), 1-11.
- Paiva, L.B., Goldbeck, R., dos Santos, W.D., Squina, F.M. 2013. Ferulic acid and derivatives: molecules with potential application in the pharmaceutical field. *Braz. J. Pharm. Sci.*, **49**(3), 395-411.
- Parracino, A., Gajula, G.P., di Gennaro, A.K., Neves-Petersen, M.T., Rafaelsen, J., Petersen, S.B. 2011. Towards Nanoscale Biomedical Devices in Medicine: Biofunctional and

- Spectroscopic Characterization of Superparamagnetic Nanoparticles. *J. Fluoresc.*, **21**(2), 663-672.
- Perez-Boada, M., Prieto, A., Prinsen, P., Forquin-Gomez, M.P., del Rio, J.C., Gutierrez, A., Martinez, A.T., Faulds, C.B. 2014. Enzymatic degradation of Elephant grass (*Pennisetum purpureum*) stems: influence of the pith and bark in the total hydrolysis. *Bioresour. Technol.*, **167**, 469-75.
- Ponnusamy, V.K., Nguyen, D.D., Dharmaraja, J., Shobana, S., Banu, J.R., Saratale, R.G., Chang, S.W., Kumar, G. 2019. A review on lignin structure, pretreatments, fermentation reactions and biorefinery potential. *Bioresour. Technol.*, **271**, 462-472.
- Prates, J., Tarbouriech, N., Charnock, S., Fontes, C., Ferreira, L., Davies, G. 2001. The structure of the feruloyl esterase module of xylanase 10B from *Clostridium thermocellum* provides insights into substrate recognition. *Structure*, **9**(12), 1183-90.
- Ramos-de-la-Peña, A.M., Contreras-Esquivel, J.C. 2016. Methods and substrates for feruloyl esterase activity detection, a review. *J. Mol. Catal., B Enzym.*, **130**, 74-87.
- Ren, Z., Zhang, R., Li, Y., Li, Y., Yang, Z., Yang, H. 2017. Ferulic acid exerts neuroprotective effects against cerebral ischemia/reperfusion-induced injury via antioxidant and anti-apoptotic mechanisms in vitro and in vivo. *Int. J. Mol. Med.*, **40**(5), 1444-1456.
- Romano, D., Bonomi, F., de Mattos, M.C., de Sousa Fonseca, T., de Oliveira Mda, C., Molinari, F. 2015. Esterases as stereoselective biocatalysts. *Biotechnol. Adv.*, **33**(5), 547-65.
- Rumbold, K., Biely, P., Mastihubova, M., Gudelj, M., Gubitz, G., Robra, K.H., Prior, B.A. 2003. Purification and Properties of a Feruloyl Esterase Involved in Lignocellulose Degradation by *Aureobasidium pullulans*. *Appl. Environ. Microbiol.*, **69**(9), 5622-5626.
- Saini, P., Gayen, P., Nayak, A., Kumar, D., Mukherjee, N., Pal, B.C., Sinha Babu, S.P. 2012. Effect of ferulic acid from *Hibiscus mutabilis* on filarial parasite *Setaria cervi*: Molecular and biochemical approaches. *Parasitol. Int.*, **61**(4), 520-531.
- Sakamoto, T., Nishimura, S., Kato, T., Sunagawa, Y., Tsuchiyama, M., Kawasaki, H. 2005. Efficient Extraction of Ferulic Acid from Sugar Beet Pulp Using the Culture Supernatant of *Penicillium chrysogenum*. *J. Appl. Glycosci.*, **52**(2), 115-120.
- Sang, S.L., Li, G., Hu, X.P., Liu, Y.H. 2011. Molecular Cloning, Overexpression and Characterization of a Novel Feruloyl Esterase from a Soil Metagenomic Library. *J. Mol. Microbiol. Biotechnol.*, **20**(4), 196-203.
- Schär, A., Sprecher, I., Topakas, E., Faulds, C.B., Nystrom, L. 2016. Hydrolysis of Nonpolar n-Alkyl Ferulates by Feruloyl Esterases. *J. Agric. Food. Chem.*, **64**(45), 8549-8554.
- Schubot, F., Kataeva, I., Blum, D., Shah, A., Ljungdahl, L., Rose, J., Wang, B. 2001. Structural basis for the substrate specificity of the feruloyl esterase domain of the cellulosomal xylanase Z from *Clostridium thermocellum*. *Biochemistry*, **40**(42), 12524-12532.
- Schulz, K., Nieter, A., Scheu, A.K., Copa-Patino, J.L., Thiesing, D., Popper, L., Berger, R.G. 2018. A type D ferulic acid esterase from *Streptomyces werraensis* affects the volume of wheat dough pastries. *Appl. Microbiol. Biotechnol.*, **102**(3), 1269-1279.
- Segato, F., Damasio, A.R.L., de Lucas, R.C., Squina, F.M., Prade, R.A. 2014. Genomics Review of Holocellulose Deconstruction by Aspergilli. *Microbiol. Mol. Biol. Rev.*, **78**(4), 588-613.

- Shi, C., Zhang, X., Sun, Y., Yang, M., Song, K., Zheng, Z., Chen, Y., Liu, X., Jia, Z., Dong, R., Cui, L., Xia, X. 2016. Antimicrobial activity of ferulic acid against *Cronobacter sakazakii* and possible mechanism of action. *Foodborne Pathog. Dis.*, **13**(4).
- Shin, H.-D., Chen, R.R. 2006. Production and characterization of a type B feruloyl esterase from *Fusarium proliferatum* NRRL 26517. *Enzyme Microb. Technol.*, **38**(3-4), 478-485.
- Shin, H.D., Chen, R.R. 2007. A type B feruloyl esterase from *Aspergillus nidulans* with broad pH applicability. *Appl. Microbiol. Biotechnol.*, **73**(6), 1323-30.
- Silva, E.O., Batista, R. 2017. Ferulic Acid and Naturally Occurring Compounds Bearing a Feruloyl Moiety: A Review on Their Structures, Occurrence, and Potential Health Benefits. *Compr. Rev. Food Sci. Food Saf.*, **16**(4), 580-616.
- Silva, M.C., Torres, J.A., Nogueira, F.G.E., Tavares, T.S., Correa, A.D., Oliveira, L.C.A., Ramalho, T.C. 2016. Immobilization of soybean peroxidase on silica-coated magnetic particles: a magnetically recoverable biocatalyst for pollutant removal. *RSC Adv.*, **6**(87), 83856-83863.
- Sompong, W., Cheng, H., Adisakwattana, S. 2017. Ferulic acid prevents methylglyoxal-induced protein glycation, DNA damage, and apoptosis in pancreatic β -cells. *J. Physiol. Biochem.*, **73**(1), 121-131.
- Srinivasan, M., Sudheer, A.R., Menon, V.P. 2007. Ferulic Acid: Therapeutic Potential Through Its Antioxidant Property. *J. Clin. Biochem. Nutr.*, **40**, 92-100.
- Sun, S., Chen, X. 2015. Kinetics of enzymatic synthesis of monoferuloyl glycerol and diferuloyl glycerol by transesterification in [BMIM]PF₆. *Biochem. Eng. J.*, **97**, 25-31.
- Suzuki, K., Hori, A., Kawamoto, K., Thangudu, R., Ishida, T., Igarashi, K., Samejima, M., Yamada, C., Arakawa, T., Wakagi, T., Koseki, T., Fushinobu, S. 2014. Crystal structure of a feruloyl esterase belonging to the tannase family: a disulfide bond near a catalytic triad. *Proteins*, **82**(10), 2857-67.
- Szwajgier, D., Waśko, A., Targoński, Z., Niedźwiadek, M., Bancarzewska, M. 2010. The Use of a Novel Ferulic Acid Esterase from *Lactobacillus acidophilus* K1 for the Release of Phenolic Acids from Brewer's Spent Grain. *J. I. Brewing*, **116**(3), 293-303.
- Terrett, O.M., Dupree, P. 2019. Covalent interactions between lignin and hemicelluloses in plant secondary cell walls. *Curr. Opin. Biotechnol.*, **56**, 97-104.
- Thörn, C., Gustafsson, H., Olsson, L. 2011. Immobilization of feruloyl esterases in mesoporous materials leads to improved transesterification yield. *J. Mol. Catal., B Enzym.*, **72**(1), 57-64.
- Thörn, C., Udatha, D.B.R.K.G., Zhou, H., Christakopoulos, P., Topakas, E., Olsson, L. 2013. Understanding the pH-dependent immobilization efficacy of feruloyl esterase-C on mesoporous silica and its structure–activity changes. *J. Mol. Catal., B Enzym.*, **93**, 65-72.
- Topakas, E., Moukouli, M., Dimarogona, M., Christakopoulos, P. 2012a. Expression, characterization and structural modelling of a feruloyl esterase from the thermophilic fungus *Myceliophthora thermophila*. *Appl. Microbiol. Biotechnol.*, **94**, 399.
- Topakas, E., Moukouli, M., Dimarogona, M., Christakopoulos, P. 2012b. Expression, characterization and structural modelling of a feruloyl esterase from the thermophilic fungus *Myceliophthora thermophila*. *Appl. Microbiol. Biotechnol.*, **94**(2), 399-411.

- Topakas, E., Stamatis, H., Biely, P., Christakopoulos, P. 2004. Purification and characterization of a type B feruloyl esterase (StFAE-A) from the thermophilic fungus *Sporotrichum thermophile*. *Appl. Microbiol. Biotechnol.*, **63**, 686-690.
- Topakas, E., Stamatis, H., Biely, P., Kekos, D., Macris, B.J., Christakopoulos, P. 2003. Purification and characterization of a feruloyl esterase from *Fusarium oxysporum* catalyzing esterification of phenolic acids in ternary water–organic solvent mixtures. *J. Biotechnol.*, **102**(1), 33-44.
- Topakas, E., Vafiadi, C., Stamatis, H., Christakopoulos, P. 2005. *Sporotrichum thermophile* type C feruloyl esterase (StFaeC): purification, characterization, and its use for phenolic acid (sugar) ester synthesis. *Enzyme Microb. Technol.*, **36**(5), 729-736.
- Tsuchiyama, M., Sakamoto, T., Fujita, T., Murata, S., Kawasaki, H. 2006. Esterification of ferulic acid with polyols using a ferulic acid esterase from *Aspergillus niger*. *Biochim. Biophys. Acta, Gen. Subj.*, **1760**(7), 1071-1079.
- Udatha, D.B., Kouskoumvekaki, I., Olsson, L., Panagiotou, G. 2011. The interplay of descriptor-based computational analysis with pharmacophore modeling builds the basis for a novel classification scheme for feruloyl esterases. *Biotechnol. Adv.*, **29**(1), 94-110.
- Udatha, D.B.R.K.G., Mapelli, V., Panagiotou, G., Olsson, L. 2012. Common and Distant Structural Characteristics of Feruloyl Esterase Families from *Aspergillus oryzae*. *PLoS One*, **7**(6), e39473.
- Uraji, M., Arima, J., Inoue, Y., Harazono, K., Hatanaka, T. 2014. Application of Two Newly Identified and Characterized Feruloyl Esterases from *Streptomyces* sp. in the Enzymatic Production of Ferulic Acid from Agricultural Biomass. *PLoS One*, **9**(8), e104584.
- Uraji, M., Tamura, H., Mizohata, E., Arima, J., Wan, K., Ogawa, K., Inoue, T., Hatanaka, T. 2018. Loop of *Streptomyces* Feruloyl Esterase Plays an Important Role in the Enzyme's Catalyzing the Release of Ferulic Acid from Biomass. *Appl. Environ. Microbiol.*, **84**(3).
- Vafiadi, C., Topakas, E., Alderwick, L.J., Besra, G.S., Christakopoulos, P. 2007. Chemoenzymatic synthesis of feruloyl d-arabinose as a potential anti-mycobacterial agent. *Biotechnol. Lett.*, **29**(11), 1771-1774.
- Vafiadi, C., Topakas, E., Alissandratos, A., Faulds, C.B., Christakopoulos, P. 2008a. Enzymatic synthesis of butyl hydroxycinnamates and their inhibitory effects on LDL-oxidation. *J. Biotechnol.*, **133**(4), 497-504.
- Vafiadi, C., Topakas, E., Christakopoulos, P. 2008b. Preparation of multipurpose cross-linked enzyme aggregates and their application to production of alkyl ferulates. *J. Mol. Catal., B Enzym.*, **54**(1), 35-41.
- Vafiadi, C., Topakas, E., Christakopoulos, P. 2006. Regioselective esterase-catalyzed feruloylation of L-arabinobiose. *Carbohydr. Res.*, **341**(12), 1992-1997.
- Varriale, S., Cerullo, G., Antonopoulou, I., Christakopoulos, P., Rova, U., Tron, T., Faure, R., Jutten, P., Piechot, A., Bras, J.L.A., Fontes, C., Faraco, V. 2018. Evolution of the feruloyl esterase MtFae1a from *Myceliophthora thermophila* towards improved catalysts for antioxidants synthesis. *Appl. Microbiol. Biotechnol.*, **102**(12), 5185-5196.

- Waldron , K.W., Ng, A., Parker Mary, L., Adrian, J.P. 1999. Ferulic Acid Dehydrodimers in the Cell Walls of Beta vulgaris and their Possible Role in Texture. *J. Sci. Food Agric.*, **74**(2), 221-228.
- Wang, L., Li, Z., Zhu, M., Meng, L., Wang, H., Ng, T.B. 2016. An acidic feruloyl esterase from the mushroom *Lactarius hatsudake*: A potential animal feed supplement. *Int. J. Biol. Macromol.*, **93**(Pt A), 290-295.
- Wang, L., Ma, Z., Du, F., Wang, H., Ng, T.B. 2014. Feruloyl esterase from the edible mushroom *Panus giganteus*: a potential dietary supplement. *J. Agric. Food Chem.*, **62**(31), 7822-7.
- Wong, D.W. 2006. Feruloyl esterase: a key enzyme in biomass degradation. *Appl. Biochem. Biotechnol.*, **133**(2), 87-112.
- Wong, D.W., Chan, V.J., Liao, H., Zidwick, M.J. 2013. Cloning of a novel feruloyl esterase gene from rumen microbial metagenome and enzyme characterization in synergism with endoxylanases. *J. Ind. Microbiol. Biotechnol.*, **40**(3-4), 287-95.
- Wu, H., Li, H., Xue, Y., Luo, G., Gan, L., Liu, J., Mao, L., Long, M. 2017. High efficiency co-production of ferulic acid and xylooligosaccharides from wheat bran by recombinant xylanase and feruloyl esterase. *Biochem. Eng. J.*, **120**, 41-48.
- Wu, M., Abokitse, K., Grosse, S., Leisch, H., Lau, P.C. 2012. New feruloyl esterases to access phenolic acids from grass biomass. *Appl. Biochem. Biotechnol.*, **168**(1), 129-43.
- Xu, Z., He, H., Zhang, S., Guo, T., Kong, J. 2017. Characterization of Feruloyl Esterases Produced by the Four Lactobacillus Species: *L. amylovorus*, *L. acidophilus*, *L. farciminis* and *L. fermentum*, Isolated from Ensiled Corn Stover. *Front. Microbiol.*, **8**, 941.
- Xue, Y., Wang, X., Chen, X., Hu, J., Gao, M.-T., Li, J. 2017. Effects of different cellulases on the release of phenolic acids from rice straw during saccharification. *Bioresour. Technol.*, **234**, 208-216.
- Yang, S.-Q., Tang, L., Yan, Q.-J., Zhou, P., Xu, H.-B., Jiang, Z.-Q., Zhang, P. 2013. Biochemical characteristics and gene cloning of a novel thermostable feruloyl esterase from *Chaetomium* sp. *J. Mol. Catal., B Enzym.*, **97**, 328-336.
- Yao, J., Chen, Q.L., Shen, A.X., Cao, W., Liu, Y.H. 2013. A novel feruloyl esterase from a soil metagenomic library with tannase activity. *J. Mol. Catal., B Enzym.*, **95**, 55-61.
- Yin, X., Hu, D., Li, J.F., He, Y., Zhu, T.D., Wu, M.C. 2015a. Contribution of Disulfide Bridges to the Thermostability of a Type A Feruloyl Esterase from *Aspergillus usamii*. *PLoS One*, **10**(5), e0126864.
- Yin, X., Li, J.F., Wang, C.J., Hu, D., Wu, Q., Gu, Y., Wu, M.C. 2015b. Improvement in the thermostability of a type A feruloyl esterase, AuFaeA, from *Aspergillus usamii* by iterative saturation mutagenesis. *Appl. Microbiol. Biotechnol.*, **99**(23), 10047-56.
- Zeng, Y., Yin, X., Wu, M.-C., Yu, T., Feng, F., Zhu, T.-D., Pang, Q.-F. 2014. Expression of a novel feruloyl esterase from *Aspergillus oryzae* in *Pichia pastoris* with esterification activity. *J. Mol. Catal., B Enzym.*, **110**, 140-146.
- Zeuner, B., Stahlberg, T., van Buu, O.N., Kunov-Kruse, A.J., Riisager, A., Meyer, A.S. 2011. Dependency of the hydrogen bonding capacity of the solvent anion on the thermal stability of feruloyl esterases in ionic liquid systems. *Green Chem.*, **13**(6), 1550-1557.

- Zhang, S.-B., Pei, X.-Q., Wu, Z.-L. 2012. Multiple amino acid substitutions significantly improve the thermostability of feruloyl esterase A from *Aspergillus niger*. *Bioresour. Technol.*, **117**, 140-147.
- Zhang, S.-B., Wu, Z.-L. 2011. Identification of amino acid residues responsible for increased thermostability of feruloyl esterase A from *Aspergillus niger* using the PoPMuSiC algorithm. *Bioresour. Technol.*, **102**(2), 2093-2096.
- Zhang, S.B., Wang, L., Liu, Y., Zhai, H.C., Cai, J.P., Hu, Y.S. 2015. Expression of feruloyl esterase A from *Aspergillus terreus* and its application in biomass degradation. *Protein Expr. Purif.*, **115**, 153-7.
- Zhang, S.B., Zhai, H.C., Wang, L., Yu, G.H. 2013. Expression, purification and characterization of a feruloyl esterase A from *Aspergillus flavus*. *Protein Expr. Purif.*, **92**(1), 36-40.
- Zhao, Z., Moghadasian, M.H. 2008. Chemistry, natural sources, dietary intake and pharmacokinetic properties of ferulic acid: A review. *Food Chem.*, **109**(4), 691-702.

CHAPTER 4

Feruloyl Esterase Activity and Its Role in Regulating the Feruloylation of Maize Cell Walls

Dyoni M. Oliveira^{1*}, Thatiane R. Mota¹, Fábio V. Salatta¹, Guilherme H. G. de Almeida¹, Vanessa G. A. Olher², Marco A. S. Oliveira¹, Rogério Marchiosi¹, Osvaldo Ferrarese-Filho¹, Wanderley D. dos Santos^{1*}

¹ Department of Biochemistry, State University of Maringá, Maringá, PR, Brazil

² Federal Institute of Paraná, Paranavaí, PR, Brazil

*** Corresponding author**

Dyoni M. Oliveira

Wanderley D. dos Santos

E-mail: dyonioliveira@gmail.com; wdsantos@uem.br

Type of chapter:

Short communication

Journal:

Plant Physiology and Biochemistry

Impact factor:

3.404

Current status:

Submitted, under review

Abstract

Cell walls of grasses have ferulic acid (FA) ester-linked to the arabinosyl substitutions of arabinoxylan (AX). Feruloyl esterases (FAE) are carboxylic acid esterases that release FA from cell walls and synthetic substrates. Despite the importance of FA for cell wall recalcitrance and in response to biotic and abiotic stresses, the physiological function of plant FAEs remains unclear. Here we reported a simple method for the determination of FAE activity (ZmFAE) in maize using the total protein extract and investigated its role in regulating the feruloylation of cell wall. The method includes a single protein extraction and enzymatic reaction with protein concentration as low as 65 μg at 35 °C for 30 min, using methyl ferulate as the substrate. The methodology allowed the determination of the apparent K_m (392.82 μM) and V_{max} (79.15 $\mu\text{kat mg}^{-1}$ protein). We also found that ZmFAE activity was correlated ($r = 0.829$) with the levels of FA in seedling roots, plant roots and leaves of maize. Furthermore, the exposure to osmotic stress resulted in a 50% increase in ZmFAE activity in seedling roots. These data suggest that FAE-catalyzed reaction is important for cell wall feruloylation during plant development and in response to abiotic stress. We conclude proposing a model for the feruloylation and deferuloylation of AX, which explains the role of FAE in regulating the levels of ester-linked FA. Our model might orient further studies investigating the role of plant FAEs and assist strategies for genetic engineering of grasses to obtain plants with reduced biomass recalcitrance.

Keywords: Cell wall; Carbohydrate esterase; Ferulic acid; Liquid chromatography; Methyl ferulate; Osmotic stress.

1. Introduction

Xylan is the main hemicellulose in grass cell walls. The xylan backbone consists of a linear chain of β -(1 \rightarrow 4)-linked D-xylopyranosyl (Xyl p) residues, which is substituted with α -(1 \rightarrow 3) and α -(1 \rightarrow 2)-linked L-arabinofuranosyl (Araf) residues, giving rise to arabinoxylan (AX) (Rennie and Scheller, 2014). Araf residues may be further esterified with ferulic acid (FA) and *p*-coumaric acid (*p*CA). Most of FA acylates AX via ester linkage, although few amounts also occur acylating lignin polymer (Ralph, 2010). Feruloyl residues ester-linked to AX can dimerize by peroxidase-mediated oxidative coupling to form a variety of ferulate dehydrodimers (diFA), cross-linking AX chains or with lignin polymer (Ralph, 2010; de Oliveira et al., 2015; Martínez-Rubio et al., 2020). In addition, cell wall-bound FA performs the key roles in cell metabolism, cessation of cell growth, anchoring lignin to cell wall polysaccharides, restricting the access of plant pathogens, and limiting the extraction of cell wall polymers for the production of biofuels and high-value chemicals (dos Santos et al., 2008b; Buanafina, 2009; Mota et al., 2018). Cell walls of grasses such as maize, sugarcane and rice, contain ester-linked FA at concentrations higher than 2 mg per gram of cell wall (Oliveira et al., 2019). We previously demonstrated that maize seedlings and plants exposed upon salt stress promote the suppression of root growth associated with the reduction in the feruloylation of AX, indicating a regulatory mechanism between feruloylation and deferuloylation processes in response to salinity (Oliveira et al., 2020b).

Feruloyl esterases (FAE; E.C. 3.1.1.73) are ubiquitous enzymes found in bacteria, fungi and plants, with the ability to catalyze the hydrolysis of the ester bonds between FA and *p*CA with Araf residues (Crepin et al., 2004). During the past two decades, more than 80 bacterial and fungal FAEs were identified and characterized, whereas much less is known about FAEs of plant origin (Oliveira et al., 2019). Using computational analysis approaches, Udatha and coworkers (2011) collected and clustered 365 putative FAE-related sequences of fungi, bacteria, and plants. The analysis of the characterized sequences revealed that 54% of FAEs are fungal, 45% of bacterial and only 1% are from plant origin. The majority of studies with FAE in plants are focused on the comprehensive genetic analysis of the functional roles in transgenic plants heterologously expressing FAEs from *Aspergillus*, with very low or absent endogenous FAE activity (Buanafina et al., 2008; Buanafina et al., 2010; Badhan et al., 2014; Reem et al., 2016). Thus, there is clear evidence regarding the importance of FA for plant cell walls, however, the biological roles underlying plant FAEs remain largely unknown.

Some methods are proposed to assay FAE activity from microbial sources. Nevertheless, the current methods to determine FAE activity in plant tissues are time-

consuming and require successive steps for protein extraction and concentration, which may result in protein loss (Sancho et al., 1999; Buanafina et al., 2010; Badhan et al., 2014). Enzyme reactions using high concentrations of substrate (24–50 mM) are also reported, with additional steps for the separation of products from the substrates followed by evaporation, or long reaction times (up to 24 h), which may lead to protein denaturation (Buanafina et al., 2008; Reem et al., 2016). Here we present a prompt protocol for protein extraction, reaction condition and single high-performance liquid chromatography (HPLC) separation system for the determination of FAE activity. We also compare the activity of FAE in different tissues of maize and provide evidence of the physiological function of FAE and its role in the deferuloylation of maize cell walls in response to osmotic stress.

2. Material and methods

2.1. Preparation and purification of methyl ferulate

Methyl ferulate was synthesized using ferulic acid (2.0 g) (Sigma-Aldrich, St. Louis, MO, USA) dissolved in 30 mL of methanol and 3 mL of concentrated H₂SO₄ as described by Borneman et al. (1992). Methyl ferulate was purified by silica gel column chromatography and analyzed by ¹H Nuclear Magnetic Resonance (NMR) spectroscopy. The NMR spectrum was recorded on a 500 MHz high field spectrometer (Bruker Avance) and tetramethylsilane was used as the internal standard. A homogenous suspension of the methyl ferulate was prepared in deuterated chloroform and a 10 ppm scan width was used.

2.2. Plant material

Maize (*Zea mays* L. cv. IPR-164) seeds were sterilized in a 2% sodium hypochlorite solution for 5 min followed by washing for 5 min in deionized water. Sterilized seeds were dark-germinated at 25 °C for three days on two sheets of moistened filter paper (Germitest, CEL 060). After germination, primary roots of seedlings were detached and the proteins were extracted from the fresh tissues for FAE assay.

To investigate the physiological role of FAE during the osmotic stress, 25 seedlings of 3-day-old were dipped into a 10 × 16 cm glass container filled with 200 mL of nutrient solution (pH 6.0) (Dong et al., 2006) supplemented with different concentrations of mannitol (0, 150 and 300 mM). Seedlings were grown for three days at 25 °C under a 12 h photoperiod and a photon flux density of 280 μmol m⁻² s⁻¹. After incubation, primary roots were detached and FAE was extracted from the fresh tissues.

For the experiments with 2-week-old plants, seedlings with 2-day-old were transferred to 500-mL pots with 400 g of vermiculite and grown for two weeks at 25 °C under a photoperiod of 12 h. The plants were watered every two days with 60 mL nutrient solution (full substrate capacity). After cultivation, primary with lateral roots and leaves without sheaths were harvested and used for the determination of FAE activity and the content of cell wall ester-linked FA.

2.3. Protein extraction and ZmFAE activity

Fresh tissues (500 mg) were ground using ice-cooled pestle and crucible with 1.5 mL of extraction buffer containing 100 mM 2-(N-morpholino)ethanesulfonic acid (MES) pH 6.0, 10% glycerol (v/v) and 100 mg polyvinylpolypyrrolidone, for 3 min on ice. The extract was centrifuged at $10,000 \times g$ for 15 min at 4 °C. The supernatant was collected and used as the crude protein extract for FAE assay. Protein concentration was determined by the Bradford method (Bradford, 1976). If the amount of tissue is limited, the entire extraction can be scaled down.

ZmFAE assays were conducted in 800 μ L of 100 mM MES pH 6.0 and 100 μ L of 1 mM methyl ferulate (for a final concentration of 100 μ M) prewarmed at 35 °C for 3 min, followed the addition of 100 μ L of crude protein extract (135 μ g of protein) to initiate the enzymatic reaction at 35 °C for 30 min. The assay was stopped by the incubation at 100 °C for 3 min. Next, the sample was centrifuged at $10,000 \times g$ for 2 min, filtered and analyzed by RP-HPLC to determine the amount of FA produced. Reactions in the absence of methyl ferulate were made to identify endogenous FA in the samples. ZmFAE activity was expressed as pkat mg^{-1} protein.

2.4. HPLC analysis

Samples from ZmFAE assay were filtered through a 0.45 μ m filter, transferred to HPLC sample vial and injected directly for HPLC separation. Quantification of FA and methyl ferulate was carried out on HPLC system (Shimadzu[®], Tokyo, Japan) equipped with LC-10AD pump, CBM-101 Communications Bus Module, a Rheodyne[®] injector, and SPD-10A UV-VIS detector. The compounds were separated at 40 °C on a C18 column (250 mm \times 4.6 mm, 5 μ m; Supelco Discovery[®]) with equivalent pre-column (10 mm \times 4.6 mm). The elution used a gradient system with solvent A (methanol) and solvent B (96/4, water/acetic acid, v/v) in the following programme: initially A 40% and B 60% over 8 min; isocratic run A 80% and B 20% over 16 min; and held isocratically at A 40% and B 60% for a further 6 min. The flow rate was

maintained at 0.8 mL.min⁻¹. The identities and quantities of the separated molecules were confirmed based on the diode array UV signatures at 322 nm, obtained in comparison with respective standards.

2.5. Determination of cell wall ester-linked ferulic acid

The cell wall residue preparation (CWR) preparation and saponification of FA were performed as described by Oliveira et al. (2020a). To release the esterified FA from cell walls, CWR (50 mg) of roots and leaves were suspended with 2.5 mL of 0.5 M NaOH and incubated at 96 °C for 2 h. After centrifugation (2,180 × g for 15 min at 4 °C), the supernatant was acidified to pH 2.0 with 6 M HCl, the phenolics were partitioned twice with anhydrous ethyl ether and dried at 40 °C. The residues after evaporation were dissolved in methanol/4% acetic acid (40/60, v/v) and filtered through a 0.45 µm filter. The separation and quantification of FA was carried out on HPLC system using the same conditions as mentioned above on item 2.4. The content of FA was expressed as µg mg⁻¹ CWR.

2.6. Statistical analysis

Data were expressed as the mean of independent biological replicates ± standard error of the mean (SEM). For 3-day-old seedlings, the biological replicate (*n*) contained 25 seedlings. For 2-week-old plants, the biological replicate contained a bulk with six plants. Analysis of variance (ANOVA) tested the significance of the observed differences using GraphPad Prism version 5.0 (GraphPad Software Inc., USA). The apparent Michaelis-Menten constant (K_m) and maximum reaction velocity (V_{max}) values were calculated by a non-linear least-squares method with GraphPad Prism.

3. Results and discussion

3.1. A standard method for protein extraction, reaction condition, and HPLC separation for FAE activity

We synthesized the methyl ferulate using FA and methanol as reagents. The ¹H-NMR spectrum of methyl ferulate showed the typical chemical shifts for methyl esters (**Fig. S1**), evidencing the identity of methyl ferulate. To determine the activity of FAE in maize (ZmFAE), fresh roots were subjected to protein extraction in 100 mM MES buffer pH 6.0 by single step and assayed with methyl ferulate (the substrate) at 35 °C (**Fig. 1A**). The temperature and pH were chosen for ZmFAE assay based on the biochemical and functional properties of characterized FAEs (Oliveira et al., 2019) and previous standard methods for enzyme assays

from maize tissues (Bevilaqua et al., 2019; Ferro et al., 2020). Previously, we reported that FAE-catalyzed reactions are optimally active between pH 6 to 7, demonstrating the clear pH-dependence for the catalytic process (Oliveira et al., 2019). The HPLC-based analysis showed that FA, produced by ZmFAE reaction, and methyl ferulate present in the reaction medium were eluted at the same retention times of their respective standards: 7.41 min (FA) and 16.05 min (methyl ferulate) (**Fig. 1B**). Moreover, under the chromatographic conditions used here, the calibration curves using the standards of FA and methyl ferulate exhibited high correlation coefficients for linear regressions ($R^2 > 0.995$).

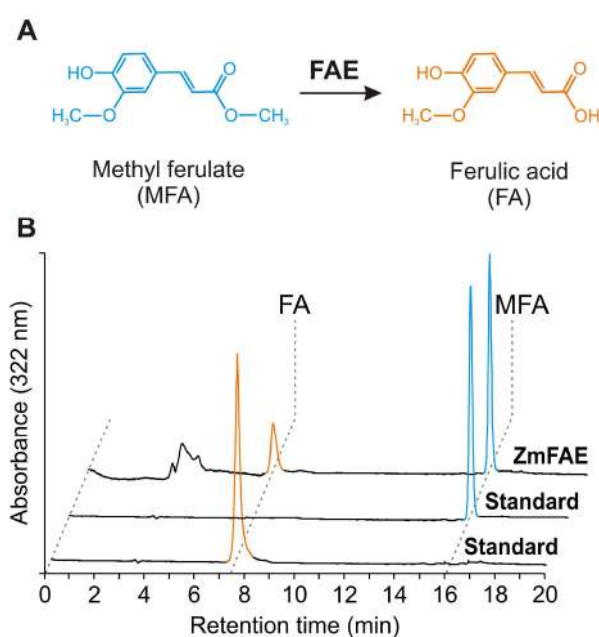


Figure 2. ZmFAE activity. **A**) Hydrolysis of methyl ferulate to ferulic acid by ZmFAE. **B**) HPLC elution profiles at 322 nm of standards of methyl ferulate (16.05 min) and ferulic acid (7.41 min), and ZmFAE activity.

We also investigated the response of ZmFAE in different concentrations of crude protein extract, to determine the optimum concentration of protein for FAE assay. **Fig. 2A** shows the high correlation between protein concentration and FA production ($R^2 = 0.981$), based on this results we used 135 μ g of protein for the subsequent assays. The data also revealed that our method had sensitivity to concentrations as low as 65 μ g of protein (**Fig. 2A**), allowing to detect low amounts of ZmFAE and the potential for incorporating in high-throughput systems for studies of large number of samples (Zhang et al., 2012).

The optimum reaction time is used to achieve the highest reaction rate. Previous studies have suggested reaction times up to 24 h for the detection of FAE activity in transgenic plants (Buanafina et al., 2008; Buanafina et al., 2010; Reem et al., 2016). In contrast, we observed linearity for enzyme reaction up to 30 min (**Fig. 2B**), followed by the tendency to plateau after

30 min, indicating that shorter reaction times may achieve the highest reaction rate for plant FAEs. Therefore, the subsequent enzyme reactions were performed for 30 min.

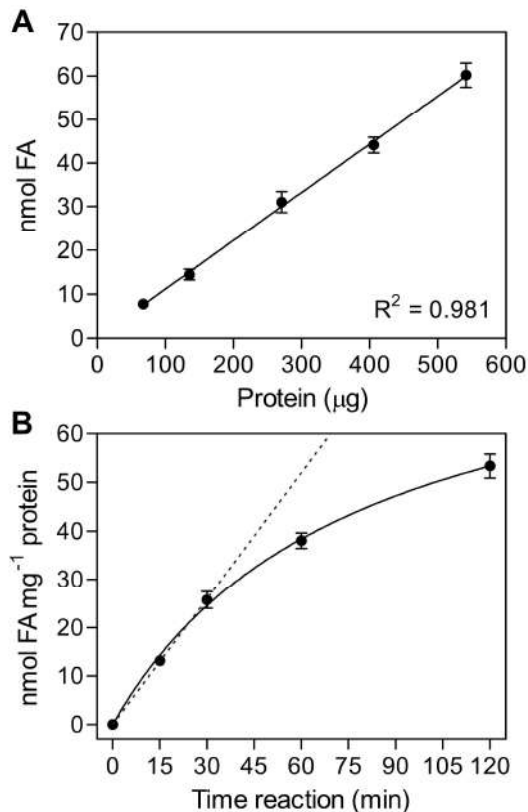


Figure 3. ZmFAE activity at 35 °C as a function of **A)** crude protein extract (for 30 min) and **B)** reaction time (with 135 µg of protein). Dashed line indicates the linearity of reaction time. Error bars indicate \pm SEM, $n = 4$ biological replicates.

We next examined whether endogenous enzymes in the crude protein preparation may consume the FA produced by ZmFAE-catalyzed reaction. Starting with 100 µM FA as the internal standard in the reaction mixture, we recovered by 97% of FA (97.4 µM) at 30 min of reaction, indicating that FA produced by ZmFAE was not significantly consumed by another enzyme present in the preparation. Although there are considerable concerns for using crude protein extract instead of purified proteins, this result indicated that the reaction medium containing a complex protein extract for ZmFAE assay did not interfere with the product formation, allowing accurate quantitation of FAE activity. Potentially, the most powerful application of this approach for FAE assay in plant tissues is its capacity to investigate the action of this esterase on plant cell wall remodeling.

3.2. Potential role of ZmFAE in controlling the feruloylation of arabinoxylan

In order to elucidate the role of ZmFAE in regulating the levels of ester-linked FA in maize cell walls, we systematically investigated the enzyme kinetics, the correlation between ZmFAE activity and FA levels in different tissues, and the changes in the activity of ZmFAE

in seedling roots exposed to osmotic stress. First, we used the method to determine the apparent K_m and maximal reaction velocity (V_{max}) for ZmFAE. The assays were performed with the concentration of methyl ferulate between 10 μM to 5 mM to ensure the substrate saturation. The apparent K_m of ZmFAE was 392.82 μM and the V_{max} was 79.15 pkat mg^{-1} of protein (**Fig. 3A**). Indeed, this apparent K_m of ZmFAE was similar to that estimated K_m of 340 μM of barley grain (*Hordeum vulgare*) using methyl ferulate as substrate (Sancho et al., 1999), and those reported of fungal FAEs, 440 μM of AfFaeA from *Aspergillus flavus* (Zhang et al., 2013) and 360 μM of FaeII from *Cellulosilyticum ruminicola* H1 (Li et al., 2011).

We also assessed whether the ZmFAE activity was correlated with the content of cell wall ester-linked FA in different maize tissues. To test this hypothesis, we determined the FA content in three different maize samples: primary roots of 3-day-old seedlings, plant roots containing primary and lateral roots and leaves of 2-week-old plants. ZmFAE activity and FA level were higher in both roots than in leaves, reflecting a substantial difference amongst the tissues (**Fig. 3B**). Interestingly, the ZmFAE activity in seedling roots, plant roots and leaves showed a high positive correlation with FA levels (Pearson correlation $r = 0.829$, $P < 0.0001$; **Fig. 3B**). The difference in the magnitude on FA level and ZmFAE activity in roots versus leaves may be due to the accumulation of FA in the cell walls of roots. Higher availability of FA in root cell walls may induce higher expression of genes encoding for FAE, which can reflect in higher ZmFAE activity. Whereas the reduced levels of FA in leaves may require a lower gene expression and consequently lower ZmFAE activity. These findings indicate that ZmFAE is required for controlling the levels of ester-linked FA on Ara f residues of AX in different maize tissues. Overexpression of genes encoding for FAE in grass crops might allow obtaining plants with reduced levels of FA and diFA cross-linking adjacent AX strands, which may generate plants with lower cell wall recalcitrance and thereupon higher saccharification. The heterologous expression of AnFaeA from *Aspergillus niger* in *Lolium multiflorum* and tall fescue resulted in reduced levels of cell wall ester-linked FA and diFA and increased biomass digestibility (Buanafina et al., 2006; Buanafina et al., 2008; Buanafina et al., 2017).

To further investigate the physiological function of ZmFAE during osmotic stress, we performed a comparative experiment growing maize seedlings for three days upon osmotic stress (150 and 300 mM mannitol) and then analyzed the ZmFAE activity in control and stressed roots (**Fig. 3C**). The results revealed that exposure to 300 mM mannitol increased by 50% ZmFAE activity in seedling roots, whereas 150 mM mannitol had no significant effect on ZmFAE, compared with control roots. We recently reported that salt stress promotes a broad cell wall remodeling in seedlings and plants of maize, with reduced feruloylation of Ara f

residues linked to AX associated with the accumulation of cytosolic FA by 1.5- to 4.3-fold (Oliveira et al., 2020b). Here, we confirm these previous findings and provide evidence that osmotic stress stimulates the activity of FAE in seedling roots of maize. Furthermore, these findings contribute to an emerging view that grasses possess esterases that are able to regulate the feruloylation of AX triggered by abiotic stress.

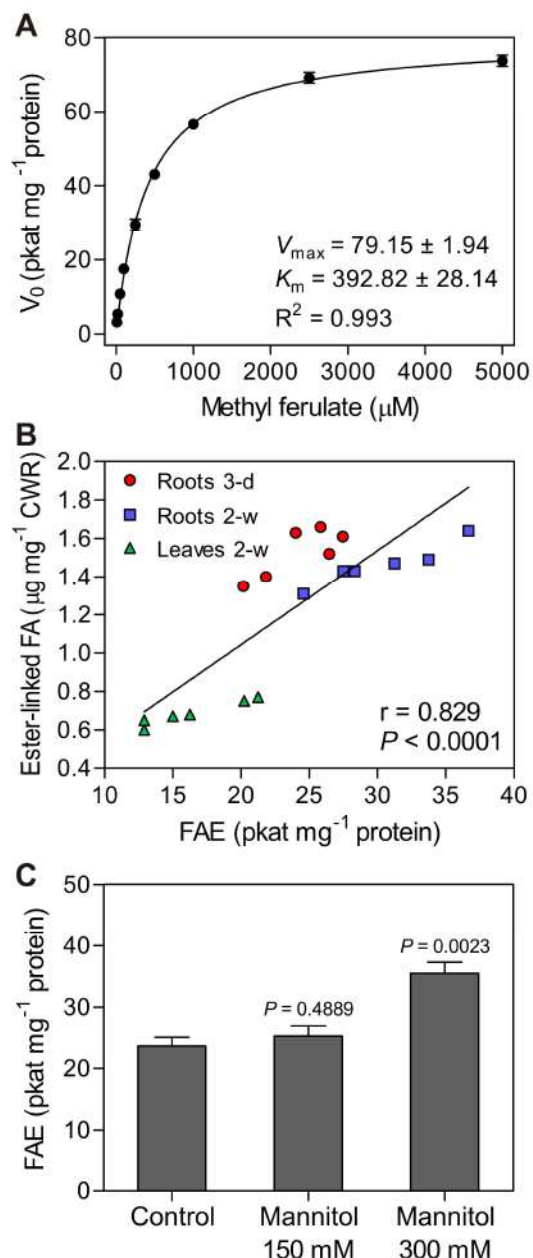


Figure 3. ZmFAE activity in maize. **A)** ZmFAE kinetics using methyl ferulate as substrate. The apparent Michaelis-Menten constant (K_m) and maximum reaction velocity (V_{max}) values were calculated by a non-linear least-squares method. $n = 4$ biological replicates. **B)** Correlation between ZmFAE activity and cell wall ester-linked ferulic acid (FA) measured in seedling roots of 3-day-old, and plant roots and leaves of 2-week-old. $n = 6$ biological replicates. **C)** ZmFAE activity in seedling roots of 3-day-old treated with 150 and 300 mM mannitol. $n = 4$ biological replicates. r , Pearson correlation coefficient. Error bars indicate \pm SEM, $P < 0.05$ is statistically significant according to Dunnett's test.

Despite the significant progress in identifying the molecular mechanism of AX feruloylation, the FAE-catalyzed reaction is not described in the current proposed model for the feruloylation of AX (Buanafina, 2009; de Oliveira et al., 2015; Hatfield et al., 2017). Nevertheless, the findings exposed herein and contextualized with the available data in the literature suggest that this esterase is implicated in regulating the feruloylation of AX in

grasses. **Fig. 4** incorporates our conclusions into a feruloyl-AX turnover model integrated with the biosynthetic pathway for phenylpropanoids and monolignols. Notably, FA biosynthesis may occur via different metabolic pathways. An evident route toward FA is one-step 3-*O*-methylation of caffeic acid by caffeate 3-*O*-methyltransferase (COMT). A second alternative route for FA formation occurs through oxidation of coniferaldehyde by hydroxycinnamaldehyde dehydrogenase (HCALDH) (Nair et al., 2004). A third route toward FA is suggested to occur via the hydrolysis of feruloyl-CoA catalyzed by a thioesterase; even though, this route is likely associated as a consequence to perturbations in lignin biosynthesis (Vanholme et al., 2012).

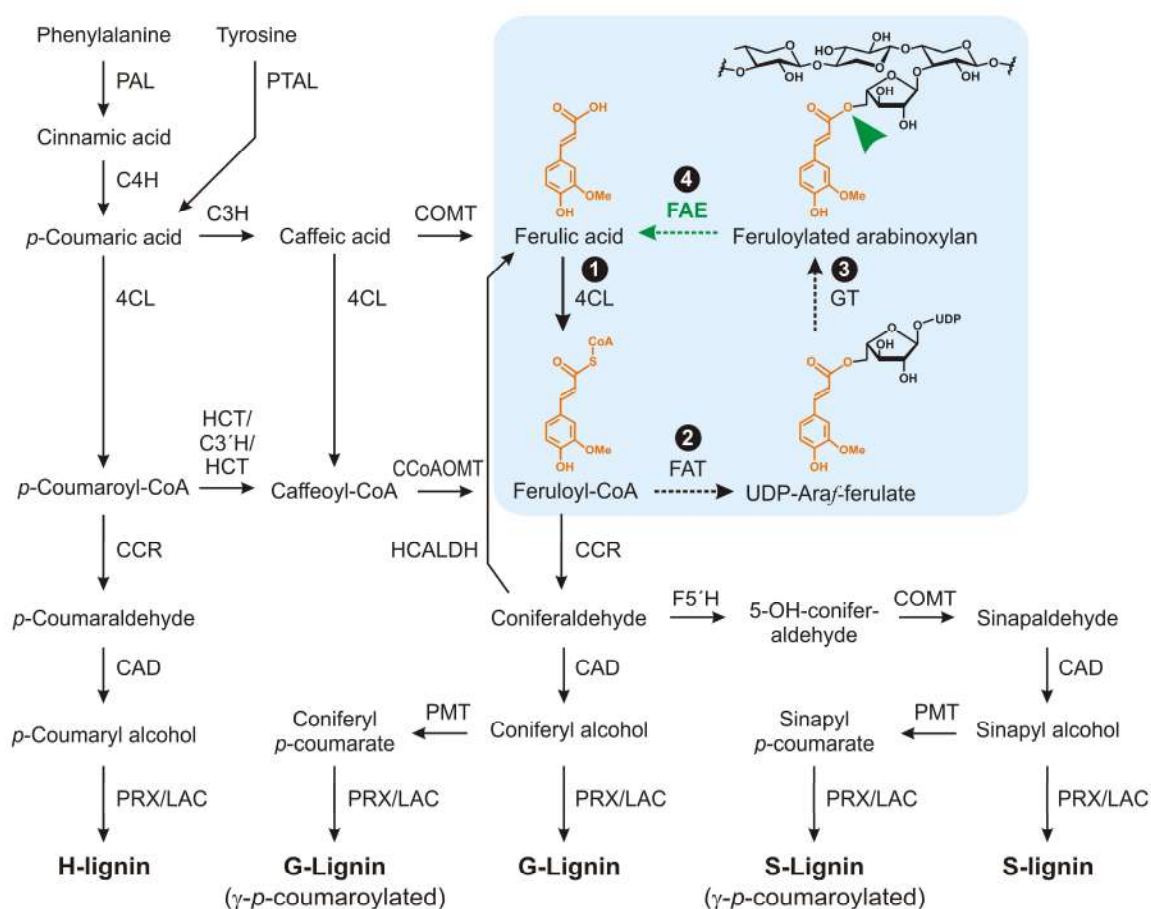


Figure 4. Lignin biosynthetic pathway in grasses and the proposed mechanism for the feruloylation and deferuloylation of arabinoxytan. The site of action and FAE-catalyzed reaction are indicated in green. Numbers in black indicate the steps for feruloylation (1 to 3) and deferuloylation (4) of arabinoxytan. Arrows with dashed lines designate putative routes. PAL, L-phenylalanine ammonia-lyase; PTAL, bifunctional L-phenylalanine/ L-tyrosine ammonia-lyase; C4H, cinnamate 4-hydroxylase; C3H, *p*-coumarate 3-hydroxylase; COMT, caffeate/5-hydroxyferulate 3-*O*-methyltransferase; 4CL, *p*-hydroxycinnamate-CoA ligase; FAT, putative feruloyl-CoA thioesterase; GT, putative glycosyl transferase; FAE, feruloyl esterase; HCT, hydroxycinnamoyl-CoA shikimate/quinat hydroxycinnamoyltransferase; C3'H, *p*-coumaroyl shikimate/quinat 3'-hydroxylase; CCoAOMT, caffeoyl-CoA 3-*O*-methyltransferase; CCR, cinnamoyl-CoA reductase; HCALDH, hydroxycinnamaldehyde dehydrogenase; F5'H, ferulate 5'-hydroxylase/coniferaldehyde 5'-hydroxylase; CAD, cinnamyl alcohol dehydrogenase; PMT, *p*-coumaroyl-CoA monolignol transferase; PRX, peroxidase; LAC, laccase.

The resulting FA is then converted to feruloyl-CoA by *p*-hydroxycinnamate-CoA ligase (4CL) (step 1 in **Fig. 4**). Alternatively, feruloyl-CoA might also be produced via methylation of caffeoyl-CoA by caffeoyl-CoA 3-*O*-methyltransferase (CCoAOMT) (Vanholme et al., 2012). The following mechanism for the transfer of feruloyl-CoA to AX remains unclear. One proposed mechanism is that acyl-CoA transferases belonging to the BAHD family of transferases, named feruloyl-CoA transferase (FAT), might transfer the feruloyl-CoA to UDP-Araf, producing the UDP-Araf-FA (step 2 in **Fig. 4**) (Buanafina, 2009; de Oliveira et al., 2015; Hatfield et al., 2017). Although the BAHD protein was not identified yet, the model is consistent with the genetic evidence provided by silencing of *BAHD01* ortholog genes in the model grass *Setaria viridis* and sugarcane (*Saccharum* spp.), which resulted in 60% and 50% decreases in cell wall ester-linked FA, respectively (de Souza et al., 2018; de Souza et al., 2019). The molecular mechanism involved in the introduction of Araf-FA into the nascent AX chain is not fully known. A glycosyl transferase (GT) from family 61, xylan arabinosyltransferase (XAT), is recognized to introduce the Araf residues into the nascent AX (step 3 in **Fig. 4**) (Anders et al., 2012; Chiniquy et al., 2012). It is likely possible that this GT may also introduce the Araf-FA into AX chain, although this molecular mechanism lacks experimental evidence.

Once the feruloylated AX is assembled into grass cell walls, we propose that FAE might hydrolyze the ester bond between FA and the *O*-5 position of Araf residues of AX (step 4 in **Fig. 4**), thereupon releasing free FA that may be recycled from the wall and likely channeled through the core phenylpropanoid pathway and contribute to carbon flux toward the biosynthesis of monolignols. Given that feruloyl-CoA is an intermediate of the phenylpropanoid pathway, free FA would be recycled back into the phenylpropanoid pathway via its activation to feruloyl-CoA by 4CL. Consistent with this hypothesis, it was demonstrated that exogenously supplied FA is converted to feruloyl-CoA and then to coniferyl and sinapyl alcohols in poplar (*Populus alba*) callus (Hamada et al., 2003). Such a redirection of the FA toward monolignols would have a particular effect in guaiacyl lignin. Exposure of soybean (*Glycine max*) seedlings to exogenous FA leads to a significant increase in the contents of lignin and over-accumulation of guaiacyl monomers, indicating the preferential redirection of the carbon flux from FA to the biosynthesis of guaiacyl lignin (dos Santos et al., 2008a; Lima et al., 2013). Alternatively, the flux may also, at least partially, redirect FA to other metabolic sinks (e.g. to feruloyl quinates, feruloyl hexose, and feruloyl malate) (Vanholme et al., 2012).

Given the widespread activity of ZmFAE in roots and leaves (**Fig. 3B**), its correlation with FA content in maize cell walls and the fundamental role that fungal and bacterial FAEs perform in plant cell wall deferuloylation, it is very likely that this esterase is responsible for

FA removal in grass species. It would be interesting to test whether the functional role of FAE in other plants is similar to the activity described in this work. Future works might investigate the expression of unknown genes encoding for FAE in maize and in other grass species. Additionally, to investigate the role of these candidate genes, the Clustered Interspaced Short Palindromic Repeats (CRISPR)/Cas9 technology may be used to obtain mutant crops with altered levels of AX feruloylation.

Conclusions

We describe a versatile and practical method to determine FAE activity in different tissues of grasses. The findings also showed that ZmFAE activity is correlated with the levels of cell wall ester-linked FA and the exposure to osmotic stress increases ZmFAE activity in seedling roots. These data suggest that FAE-catalyzed reaction is important for cell wall feruloylation during plant development and in response to abiotic stress. The collected information using this method and surveying the related literature allowed us to propose a model for the feruloylation and deferuloylation of AX, which explains the role of FAE in regulating the levels of ester-linked FA. Our model might orient further investigations of the roles of FAEs in plants and assist strategies for genetic engineering of grass crops to obtain lignocellulosic biomass with reduced recalcitrance.

Acknowledgements

This work was supported by the Brazilian National Council for Scientific and Technological Development (CNPq) and the Coordination of Enhancement of Higher Education Personnel (CAPES). DMO, TRM, FVS and GHGA gratefully acknowledge the doctoral scholarships granted by CNPq (GM/GD – 141076/2016-0) and CAPES (Code 001). RM and OFF are research fellows of CNPq.

Conflict of Interest

The authors have no conflicts of interest to disclose.

References

- Anders N, Wilkinson MD, Lovegrove A, Freeman J, Tryfona T, Pellny TK, Weimar T, Mortimer JC, Stott K, Baker JM, Defoin-Platel M, Shewry PR, Dupree P, Mitchell RA. 2012. Glycosyl transferases in family 61 mediate arabinofuranosyl transfer onto xylan in grasses. *Proc. Natl. Acad. Sci. USA* 109(3): 989-993.
- Badhan A, Jin L, Wang Y, Han S, Kowalczyk K, Brown DCW, Ayala CJ, Latoszek-Green M, Miki B, Tsang A, McAllister T. 2014. Expression of a fungal ferulic acid esterase in alfalfa modifies cell wall digestibility. *Biotechnol. Biofuels* 7(1): 39.
- Bevilaqua JM, Finger-Teixeira A, Marchiosi R, Oliveira DM, Joia BM, Ferro AP, Parizotto ÂV, dos Santos WD, Ferrarese-Filho O. 2019. Exogenous application of rosmarinic acid improves saccharification without affecting growth and lignification of maize. *Plant Physiol. Biochem.* 142: 275-282.
- Borneman WS, Ljungdahl LG, Hartley RD, Akin DE. 1992. Purification and partial characterization of two feruloyl esterases from the anaerobic fungus *Neocallimastix* strain MC-2. *Appl. Environ. Microbiol.* 58(11): 3762-3766.
- Bradford MM. 1976. A rapid and sensitive method for the quantitation of microgram quantities of protein utilizing the principle of protein-dye binding. *Anal. Biochem.* 72(1): 248-254.
- Buanafina MMO, Langdon T, Hauck B, Dalton S, Morris P. 2008. Expression of a fungal ferulic acid esterase increases cell wall digestibility of tall fescue (*Festuca arundinacea*). *Plant Biotechnol. J.* 6(3): 264-280.
- Buanafina MMO, Langdon T, Hauck B, Dalton S, Timms-Taravella E, Morris P. 2010. Targeting expression of a fungal ferulic acid esterase to the apoplast, endoplasmic reticulum or golgi can disrupt feruloylation of the growing cell wall and increase the biodegradability of tall fescue (*Festuca arundinacea*). *Plant Biotechnol. J.* 8(3): 316-331.
- Buanafina MMO. 2009. Feruloylation in grasses: current and future perspectives. *Mol Plant* 2(5): 861-872.
- Buanafina MMO, Iyer PR, Buanafina MF, Shearer EA. 2017. Reducing cell wall feruloylation by expression of a fungal ferulic acid esterase in *Festuca arundinacea* modifies plant growth, leaf morphology and the turnover of cell wall arabinoxylans. *PLoS One* 12(9): e0185312.
- Buanafina MMO, Langdon T, Hauck B, Dalton SJ, Morris P. 2006. Manipulating the phenolic acid content and digestibility of italian ryegrass (*Lolium multiflorum*) by vacuolar-targeted expression of a fungal ferulic acid esterase. *Appl. Biochem. Biotechnol.* 129: 416-426.
- Chiniquy D, Sharma V, Schultink A, Baidoo EE, Rautengarten C, Cheng K, Carroll A, Ulvskov P, Harholt J, Keasling JD, Pauly M, Scheller HV, Ronald PC. 2012. XAX1 from glycosyltransferase family 61 mediates xylosyltransfer to rice xylan. *Proc. Natl. Acad. Sci. USA* 109(42): 17117-17122.
- Crepin VF, Faulds CB, Connerton IF. 2004. Functional classification of the microbial feruloyl esterases. *Appl. Microbiol. Biotechnol.* 63(6): 647-652.
- de Oliveira DM, Finger-Teixeira A, Mota TR, Salvador VH, Moreira-Vilar FC, Molinari HB, Mitchell RA, Marchiosi R, Ferrarese-Filho O, dos Santos WD. 2015. Ferulic acid: a key

- component in grass lignocellulose recalcitrance to hydrolysis. *Plant Biotechnol. J.* 13(9): 1224-1232.
- de Souza WR, Martins PK, Freeman J, Pellny TK, Michaelson LV, Sampaio BL, Vinecky F, Ribeiro AP, da Cunha B, Kobayashi AK, de Oliveira PA, Campanha RB, Pacheco TF, Martarello DCI, Marchiosi R, Ferrarese-Filho O, dos Santos WD, Tramontina R, Squina FM, Centeno DC, Gaspar M, Braga MR, Tine, MAS, Ralph J, Mitchell RAC, Molinari HBC. 2018. Suppression of a single BAHD gene in *Setaria viridis* causes large, stable decreases in cell wall feruloylation and increases biomass digestibility. *New Phytol.* 218(1): 81-93.
- de Souza WR, Pacheco TF, Duarte KE, Sampaio BL, de Oliveira Molinari PA, Martins PK, Santiago TR, Formighieri EF, Vinecky F, Ribeiro AP, da Cunha B, Kobayashi AK, Mitchell RAC, Gambetta DSR, Molinari HBC. 2019. Silencing of a BAHD acyltransferase in sugarcane increases biomass digestibility. *Biotechnol. Biofuels* 12(1).
- Dong J, Wu F, Zhang G. 2006. Influence of cadmium on antioxidant capacity and four microelement concentrations in tomato seedlings (*Lycopersicon esculentum*). *Chemosphere* 64(10): 1659-1666.
- dos Santos WD, Ferrarese MLL, Nakamura CV, Mourão KS, Mangolin CA, Ferrarese-Filho O. 2008a. Soybean (*Glycine max*) root lignification induced by ferulic acid. The possible mode of action. *J. Chem. Ecol.* 34(9): 1230-1241.
- dos Santos WD, Ferrarese MLL, Ferrarese-Filho O. 2008b. Ferulic acid: an allelochemical troublemaker. *Funct. Plant Sci. Biotechnol.* 2: 47-55.
- Ferro AP, Flores Júnior R, Finger-Teixeira A, Parizotto AV, Bevilaqua JM, Oliveira DM, Molinari HBC, Marchiosi R, dos Santos WD, Seixas FAV, Ferrarese-Filho, O. 2020. Inhibition of *Zea mays* coniferyl aldehyde dehydrogenase by daidzin: A potential approach for the investigation of lignocellulose recalcitrance. *Process Biochem.* 90: 131-138.
- Hamada K, Tsutsumi Y, Nishida T. 2003. Treatment of poplar callus with ferulic and sinapic acids II: effects on related monolignol biosynthetic enzyme activities. *J. Wood Sci.* 49(4): 366-370.
- Hatfield RD, Rancour DM, Marita JM. 2017. Grass cell walls: a story of cross-linking. *Front. Plant Sci.* 7: 2056.
- Li J, Cai S, Luo Y, Dong X. 2011 Three feruloyl esterases in *Cellulosilyticum ruminicola* H1 act synergistically to hydrolyze esterified polysaccharides. *Appl. Environ. Microbiol.* 77: 6141-6147.
- Lima RB, Salvador VH, dos Santos WD, Bubna GA, Finger-Teixeira A, Soares AR, Marchiosi R, L. FM, Ferrarese-Filho O. 2013. Enhanced lignin monomer production caused by cinnamic acid and its hydroxylated derivatives inhibits soybean root growth. *PLoS One* 8(12): e80542.
- Martínez-Rubio R, Centeno ML, García-Angulo P, Álvarez JM, Acebes JL, Encina A. 2020. The role of cell wall phenolics during the early remodelling of cellulose-deficient maize cells. *Phytochemistry* 170: 112219.

- Mota TR, Oliveira DM, Marchiosi R, Ferrarese-Filho O, dos Santos WD. 2018. Plant cell wall composition and enzymatic deconstruction. *AIMS Bioeng.* 5(1): 63-77.
- Nair RB, Bastress KL, Ruegger MO, Denault JW, Chapple C. 2004. The *Arabidopsis thaliana* *REDUCED EPIDERMAL FLUORESCENCE1* gene encodes an aldehyde dehydrogenase involved in ferulic acid and sinapic acid biosynthesis. *Plant Cell* 16(2): 544-554.
- Oliveira DM, Mota TR, Grandis A, de Moraes GR, de Lucas RC, Polizeli MLTM, Marchiosi R, Buckeridge MS, Ferrarese-Filho O, dos Santos WD. 2020a. Lignin plays a key role in determining biomass recalcitrance in forage grasses. *Renew. Energy* 147: 2206-2217.
- Oliveira DM, Mota TR, Oliva B, Segato F, Marchiosi R, Ferrarese-Filho O, Faulds CB, dos Santos WD. 2019. Feruloyl esterases: Biocatalysts to overcome biomass recalcitrance and for the production of bioactive compounds. *Bioresour. Technol.* 278: 408-423.
- Oliveira DM, Mota TR, Salatta FV, Sinzker RC, Končítíková R, Kopečný D, Simister R, Silva M, Goeminne G, Morreel K, Rencoret J, Gutiérrez A, Tryfona T, Marchiosi R, Dupree P, del Río JC, Boerjan W, McQueen-Mason SJ, Gomez LD, Ferrarese-Filho O, dos Santos WD. 2020b. Cell wall remodeling under salt stress: Insights into changes in polysaccharides, feruloylation, lignification, and phenolic metabolism in maize. In press *Plant Cell Environ.* DOI: 10.1111/pce.13805
- Ralph J. 2010. Hydroxycinnamates in lignification. *Phytochem. Rev.* 9: 65-83.
- Reem NT, Pogorelko G, Lionetti V, Chambers L, Held MA, Bellincampi D, Zabolina OA. 2016. Decreased polysaccharide feruloylation compromises plant cell wall integrity and increases susceptibility to necrotrophic fungal pathogens. *Front. Plant Sci.* 7: 630.
- Rennie EA, Scheller HV. 2014. Xylan biosynthesis. *Curr. Opin. Biotechnol.* 26: 100-107.
- Sancho AI, Faulds CB, Bartolomé B, Williamson G. 1999. Characterisation of feruloyl esterase activity in barley. *J. Sci. Food Agric.* 79(3): 447-449.
- Udatha DB, Kouskoumvekaki I, Olsson L, Panagiotou G. 2011. The interplay of descriptor-based computational analysis with pharmacophore modeling builds the basis for a novel classification scheme for feruloyl esterases. *Biotechnol. Adv.* 29(1): 94-110.
- Vanholme R, Storme V, Vanholme B, Sundin L, Christensen JH, Goeminne G, Halpin C, Rohde A, Morreel K, Boerjan W. 2012. A systems biology view of responses to lignin biosynthesis perturbations in *Arabidopsis*. *Plant Cell* 24(9): 3506-3529.
- Zhang S-B, Ma X-F, Pei X-Q, Liu J-Y, Shao H-W, Wu Z-L. 2012. A practical high-throughput screening system for feruloyl esterases: Substrate design and evaluation. *J. Mol. Catal. B Enzym.* 74(1-2): 36-40.
- Zhang SB, Zhai HC, Wang L, Yu GH. 2013. Expression, purification and characterization of a feruloyl esterase A from *Aspergillus flavus*. *Protein Expr. Purif.* 92(1): 36-40.

CHAPTER 5

Designing Xylan for Improved Sustainable Biofuel Production

Dyoni M. Oliveira^{1*}, Thatiane R. Mota¹, Fábio V. Salatta¹, Rogério Marchiosi¹, Leonardo D. Gomez², Simon J. McQueen-Mason², Osvaldo Ferrarese-Filho¹, Wanderley D. dos Santos^{1*}

¹ Laboratory of Plant Biochemistry, Department of Biochemistry, State University of Maringá, Maringá, Paraná, Brazil

² Centre for Novel Agricultural Products, Department of Biology, University of York, York YO10 5DD, UK

* Corresponding author

Dyoni M. Oliveira

Wanderley D. dos Santos

E-mail: dyonioliveira@gmail.com; wdsantos@uem.br

Type of chapter:	Brief Communication
Journal:	Plant Biotechnology Journal
Impact factor:	6.840
Volume/issue, pages:	17(12), 2225-2227
Date of publication:	December 2019
DOI:	10.1111/pbi.13150

1. Background

Increasing greenhouse gas emissions and diminishing supplies of fossil-derived fuels underline the need for environmentally sustainable energy resources. Lignocellulose, more generically named simply as plant biomass, represent one of the most abundant renewable resources for biofuels. Lignocellulosic biomass from forest residues, agro-wastes and energy grasses is extensively exploited for bioenergy production. This renewable biomass source is abundant, highly accessible, relatively cheap, and diversifies the energy matrix (Marriott *et al.*, 2016). Grass lignocellulosic material consists mostly of secondary cell walls and is composed mainly of cellulose (25%-55%), hemicellulose xylan (20%-50%), lignin (10%-35%), and small amount of pectin, depending on plant species, organ, cell types and developmental stage of the tissue. Although pectin is a minor cell wall component, there is increasing evidence suggesting that pectic polysaccharides are involved in cell wall recalcitrance (Biswal *et al.*, 2018).

The most important crops farmed at large scale are grasses, where xylan is the main hemicellulose component in their cell walls. Xylan is tightly associated with cellulose microfibrils, connecting them through hydrogen bonds. Recently, it was demonstrated that xylan interacts with cellulose by two-fold helical screw conformation and the interaction is influenced by xylan substitution patterns (Simmons *et al.*, 2016). The xylan backbone consists of a linear chain of β -(1,4)-D-xylosyl residues (Xylp) and makes up between 20% and 35% of the total cell wall. Arabinofuranose residues (Araf) may be α -(1,2)- or α -(1,3)-linked to the xylan backbone forming arabinoxylan (AX), which may be further substituted with ferulic (FA) or *p*-coumaric acid residues (**Figure 1**). The side-chain decorations on the AX backbone vary between plant species and tissues. In grasses, the primary and secondary cell walls contain substantial amounts of AX, which is also found at much lower abundance in primary cell walls of dicots. For more background information of xylan biosynthesis and modifications, see the review by Smith *et al.* (2017).

FA esters in AX might undergo oxidative dimerization to form crosslinks at adjacent AX chains or lignin, thereby generating intra-molecular and inter-molecular crosslinks of AXs with lignin and structural proteins that contribute to the recalcitrance of grass biomass for saccharification. FA may act as a nucleating site for the formation of lignin, hence linking AXs to lignin by forming a lignin-AX complex (Oliveira *et al.*, 2015). Recent studies of the lignin-polysaccharide interactions in secondary cell walls demonstrated that the hydroxyl groups in xylan have abundant electrostatic interactions with lignin methoxyl groups found mainly in S-lignin (Kang *et al.*, 2019).

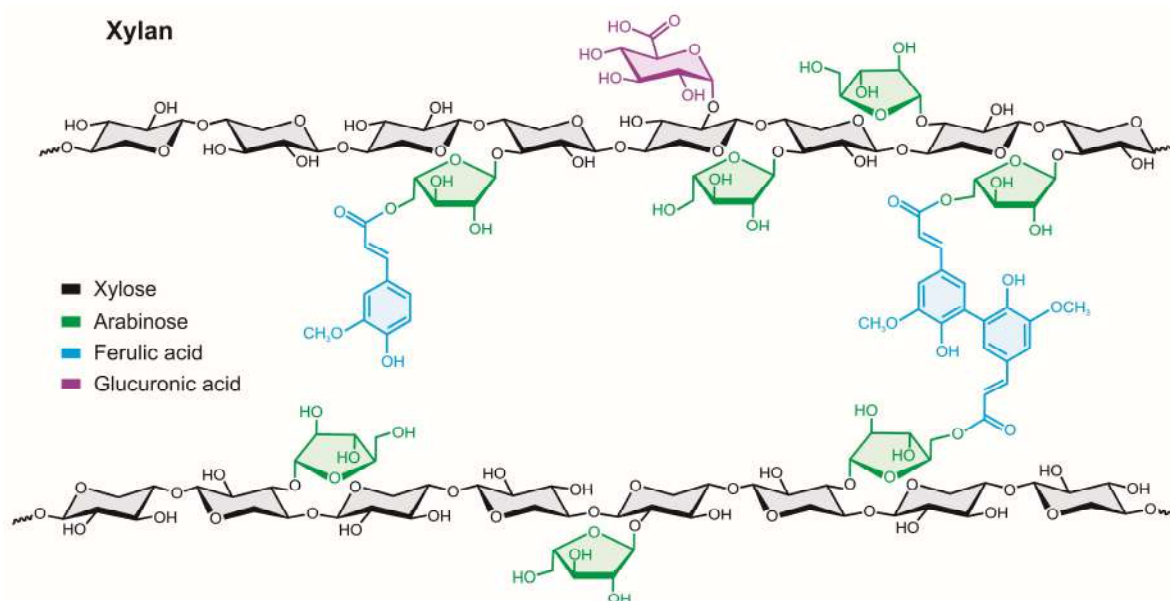


Figure 1. Generalized structure of xylan branched with arabinose, ferulic acid and glucuronic acid.

AX also influences the enzymatic hydrolysis of cellulose and it requires different enzymes from those used to hydrolyse cellulose. Lowering AX content and/or its decorations (with Araf and FA) reduces the cross-linkages among AX, lignin and cellulose in plant cell walls, decreasing biomass recalcitrance (Smith *et al.*, 2017). Research aiming at elucidating the genes required for xylan biosynthesis, the way they are controlled, and how changes in these genes influence plant development has been boosted by the potential of plant biomass as a source of renewable energy. Recent studies have highlighted the key role that xylan plays in the conversion of lignocellulosic feedstocks to fuels and other value-added products.

2. Tailoring xylan structure

The glycosyltransferases (GTs) required for xylan biosynthesis were first identified in *Arabidopsis thaliana*. These enzymes catalyze the biosynthesis of the xylan backbone, transferring nucleotide sugars to the growing AX chain within the Golgi apparatus. Two members of the glycosyltransferase family 43 (GT43), IRREGULAR XYLEM9 (IRX9) and IRX14 proteins, and one member of GT47, IRX10, are implicated in the biosynthesis of the xylan backbone, but the specific role is not completely established (Brown *et al.*, 2007; Smith *et al.*, 2017). Subsequent works confirmed that IRX10 is the β-1,4-xylan xylosyl transferase responsible for xylan polymer extension, transferring xylosyl residues from UDP-xylose to xylo-oligosaccharides at the reducing end, whereas IRX9 and IRX14 are accessory proteins involved in the elongation of the xylan backbone and are structural components of the functioning xylan synthase complex (XSC). Additionally, glucuronosyltransferases (GUX)

from the GT8 family and arabinosyltransferases (XAT) from the GT61 family are responsible for the addition of glucuronosyl and arabinosyl on the xylan backbone, respectively (Smith *et al.*, 2017).

Despite the importance of AX for biofuels, the biochemical function and structure of GT43 enzymes are still unclear. GTs are difficult to study because they are labile, present in multimeric complexes and encoded by large gene families whose members can have overlapping functions. Almost all the studies with the GT43 family are limited to comprehensive genetic analysis of the functional roles of GT43, mutations in the genes *IRX9* and *IRX14* result in decreased xylan synthase activity and xylose content, accompanied by a shorter xylan backbone (Brown *et al.*, 2007).

Recent advances provided important evidence that *BdGT43A*, the orthologue of *IRX14* in *Arabidopsis*, is involved in xylan backbone biosynthesis in *Brachypodium distachyon* (Whitehead *et al.*, 2018). Using commercial cellulases, *B. distachyon* recombinant inbred lines (RILs) were screened, associating them with a single quantitative trait locus (QTL) for saccharification. The study revealed that RNAi suppression of *BdGT43A* in *Brachypodium* decreases xylose and arabinose content and increases stem saccharification relative to the wild-type, which is clear genetic evidence that *BdGT43A* is involved in xylan biosynthesis. In addition, the transgenic lines showed a decrease in FA and an increase in *p*-coumaric acid, compared to the wild type. Similarly, plants of hybrid aspen (*Populus tremula* × *tremuloides*) downregulated simultaneously for *PtGT43B* and *PtGT43C*, the orthologues of *IRX9* and *IRX14*, respectively, present reduced xylose content relative to the reducing end sequence in xylan, with slight alteration in the chemical composition of wood, a small decrease in S and H lignin, accompanied by a higher lignocellulose saccharification efficiency (Ratke *et al.*, 2018).

It is interesting to note that the underlying mechanisms for the reduced recalcitrance in *Brachypodium* and hybrid aspen transgenic lines are quite different. In *BdGT43A* silenced lines the lower xylan content associated with decreased FA content is the main factor responsible for the increased saccharification efficiency. Alternatively, the reduction in the xylan in hybrid aspen *GT43* suppressed lines is associated with a small decrease in S and H lignin content, being this the main contribution to the higher saccharification efficiency. Different responses to the suppression of orthologues genes are due in part to the largely unpredictable pleiotropic effects and phenotypes associated with the mutations. Additionally, the mechanistic relationship between *GT43* gene repression and cell wall modifications require more investigation.

Further examination of AX feruloylation (de Souza *et al.*, 2018) identified a member of the BAHD acyltransferase family involved in the transference of FA residues to the AX backbone. Silencing the *SvBAHD01* gene by RNAi in *Setaria viridis* reduced FA content by 60% and increased stem saccharification efficiency (from 40 to 60%), without changing biomass productivity. Therefore, the increase in stem saccharification obtained by Whitehead *et al.* (2018) reflect a synergic effect of the overall decrease in feruloylation of arabinosyl moieties linked to AXs. The elucidation of the genes involved in xylan biosynthesis and feruloylation, the way they are controlled, and how changes in these genes influence plant growth can facilitate the design of strategies aimed at engineering plants to exhibit modified xylan for improved biofuel production. These recent insights emphasize the importance of generating plants with reduced FA and AX content in the search for improved feedstocks for biorefineries.

Future perspectives

AXs are abundant in nature and in the grass cell wall. AX and FA are essential components, cross-linking polysaccharides to lignin and increasing the cell wall resistance to hydrolysis. Although further elucidation of xylan biosynthesis mechanisms are still necessary, a possible model to explain how it is associated with biomass digestibility is emerging. The advantage of discovering the genes associated with the expression of the enzymes in the biosynthesis of xylan is that there are now more ways to design this structure. Genetic manipulation of xylan biosynthesis and feruloylation raise many interesting questions that should be addressed in the future and is a potential approach to engineering crops that match the industrial requirements for food, cellulosic ethanol, and biorefineries.

Acknowledgments

This work was supported by grants from the The National Council for Scientific and Technological Development (CNPq) and Coordination for Enhancement of Higher Education Personnel (CAPES).

Competing interests

The authors declare no competing interests.

References

- Biswal, A.K., Atmodjo, M.A., Li, M., Baxter, H.L., Yoo, C.G., Pu, Y., Lee, Y.C., Mazarei, M., Black, I.M., Zhang, J.Y., Ramanna, H., Bray, A.L., King, Z.R., LaFayette, P.R., Pattathil, S., Donohoe, B.S., Mohanty, S.S., Ryno, D., Yee, K., Thompson, O.A., Rodriguez, M., Jr., Dumitrache, A., Natzke, J., Winkeler, K., Collins, C., Yang, X., Tan, L., Sykes, R.W., Gjersing, E.L., Ziebell, A., Turner, G.B., Decker, S.R., Hahn, M.G., Davison, B.H., Udvardi, M.K., Mielenz, J.R., Davis, M.F., Nelson, R.S., Parrott, W.A., Ragauskas, A.J., Neal Stewart, C., Jr. and Mohnen, D. (2018) Sugar release and growth of biofuel crops are improved by downregulation of pectin biosynthesis. *Nat. Biotechnol.* **36**, 249-257.
- Brown, D.M., Goubet, F., Wong, V.W., Goodacre, R., Stephens, E., Dupree, P. and Turner, S.R. (2007) Comparison of five xylan synthesis mutants reveals new insight into the mechanisms of xylan synthesis. *Plant J.* **52**, 1154-1168.
- de Oliveira, D.M., Finger-Teixeira, A., Mota, T.R., Salvador, V.H., Moreira-Vilar, F.C., Molinari, H.B., Mitchell, R.A., Marchiosi, R., Ferrarese-Filho, O. and dos Santos, W.D. (2015) Ferulic acid: a key component in grass lignocellulose recalcitrance to hydrolysis. *Plant Biotechnol. J.* **13**, 1224-1232.
- de Souza, W.R., Martins, P.K., Freeman, J., Pellny, T.K., Michaelson, L.V., Sampaio, B.L., Vinecky, F., Ribeiro, A.P., da Cunha, B., Kobayashi, A.K., de Oliveira, P.A., Campanha, R.B., Pacheco, T.F., Martarello, D.C.I., Marchiosi, R., Ferrarese-Filho, O., dos Santos, W.D., Tramontina, R., Squina, F.M., Centeno, D.C., Gaspar, M., Braga, M.R., Tine, M.A.S., Ralph, J., Mitchell, R.A.C. and Molinari, H.B.C. (2018) Suppression of a single BAHD gene in *Setaria viridis* causes large, stable decreases in cell wall feruloylation and increases biomass digestibility. *New Phytol.* **218**, 81-93.
- Kang, X., Kirui, A., Dickwella Widanage, M.C., Mentink-Vigier, F., Cosgrove, D.J. and Wang, T. (2019) Lignin-polysaccharide interactions in plant secondary cell walls revealed by solid-state NMR. *Nat. Commun.* **10**, 347.
- Marriott, P.E., Gomez, L.D. and McQueen-Mason, S.J. (2016) Unlocking the potential of lignocellulosic biomass through plant science. *New Phytol.* **209**, 1366-1381.
- Ratke, C., Terebieniec, B.K., Winstrand, S., Derba-Maceluch, M., Grahn, T., Schiffthaler, B., Ulvcróna, T., Ozparpucu, M., Rüggeberg, M., Lundqvist, S.O., Street, N.R., Jonsson, L.J. and Mellerowicz, E.J. (2018) Downregulating aspen xylan biosynthetic GT43 genes in developing wood stimulates growth via reprogramming of the transcriptome. *New Phytol.* **219**, 230-245.
- Simmons, T.J., Mortimer, J.C., Bernardinelli, O.D., Poppler, A.C., Brown, S.P., deAzevedo, E.R., Dupree, R. and Dupree, P. (2016) Folding of xylan onto cellulose fibrils in plant cell walls revealed by solid-state NMR. *Nat. Commun.* **7**, 13902.
- Smith, P.J., Wang, H.T., York, W.S., Pena, M.J. and Urbanowicz, B.R. (2017) Designer biomass for next-generation biorefineries: leveraging recent insights into xylan structure and biosynthesis. *Biotechnol. Biofuels* **10**, 286.
- Whitehead, C., Garrido, F.J.O., Reymond, M., Simister, R., Distelfeld, A., Atienza, S.G., Piston, F., Gomez, L.D. and McQueen-Mason, S.J. (2018) A glycosyl transferase family 43 protein involved in xylan biosynthesis is associated with straw digestibility in *Brachypodium distachyon*. *New Phytol.* **218**, 974-985.

CHAPTER 6

Cell Wall Remodeling Under Salt Stress: Insights into Changes in Polysaccharides, Feruloylation, Lignification, and Phenolic Metabolism in Maize

Dyoni M. Oliveira^{1*}, Thatiane R. Mota¹, Fábio V. Salatta¹, Renata C. Sinzker¹, Radka Končítíková², David Kopečný², Rachael Simister³, Mariana Silva³, Geert Goeminne^{4,5}, Kris Morreel^{4,5}, Jorge Rencoret⁶, Ana Gutiérrez⁶, Theodora Tryfona⁷, Rogério Marchiosi¹, Paul Dupree⁷, José C. del Río⁶, Wout Boerjan^{4,5}, Simon J. McQueen-Mason³, Leonardo D. Gomez³, Osvaldo Ferrarese-Filho¹, Wanderley D. dos Santos^{1*}

¹ Department of Biochemistry, State University of Maringá, Maringá, Brazil

² Department of Protein Biochemistry and Proteomics, Centre of the Region Haná for Biotechnological and Agricultural Research, Faculty of Science, Palacký University, Olomouc, Czech Republic

³ Centre for Novel Agricultural Products, Department of Biology, University of York, York, United Kingdom

⁴ Department of Plant Biotechnology and Bioinformatics, Ghent University, Ghent, Belgium

⁵ Center for Plant Systems Biology, VIB, Ghent, Belgium

⁶ Instituto de Recursos Naturales y Agrobiología de Sevilla, CSIC, Seville, Spain

⁷ Department of Biochemistry, University of Cambridge, Cambridge, United Kingdom

* Corresponding author

Dyoni M. Oliveira

Wanderley D. dos Santos

E-mail: dyonioliveira@gmail.com; wdsantos@uem.br

Type of chapter:

Research article

Journal:

Plant, Cell & Environment

Impact factor:

5.624

Current status:

Submitted, under review

Abstract

Although cell wall polymers play important roles in the tolerance of plants to abiotic stress, the effects of salinity on cell wall composition and metabolism in grasses remain largely unexplored. Here, we conducted an in-depth study of changes in cell wall composition and phenolic metabolism induced upon salinity in maize seedlings and plants. Cell wall characterization revealed that salt stress modulated the deposition of cellulose, matrix polysaccharides and lignin in seedling roots, plant roots and stems. The extraction and analysis of arabinoxylans by size-exclusion chromatography, 2D-NMR spectroscopy and carbohydrate gel electrophoresis showed a reduction of arabinoxylan content in salt-stressed roots. Saponification and mild acid hydrolysis revealed that salinity also reduced the feruloylation of arabinoxylans in roots of seedlings and plants. Determination of lignin content and composition by nitrobenzene oxidation and 2D-NMR confirmed the increased incorporation of syringyl units in lignin of maize roots. Salt stress also induced the expression of genes and the activity of enzymes enrolled in phenylpropanoid biosynthesis. The UHPLC-MS-based metabolite profiling confirmed the modulation of phenolic profiling by salinity and the accumulation of ferulate and its derivatives 3- and 4-*O*-feruloyl quinate. In conclusion, we present a model for explaining cell wall remodeling in response to salinity.

Keywords: Abiotic stress, cell wall, ferulic acid, lignification, *p*-coumaric acid, salinity, xylan, *Zea mays*.

Significance statement

We demonstrate the modulations induced by salt stress in the amounts of cellulose, matrix polysaccharides and lignin in roots of maize seedlings and roots, stems and leaves of maize plants. Salt stress reduced the feruloylation of arabinoxylan, increased the incorporation of syringyl lignin, and induced the biosynthesis and accumulation of ferulic acid and its derivatives. Based on these findings, we propose a model of grass cell wall remodeling in response to salinity.

1. Introduction

Soil salinity is an important environmental problem for over 800 million hectares of land (*ca.* 6% of the world's total land), which are affected by either salinity (397 million ha) or sodicity (434 million ha) (Munns and Tester, 2008). Salt stress results in ionic imbalances, osmotic stress, ion toxicity, oxidative damage and complex effects on the physiology and metabolism of the plant (Negrão *et al.*, 2017). The growth of most cereal crops is reduced when the soil salinity exceeds the electrical conductivity of 4 dS/m, which is equivalent to 40 mM sodium chloride (Munns and Tester, 2008; Munns *et al.*, 2019). Maize (*Zea mays* L.) is the crop with the highest global annual grain yield and manifests biochemical and physiological adaptations that allow it to grow under exposure to salt concentrations of up to 200 mM sodium chloride (Farooq *et al.*, 2015).

Plant cell walls are highly dynamic and responsive structures that can be remodeled during plant growth, development and in response to various abiotic and biotic stresses (Tenhaken, 2014; Le Gall *et al.*, 2015; Voiniciuc *et al.*, 2018; Cesarino, 2019). The complex arrangement of cell wall polymers provides mechanical and structural integrity to each cell, sustains the differential growth during cell division and expansion, and serves as sensory interfaces between plants and their environment (Burton *et al.*, 2010; Vaahtera *et al.*, 2019). The tolerance of plants to salinity is closely related to the formation of secondary cell walls and the deposition pattern of cellulose and lignin (Wang *et al.*, 2016; Byrt *et al.*, 2018). Most of the studies on cell wall modifications upon abiotic stress focus primarily on genes and proteins putatively involved in cell wall metabolism, consequently modulations of chemical nature are not fully understood (Tenhaken, 2014; Le Gall *et al.*, 2015; Rui and Dinneny, 2019).

Cellulose is a fundamental component of the cell walls. This macromolecule consists of unbranched and unsubstituted β -(1,4)-D-linked glucan chains that form non-covalent microfibrillar complexes through extensive intra and intermolecular hydrogen bonding and hydrophobic interactions (Burton *et al.*, 2010). Exposure to salinity directly or indirectly modulates cellulose biosynthesis by regulating cellulose synthase genes and the arrangement of cellulose microfibrils (Endler *et al.*, 2015; Wang *et al.*, 2016; Kesten *et al.*, 2019).

Lignin impregnates the secondary cell walls of vascular plants, providing mechanical support, impermeability and resistance to biodegradation (Moura *et al.*, 2010; Mota *et al.*, 2019; Ralph *et al.*, 2019). Lignin is synthesized via the phenylpropanoid pathway followed by oxidative radical coupling of lignin monomers. The main canonical monolignols, *p*-coumaryl, coniferyl and sinapyl alcohols, constitute the *p*-hydroxyphenyl (H), guaiacyl (G), and syringyl (S) units in lignin polymer, respectively (Ralph *et al.*, 2004; Vanholme *et al.*, 2010). Additional

monomers are also incorporated into lignin polymer, for example, grasses incorporate γ -*p*-coumaroylated monolignols during lignification, producing γ -acylated lignin units (Ralph, 2010; Petrik *et al.*, 2014). Notably, biotic and abiotic stresses can rapidly induce the biosynthesis and deposition of lignin in secondary cell walls (Moura *et al.*, 2010; Cesarino, 2019; Vanholme *et al.*, 2019).

Ferulic (FA) and *p*-coumaric acids (*p*CA) are also produced by the phenylpropanoid pathway. Activated with coenzyme A (CoA), as feruloyl- and *p*-coumaroyl-CoA, they are intermediary metabolites toward the formation of monolignols and precursors for the acylation of xylan and lignin (Hatfield *et al.*, 2009; Ralph, 2010; Hatfield *et al.*, 2017). Xylan is the main hemicellulose of grasses and its backbone consists of a linear chain of β -(1,4)-D-linked xylopyranosyl residues (Xylp) (Rennie and Scheller, 2014). Arabinofuranosyl residues (Araf) are α -(1,2)- or α -(1,3)-linked to the xylan chain assembling the arabinoxylan (AX), which may be further esterified with FA (and *p*CA at lower levels) residues at *O*-5 position of Araf residues. Feruloylation of AX may act as cross-links between AX chains to each other or between AX to lignins, resulting in a highly recalcitrant lignin–hydroxycinnamate– carbohydrate complex (Grabber *et al.*, 2000; Buanafina, 2009; de Oliveira *et al.*, 2015; Hatfield *et al.*, 2017; Oliveira *et al.*, 2020).

Little is known about the chemical nature and particularly the structural features underlying cell wall compositional shifts in response to abiotic stresses (Tenhaken, 2014; Le Gall *et al.*, 2015; Cesarino, 2019; Zhao *et al.*, 2019). During recent years, our understanding of the cell wall biosynthesis and structure has improved profoundly, for instance, the feruloylation and *p*-coumaroylation of AX (Bartley *et al.*, 2013; Buanafina *et al.*, 2016; de Souza *et al.*, 2018; de Souza *et al.*, 2019), lignin acylation (Withers *et al.*, 2012; Petrik *et al.*, 2014; Wilkerson *et al.*, 2014; Karlen *et al.*, 2016; Karlen *et al.*, 2018), xylan biosynthesis and structure (Anders *et al.*, 2012; Grantham *et al.*, 2017; Whitehead *et al.*, 2018; Zhong *et al.*, 2018; Tryfona *et al.*, 2019), and covalent interactions between lignin, xylan and cellulose (Busse-Wicher *et al.*, 2016; Simmons *et al.*, 2016; Kang *et al.*, 2019). Here, we examined how salt stress affects the cell wall structure of maize seedlings and plants, determining the polysaccharides, lignin and feruloylation, investigating the genes and enzymes related to FA biosynthesis, and the abundance of phenolic metabolites differentially expressed upon salinity. We demonstrate how maize copes with saline environment remodeling its cell wall structure, modulating the feruloylation of AX and the differential incorporation of lignin monomers.

2. Materials and Methods

2.1. Plant material and growth conditions

Maize (*Zea mays* L. cv. IPR-164) seeds were surface sterilized with 2% NaClO and germinated at 25 °C on moistened filter paper under dark conditions. For the experiments with seedlings, 25 seedlings of 3-day-old with uniform growth were transferred to hydroponic nutrient solution (Dong *et al.*, 2006) supplemented with different NaCl concentrations (0 to 200 mM), and grown for three days at 25 °C under a 12 h photoperiod. The initial screening with different concentrations of NaCl showed that 200 mM NaCl changed simultaneously the amounts of cell wall-bound FA, pCA and lignification in roots of seedlings (**Fig. S1**). Based on this screening, 200 mM NaCl was selected for subsequent experiments in seedlings. For the experiments with maize plants, 2-day-old seedlings were transferred to 500-ml pots with 400 g of vermiculite and grown at 25 °C under a photoperiod of 12 h light/12 h dark. After the fifth day, the plants were watered every two days with 60 ml nutrient solution (full substrate capacity) in the absence (control) or presence of NaCl. The concentration was selected based on the initial screening in plants exposed upon different NaCl concentrations (0 to 200 mM), using lignin amount as the measure (**Fig. S2**). Similarly to seedlings, 200 mM NaCl increased lignin content in roots and stems, thereupon this concentration was employed for subsequent experiments. After 17 days of cultivation, the roots, stems and leaves without sheaths were harvested and used for the experiments.

Plant growth parameters were obtained at the end of the cultivation of seedlings and plants. The lengths and fresh weights of roots, stems and leaves were measured immediately after harvesting, whereas the dry weights were determined after drying the plant material in an oven at 60 °C for three days. Relative water content (RWC) was calculated as follow: $RWC\% = (\text{Fresh weight} - \text{Dry weight}) / \text{Fresh weight} \times 100$. Thiobarbituric acid reactive substances (TBARS) content was determined as detailed in **Methods S1**. The schematic flowchart summarizing the experimental design and the methodologies applied in this study is shown in **Fig. S3**.

2.2. Alcohol insoluble residue preparation

A total of ~200 mg of milled material was incubated in 5 ml of phenol for 30 min at room temperature under agitation, followed by centrifugation at 3,000×g for 20 min. The supernatant was removed and the pellet was washed twice with chloroform:methanol (2:1, v/v) and once with absolute ethanol. After centrifugation, the pellet was incubated over-night with

90% aqueous dimethyl sulfoxide (v/v) at room temperature under agitation, followed by centrifugation and washed thrice with absolute ethanol. The pellets were dried at 45 °C and considered as the alcohol insoluble residue (AIR).

2.3. ATR-FTIR spectroscopy

Attenuated Total Reflectance-Fourier Transform Infrared (ATR-FTIR) spectra of AIR samples were obtained between 850–1850 cm^{-1} using a Spectrum One spectrometer (Perkin-Elmer) as previously reported (Marriott *et al.*, 2014). Spectral assignments were made according to the literature (**Table S1**).

2.4. Matrix monosaccharide compositional analysis and crystalline cellulose content

The AIR (4 mg) was hydrolyzed with 500 μl of 2 M trifluoroacetic acid (TFA) at 100 °C for 4 h, under oxygen-free condition. Following the evaporation under vacuum for the removal of TFA, the samples were rinsed twice with isopropanol and resuspended in 200 μl of water. Samples were filtered with 0.45 μm polytetrafluoroethylene filters and analyzed by high-performance anion-exchange chromatography with pulsed amperometric detection (HPAEC-PAD) (Carbopac PA10 column; Dionex ICS3000 system, Camberley, UK) (Jones *et al.*, 2003). The residue following 2 M TFA hydrolysis was used for the determination of crystalline cellulose content using the anthrone-sulfuric acid method as previously described by Foster *et al.* (2010) with modifications (see **Methods S1** for a detailed description).

2.5. Sequential extraction and analysis of xylan

For xylan extraction, the AIR was firstly destarched as described by Whitehead and coworkers (2018). Next, the sequential extraction of xylan was performed by agitating 20 mg of destarched AIR in 2 ml of 50 mM 1,2-cyclohexylenedinitrilotetraacetic acid (CDTA) (pH 6.5) for 24 h at room temperature. The suspension was centrifuged (14,000 \times g, 4 °C for 10 min) and the pellet washed once with deionized water. The pellets were subsequently extracted under oxygen-free conditions using 50 mM Na_2CO_3 containing 10 mM NaBH_4 for 24 h at 4 °C, 1 M KOH with 10 mM NaBH_4 for 24 h at 4 °C and 4 M KOH with 10 mM NaBH_4 for 24 h at 4 °C. The KOH-soluble fractions were adjusted to pH 5 with 100 μl of glacial acetic acid, dialyzed extensively against deionized water for 24 h at 4 °C and freeze-dried. For the monosaccharide analysis, 1 mg of freeze-dried KOH fraction was hydrolyzed with 2 M TFA followed by HPAEC-PAD analysis.

2.6. Xylan analysis by size-exclusion chromatography coupled to multi-angle light-scattering (SEC-MALS)

The analysis of the molecular weight of the xylan was conducted using a size-exclusion chromatography (SEC) method described by Brown and coworkers (2009) with minor modifications (Whitehead *et al.*, 2018). The 1 and 4 M KOH fractions (1 mg) were suspended in 1 ml of 50 mM sodium acetate and filtered with 0.2 μm polytetrafluoroethylene filters. The fractions were separated by SEC (Superdex S200 10/300 GL #0805015, G.E. Healthcare), followed by analyses with Wyatt HELEOS-II multi-angle light-scattering (MALLS) detector and a Wyatt rEX refractive index detector system linked to a Shimadzu HPLC system (SPD-20A UV detector, LC20-AD isocratic pump system, DGU-20A3 degasser and SIL-20A autosampler). Data were analysed using the Astra V software. A value of 0.145 was used for sample refractive index increment (dn/dc).

2.7. Enzymatic hydrolysis of xylan and polysaccharide analysis by carbohydrate gel electrophoresis (PACE)

The enzymatic hydrolysis of destarched AIR of seedling roots and plant roots, derivatization of released oligosaccharides, carbohydrate electrophoresis, PACE gel scanning and quantification was performed as described by Goubet *et al.* (2002) and Goubet *et al.* (2009) (see **Methods S1** for a detailed description). The enzymes used for xylan digestion were: GH10 endo- β -1,4-xylanase from *Cellvibrio japonicus* (CjGH10A); GH11 endo- β -1,4-xylanase from *Neocallimastix patriciarum* (NpGH11A); GH62 α -arabinofuranosidase from *Penicillium aurantiogriseum* (PaGH62) and GH115 α -glucuronidase from *Bacteroides ovatus* (BoGH115).

2.8. Determination of total cell wall ester-linked hydroxycinnamates

To release esterified hydroxycinnamic acids from the cell walls, 700 μl of 2 M NaOH was added to 10 mg of AIR and incubated at 25 $^{\circ}\text{C}$ for 16 h. After addition of 200 μl of 10 M HCl, phenolics were partitioned three times with anhydrous ethyl ether and dried. The residue after evaporation was dissolved in acetonitrile 50% (v/v) and filtered through a 0.45 μm filter. Quantification of hydroxycinnamic acids was carried out on a HPLC system (Shimadzu[®], Tokyo, Japan) with SPD-10A UV-VIS detector. The compounds were separated at 35 $^{\circ}\text{C}$ on a C18 column (150 \times 4.6 mm, 5 μm ; Supelco Discovery[®]). The mobile phase was acetonitrile 90%/formic acid 0.1% (20/80, v/v) with a flow rate of 1.0 ml/min in isocratic mode. The

identities and quantities of the separated molecules were confirmed based on the UV signatures at 322 nm for FA and 309 nm for *p*CA, obtained in comparison with the respective standards.

2.9. Determination of hydroxycinnamate conjugates released by mild acidolysis

AIR (10 mg) was hydrolyzed with 1 ml of 50 mM TFA and incubated at 99 °C for 4 h as described by Bartley *et al.* (2013) and de Souza *et al.* (2018) with modifications. After centrifugation for 10 min at 10,000×*g*, 400 µl of TFA-supernatant was freeze-dried. The pellet was washed twice with water and acetone, and left to dry at 45 °C. Next, dried pellets and TFA-extracts were saponified with 700 µl of 2 M NaOH at 25 °C for 16 h. After acidification with 200 µl of 10 M HCl, phenolics were partitioned three times with anhydrous ethyl ether and dried. The residue after evaporation was resuspended in acetonitrile 50% (*v/v*) and filtered through a 0.45 µm filter for HPLC analysis. Released FA and *p*CA from the TFA-soluble fractions are esterified to AX and those released from the pellets are esterified to lignin fraction.

2.10. Quantitative real-time PCR

RNA was isolated from maize tissues using the RNAqueous kit (Ambion) and treated twice with a Turbo DNase-free kit (Ambion) (see **Methods S1** for a detailed description). Gene identifiers, probes and primer pairs are given in **Table S2**.

2.11. Enzymatic assays

For all the enzymatic assays, fresh tissues (1 g) were ground using ice-cooled pestle and mortar with 1.5 ml of extraction buffer (as indicated for each enzyme) for 3 min. After centrifugation (10,000×*g*, 15 min, 4 °C), the supernatant was collected and used for the enzymatic assay. The activities were expressed as nmol product min⁻¹ mg⁻¹ of fresh weight. Control experiments without substrates were performed under the same conditions to identify any endogenous compounds in the enzymatic extracts.

p-Hydroxycinnamate-CoA ligase (4CL) activity was carried out as described by Bevilaqua *et al.* (2019), using *p*-coumaric acid or ferulic acid as substrates. The extraction buffer contained 200 mM Tris-HCl (pH 7.5), 10 mM MgCl₂, 5 mM DTT and 20% glycerol (*v/v*). The reaction mixture contained 200 mM Tris-HCl (pH 7.2), 10 mM MgCl₂, 5 mM DTT, 4 mM ATP, 100 µl of protein extract, 0.4 mM *p*-coumaric acid or ferulic acid, and 0.2 mM Coenzyme A (CoA) to initiate the reaction. After the addition of CoA, the reaction was incubated at 35 °C for 10 min. The increase in absorbance at 333 nm for *p*-coumaroyl-CoA and 346 nm for feruloyl-CoA were spectrophotometrically monitored.

Hydroxycinnamaldehyde dehydrogenase (HCALDH) activity was carried out as described by Nair *et al.* (2004) and Ferro *et al.* (2020). The extraction buffer for HCALDH activity contained 50 mM Hepes-HCl (pH 8.0), 5 mM DTT, 1 mM EDTA and 10% glycerol (*v/v*). After precipitation with 70% saturated ammonium sulfate, the pellet was homogenized in extraction buffer and used as the enzyme extract. The reaction mixture contained 50 mM Hepes-HCl (pH 8.0), 5 mM DTT, 1 mM NAD⁺, 100 μ l of enzyme extract, 100 μ M coniferaldehyde (to initiate the reaction), and was incubated for 10 min at 40 °C. The reaction was terminated with the addition of 3 M HCl. After centrifugation (10,000 \times *g*, 2 min), the samples were filtered through a 0.45 μ m filter and submitted to HPLC analysis, following the same experimental conditions for the quantification of ester-linked hydroxycinnamates.

Caffeic acid 3-*O*-methyltransferase (COMT) activity was performed as described by Bevilaqua *et al.* (2019). The extraction buffer contained 100 mM Tris-HCl (pH 7.2), 0.2 mM MgCl₂, 2 mM DTT and 10% glycerol (*v/v*). The reaction mixture contained 100 mM Tris-HCl (pH 7.2), 0.2 mM MgCl₂, 2 mM DTT, 1 mM S-adenosyl-L-methionine, 200 μ l of enzyme extract, 60 μ M caffeic acid (to initiate the reaction), and was incubated for 30 min at 30 °C. The reaction was terminated by the addition of 3 M HCl. After centrifugation (10,000 \times *g*, 2 min), the samples were filtered through a 0.45 μ m filter and submitted to HPLC analysis, following the same experimental conditions for the quantification of ester-linked hydroxycinnamates.

For the activity of feruloyl esterase (FAE), the extraction was carried out in 100 mM 2-(*N*-morpholino) ethanesulfonic acid (MES) pH 6.0, 10% glycerol (*v/v*) and 0.2 g polyvinylpolypyrrolidone. The reaction mixture contained 100 mM MES (pH 6.0), 100 μ l of enzyme extract, 100 μ M methyl ferulate (to initiate the reaction), and was incubated for 30 min at 35 °C. The reaction was terminated by boiling for 3 min at 100 °C. After centrifugation (10,000 \times *g*, 2 min), the samples were filtered through a 0.45 μ m filter and submitted to HPLC analysis.

2.12. Metabolic profiling

Fresh roots of seedlings and plants (~7 mg dry weight per sample) were homogenized in liquid nitrogen and extracted with 500 μ l of methanol for 15 min at 70 °C. The methanol extract was then evaporated and the pellet dissolved in 200 μ l water/cyclohexane (1/1, *v/v*). 10 μ l of the aqueous phase was analyzed via reverse-phase Ultra High Performance Liquid Chromatography (UHPLC; Acquity UPLC Class 1 system consisting of a Sample Manager-FTN, a Binary Solvent Manager and a Column Manager, Waters Corporation, Milford, MA) coupled to negative ion ElectroSpray Ionization-Quadrupole-Time-of-Flight Mass Spectrometry (ESI-Q-ToF-MS; Vion

IMS Q-ToF, Waters Corporation) using an Acquity UPLC BEH C18 column (2.1 mm × 150 mm, 1.7 μm, Waters Corporation). Using a flow rate of 350 μl/min, a linear gradient was run from 95% aqueous formic acid (0.1%, buffer A) to 50% acetonitrile (0.1% formic acid, buffer B) in 30 min, followed by a concave gradient (curve 3) in 10 min to 100% buffer B. Full MS spectra (m/z 50 – m/z 1,500) were recorded at a scan rate of 10 Hz.

Integration and alignment of the m/z features were performed via Progenesis QI software version 2.1 (Waters Corporation). Peak picking was based on all runs with a sensitivity set on ‘automatic’ (value = 5). The normalization was set on ‘external standards’ and was based on the dry weight of the samples (Morreel *et al.*, 2006). The precursor ion search (10 ppm tolerance) was based on a compound database constructed via instant JChem (ChemAxon, Hungary), whereas MS/MS identities were obtained by matching against an in-house mass spectral database (200 ppm fragment tolerance). Using R vs 3.4.2., m/z features representing the same compound were grouped following the algorithm described by Morreel and coworkers (2014). Abundance values that were lower than the detection threshold, and ‘NA’s were replaced randomly by either 1 or 2. Differential m/z features were defined as those for which the abundance was (i) significantly different and (ii) at least two-fold changed between control and salt-stressed plants.

2.13. Determination of lignin content and composition

Lignin content was determined by the acetyl bromide method and the monomeric composition was assessed using alkaline nitrobenzene oxidation as described by Moreira-Vilar *et al.* (2014) with modifications (see Methods S1 for a detailed description).

2.14. Cell wall characterization by two-dimensional NMR

The whole-cell walls of maize tissues were characterized using two-dimensional heteronuclear single-quantum coherence NMR (2D-HSQC-NMR) at solution state as previously described (Kim *et al.*, 2008; Rencoret *et al.*, 2009) (see **Methods S1** for a detailed description). 2D-HSQC-NMR cross-signals were assigned by literature comparison (Fornalé *et al.*, 2017; Kim *et al.*, 2017). Assignments of the lignin and protein $^1\text{H}/^{13}\text{C}$ correlation signals in the 2D-HSQC-NMR spectra from the whole cell walls are given in **Table S3**.

2.15. Statistical analysis

In the experiments with maize seedlings, each biological replicate (n) consisted of a bulk containing 25 seedlings, whereas in the experiments with maize plants, each biological replicate consisted of a bulk containing six plants. The two-sample Student’s t -test (two-tailed

distribution) was applied to compare control and salt-treated samples. Statistical significance was defined as * $0.05 \geq P > 0.01$, ** $0.01 \geq P > 0.001$, and *** $P \leq 0.001$.

3. Results

3.1. Salt stress induces changes in plant growth and cell wall polysaccharides

To investigate the chemical nature and structural features of the cell walls of maize tissues exposed to salt stress, we cultivated seedlings for three days and plants for 12 days on control and 200 mM NaCl conditions. In seedlings, we studied the roots (S-roots) and in plants, we studied the roots, stems and leaves. The phenotypic response of seedlings and plants showed a significant restriction of the growth (**Fig. 1a**). Notably, salt stress promoted reductions in all the growth parameters (length, fresh biomass, dry biomass, and relative water content) in S-roots, and roots, stems and leaves of plants (**Fig. S4**). The amounts of thiobarbituric acid reactive substances (TBARS) significantly increased in all the salt-stressed tissues, suggesting oxidative damage caused by salt stress on maize tissues.

We then prepared the alcohol insoluble residue (AIR) and analyzed the cell wall composition using state-of-the-art analytical tools (see **Fig. S3** for details). First, the AIR was subjected to Fourier transform infrared (FTIR) spectroscopy to verify the similarities in cell wall composition between the samples (Marriot *et al.*, 2016). Principal component analysis (PCA) of the FTIR data showed a clear separation between spectra derived from control and NaCl-treated samples, with S-roots from seedlings exposed to salinity showing the most extreme separation (**Fig. 1b**). The corresponding loading plots show the contribution of each wavelength to the separation of the samples on each principal component (PC). The loading plots for PC1 and PC2 (**Fig. 1c**) revealed two large peaks at wavelengths corresponding to C–O and C–O–C stretching assigned to cell wall polysaccharides ($950\text{--}1,100\text{ cm}^{-1}$) and C=C stretching and aromatic skeletal vibrations assigned to lignin ($1,510\text{--}1,630\text{ cm}^{-1}$) (Oliveira *et al.*, 2020).

The amount of crystalline cellulose measured by the anthrone-sulfuric acid method in AIR of plant roots and stems was significantly reduced (-11% and -29% , respectively) upon salt stress, while that of S-roots and leaves was similar to that of the corresponding controls (**Fig. 1d**). We also observed a reduction in matrix polysaccharide content of S-roots (-24%) and roots of plants (-18%) as compared to respective controls. Conversely, in leaves, the matrix polysaccharide content was increased by 18% , whereas no significant differences were observed in matrix polysaccharide content in stems upon NaCl exposure.

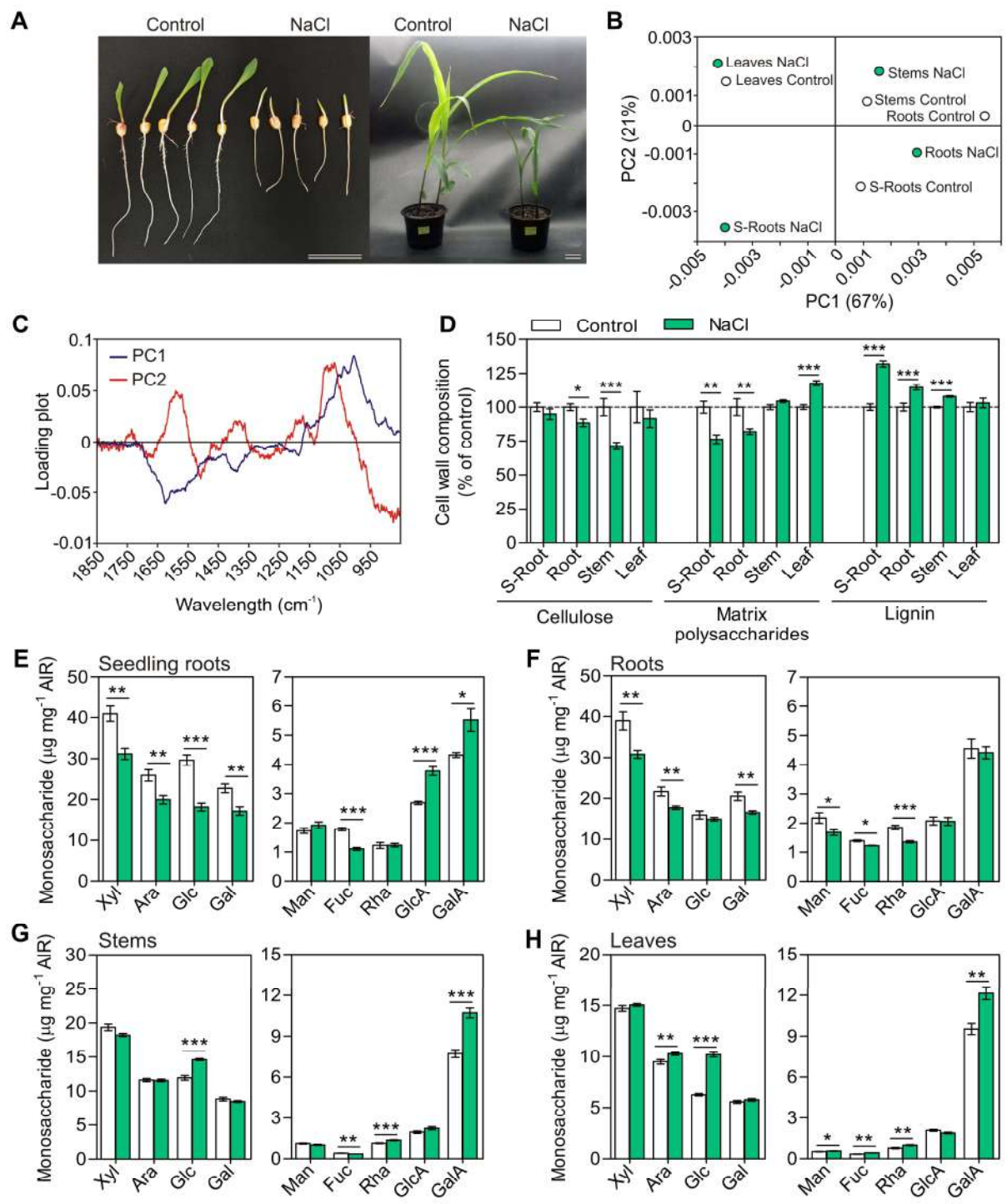


Figure 1. Phenotype of maize seedlings and plants and chemical characterization of cell walls affected by salt stress. (A) Representative images of seedlings and plants indicating the suppression of growth under 200 mM NaCl conditions. Scale bar = 5 cm. (B) Principal component analysis (PCA) of baseline corrected and peak normalized FTIR spectra and (C) loading plots of PC1 and PC2 from the PCA ($n = 3$ biological replicates). (D) Cellulose, matrix polysaccharides and lignin contents expressed as percentage of control plants. (E-H) Non-cellulosic monosaccharide composition of alcohol insoluble residue (AIR). Xyl, xylose; Ara, arabinose; Glc, glucose; Gal, galactose; Man, mannose; Fuc, fucose; Rha, rhamnose; GlcA, glucuronic acid; GalA, galacturonic acid; S-Root, seedling root; Error bars represent SEM, $n = 7$ biological replicates. * $0.05 \geq P > 0.01$, ** $0.01 \geq P > 0.001$, and *** $P \leq 0.001$, unpaired two-sided t -test.

Analysis of the matrix polysaccharide composition revealed that the major glycosyl residues were xylose (26–35%), arabinose (17–20%) and glucose (15–22%) (**Fig. S5**). We found significant changes in the monosaccharide profiles in S-roots and plant roots in response to salinity. **Fig. 1e, f** shows a marked decrease of 18–24% in xylose and arabinose contents in S-roots and plant roots. In stems, neither xylose nor arabinose contents were altered by salt-stress, whilst in leaves only arabinose increased (11%) (**Fig. 1g, h**). In addition, exposure to NaCl reduced the glucose content in S-roots (–39%), whereas higher levels of glucose were observed in stems (22%) and leaves (62%). The abundance of several other monosaccharides, including galactose, fucose, mannose, rhamnose, glucuronic and galacturonic acids, which are derived from less abundant polysaccharides in maize cell walls, were also significantly altered by NaCl treatment.

2.2. Salt-stressed roots exhibit reduced arabinoxylan content

To determine structural shifts in xylan of S-roots and plant roots, the destarched AIR was sequentially extracted with CDTA and Na₂CO₃ to remove pectins, followed by extraction with 1 and 4 M KOH to produce the xylan-enriched fractions. Monosaccharide analysis of 1 and 4 M KOH fractions revealed lower levels of xylose (–18% to –24%) and arabinose (–19% to –23%) in stressed S-roots and plant roots when compared with those of controls (**Fig. 2a**). The decrease in xylose in the xylan fractions was highly correlated with the decrease in arabinose (Pearson's correlation, $r = 0.984$, $P < 0.0001$). The ratios of xylosyl to arabinosyl substitutions in grass xylans can vary from 2:1 to 30:1, depending on the tissue and developmental stage of the specific grass evaluated (Hatfield *et al.*, 2017). Our analysis revealed that xylans of maize roots have a high degree of arabinosyl substitutions, with xylose/arabinose ratio between 1.6/1 to 1.9/1. Nevertheless, no differences were observed between the xylose/arabinose ratios of xylans extracted from salt-stressed and control roots.

We next examined whether salt stress led to a reduced abundance of AX or the chain length of AX molecules using size-exclusion chromatography coupled to a multi-angle light scattering detector (SEC-MALS) of 1 M and 4 M KOH xylan-enriched fractions (**Fig. 2b**). The average chain lengths of AXs were not different between control and salt-stressed S-roots and plant roots. Although it was difficult to establish the difference in AX abundance between S-roots control and salt-treated in 1 M KOH fractions due to the high baseline, the peak at 16 min in 1 M KOH fractions and at 16 min and 41 min in 4 M KOH fractions indicated that the abundances of AXs from stressed roots were lower compared to the respective controls.

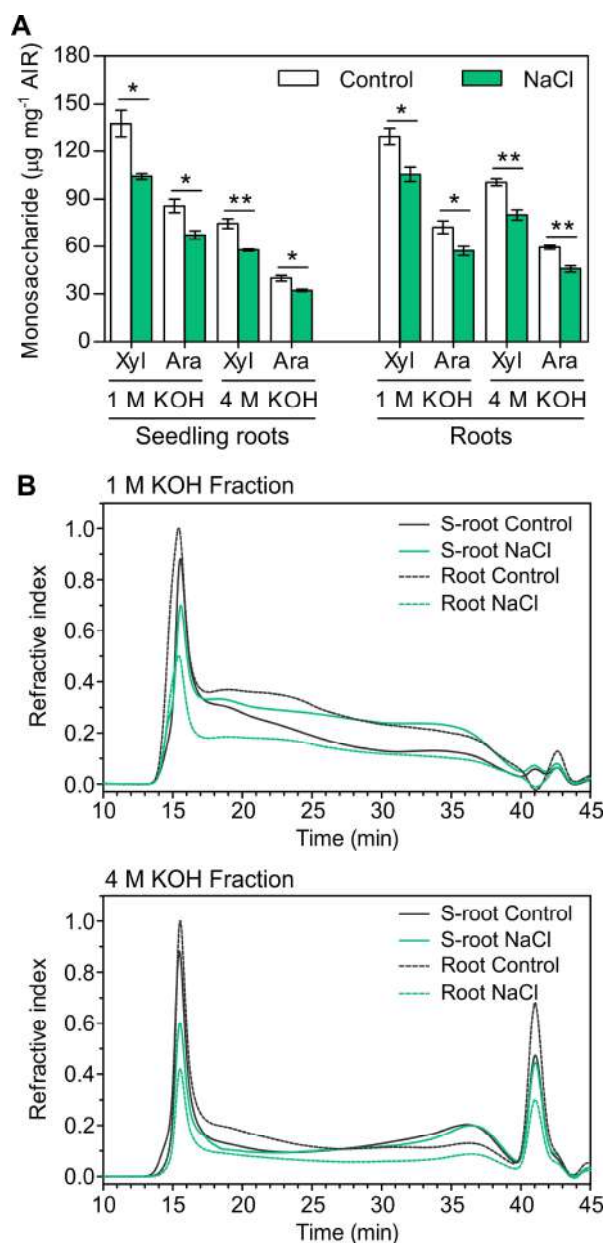


Figure 2. Cell walls of seedling roots and plant roots exhibit reduced arabinoxylan content in response to salinity. (A) Xylose and arabinose amounts in the 1 M KOH and 4 M KOH cell wall fractions of seedling roots (S-roots) and plant roots during exposition to 200 mM NaCl. Error bars represent SEM. * $0.05 \geq P > 0.01$, ** $0.01 \geq P > 0.001$, and *** $P \leq 0.001$, unpaired two-sided t-test. (B) SEC-MALS analysis of xylan chain length in 1 M KOH and 4 M KOH fractions ($n = 4$ biological replicates). Data shown are representative of the results obtained for all KOH extracts.

Further analysis of the anomeric regions of the two-dimensional heteronuclear single quantum coherence NMR (2D-HSQC-NMR) spectra of S-roots and plant roots confirmed the decrease in AX content in response to salinity (**Fig. 3a**). The NMR data also confirmed that the relative abundances of xylosyl and arabinosyl residues remained constant in the controls and the stressed roots, suggesting that the AX structure was maintained upon salt stress. We also performed a polysaccharide analysis by carbohydrate gel electrophoresis (PACE) to determine whether changes in AX content had concomitant changes in its decorations. AIRs of S-roots and plant roots were separately digested with glycosyl hydrolase (GH) family 10 and 11 endo- β 1,4-xylanases, followed by hydrolysis with GH62 α -arabinofuranosidase or GH115 α -glucuronidase, and the resulting oligosaccharides were analyzed by PACE (**Fig. 3b**). Compared to the controls, salt-stressed S-roots and plant roots had no significant differences in the pattern

of oligosaccharides released by xylanases. The intensity of each band and the number of fragments were similar for control and NaCl-treated roots. Although PACE analysis revealed no significant changes in quantity and structure of the xylanase digestible fraction of AX, the monosaccharide analysis, SEC-MALS and 2D-NMR results supported an overall reduction in AX quantity.

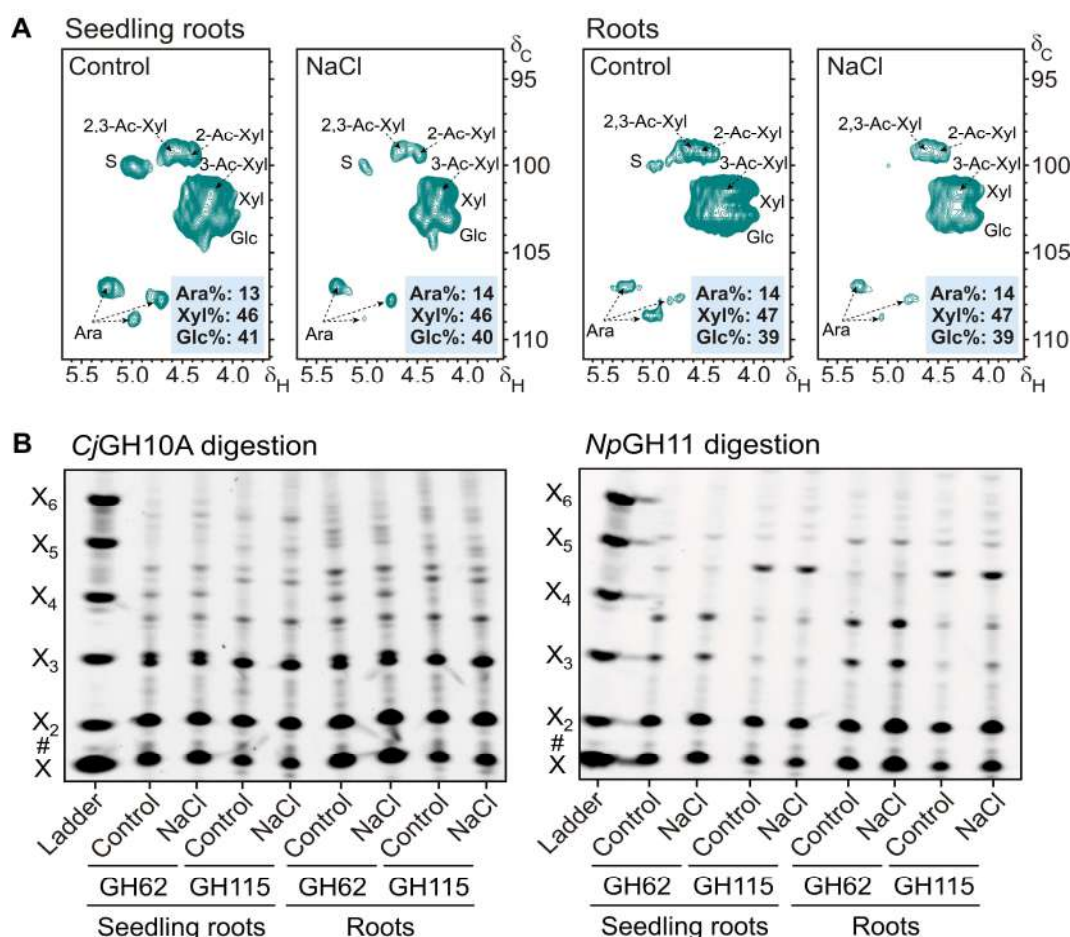


Figure 3. Structural characterization of arabinoxylans from seedling roots and plant roots. (A) 2D- HSQC-NMR spectra of whole-cell walls showing anomeric carbons of non-cellulosic polysaccharides (Xyl: β -D-xylopyranoside; 2-Ac-Xyl: 2-*O*-acetyl- β -D-xylopyranoside; 3-Ac-Xyl: 3-*O*-acetyl- β -D-xylopyranoside; 2,3-Ac-Xyl: 2,3-di-*O*-acetyl- β -D-xylopyranoside; Ara: α -L-arabinofuranoside; Glc: β -D-glucopyranoside; S: residual starch). The spectra were normalized to the same intensity of the DMSO signals, since the same DMSO volume and amount of sample were used in all cases. (B) Digestion of cell walls of seedling roots (S-roots) and plant roots with *CjGH10A* and *NpGH11* analyzed by PACE. Ladder: xylose (X1) to xylohexose (X6). # indicates background bands. Representative gel of three independent experiments is shown.

3.3. Salinity modulates cell wall-esterified FA and *pCA*

The total content of cell wall ester-linked FA and *pCA* was determined by saponification with 2 M NaOH followed by RP-HPLC analysis to evaluate the effects of salt stress on cell wall feruloylation and *p*-coumaroylation. Our data show that salt exposure reduced the esterified FA levels by \sim 30% in S-roots and plant roots, compared to the controls (Fig. 4a). By

contrast, the stems of salt-stressed plants had ~80% more esterified FA in comparison to the control, whereas no significant differences were observed in leaves. Ester-linked *p*CA decreased in stressed S-roots (-31%) and stems (-25%), while esterified *p*CA was not significantly affected in plant roots and leaves (**Fig. 4b**).

In grass cell walls, FA and *p*CA (at lower levels) are esterified at the xylan *O*-5 position of α -(1,2) or α -(1,3)-*Araf* residues (Hatfield *et al.*, 2017). To gain further insight into the nature of the modulation of *Araf*-bound FA and *Araf*-bound *p*CA levels in response to salt stress, the AIR was subjected to mild acid hydrolysis in 50 mM TFA to leave the *Araf* residues esterified to FA or *p*CA (the FA-*Araf* or *p*CA-*Araf*) followed by saponification and analysis. The content of FA esterified to AX followed the same modulation pattern as found for total ester-linked FA: salt exposure decreased the FA levels in S-roots and plant roots by 38% and 50%, respectively (**Fig. 4c**), albeit an 82% increase was observed in stems, and no significant difference was observed in leaves. In contrast, salt exposure reduced the *p*CA content esterified to AX only in S-roots (-34%) (**Fig. 4d**). Accordingly, the reductions in FA esterified to AX were strongly correlated with the reduction in xylose (Pearson's correlation, $r = 0.922$, $P < 0.0011$) and arabinose ($r = 0.962$, $P < 0.0001$) from xylan fractions (**Fig. 2a**). There was, however, no significant correlation between *p*CA esterified to AX with xylose ($r = 0.575$, $P = 0.136$) or arabinose ($r = 0.443$, $P = 0.271$). We also examined the ratios between arabinose/FA-*Araf* in response to salinity. In S-roots, arabinose/FA-*Araf* ratio increased from 17.6/1 (control samples) to 22.1/1 (salt-stressed samples), with similar increase in plant roots, from 13.9/1 to 22.4/1. Differently, stems reduced the ratio from 18.7/1 to 10.2/1, while leaves exhibited no significant difference (9.4/1 to 9.6/1).

The analysis of alkali-released FA and *p*CA from the remaining TFA-insoluble residue showed that ~80% of the ester-linked FA of maize cell walls was associated with AX, albeit ~20% of FA remained in the lignin fraction. The reverse was observed for *p*CA, with 77–94% of the *p*CA remaining in the pellet, mostly linked to lignin, whereas only 6–23% of *p*CA was esterified to AX fraction. Furthermore, the amounts of FA in the lignin fractions were not altered in response to salt stress (**Fig. 4e**), whereas the amounts of *p*CA in the pellets were reduced by ~30% in S-roots and plant stems (**Fig. 4f**). Taken together, the reduction in FA content in S-roots and plant roots and the increase in stems occurred in the AX fraction but not in the lignin fraction, suggests that salinity modulates the incorporation of FA to the *Araf* residues of AX.

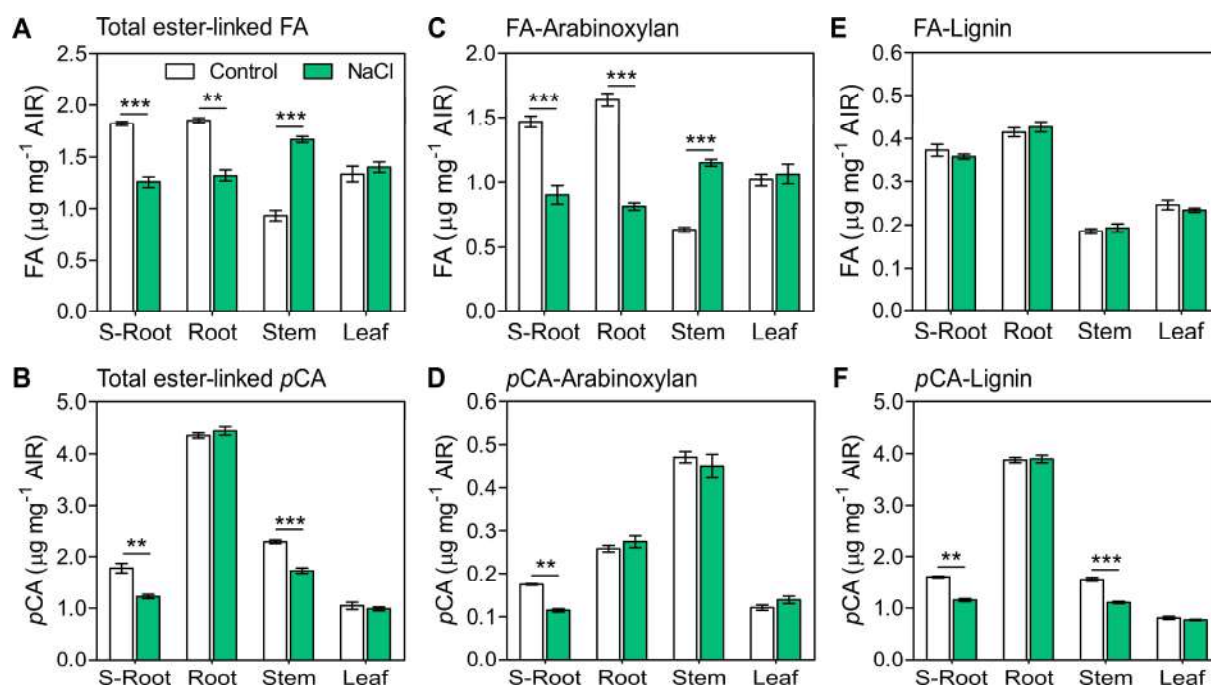


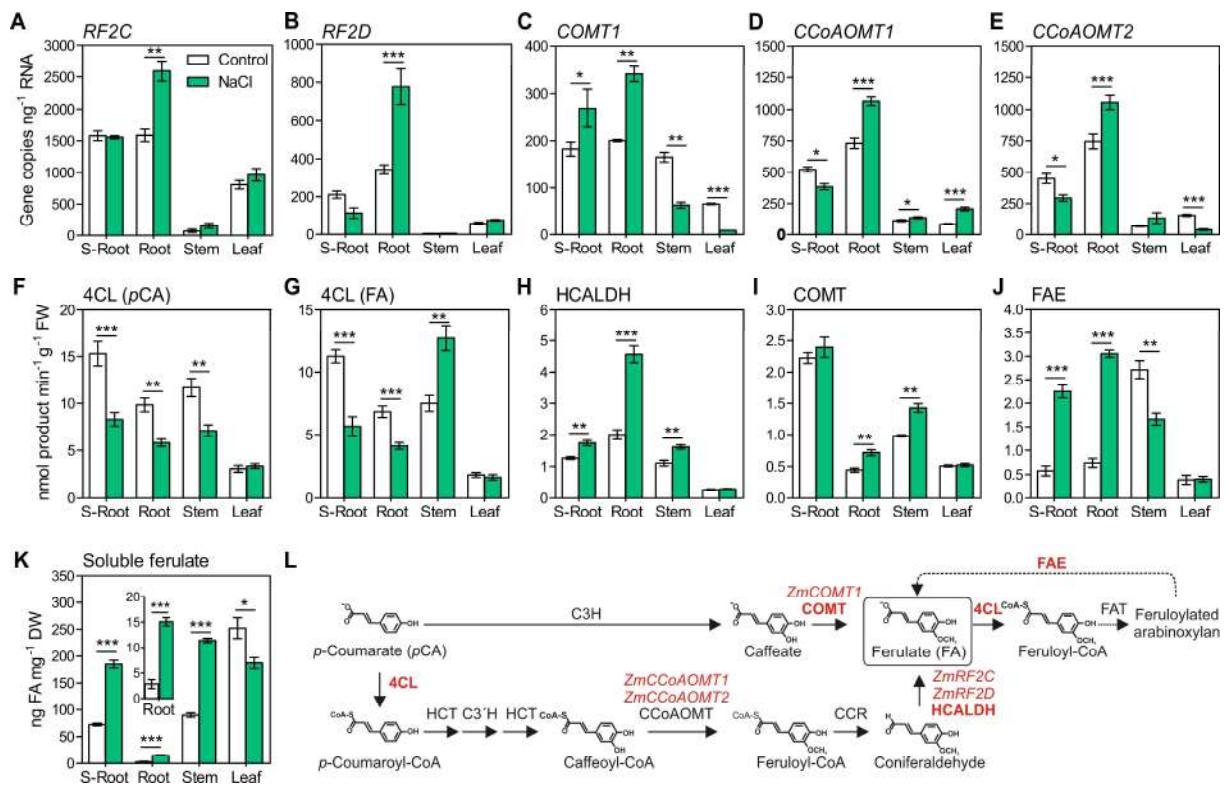
Figure 4. Modulation of cell wall ester-linked hydroxycinnamates in response to salt stress. (A,B) Total ester-linked FA and *pCA*. **(C,D)** FA and *pCA* esterified to AX. **(E,F)** FA and *pCA* esterified to lignin. AIR, alcohol insoluble residue; S-Root, seedling roots. Error bars represent SEM, $n = 5$ biological replicates. * $0.05 \geq P > 0.01$, ** $0.01 \geq P > 0.001$, and *** $P \leq 0.001$, unpaired two-sided *t*-test.

3.4. Salt stress induces the biosynthesis and accumulation of ferulic acid

In order to elucidate the molecular basis of the modulation in cell wall ester-linked FA content, we further investigated the changes in the expression of genes and the activity of enzymes required to FA biosynthesis in seedlings and plants exposed to salinity. Genes encoding hydroxycinnamaldehyde dehydrogenase (*RF2C* and *RF2D*), caffeoyl-CoA 3-*O*-methyltransferase (*CCoAOMT1* and *CCoAOMT2*) and caffeic acid 3-*O*-methyltransferase (*COMT1*) were differentially expressed in response to salt stress (**Fig. 5a-e**). Although S-roots had no significant differences in *RF2C* and *RF2D* transcript levels in response to salt stress, the plant roots of salt-stressed plants showed higher *RF2C* (64%) and *RF2D* (126%) transcript levels compared to control plants (**Fig. 5a,b**). Stems and leaves displayed similar transcript levels of *RF2C* and *RF2D* in control and stressed plants. The transcript abundance of *COMT1* was higher in stressed S-roots (47%) and roots (70%), and lower in stems (−62%) and leaves (−85%) (**Fig. 5c**). Whereas *CCoAOMT1* and *CCoAOMT2* expression were ~30% lower in stressed S-roots, their levels were ~45% higher in plant roots (**Fig. 5d,e**). Overall, our qPCR-based data suggest that FA biosynthesis is upregulated mainly in plant roots in response to salt stress.

Next, we found that the activity of *p*-hydroxycinnamate-CoA ligase (4CL), which catalyzes the ATP-dependent activation of *pCA* to *p*-coumaroyl-CoA, was changed upon salt stress when using *pCA* as substrate (**Fig. 5f**). Relatively higher activity was observed for 4CL

compared to the other enzymes. Salt stress reduced 4CL activity by ~40% in S-roots, roots and stems. We also evaluated the 4CL activity using FA as the substrate. 4CL activity for the formation of feruloyl-CoA was 50% lower in stressed S-roots and 40% lower in plant roots, while stressed stems presented ~70% higher activity, compared to controls (Fig. 5g). Accordingly, 4CL activity followed the similar pattern as found for total ester-linked FA and FA esterified to AX. Hydroxycinnamaldehyde dehydrogenase (HCALDH) and COMT activities were higher in response to salt stress in plant roots and stems. In salt-stressed tissues, HCALDH activity increased by 38% in S-roots, 128% in plant roots and 45% in stems, compared to control plants (Fig. 5h). Similarly, COMT activity increased by 60% and 45% in salt-stressed plant roots and stems, respectively (Fig. 5i), with no significant differences in S-roots. Leaves had similar levels of 4CL, HCALDH and COMT activities in control and stressed plants.



Feruloyl esterase (FAE) hydrolyzes the ester-linkage between FA and the Araf residue of AX (Oliveira *et al.*, 2019). Salt stress strongly increased the FAE activity by ~300% in S-roots and plant roots, while it decreased by 40% in stems (**Fig. 5j**). The inverse relation between 4CL (using FA as substrate) and FAE activities observed in S-roots, and plant roots, suggests a regulatory mechanism between cell wall feruloylation and deferuloylation processes. The upregulation of genes and enzymes involved in FA biosynthesis increased the cytosolic FA levels by ~150% in salt-stressed S-roots and stems, and by 430% in plant roots (**Fig. 5k,l**).

3.5. Phenolic profile changes following salt exposure

Because FA biosynthesis was markedly induced by salt treatment in S-roots and plant roots, we investigated possible shifts in the phenolic profiles in response to salinity via reverse-phase UHPLC-ESI-Q-ToF-MS of methanol extracts. The differential compounds in each data set are displayed in **Table 1** and **2**. A total of 16,159 peaks (mass-to-charge ratio [m/z] features) were integrated and aligned across all chromatograms. The PCA analysis of metabolites measured by untargeted metabolomic profiling showed significant differences between control and salt-treated samples (**Fig. 6a**). PC1 (explaining 29% of the variance) discriminated the phenolic profiles of S-roots and plant roots, while PC2 (explaining 19% of the variance) provided separation of the profiles of S-roots control from the other profiles (S-roots NaCl, plant roots control and NaCl).

Table 1. Differential phenolic compounds in seedling roots. Characterization of the compounds is based on MS/MS fragmentation spectra. Peak area is expressed in counts. $n = 8$ biological replicates. RT, retention time. The detection limit was set at a peak intensity of 100 counts.

Compound	m/z	RT (min)	Control (mean)	NaCl	Fold change	P (t test)
4- <i>O</i> -Feruloyl quinic acid	367.1031	6.58	423	3004	7.10	1.3E-04
3- <i>O</i> -Feruloyl quinic acid	367.1032	4.60	2232	9779	4.38	1.9E-04
Sinapoyl hexose	385.1137	5.40	4371	2089	0.48	2.6E-07
DIMBOA glucoside	372.0931	5.81	17567	7909	0.45	1.1E-04
Syringoyl sinapoyl hexose	565.1553	5.81	1080	469	0.43	4.2E-04
DIMBOA glucoside	372.0933	4.50	8520	3593	0.42	5.2E-05
Apigenin-6,8- <i>C</i> -dihexoside	593.1502	5.90	1009	389	0.39	7.7E-04
Feruloyl hexose	355.1032	5.21	6575	2216	0.34	3.8E-06
Tricin + hexuronic acid + pentose	637.1398	10.77	514	170	0.33	1.5E-05
DIMBOA + hexose + hexose	534.1456	5.62	2485	806	0.32	2.5E-05
Isorhamnetin hexoside deoxyhexoside	623.1605	10.02	1658	313	0.19	1.0E-04
Vanilloyl hexose	329.0873	3.07	2513	310	0.12	1.6E-11

Table 2. Differential phenolic compounds in plant roots. Characterization of the compounds is based on MS/MS fragmentation spectra. Peak area is expressed in counts. $n = 8$ biological replicates. RT, retention time. The detection limit was set at a peak intensity of 100 counts.

Compound	m/z	RT	Control (mean)	NaCl	Fold change	P (t test)
Feruloyl hexose	355.1032	5.21	86	628	7.34	4.2E-04
3- <i>O</i> -Feruloyl quinic acid	367.1032	4.60	1000	6667	6.66	1.0E-04
DIMBOA glucoside	372.0933	4.50	644	2793	4.34	1.4E-07
Sinapoyl hexose	385.1137	5.40	412	1625	3.94	2.8E-05
4- <i>O</i> -Feruloyl quinic acid	367.1031	6.58	354	1304	3.68	5.2E-04
Sinapoyl hexose + 226 kDa	611.1966	7.99	223	788	3.53	2.4E-06
Sinapoyl hexose + 210 kDa	595.2023	9.25	1318	4517	3.43	4.7E-07
HBOA-2- <i>O</i> -hexoside	326.0877	4.40	1393	636	0.46	9.8E-04
Azelaic acid	187.0973	10.79	764	244	0.32	2.8E-06
9,12,13-Trihydroxy-10(E)-octadecadienoic acid	329.2328	20.05	1140	324	0.28	4.2E-04
Hydroxybenzoic acid hexoside	599.1603	1.79	1207	331	0.27	8.9E-05
9,12,13-Trihydroxy-10(E),15(Z)-octadecadienoic acid	327.2171	18.27	994	167	0.17	1.4E-04
Trihydroxy-octadecadienoic acid	329.2330	19.93	3852	613	0.16	1.7E-04

Data sets of S-roots and plant roots presented 175 and 86 differentially abundant compounds caused by salt stress, respectively. From those, 19 were found in common between both data sets. In the data set of S-roots, 60 compounds increased and 115 decreased in the salt-stressed samples when compared with control samples. In plant roots, 20 compounds increased, and 66 compounds decreased in salt-stressed tissues. Comparative analysis of the 19 differential compounds in common between both data sets, five were increased in response to salinity including 4-*O*-feruloyl quinic acid (7-fold in S-roots and 4-fold in plant roots) and 3-*O*-feruloyl quinic acid (4-fold in S-roots and 7-fold in plant roots) (**Fig. 6b**). Ten common differential compounds decreased due to salt stress in both data sets and four decreased in the S-roots but increased in the roots data set due to salt stress. Among them, sinapoyl hexose (~0.5-fold in S-roots and 4-fold in roots), DIMBOA glucoside (0.4-fold in S-roots and 4-fold in roots) and feruloyl hexose (0.3-fold in S-roots and 7-fold in roots). Furthermore, feruloyl quinic acid isomers were consistently higher under salt stress, whereas the hexosylated phenylpropanoids were lower in the data set of S-roots but restored to normal levels or were even up in the data set of plant roots. Therefore, our new findings revealed that salt stress stimulated the accumulation of FA and its derivatives, 3- and 4-*O*-feruloyl quinic acid.

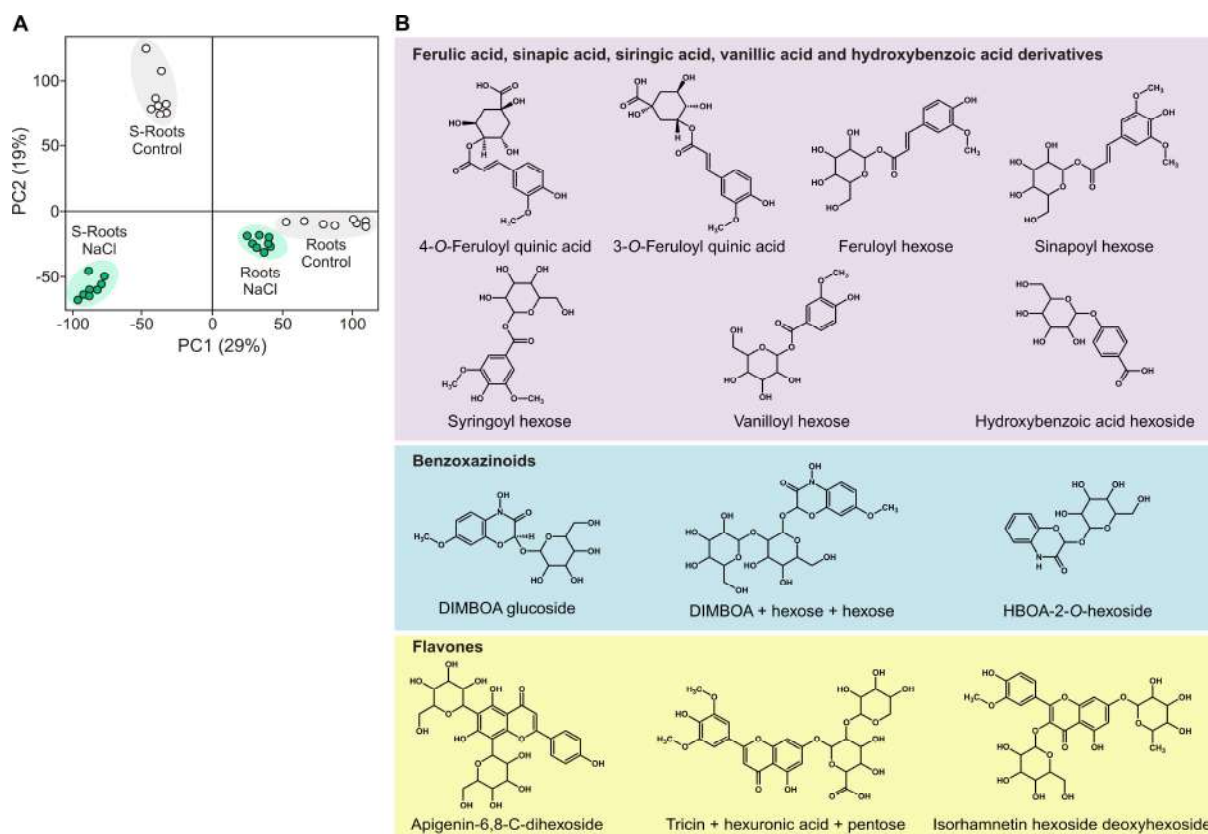


Figure 6. Phenolic profiles of seedling roots and plant roots during salt exposure. (A) Principal component analysis (PCA) of the untargeted phenolic profiling using UHPLC-ESI-Q-ToF-MS negative ion mode and **(B)** structures of metabolites differentially expressed upon salinity presented in Tables 1 and 2. Data represent eight biological replicates of pools of roots.

3.6. Salt stress increases lignin content and incorporation of S-units

To investigate the impact of salt stress on lignification, we determined the lignin content and its monomeric composition. Determination of lignin content using the acetyl bromide method revealed that stressed S-roots, plant roots and stems had 32%, 15% and 8% more lignin than the controls, respectively (**Fig. 1d**). No change in lignin content was observed in plant leaves after NaCl treatment.

We next examined the lignin composition using nitrobenzene oxidation. Compared to controls, the total monomeric yields (G+S) was higher in stressed S-roots, roots and stems, organs that also had increases in lignin amount (**Table 3**). Salt stress increased the amount of S-unit in all the organs (from 21% to 147%), and to a lesser extent, the amount of G-lignin (from 7% to 72%). The mol % of S-unit increased by 37% in S-roots and by 27% in plant roots, whereas the mol % of G-unit slightly decreased by ~12% in S-roots and plants roots, indicating that salt stress increased the incorporation of S-units. The increase in S-lignin upon salt stress caused an increase in the S/G ratios, which were ~50% higher in S-roots and plant roots, when compared with the respective controls.

Table 3. Lignin monomeric composition of control and salt-stressed maize tissues determined by alkaline nitrobenzene oxidation. AIR, alcohol insoluble residue; G, guaiacyl unit; S, syringyl unit. Values of difference indicate significantly increased or decreased percentage, as compared with those of respective control. $n = 5-6$. * $0.05 \geq P > 0.01$, ** $0.01 \geq P > 0.001$, and *** $P \leq 0.001$, unpaired two-sided t -test.

Plant material	Treatment	G	S	G+S	G	S	S/G ratio
		($\mu\text{g mg}^{-1}$ AIR)	($\mu\text{g mg}^{-1}$ AIR)	($\mu\text{g mg}^{-1}$ AIR)	(mol %)	(mol %)	
Seedling roots	Control	4.27 \pm 0.14	1.74 \pm 0.08	6.01 \pm 0.08	74.56 \pm 1.12	25.44 \pm 1.12	0.34 \pm 0.02
	NaCl	4.67 \pm 0.06	2.99 \pm 0.10***	7.65 \pm 0.13***	65.23 \pm 0.82***	34.77 \pm 0.81***	0.53 \pm 0.02***
	Difference (%)	9	72	27	-13	37	56
Roots	Control	4.51 \pm 0.23	2.29 \pm 0.14	6.80 \pm 0.34	70.29 \pm 0.81	29.71 \pm 0.81	0.42 \pm 0.02
	NaCl	7.78 \pm 0.30***	5.65 \pm 0.18***	13.43 \pm 0.42***	62.24 \pm 0.92***	37.76 \pm 0.92***	0.61 \pm 0.02***
	Difference (%)	72	147	97	-11	27	45
Stems	Control	5.65 \pm 0.15	2.93 \pm 0.04	8.58 \pm 0.16	69.76 \pm 0.61	30.24 \pm 0.62	0.43 \pm 0.01
	NaCl	6.31 \pm 0.32*	3.63 \pm 0.09***	9.94 \pm 0.27**	67.33 \pm 1.45	32.67 \pm 1.45	0.48 \pm 0.03
	Difference (%)	12	24	16	-3	8	12
Leaves	Control	2.81 \pm 0.21	0.80 \pm 0.04	3.61 \pm 0.22	80.51 \pm 1.60	19.49 \pm 1.60	0.24 \pm 0.01
	NaCl	3.02 \pm 0.19	0.97 \pm 0.06*	3.98 \pm 0.25	78.84 \pm 0.54	21.16 \pm 0.53	0.27 \pm 0.04
	Difference (%)	7	21	6	-2	9	13

To further explore the lignin compositional shifts, whole-cell walls were analyzed by 2D-HSQC-NMR at the gel-state (Kim *et al.*, 2008; Rencoret *et al.*, 2009). The aromatic/unsaturated regions (δ_C/δ_H 90–150/5.90–7.90) of the 2D-HSQC-NMR spectra, together with the main substructures identified, are shown in **Fig. 7**. The cross-signals assigned in the HSQC spectra are listed in **Table S3**. The intensities of the lignin signals, and particularly those of the S-units, increased in cell walls submitted to salt stress of S-roots and plant roots, consistent with the total monomeric yields observed by nitrobenzene oxidation and the higher lignin content. The magnitude of the increase in S-units estimated from the normalized integrals (24–37%) was quite similar to that estimated biochemically (27–37%) for roots of seedlings and plants. In general, the NMR data largely corroborated the data obtained by nitrobenzene oxidation analysis, indicating a higher deposition of S-units in lignin of S-roots and plant roots in response to salt stress and, consequently, an overall increase in the S/G ratios. In accordance with the biochemical determination, the total FA identified by 2D-NMR was reduced by 48% in S-roots and by 39% in plant roots, and increased by 75% in stems, in response to salt stress. The cross-signals corresponding to H-lignin units overlapped with intense signals of phenylalanine residues from proteins. Therefore, the relative abundance of H-units could not be determined. Signals for tricetin, a flavone that is incorporated into the lignin of grasses (del Río *et al.*, 2012; Lan *et al.*, 2015), were observed in the HSQC spectra of the aerial parts of the plants (stems and leaves) but were absent in roots of seedlings and plants. Nevertheless, no major differences were observed in the relative abundances of tricetin in stems and leaves of plants grown under salt stress, compared to the controls.

4. Discussion

Plant cell wall composition and metabolism are dynamically regulated in response to a variety of environmental stresses. Our data represents the first detailed study of changes in cell wall polysaccharides, feruloylation, lignification and phenolic metabolism upon exposure to salinity in a grass species. Salt stress modulated the deposition of cellulose, matrix polysaccharides and lignin in tissues of roots and stems of maize (see **Table 4** for the summary of the main alterations in response to salinity). We show reductions of AX content and its feruloylation triggered by salinity, followed by increases in lignin amounts and the incorporation of S-units in S-roots and plant roots. The expression of genes and enzyme activities enrolled in phenylpropanoid biosynthesis were modified by salinity in a consistent manner with the structural changes observed in each studied organ. **Fig. 8** shows a model of

grass cell wall biosynthesis integrating the extensive cell wall remodeling in response to salinity.

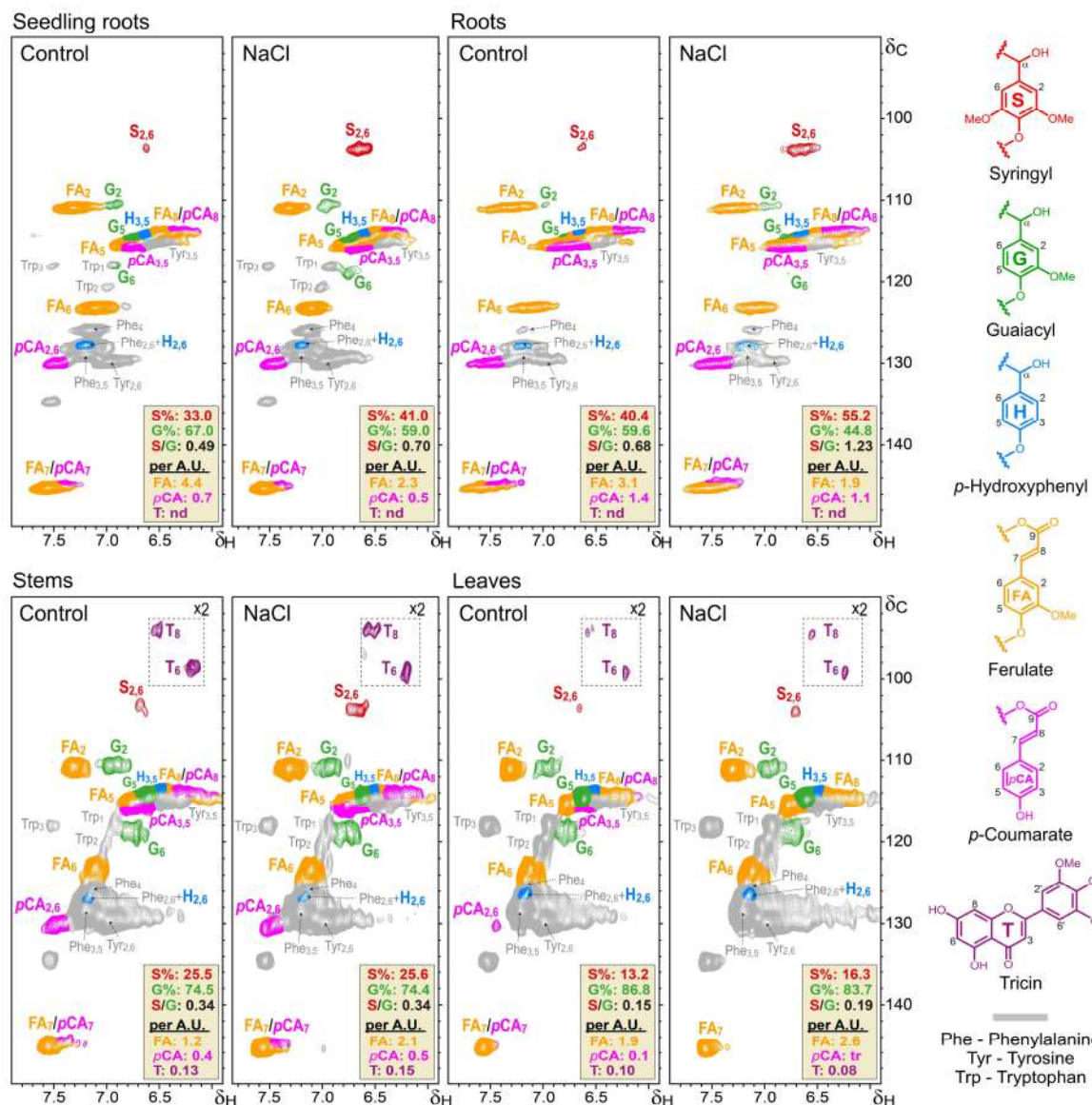


Figure 7. 2D-HSQC-NMR spectra (δ_C/δ_H 90–150/5.90–7.90) of whole-cell walls of maize tissues submitted to salt stress. The colors of the main lignin structures identified in the NMR spectra match those of the corresponding signals. The signal intensities corresponding to triclin in the framed areas are amplified at twice the intensity.

Our data indicate that different tissues respond differently to salinity. Although maize leaves had significant reductions of growth parameters (**Fig. S4**), they presented subtle alterations in cell wall composition triggered by salt stress (**Table 4**). The effects were restricted to a slight increase in the content of matrix polysaccharides, arabinose, glucose, and the frequency of S-units in lignin assessed by 2D-NMR. In turn, S-roots, plant roots and, to a lesser extent the stems, exhibited more significant changes in their cell walls. In addition to increased

lignin content, stressed S-roots and plant roots showed a significant reduction in the content of xylose, arabinose, galactose and FA. Given that roots are the first organ confronted with salinity, the effects of exposure to high concentrations of salt and the ions Na^+ and Cl^- are expected to be more evident in roots than in aerial parts of the plant (Farooq *et al.*, 2015; Dinneny, 2019).

Despite the recent progress in our understanding of cell wall feruloylation (Bartley *et al.*, 2013; Buanafina *et al.*, 2016; de Souza *et al.*, 2018; de Souza *et al.*, 2019), the modulation of this process in response to abiotic stress is still not well understood. In wheat coleoptiles, osmotic stress suppresses cell wall stiffening and reduces the total FA content (Wakabayashi *et al.*, 1997). Later work demonstrated that an increase in FA content in maize cell walls in response to salt stress is associated with the suppression of shoot growth (Uddin *et al.*, 2014). Our study demonstrates that salt stress causes reductions in the feruloylation of AX in S-roots and plant roots, at least in part due to the lower abundance of AX (**Fig. 2, 4**). In addition to decreased xylose residues, stressed S-roots and roots had a significant reduction in arabinose residues in the 1 M and 4 M KOH cell wall fractions, reflecting an overall decrease in AX abundance. Our data indicate that reductions in xylosyl residues lead, consequently, to a reduction in arabinosyl residues carrying feruloyl esters. The reduced level of cell wall-bound FA in the salt-stressed roots reduces the cross-links between AXs and lignin. Rice mutants lacking the xylosyltransferase activity from glycosyltransferase family GT61, *XAX1*, had reduced FA and xylosyl residues of xylan (Chiniquy *et al.*, 2012). Similarly, suppression of the *Brachypodium* glycosyltransferase family 43 *BdGT43A*, which is implicated in the xylan backbone elongation, leads to a decrease in AX abundance associated with lower levels of FA (Whitehead *et al.*, 2018).

Besides the reduced AX abundance in salt-stressed S-roots and plant roots, the increases in arabinose/FA-Araf ratios in these organs demonstrate that FA-Araf amounts reduced to a greater extent. A possible explanation for this phenomenon is the decrease of 4CL activity in S-roots and plant roots. This enzyme converts FA to feruloyl-CoA, an essential step for feruloylation of AX. In addition, stems presented significantly higher FA-Araf content (~80%) and 4CL activity (~70%) in response to salinity. Feruloylation of AXs and lignins are both known to be catalyzed by BAHD acyl-CoA transferases, using feruloyl-CoA as acyl-donor. Specific BAHD acyl-CoA transferases are involved in the feruloylation of AXs in grasses, *B. distachyon* (Buanafina *et al.*, 2016), *Setaria viridis* (de Souza *et al.*, 2018) and sugarcane (de Souza *et al.*, 2019). Although further studies are required to demonstrate that the *BAHD* genes are responsive to salinity, our results suggest a regulatory mechanism between cell wall

feruloylation and deferuloylation. In addition, the increase in FAE activity in response to salinity in S-roots and plant roots can also lead to a higher FA removal from *Araf* residues, contributing to the deferuloylation of AX (**Fig. 8**). Therefore, maize FAE is likely to be implicated in controlling the degree of AX feruloylation during abiotic stress.

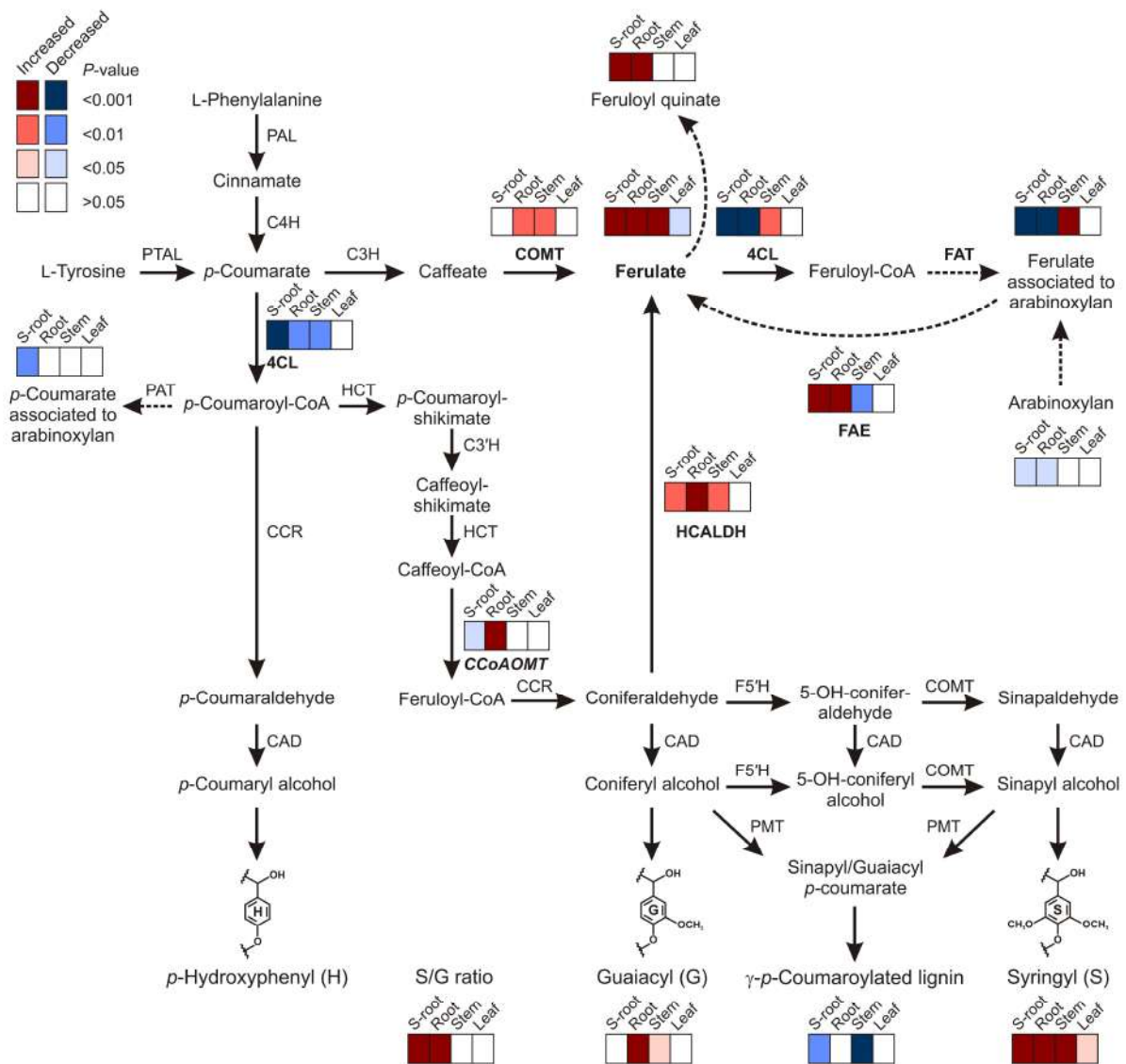


Figure 8. Metabolic map integrating lignin and ferulic acid biosynthesis with feruloylation in response to salt stress in maize. The differential modulation of genes, enzymes, metabolites and cell wall components are shown for seedling roots, plant roots, stems and leaves. The colors of the cells indicate the increased (red) or decreased (blue) parameter in the salt-stressed samples compared to respective controls. Arrows with dashed lines designate putative routes. PAL, L-phenylalanine ammonia-lyase; PTAL, bifunctional L-phenylalanine/ L-tyrosine ammonia-lyase; C4H, cinnamate 4-hydroxylase; C3H *p*-coumarate 3-hydroxylase; COMT, caffeate/5-hydroxyferulate 3-*O*-methyltransferase; 4CL, *p*-hydroxycinnamate-CoA ligase; FAT, putative feruloyl-CoA transferase; FAE, feruloyl esterase; PAT, putative *p*-coumaroyl-CoA transferase; HCT, hydroxycinnamoyl-CoA shikimate/quinic acid hydroxycinnamoyltransferase; C3H, *p*-coumaroyl shikimate/quinic acid 3'-hydroxylase; CCoAOMT, caffeoyl-CoA 3-*O*-methyltransferase; CCR, cinnamoyl-CoA reductase; HCALDH, hydroxycinnamaldehyde dehydrogenase; F5'H, ferulate 5'-hydroxylase/coniferaldehyde 5'-hydroxylase; CAD, cinnamyl alcohol dehydrogenase; PMT, *p*-coumaroyl-CoA monolignol transferase.

We observed higher lignin content in secondary cell walls in response to salt stress. Lignin is involved in plant responses to abiotic stress and lignin biosynthetic genes are induced during plant acclimation to salt stress (Moura *et al.*, 2010; Neves *et al.*, 2010). The overexpression of *MYB46* and *NAC012* transcription factors responsible for the coordinated expression of secondary cell wall biosynthetic genes led to enhanced tolerance to salt and osmotic stress, by upregulating the expression of genes encoding lignin biosynthetic enzymes, resulting in higher lignin deposition in secondary cell walls (Guo *et al.*, 2017; Hu *et al.*, 2019). Salt stress also promoted reductions in cellulose and/or matrix polysaccharides, concomitantly with increases in lignin content (**Fig. 1d**). The regulation of cellulose and lignin deposition in response to salinity may represent an adaptation to provide mechanical support to cell walls, suggesting crosstalk during cell wall biosynthesis (Hu *et al.*, 1999; Burton *et al.*, 2010; Byrt *et al.*, 2018). This crosstalk is consistent with the fact that during cell wall formation plants regulate the deposition of lignin and cellulose (Hu *et al.*, 1999; Burton *et al.*, 2010; Byrt *et al.*, 2018), and matrix polysaccharides (Van Acker *et al.*, 2013).

2D-HSQC-NMR spectroscopy of whole-cell walls and lignin compositional analysis with alkaline nitrobenzene oxidation followed by liquid chromatography revealed that salt stress increases lignin content and promotes higher incorporation of predominantly S-units, with the consequent increase in the S/G ratio (**Table 3**). This finding suggests that maize cells can redirect the carbon flux upon salinity from the biosynthesis of cell wall polysaccharides to lignin, such redirection of the flux has a particularly strong effect toward S-units, resulting in plants with increased S-units in lignin polymer (Hu *et al.*, 1999; Verbancic *et al.*, 2018). Lignin enriched in S-units is composed primarily of ether-type β -O-4 bonds, due to the presence of a methoxyl group at the C5 position of the syringyl moiety that prevents the formation of covalent bonds at this position (Ralph *et al.*, 2004). The methoxyl group at the C5 position diminishes the complexity of the lignin polymer, as compared to the G-rich lignins that are richer in condensed β -5 and 5-5/4-O- β bonds (Mottiar *et al.*, 2016; Ralph *et al.*, 2019). More importantly, the higher lignin content in secondary cell walls acts as diffusion barrier to limit salt, Na⁺ and Cl⁻ entry into xylem vessels and ultimately into the shoots (Byrt *et al.*, 2018). This suggests that lignin deposition during salt stress is a dynamic process for the reinforcement of cell walls (Vaahtera *et al.*, 2019).

The decreased content of *pCA* ester-linked to lignin in stressed tissues is interesting and somewhat unexpected. Maize lignins contain relatively large amounts of *pCA* acylating preferentially S-units, but also G-units (Grabber *et al.*, 1996; Hatfield *et al.*, 2009). Although it was envisioned that S-enriched lignins in salt-stressed tissues would present higher levels of

*p*CA, we observed the contrary (**Fig. 4f**). It is known that γ -*p*-coumaroylation of monolignols occurs through acylation of canonical monolignols using *p*-coumaroyl-CoA as the acyl-donor, and catalyzed by *p*-coumaroyl-CoA:monolignol transferase (PMT) (Withers *et al.*, 2012; Petrik *et al.*, 2014). Considering that grasses produce γ -*p*-coumaroylated S-lignins when concentrations of sinapyl alcohol and *p*-coumaroyl-CoA as substrates are sufficient and available for PMT activity (Takeda *et al.*, 2018), the reduced 4CL activity in response to salinity may have resulted in lower concentrations of *p*-coumaroyl-CoA available to PMT, in turn resulting in a diminished cellular pool of substrate for the γ -*p*-coumaroylation of lignins (**Fig. 8**).

Given that salt stress reduces the abundance of feruloylated AX, and concomitantly increases S-lignin content, we infer that cell walls of salt-stressed tissues present fewer covalent linkages between polysaccharides and lignin components. A recent study demonstrated that hydroxyl groups in xylan of secondary cell walls have abundant electrostatic interactions with methoxyl groups found mainly on S-units of the lignin polymer (Kang *et al.*, 2019). In turn, xylan substitutions with arabinose residues determine the strength of the covalent interactions of wall polysaccharides (*i.e.* binding of xylan to cellulose), modifying the mechanical properties of the wall (Simmons *et al.*, 2016; Grantham *et al.*, 2017; Hatfield *et al.*, 2017).

Genetic and biochemical studies suggest that FA can be biosynthesized via two different metabolic pathways (de Oliveira *et al.*, 2015). In maize, two cytosolic aldehyde dehydrogenases, REF2C and REF2D, catalyze the oxidation of coniferaldehyde to FA (Nair *et al.*, 2004; Končítíková *et al.*, 2015; Ferro *et al.*, 2020). Alternatively, FA might also be produced from caffeic acid via 3-*O*-methylation by COMT (Fornalé *et al.*, 2017). Our RT-qPCR-based analysis and enzyme assays revealed differential expression patterns for FA biosynthesis (**Fig. 5**).

We observed an increase in cytosolic FA by 150% to 430% in S-roots, roots and stems in response to salinity, which can be attributed, at least in part, to the redirection of carbon flux from the biosynthesis of G-unit to the biosynthesis of cytosolic FA, by the oxidation of coniferaldehyde to FA by HCALDH (**Fig. 8**). Our findings revealed that salt stress increases cytosolic FA levels by increasing its *de novo* biosynthesis, and by removing the ester-linked FA from AX. *De novo* biosynthesis of FA also increases in stems, but in contrast, it is followed by FA activation to feruloyl-CoA and subsequent esterification to AX accompanied by reduced FAE activity.

Table 4. Summary of the main alterations of cell wall composition and phenolic metabolites in response to salinity. ↑ indicates increased parameter, ↓ indicates decreased parameter and = indicates no significant difference in the salt-stressed samples compared to respective controls. nd, not detected or not determined.

Parameter	Seedlings		Plants	
	Roots	Roots	Stems	Leaves
Cellulose	=	↓	↑	=
Matrix polysaccharides	↓	↓	=	↑
Xylose	↓	↓	=	=
Arabinose	↓	↓	=	↑
Glucose	↓	=	↑	↑
Arabinoxylan (AX)	↓	↓	nd	nd
Xylose	↓	↓	nd	nd
Arabinose	↓	↓	nd	nd
AX by SEC-MALS (Abundance)	↓	↓	nd	nd
AX by SEC-MALS (Chain length)	=	=	nd	nd
AX by NMR	↓	↓	nd	nd
AX by PACE	=	=	nd	nd
Total ester-linked FA	↓	↓	↑	=
Ester-linked FA to AX	↓	↓	↑	=
Ester-linked FA to lignin	=	=	=	=
Total ester-linked <i>p</i> CA	↓	=	↓	=
Ester-linked <i>p</i> CA to AX	↓	=	=	=
Ester-linked <i>p</i> CA to lignin	↓	=	↓	=
Gene expression				
<i>RF2C</i>	=	↑	=	=
<i>RF2D</i>	=	↑	=	=
<i>COMT1</i>	↑	↑	↓	↓
<i>CCoAOMT1</i>	↓	↑	↑	↑
<i>CCoAOMT2</i>	↓	↑	=	↓
Enzyme activity				
4CL (<i>p</i> CA)	↓	↓	↓	=
4CL (FA)	↓	↓	↑	=
Hcaldh	↑	↑	↑	=
COMT	=	↑	↑	=
FAE	↑	↑	↓	=
Lignin content	↑	↑	↑	=
Lignin composition (mol %)				
G-unit by nitrobenzene oxidation	↓	↓	=	=
G-unit by NMR	↓	↓	=	↓
S-unit by nitrobenzene oxidation	↑	↑	=	=
S-unit by NMR	↑	↑	=	↑
S/G ratio nitrobenzene oxidation	↑	↑	↑	=
S/G ratio by NMR	↑	↑	↑	↑
Tricin by NMR	nd	nd	=	=
Phenolic metabolites				
FA	↑	↑	↑	↓
3- <i>O</i> -Feruloyl quinic acid	↑	↑	nd	nd
4- <i>O</i> -Feruloyl quinic acid	↑	↑	nd	nd

The phenolic profiling of S-roots and plant roots allowed to evaluate how the carbon flux through the phenylpropanoid pathway was redirected in response to salt stress. We found

that most of the compounds with increased abundance in S-roots and plant roots were the FA derivatives 3- and 4-*O*-feruloyl quinic acids, consistent with the increased flux towards FA formation (**Fig. 8**). The increase in cytosolic FA is likely associated with the increase in the osmotic pressure promoted by the external NaCl, and to play antioxidant protection against the toxicity of the absorbed NaCl (de Oliveira *et al.*, 2015).

In conclusion, our results reveal that the broad compositional alterations in maize cell walls in response to salinity are largely attributed to the reductions in cellulose and/or matrix polysaccharide amounts, the reduced feruloylation of arabinosyl moieties linked to AXs, and higher incorporation of S-units in lignin polymer. Moreover, this study provides new insights into salt-induced modulations in the expression of genes and enzyme activities required for FA biosynthesis and cell wall feruloylation, such as 4CL, HCALDH and FAE. Genetic modification of these candidate targets may contribute to develop resilient crops to increased salinity. This study provides a better understanding of how plants cope with a saline environment by modulating the composition and structure of their cell walls and the phenolic metabolism.

Acknowledgments

D.M.O. and T.R.M. gratefully acknowledge the doctoral scholarships granted by CNPq (GM/GD – 141076/2016-0) and the doctoral scholarships abroad granted by CAPES (PDSE – 88881.188627/2018-01). We are also grateful to the University of York Bioscience Technology Facility for performing the SEC-MALS analysis.

Funding information

This work was supported by the Brazilian National Council for Scientific and Technological Development (CNPq) and the Coordination of Enhancement of Higher Education Personnel (CAPES). D.M.O. and T.R.M. gratefully acknowledge the doctoral scholarships granted by CNPq (GM/GD – 141076/2016-0) and the doctoral scholarships abroad granted by CAPES (PDSE – 88881.188627/2018-01). D.K. and R.K. were supported by the Czech Science Foundation (grant No. 18-07563S) and the Ministry of Education, Youth and Sports of the Czech Republic (CZ.02.1.01/0.0/0.0/16_019/0000827). J.C.d.R., J.R., and A.G. were funded by the Spanish project AGL2017-83036-R (financed by Ministerio de Economía y Competitividad, Agencia Estatal de Investigación, AEI, and Fondo Europeo de Desarrollo Regional, FEDER).

Author contributions

D.M.O. and W.D.S. designed the research. D.M.O., T.R.M., F.V.S., R.C.S., R.K., D.K., R.S., M.S., G.G., K.M., J.R., A.G. and T.T. performed the experiments. D.M.O., K.M., J.R., R.M., P.D., J.C.d.R., W.B., S.M.M., L.D.G., O.F.F. and W.D.S. assisted the experimental design, analyzed and discussed the data. D.M.O. wrote the manuscript with contributions from all the coauthors. All authors approved the final version of the manuscript.

Conflict of interest

The authors declare no conflict of interest.

Supporting information

Additional Supporting Information may be found in the online version of this article at the publisher's website:

Figure S1. Screening for cell wall ester-linked hydroxycinnamates and total lignin in maize seedling roots.

Figure S2. Screening for total lignin in maize plant roots, stems and leaves.

Figure S3. Schematic flowchart summarizing the experimental design and the methodologies applied in this study.

Figure S4. Growth parameters of maize seedlings and plants in response to salinity.

Figure S5. Matrix polysaccharide composition of S-roots, plant roots, stems and leaves expressed as relative abundance.

Table S1. Assignments of the main bands in the ATR-FTIR spectra.

Table S2. Gene identifiers, probes, primer pairs for RT-qPCR.

Table S3. Assignments of the lignin and protein $^1\text{H}/^{13}\text{C}$ correlation signals in the 2D-HSQC-NMR spectra from the whole cell walls.

Methods S1. Detailed description of methods.

References

- Anders, N., Wilkinson, M.D., Lovegrove, A., Freeman, J., Tryfona, T., Pellny, T.K., Weimar, T., Mortimer, J.C., Stott, K., Baker, J.M., Defoin-Platel, M., Shewry, P.R., Dupree, P. & Mitchell, R.A. (2012) Glycosyl transferases in family 61 mediate arabinofuranosyl transfer onto xylan in grasses. *Proceedings of the National Academy of Sciences of the United States of America*, 109, 989-993.
- Bartley, L.E., Peck, M.L., Kim, S.R., Ebert, B., Manisseri, C., Chiniquy, D.M., Sykes, R., Gao, L., Rautengarten, C., Vega-Sanchez, M.E., Benke, P.I., Canlas, P.E., Cao, P., Brewer, S., Lin, F., Smith, W.L., Zhang, X., Keasling, J.D., Jentoff, R.E., Foster, S.B., Zhou, J., Ziebell, A., An, G., Scheller, H.V. & Ronald, P.C. (2013) Overexpression of a BAHD acyltransferase, *OsAt10*, alters rice cell wall hydroxycinnamic acid content and saccharification. *Plant Physiology*, 161, 1615-1633.
- Bevilaqua, J.M., Finger-Teixeira, A., Marchiosi, R., Oliveira, D.M., Joia, B.M., Ferro, A.P., Parizotto, A.V., dos Santos, W.D. & Ferrarese-Filho, O. (2019) Exogenous application of rosmarinic acid improves saccharification without affecting growth and lignification of maize. *Plant Physiology and Biochemistry*, 142, 275-282.
- Brown, D.M., Zhang, Z., Stephens, E., Dupree, P. & Turner, S.R. (2009) Characterization of IRX10 and IRX10-like reveals an essential role in glucuronoxylan biosynthesis in *Arabidopsis*. *Plant Journal*, 57(4), 732-746.
- Buanafina, M.M., Fescemyer, H.W., Sharma, M. & Shearer, E.A. (2016) Functional testing of a PF02458 homologue of putative rice arabinoxylan feruloyl transferase genes in *Brachypodium distachyon*. *Planta*, 243, 659-674.
- Burton, R.A., Gidley, M.J. & Fincher, G.B. (2010) Heterogeneity in the chemistry, structure and function of plant cell walls. *Nature Chemical Biology*, 6, 724-732.
- Busse-Wicher, M., Li, A., Silveira, R.L., Pereira, C.S., Tryfona, T., Gomes, T.C., Skaf, M.S. & Dupree, P. (2016) Evolution of xylan substitution patterns in gymnosperms and angiosperms: implications for xylan interaction with cellulose. *Plant Physiology*, 171, 2418-2431.
- Byrt, C.S., Munns, R., Burton, R.A., Gilliam, M. & Wege, S. (2018) Root cell wall solutions for crop plants in saline soils. *Plant Science*, 269, 47-55.
- Cesarino, I. (2019) Structural features and regulation of lignin deposited upon biotic and abiotic stresses. *Current Opinion in Biotechnology*, 56, 209-214.
- Chiniquy, D., Sharma, V., Schultink, A., Baidoo, E.E., Rautengarten, C., Cheng, K., Carroll, A., Ulvskov, P., Harholt, J., Keasling, J.D., Pauly, M., Scheller, H.V. & Ronald, P.C. (2012) XAX1 from glycosyltransferase family 61 mediates xylosyltransfer to rice xylan. *Proceedings of the National Academy of Sciences of the United States of America*, 109, 17117-17122.
- de Oliveira, D.M., Finger-Teixeira, A., Mota, T.R., Salvador, V.H., Moreira-Vilar, F.C., Molinari, H.B., Mitchell, R.A., Marchiosi, R., Ferrarese-Filho, O. & dos Santos, W.D. (2015) Ferulic acid: a key component in grass lignocellulose recalcitrance to hydrolysis. *Plant Biotechnology Journal*, 13, 1224-1232.
- de Souza, W.R., Martins, P.K., Freeman, J., Pellny, T.K., Michaelson, L.V., Sampaio, B.L., Vinecky, F., Ribeiro, A.P., da Cunha, B., Kobayashi, A.K., de Oliveira, P.A., Campanha, R.B., Pacheco, T.F., Martarello, D.C.I., Marchiosi, R., Ferrarese-Filho, O., dos Santos,

- W.D., Tramontina, R., Squina, F.M., Centeno, D.C., Gaspar, M., Braga, M.R., Tine, M.A.S., Ralph, J., Mitchell, R.A.C. & Molinari, H.B.C. (2018) Suppression of a single BAHD gene in *Setaria viridis* causes large, stable decreases in cell wall feruloylation and increases biomass digestibility. *New Phytologist*, 218, 81-93.
- de Souza, W.R., Pacheco, T.F., Duarte, K.E., Sampaio, B.L., de Oliveira Molinari, P.A., Martins, P.K., Santiago, T.R., Formighieri, E.F., Vinecky, F., Ribeiro, A.P., da Cunha, B.A.D.B., Kobayashi, A.K., Mitchell, R.A.C., Gambetta D.S.R. & Molinari, H.B.C. (2019) Silencing of a BAHD acyltransferase in sugarcane increases biomass digestibility. *Biotechnology for Biofuels*, 12, 111.
- del Río, J.C., Rencoret, J., Prinsen, P., Martínez, Á.T., Ralph, J. & Gutiérrez, A. (2012) Structural characterization of wheat straw lignin as revealed by analytical pyrolysis, 2D-NMR, and reductive cleavage methods. *Journal of Agricultural and Food Chemistry*, 60, 5922-5935.
- Dinneny, J.R. (2019) Developmental responses to water and salinity in root systems. *Annual Review of Cell and Developmental Biology*, 35, 239-257.
- Dong, J., Wu, F., & Zhang, G. (2006) Influence of cadmium on antioxidant capacity and four microelement concentrations in tomato seedlings (*Lycopersicon esculentum*). *Chemosphere*, 64, 1659-1666
- Endler, A., Kesten, C., Schneider, R., Zhang, Y., Ivakov, A., Froehlich, A., Funke, N. & Persson, S. (2015) A mechanism for sustained cellulose synthesis during salt stress. *Cell*, 162, 1353-1364.
- Farooq, M., Hussain, M., Wakeel, A. & Siddique, K.H.M. (2015) Salt stress in maize: effects, resistance mechanisms, and management. A review. *Agronomy for Sustainable Development*, 35, 461-481.
- Ferro, A.P., Flores Júnior, R., Finger-Teixeira, A., Parizotto, A.V., Bevilaqua, J.M., Oliveira, D.M., Molinari, H.B.C., Marchiosi, R., dos Santos, W.D., Seixas, F.A.V. & Ferrarese-Filho, O. (2020). Inhibition of *Zea mays* coniferyl aldehyde dehydrogenase by daidzin: A potential approach for the investigation of lignocellulose recalcitrance. *Process Biochemistry*, 90, 131-138.
- Fornalé, S., Rencoret, J., García-Calvo, L., Encina, A., Rigau, J., Gutiérrez, A., del Río, J.C. & Caparrós-Ruiz, D. (2017) Changes in cell wall polymers and degradability in maize mutants lacking 3'- and 5'-O-methyltransferases involved in lignin biosynthesis. *Plant and Cell Physiology*, 58(2), 240-255.
- Foster, C.E., Martin, T.M. & Pauly, M. (2010). Comprehensive compositional analysis of plant cell walls (lignocellulosic biomass) part II: carbohydrates. *Journal of Visualized Experiments* (37), 1837.
- Gladala-Kostarz, A., Doonan, J. H., & Bosch, M. (2020). Mechanical stimulation in *Brachypodium distachyon*: Implications for fitness, productivity, and cell wall properties. *Plant, Cell & Environment*. DOI:10.1111/pce.13724
- Goubet, F., Barton, C.J., Mortimer, J.C., Yu, X., Zhang, Z., Miles, G.P., Richens, J., Liepman, A.H., Seffen, K. & Dupree, P. (2009) Cell wall glucomannan in *Arabidopsis* is synthesised by CSLA glycosyltransferases, and influences the progression of embryogenesis. *Plant Journal*, 60(3), 527-538.

- Goubet, F., Jackson, P., Deery, M.J. & Dupree, P. (2002) Polysaccharide analysis using carbohydrate gel electrophoresis: a method to study plant cell wall polysaccharides and polysaccharide hydrolases. *Analytical Biochemistry*, 300(1), 53-68.
- Grabber, J.H., Quideau, S. & Ralph, J. (1996) *p*-Coumaroylated syringyl units in maize lignin: Implications for β -ether cleavage by thioacidolysis. *Phytochemistry*, 43, 1189-1194.
- Grabber, J.H., Ralph, J. & Hatfield, R.D. (2000) Cross-linking of maize walls by ferulate dimerization and incorporation into lignin. *Journal of Agricultural and Food Chemistry*, 48, 6106-6113.
- Grantham, N.J., Wurman-Rodrich, J., Terrett, O.M., Lyczakowski, J.J., Stott, K., Iuga, D., Simmons, T.J., Durand-Tardif, M., Brown, S.P., Dupree, R., Busse-Wicher & M., Dupree, P. (2017) An even pattern of xylan substitution is critical for interaction with cellulose in plant cell walls. *Nature Plants*, 3, 859-865.
- Guo, H., Wang, Y., Wang, L., Hu, P., Wang, Y., Jia, Y., Zhang, C., Zhang, Y., Zhang, Y., Wang, C. & Yang, C. (2017) Expression of the MYB transcription factor gene BpIMYB46 affects abiotic stress tolerance and secondary cell wall deposition in *Betula platyphylla*. *Plant Biotechnology Journal*, 15, 107-121.
- Hatfield, R.D., Marita, J.M., Frost, K., Grabber, J., Ralph, J., Lu, F. & Kim, H. (2009) Grass lignin acylation: *p*-coumaroyl transferase activity and cell wall characteristics of C3 and C4 grasses. *Planta*, 229, 1253-1267.
- Hatfield, R.D., Rancour, D.M. & Marita, J.M. (2017) Grass cell walls: a story of cross-linking. *Frontiers in Plant Science*, 7, 2056.
- Hu, P., Zhang, K. & Yang, C. (2019) BpNAC012 positively regulates abiotic stress responses and secondary wall biosynthesis. *Plant Physiology*, 179, 700-717.
- Hu, W.-J., Harding, S.A., Lung, J., Popko, J.L., Ralph, J., Stokke, D.D., Tsai, C.-J. & Chiang, V.L. (1999) Repression of lignin biosynthesis promotes cellulose accumulation and growth in transgenic trees. *Nature Biotechnology*, 17, 808-812.
- Jones, L., Milne, J.L., Ashford, D. & McQueen-Mason, S.J. (2003) Cell wall arabinan is essential for guard cell function. *Proceedings of the National Academy of Sciences of the United States of America*, 100, 11783-11788.
- Kang, X., Kirui, A., Widanage, M.C.D., Mentink-Vigier, F., Cosgrove, D.J. & Wang, T. (2019) Lignin-polysaccharide interactions in plant secondary cell walls revealed by solid-state NMR. *Nature Communications*, 10, 347.
- Karlen, S.D., Free, H.C., Padmakshan, D., Smith, B.G., Ralph, J. & Harris, P.J. (2018) Commelinid monocotyledon lignins are acylated by *p*-coumarate. *Plant Physiology*, 177, 513-521.
- Karlen, S.D., Zhang, C., Peck, M.L., Smith, R.A., Padmakshan, D., Helmich, K.E., Free, H.C.A., Lee, S., Smith, B.G., Lu, F., Sedbrook, J.C., Sibout, R., Grabber, J.H., Runge, T.M., Mysore, K.S., Harris, P.J., Bartley, L.E. & Ralph, J. (2016) Monolignol ferulate conjugates are naturally incorporated into plant lignins. *Science Advances*, 2, e1600393.
- Kesten, C., Wallmann, A., Schneider, R., McFarlane, H.E., Diehl, A., Khan, G.A., van Rossum, B.J., Lampugnani, E.R., Szymanski, W.G., Cremer, N., Schmieder, P., Ford, K.L., Seiter, F., Heazlewood, J.L., Sanchez-Rodriguez, C., Oschkinat, H. & Persson, S. (2019) The companion of cellulose synthase 1 confers salt tolerance through a Tau-like mechanism in plants. *Nature Communications*, 10, 857.

- Kim, H., Padmakshan, D., Li, Y., Rencoret, J., Hatfield, R.D. & Ralph, J. (2017) Characterization and elimination of undesirable protein residues in plant cell wall materials for enhancing lignin analysis by solution-state Nuclear Magnetic Resonance spectroscopy. *Biomacromolecules*, 18(12), 4184-4195.
- Kim, H., Ralph, J. & Akiyama, T. (2008) Solution-state 2D NMR of ball-milled plant cell wall gels in DMSO-d₆. *Bioenergy Research*, 1, 56-66.
- Končítíková, R., Vigouroux, A., Kopečná, M., Andree, T., Bartos, J., Sebela, M., Morera, S. & Kopečný, D. (2015) Role and structural characterization of plant aldehyde dehydrogenases from family 2 and family 7. *Biochemical Journal*, 468, 109-123.
- Lan, W., Lu, F., Regner, M., Zhu, Y., Rencoret, J., Ralph, S.A., Zakai, U.I., Morreel, K., Boerjan, W. & Ralph, J. (2015) Tricin, a flavonoid monomer in monocot lignification. *Plant Physiology*, 167, 1284-1295.
- Le Gall, H., Philippe, F., Domon, J.M., Gillet, F., Pelloux, J. & Rayon, C. (2015) Cell wall metabolism in response to abiotic stress. *Plants (Basel)*, 4, 112-166.
- Marriott, P.E., Sibout, R., Lapierre, C., Fangel, J.U., Willats, W.G., Hofte, H., Gomez, L.D. & McQueen-Mason, S.J. (2014) Range of cell-wall alterations enhance saccharification in *Brachypodium distachyon* mutants. *Proceedings of the National Academy of Sciences of the United States of America*, 111, 14601-14606.
- Moreira-Vilar, F.C., Siqueira-Soares, R.d.C., Finger-Teixeira, A., de Oliveira, D.M., Ferro, A.P., da Rocha, G.J., Ferrarese, M.L.L., dos Santos, W.D. & Ferrarese-Filho, O. (2014) The acetyl bromide method is faster, simpler and presents best recovery of lignin in different herbaceous tissues than kladon and thioglycolic acid methods. *PLOS ONE*, 9(10), e110000.
- Morreel, K., Goeminne, G., Storme, V., Sterck, L., Ralph, J., Coppin, W., Breyne, P., Steenackers, M., Georges, M., Messens, E. & Boerjan, W. (2006) Genetical metabolomics of flavonoid biosynthesis in *Populus*: a case study. *Plant Journal*, 47, 224-237.
- Morreel, K., Saeys, Y., Dima, O., Lu, F., Van de Peer, Y., Vanholme, R., Ralph, J., Vanholme, B. & Boerjan, W. (2014) Systematic structural characterization of metabolites in *Arabidopsis* via candidate substrate-product pair networks. *Plant Cell*, 26, 929-945.
- Mota, T.R., Oliveira, D.M., Morais, G.R., Marchiosi, R., Buckeridge, M.S., Ferrarese-Filho, O., & dos Santos, W.D. (2019). Hydrogen peroxide-acetic acid pretreatment increases the saccharification and enzyme adsorption on lignocellulose. *Industrial Crops and Products*, 140, 111657.
- Mottiar, Y., Vanholme, R., Boerjan, W., Ralph, J. & Mansfield, S.D. (2016) Designer lignins: harnessing the plasticity of lignification. *Current Opinion in Biotechnology*, 37, 190-200.
- Moura, J.C., Bonine, C.A., de Oliveira Fernandes Viana, J., Dornelas, M.C. & Mazzafera, P. (2010) Abiotic and biotic stresses and changes in the lignin content and composition in plants. *Journal of Integrative Plant Biology*, 52, 360-376.
- Munns, R., Passioura, J.B., Colmer, T.D. & Byrt, C.S. (2019) Osmotic adjustment and energy limitations to plant growth in saline soil. *New Phytologist*, 225(3), 1091-1096.
- Munns, R. & Tester, M. (2008) Mechanisms of salinity tolerance. *Annual Review of Plant Biology*, 59, 651-681.
- Nair, R.B., Bastress, K.L., Ruegger, M.O., Denault, J.W. & Chapple, C. (2004) The *Arabidopsis thaliana* *REDUCED EPIDERMAL FLUORESCENCE1* gene encodes an aldehyde

- dehydrogenase involved in ferulic acid and sinapic acid biosynthesis. *Plant Cell*, 16, 544-554.
- Negrão, S., Schmockel, S.M. & Tester, M. (2017) Evaluating physiological responses of plants to salinity stress. *Annals of Botany*, 119, 1-11.
- Neves, G.Y.S., Marchiosi, R., Ferrarese, M.L.L., Siqueira-Soares, R.C. & Ferrarese-Filho, O. (2010) Root growth inhibition and lignification induced by salt stress in soybean. *Journal of Agronomy and Crop Science*, 196, 467-473.
- Oliveira, D.M., Mota, T.R., Grandis, A., de Moraes, G.R., de Lucas, R.C., Polizeli, M.L.T.M., Marchiosi, R., Buckeridge, M.S., Ferrarese-Filho, O. & dos Santos, W.D. (2020) Lignin plays a key role in determining biomass recalcitrance in forage grasses. *Renewable Energy*, 147, 2206-2217.
- Oliveira, D.M., Mota, T.R., Oliva, B., Segato, F., Marchiosi, R., Ferrarese-Filho, O., Faulds, C.B. & dos Santos, W.D. (2019) Feruloyl esterases: Biocatalysts to overcome biomass recalcitrance and for the production of bioactive compounds. *Bioresource Technology*, 278, 408-423.
- Petrik, D.L., Karlen, S.D., Cass, C.L., Padmakshan, D., Lu, F., Liu, S., Le Bris, P., Antelme, S., Santoro, N., Wilkerson, C.G., Sibout, R., Lapierre, C., Ralph, J. & Sedbrook, J.C. (2014) *p*-Coumaroyl-CoA:monolignol transferase (PMT) acts specifically in the lignin biosynthetic pathway in *Brachypodium distachyon*. *Plant Journal*, 77, 713-726.
- Ralph, J. (2010) Hydroxycinnamates in lignification. *Phytochemistry Reviews*, 9, 65-83.
- Ralph, J., Lapierre, C. & Boerjan, W. (2019) Lignin structure and its engineering. *Current Opinion in Biotechnology*, 56, 240-249.
- Ralph, J., Lundquist, K., Brunow, G., Lu, F., Kim, H., Schatz, P.F., Marita, J.M., Hatfield, R.D., Ralph, S.A., Christensen, J.H. & Boerjan, W. (2004) Lignins: Natural polymers from oxidative coupling of 4-hydroxyphenyl- propanoids. *Phytochemistry Reviews*, 3, 29-60.
- Rencoret, J., Marques, G., Gutiérrez, A., Nieto, L., Santos, J.I., Jiménez-Barbero, J., Martínez, Á.T. & del Río, J.C. (2009) HSQC-NMR analysis of lignin in woody (*Eucalyptus globulus* and *Picea abies*) and non-woody (*Agave sisalana*) ball-milled plant materials at the gel state. *Holzforschung*, 63, 691-698.
- Rennie, E.A. & Scheller, H.V. (2014) Xylan biosynthesis. *Current Opinion in Biotechnology*, 26, 100-107.
- Rui, Y. and Dinneny, J.R. (2019) A wall with integrity: surveillance and maintenance of the plant cell wall under stress. *New Phytologist*, 225 (4), 1428-1439.
- Simmons, T.J., Mortimer, J.C., Bernardinelli, O.D., Poppler, A.C., Brown, S.P., de Azevedo, E.R., Dupree, R. & Dupree, P. (2016) Folding of xylan onto cellulose fibrils in plant cell walls revealed by solid-state NMR. *Nature Communications*, 7, 13902.
- Takeda, Y., Tobimatsu, Y., Karlen, S.D., Koshiba, T., Suzuki, S., Yamamura, M., Murakami, S., Mukai, M., Hattori, T., Osakabe, K., Ralph, J., Sakamoto, M. & Umezawa, T. (2018) Downregulation of *p*-COUMAROYL ESTER 3-HYDROXYLASE in rice leads to altered cell wall structures and improves biomass saccharification. *Plant Journal*, 95(5), 796-811.
- Tenhaken, R. (2014) Cell wall remodeling under abiotic stress. *Frontiers in Plant Science*, 5, 771.
- Tryfona, T., Sorieul, M., Feijao, C, Stott, K., Rubtsov, D.V., Anders, N. & Dupree, P. (2019) Development of an oligosaccharide library to characterise the structural variation in

- glucuronoarabinoxylan in the cell walls of vegetative tissues in grasses. *Biotechnology for Biofuels*, 12, 109.
- Uddin, M.N., Hanstein, S., Faust, F., Eitenmuller, P.T., Pitann, B. & Schubert, S. (2014) Diferulic acids in the cell wall may contribute to the suppression of shoot growth in the first phase of salt stress in maize. *Phytochemistry*, 102, 126-136.
- Vaahtera, L., Schulz, J. & Hamann, T. (2019) Cell wall integrity maintenance during plant development and interaction with the environment. *Nature Plants*, 5, 924-932.
- Van Acker, R., Vanholme, R., Storme, V., Mortimer, J.C., Dupree, P. & Boerjan, W. (2013) Lignin biosynthesis perturbations affect secondary cell wall composition and saccharification yield in *Arabidopsis thaliana*. *Biotechnology for Biofuels*, 6, 46.
- Vanholme, R., De Meester, B., Ralph, J. & Boerjan, W. (2019) Lignin biosynthesis and its integration into metabolism. *Current Opinion in Biotechnology*, 56, 230-239.
- Vanholme, R., Demedts, B., Morreel, K., Ralph, J. & Boerjan, W. (2010) Lignin biosynthesis and structure. *Plant Physiology*, 153, 895-905.
- Verbancic, J., Lunn, J.E., Stitt, M. & Persson, S. (2018) Carbon supply and the regulation of cell wall synthesis. *Molecular Plant*, 11, 75-94.
- Voiniciuc, C., Pauly, M. & Usadel, B. (2018) Monitoring polysaccharide dynamics in the plant cell wall. *Plant Physiology*, 176, 2590-2600
- Wakabayashi, K., Hoson, T. & Kamisaka, S. (1997) Osmotic stress suppresses cell wall stiffening and the increase in cell wall-bound ferulic and diferulic acids in wheat coleoptiles. *Plant Physiology*, 113, 967-973.
- Wang, T., McFarlane, H.E. & Persson, S. (2016) The impact of abiotic factors on cellulose synthesis. *Journal of Experimental Botany*, 67, 543-552.
- Whitehead, C., Garrido, F.J.O., Reymond, M., Simister, R., Distelfeld, A., Atienza, S.G., Piston, F., Gomez, L.D. & McQueen-Mason, S.J. (2018) A glycosyl transferase family 43 protein involved in xylan biosynthesis is associated with straw digestibility in *Brachypodium distachyon*. *New Phytologist*, 218, 974-985.
- Wilkerson, C.G., Mansfield, S.D., Lu, F., Withers, S., Park, J.Y., Karlen, S.D., Gonzales-Vigil, E., Padmakshan, D., Unda, F., Rencoret, J. & Ralph, J. (2014) Monolignol ferulate transferase introduces chemically labile linkages into the lignin backbone. *Science*, 344, 90-93.
- Withers, S., Lu, F., Kim, H., Zhu, Y., Ralph, J. & Wilkerson, C.G. (2012) Identification of grass-specific enzyme that acylates monolignols with *p*-coumarate. *Journal of Biological Chemistry*, 287, 8347-8355.
- Zhao, C., Zayed, O., Zeng, F., Liu, C., Zhang, L., Zhu, P., Hsu, C.C., Tuncil, Y.E., Tao, W.A., Carpita, N.C. & Zhu, J.K. (2019) Arabinose biosynthesis is critical for salt stress tolerance in *Arabidopsis*. *New Phytologist*, 224, 274-290.

Supporting Information

Chapter 6. Cell Wall Remodeling Under Salt Stress: Insights into Changes in Polysaccharides, Feruloylation, Lignification, and Phenolic Metabolism in Maize

Dyoni M. Oliveira, Thatiane R. Mota, Fábio V. Salatta, Renata C. Sinzker, Radka Končítíková, David Kopečný, Rachael Simister, Mariana Silva, Geert Goeminne, Kris Morreel, Jorge Rencoret, Ana Gutiérrez, Theodora Tryfona, Rogério Marchiosi, Paul Dupree, José C. del Río, Wout Boerjan, Simon J. McQueen-Mason, Leonardo D. Gomez, Osvaldo Ferrarese-Filho, Wanderley D. dos Santos

The following Supporting Information is available for this article:

Figure S1. Screening for cell wall ester-linked hydroxycinnamates and total lignin in maize seedling roots.

Figure S2. Screening for total lignin in maize plant roots, stems and leaves.

Figure S3. Schematic flowsheet summarizing the experimental design and the methodologies applied in this study.

Figure S4. Growth parameters of maize seedlings and plants in response to salinity.

Figure S5. Cell wall acetylation in maize seedling roots (S-roots) and plant roots.

Table S1. Assignments of the lignin and protein $^1\text{H}/^{13}\text{C}$ correlation signals in the 2D-HSQC-NMR spectra from the whole cell walls.

Table S2. Assignment of the main bands of ATR-FTIR.

Table S3. Gene identifiers, probes, primer pairs for RT-qPCR.

Methods S1. Detailed description of methods.

Supporting figures

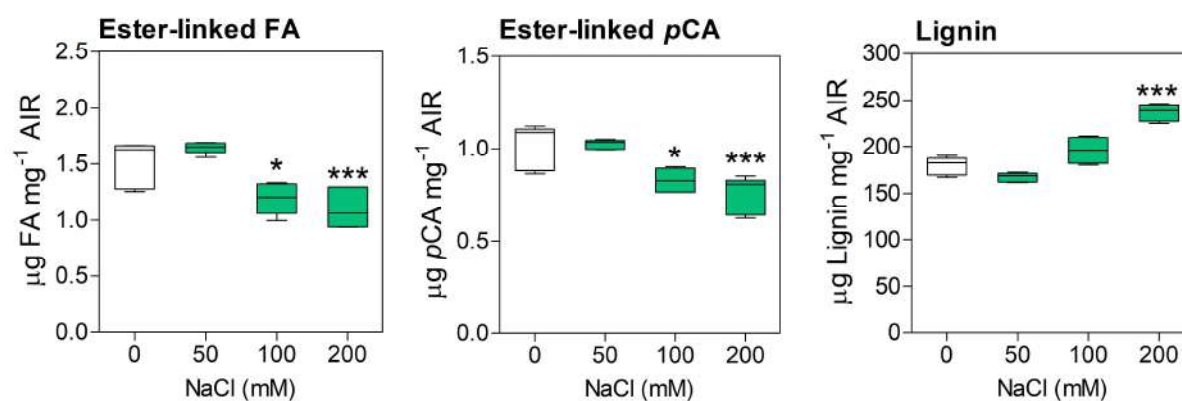


Figure S1. Screening for cell wall ester-linked hydroxycinnamates and total lignin in maize seedling roots. Error bars represent SEM, $n = 6$ biological replicates, * $0.05 \geq P > 0.01$, ** $0.01 \geq P > 0.001$, and *** $P \leq 0.001$, Dunnett's test.

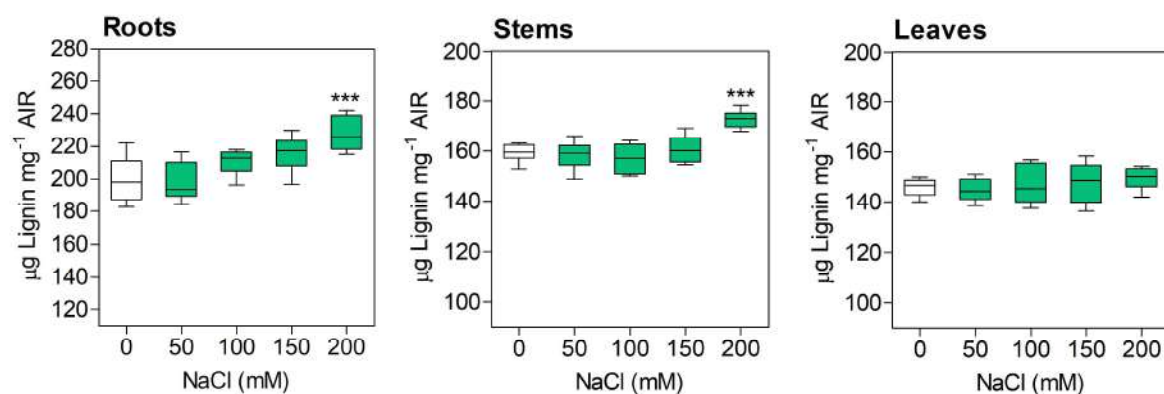


Figure S2. Screening for total lignin in maize plant roots, stems and leaves. Error bars represent SEM, $n = 6$ biological replicates, * $0.05 \geq P > 0.01$, ** $0.01 \geq P > 0.001$, and *** $P \leq 0.001$, Dunnett's test.

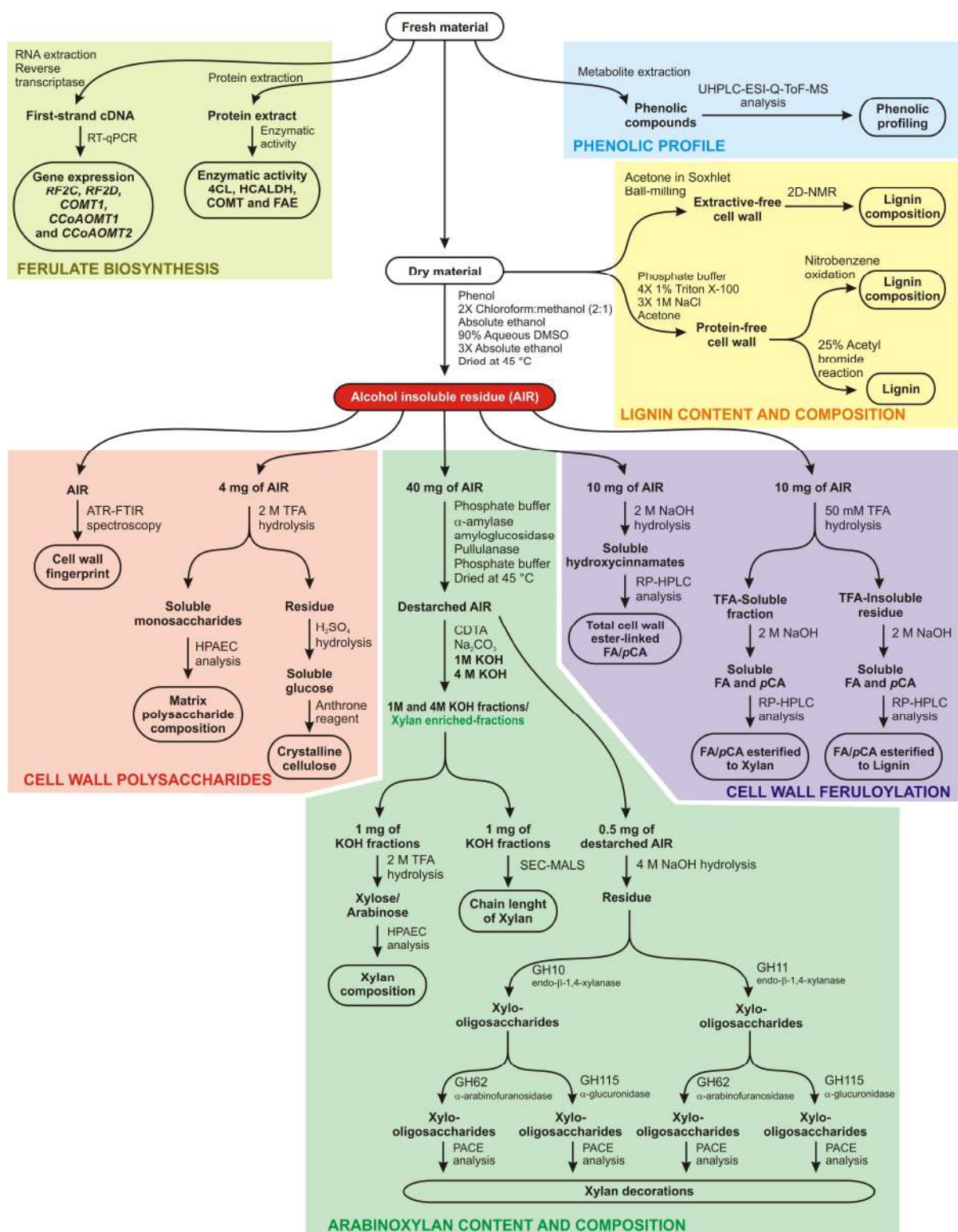


Figure S3. Schematic flowchart summarizing the experimental design and the methodologies applied in this study. ATR-FTIR, attenuated total reflectance-fourier transform infrared; CDTA, 1,2-cyclohexylenedinitrotetraacetic acid; FA, ferulic acid; GH10, endo- β -1,4-xylanase from *Cellvibrio japonicus*; GH11, endo- β -1,4-xylanase from *Neocallimastix patriciarum*; GH62, α -arabinofuranosidase from *Penicillium aurantiogriseum*; GH115 α -glucuronidase from *Bacteroides ovatus*; HPAEC, high-performance anion-exchange chromatography; PACE, polysaccharide analysis by carbohydrate gel electrophoresis; pCA, p-coumaric acid; SEC-MALS, size-exclusion chromatography coupled to multi-angle light-scattering; TFA, trifluoroacetic acid.

Maize material	Growth parameters	Control	200 mM NaCl	Difference (%)
SEEDLINGS	Length (cm)	14.77 ± 0.58	5.59 ± 0.25***	-62
	Roots			
	Fresh weight (g)	3.50 ± 0.22	1.04 ± 0.08***	-70
	Dry weight (g)	0.21 ± 0.01	0.09 ± 0.00***	-57
	Relative water content (%)	94.44 ± 0.28	92.45 ± 0.15***	-2
	TBARS (nmol g ⁻¹ FW)	15.03 ± 0.97	33.71 ± 1.57***	124
PLANTS	Plant height (cm)	48.26 ± 0.99	33.44 ± 1.09***	-31
	Total fresh weight: roots+stem+leaves (g)	12.06 ± 0.54	5.46 ± 0.37***	-55
	Total dry weight: roots+stem+leaves (g)	0.83 ± 0.04	0.53 ± 0.03***	-36
Roots	Length (cm)	32.83 ± 0.95	24.96 ± 0.65***	-24
	Fresh weight (g)	3.23 ± 0.15	1.79 ± 0.16***	-45
	Dry weight (g)	0.15 ± 0.01	0.11 ± 0.01**	-25
	Relative water content (%)	95.11 ± 0.35	92.99 ± 0.12***	-2
	TBARS (nmol g ⁻¹ FW)	9.19 ± 1.52	18.09 ± 2.28**	97
Stems	Length (cm)	5.97 ± 0.24	4.86 ± 0.18**	-20
	Diameter (mm)	5.66 ± 0.15	4.36 ± 0.10***	-23
	Fresh weight (g)	2.63 ± 0.12	1.27 ± 0.06***	-52
	Dry weight (g)	0.15 ± 0.01	0.10 ± 0.00**	-20
	Relative water content (%)	94.75 ± 0.11	91.13 ± 0.10***	-4
	TBARS (nmol g ⁻¹ FW)	34.21 ± 3.30	141.40 ± 4.04***	313
Leaves	Length of leaf +1 (cm)	39.46 ± 1.08	26.18 ± 1.34***	-34
	Width of leaf +1 (cm)	2.34 ± 0.07	1.46 ± 0.05***	-38
	Fresh weight (g)	6.19 ± 0.26	2.38 ± 0.13***	-62
	Dry weight (g)	0.53 ± 0.02	0.32 ± 0.02***	-40
	Relative water content (%)	91.51 ± 0.10	86.70 ± 0.27***	-5
	TBARS (nmol g ⁻¹ FW)	30.45 ± 3.78	46.79 ± 2.36**	54

Figure S4. Growth parameters of maize seedlings and plants in response to salinity. Values of difference indicate significantly increased or decreased percentage, as compared with those of respective control. $n = 8$ biological replicates. * $0.05 \geq P > 0.01$, ** $0.01 \geq P > 0.001$, and *** $P \leq 0.001$, unpaired two-sided t -test. TBARS, thiobarbituric acid reactive substances.

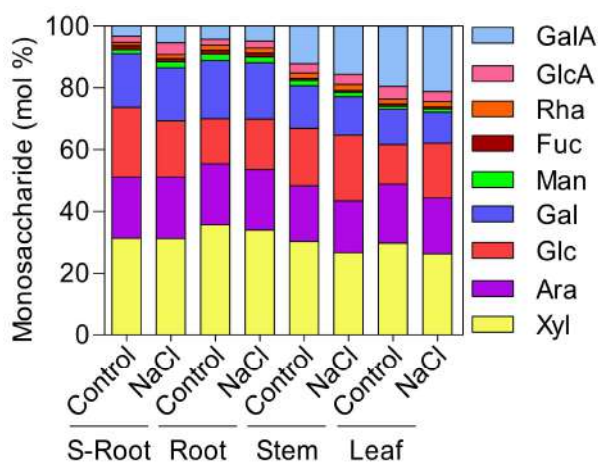


Figure S5. Matrix polysaccharide composition of S-roots, plant roots, stems and leaves expressed as relative abundance. Xyl, xylose; Ara, arabinose; Glc, glucose; Gal, galactose; Man, mannose; Fuc, fucose; Rha, rhamnose; GlcA, glucuronic acid; GalA, galacturonic acid; S-Root, seedling root. $n = 7$ biological replicates.

Supporting tables

Table S1. Assignments of the main bands in the ATR-FTIR spectra. Bands were assigned by comparison with the literature (Oliveira *et al.* 2020).

Vibration (cm ⁻¹)	Assignment	Cell wall component
1735	Unconjugated C=O stretching	Lignin
1633	C–C stretch of coniferaldehyde and sinapaldehyde	Lignin
1600	Lignin aromatic skeletal vibrations	Lignin
1510	Aryl ring stretch, asymmetric	Lignin
1378	Symmetric C-H deformation and phenolic OH	Crystalline cellulose; lignin
1150	C-O-C asymmetric stretching	Crystalline cellulose
1095	C–C and C–O stretching	Crystalline cellulose
1053	C–C and C–O stretching	Crystalline cellulose

Table S2. Gene identifiers, probes, primer pairs for RT-qPCR. Primers and TaqManTM probes were designed using Primer Express 3.0 software (Thermo Scientific).

Gene name	GenBank ID/ Phytozome ID	Sequences
RF2A	KJ004510 GRMZM2G058675	5'-CAGGACAGTGCCTGCAGATG-3', 5'-TGCTGCTGCAGTGCTGAAC-3', 5'-FAM-CACAGGCTGTTGCCAGGTGTCCCTTC-TAM-3'
RF2B	KJ004511 GRMZM2G125268	5'-TGTACGACGAGTTCGTGGAGAA-3', 5'-ACTGGACGTACCGCAAGATCTT-3', 5'-FAM-CGTCGTCGGCGACCCCTTCA-TAM-3'
RF2C	KJ004512 GRMZM2G071021	5'-CTCCCGTCATCGTCTTCGA-3', 5'-CTCGCCCTTGTGTTGTTAGGT-3', 5'-FAM-ACCTCGACATGGCCGTTAACCTCGT-TAM-3'
RF2D	KM225857 GRMZM2G097706	5'-TGTGGTGGTACCGGAGATCA-3', 5'-ATCAGCTTTGTCTGCCTCTGCTA-3', 5'-FAM-CGCCTCCGGCAAGACATTCGATAC-TAM-3'
COMT	AY323283 AC196475	5'-AACAAAGGCGTACGGGATGAC-3', 5'-TTCATGCCCTCGTTCAACAC-3', 5'-FAM-CGTTTCGAGTACCACGGCACGGAC-TAM-3'
CCoAOMT1	AJ242980 GRMZM2G127948	5'-GGACGCCGACAAGGACAA-3', 5'-CCGTTCCACAGCGTGTTG-3', 5'-FAM-TACCTCAACTACCACGAGCGGCTGCT-TAM-3'
CCoAOMT2	NP_001337196 GRMZM2G099363	5'-GCACCCATGGAACCTGATG-3', 5'-CCGATCTCCATGGTCTTCTTG-3', 5'-FAM-CCGACGAGGGCCAGTTCCTCAA-TAM-3'
EFa	AF136829 GRMZM2G154218	5'-TGATACCCACCAAGCCTATGGT-3', 5'-CATGTCGCGGACAGCAAAC-3', 5'-FAM-AGACATTCTCCGCGTTTCTCCCT-TAM-3'
ACT	BT086225 GRMZM2G053284	5'-CCGCATGAGCAAGGAGATTAC-3', 5'-GCGGAGCAACCACCTTCA-3', 5'-CACTTGCCCCCAGCAGCATGAA-TAM-3'

Table S3. Assignments of the lignin and protein $^1\text{H}/^{13}\text{C}$ correlation signals in the 2D-HSQC-NMR spectra from the whole cell walls. Signals were assigned by comparison with the literature (Fornalé *et al.* 2017; Kim *et al.* 2017).

Label	$\delta_{\text{C}}/\delta_{\text{H}}$ (ppm)	Assignment
T₈	94.0/6.50	C ₈ /H ₈ in tricin units (T)
T₆	98.5/6.18	C ₆ /H ₆ in tricin units (T)
S_{2,6}	103.8/6.69	C ₂ /H ₂ and C ₆ /H ₆ in etherified syringyl units (S)
G₂	110.9/6.99	C ₂ /H ₂ in guaiacyl units (G)
FA₂	110.9/7.31	C ₂ /H ₂ in ferulates (FA)
pCA₈ and FA₈	113.9/6.48	C ₈ /H ₈ in <i>p</i> -coumarates (pCA) and ferulates (FA)
G_{5/6}	114.9/6.72	C ₅ /H ₅ and C ₆ /H ₆ in guaiacyl units (G)
G₆	119.0/6.76	C ₆ /H ₆ in guaiacyl units (G)
FA₅	115.3/6.77	C ₅ /H ₅ in ferulates (FA)
pCA_{3,5}	115.5/6.77	C ₃ /H ₃ and C ₅ /H ₅ in <i>p</i> -coumarates (pCA)
FA₆	123.1/7.11	C ₆ /H ₆ in ferulates (FA)
H_{2,6}	128.9/7.20	C ₂ /H ₂ and C ₆ /H ₆ in <i>p</i> -hydroxyphenyl units (H)
pCA_{2,6}	130.1/7.45	C ₂ /H ₂ and C ₆ /H ₆ in <i>p</i> -coumarates (pCA)
pCA₇ and FA₇	145.2/7.56	C ₇ /H ₇ in <i>p</i> -coumarates (pCA) and ferulates (FA)
Proteins		
Tyr_{3,5}	114.7/6.60	C ₃ /H ₃ and C ₅ /H ₅ in tyrosine (Tyr)
Trp₁	117.9/6.93	C ₁ /H ₁ in tryptophan (Trp)
Trp₃	118.1/7.51	C ₃ /H ₃ in tryptophan (Trp)
Trp₂	120.8/6.99	C ₂ /H ₂ in tryptophan (Trp)
Phe₄	125.9/7.15	C ₄ /H ₄ in phenylalanine (Phe)
Phe_{3,5}	127.8/7.20	C ₃ /H ₃ and C ₅ /H ₅ in phenylalanine (Phe)
Phe_{2,6}	128.9/7.20	C ₂ /H ₂ and C ₆ /H ₆ in phenylalanine (Phe)
Tyr_{2,6}	129.8/6.98	C ₂ /H ₂ and C ₆ /H ₆ in in tyrosine (Tyr)

Methods S1. Detailed description of methods

Determination of thiobarbituric acid reactive substances (TBARS)

The determination of TBARS content was performed as previously described by Hodges *et al.* (1999) with minor modifications. 300 mg of fresh tissues were homogenized with 3 mL of 80% ethanol (v/v) and centrifuged (10,000×g, 10 min, and 4 °C). Next, 1 mL of the supernatant was mixed with 1 mL of 0.65% thiobarbituric acid (TBA) (w/v) in 20% trichloroacetic acid (TCA) (w/v) and incubated at 95 °C for 25 min. After centrifugation (10,000×g, 10 min, and 4 °C), the supernatant was spectrophotometrically monitored at 532 nm and 600 nm. TBARS content was obtained using the following equation and expressed in nmol g⁻¹ fresh weight:

$$\text{TBARS (nmol g}^{-1}\text{ fresh weight)} = [(\text{Abs at 532 nm} - \text{Abs at 600 nm})/155,000] \times 10^6$$

where 532 nm indicated the maximum absorbance of the TBARS, 600 nm indicated the correction for non-specific turbidity, and 155,000 was the molar extinction coefficient for TBARS as previously described by Hodges *et al.* (1999).

Crystalline cellulose content

Crystalline cellulose content was determined using the anthrone-sulfuric acid method as previously described by Foster *et al.* (2010) with modifications. The residue following 2 M TFA hydrolysis (from matrix monosaccharide analysis) was washed once with deionized water and thrice with acetone and left to dry at room temperature. Remaining pellet was hydrolyzed with 90 µl of 72 % sulphuric acid at 25 °C for 4 h under oxygen-free condition. Samples were then diluted to 4 % H₂SO₄ and incubated at 120 °C for 4 h under oxygen-free condition. After centrifugation (10,000×g, 5 min), the glucose of the supernatants was determined by the colorimetric anthrone-sulfuric acid method.

Enzymatic hydrolysis of xylan and polysaccharide analysis by carbohydrate gel electrophoresis (PACE)

Destarched AIR (500 µg) of seedling and plant roots was initially saponified with 4 M NaOH for 1 h at room temperature, neutralized with HCl and hydrolyzed in 100 mM ammonium acetate buffer pH 6.0 overnight at room temperature under agitation. The enzymes used were: GH10 endo-β-1,4-xylanase from *Cellvibrio japonicus* (CjGH10A); GH11 endo-β-1,4-xylanase from *Neocallimastix patriciarum* (NpGH11A); GH62 α-arabinofuranosidase from *Penicillium*

aurantiigriseum (PaGH62) and GH115 α -glucuronidase from *Bacteroides ovatus* (BoGH115). The reactions were stopped by boiling for 10 min. The samples were dried using a centrifugal vacuum evaporator. CjGH10A, NpGH11A and BoGH115 enzymes were kind gifts from Prof. Harry Gilbert (Newcastle University) and the PaGH62 enzyme was a gift from Novozymes.

The derivatization of oligosaccharides for PACE was performed as previously described by Goubet *et al.* (2002) with some modifications. Dried samples and xylooligosaccharide standards [xylose (X1), xylobiose (X2), xylotriose (X3), xylotetraose (X4), xylopentose (X5) and xylohexose (X6) (Megazyme)] were derivatized with 8-aminonaphthalene-1,3,6-trisulfonic acid (ANTS) and 2-picoline-borane (2-PB). Briefly, ANTS was prepared in acetic acid/water (3/17, v/v) at 0.2 M as final concentration. 2-PB was solubilized in DMSO for ANTS derivatization at 0.2 M final concentration and a DMSO buffer in acetic acid/water (3/17/20, v/v) was prepared freshly every time. 400 μ l of each of the above reagents were mixed to yield a final ANTS stock solution (stored at -20 °C) and 20 μ l of this stock solution were added to each dry sample. The samples were mixed, centrifuged and incubated at 37 °C overnight.

Carbohydrate electrophoresis, PACE gel scanning and quantification was performed as described by Goubet *et al.* (2002) and Goubet *et al.* (2009). Control experiments without substrates or enzymes were performed under the same conditions to identify any non-specific compounds in the enzymes, polysaccharides/cell walls or labelling reagents. All analyzes were repeated a minimum of three times.

Quantitative real-time PCR

RNA was isolated from maize tissues using the RNAqueous kit (Ambion) and treated twice with a Turbo DNase-free kit (Ambion) (Končítíková *et al.*, 2015). First-strand cDNA was synthesized by RevertAid H Minus reverse transcriptase and oligo(dT) primers (Thermo Fisher Scientific). Diluted cDNA samples were used as templates in real-time PCRs containing TaqMan Gene Expression MasterMix (Life Technologies), both primers at 300 nM concentrations and 250 nM TaqMan 6-FAM TAMRA probe on a StepOnePlus Real-Time PCR System. Plasmid DNA carrying the ORF of the respective maize *RF2C*, *RF2D*, *COMT1*, *CCoAOMT1* and *CCoAOMT2* genes was used as a template for a calibration curve to determine the PCR efficiencies of designed probes and primer pairs as well as to verify their specificity. Cycle threshold values were normalized with respect to elongation factor 1 α and β -actin genes and amplification efficiency. Expression values were determined and statistically evaluated using the DataAssist v3.0 Software package (Life Technologies). Gene identifiers, probes and primer pairs are given in **Table S2**.

Determination of lignin content and composition

Lignin content was determined by the acetyl bromide method (Moreira-Vilar *et al.*, 2014). Protein-free cell wall (2 mg) was incubated with 150 μ L of freshly prepared acetyl bromide solution (25% *v/v* acetyl bromide/glacial acetic acid) at 70 °C for 30 min. After digestion, the sample was ice-cooled, and then mixed with 270 μ L of 2 M NaOH, 30 μ L of 5 M hydroxylamine-HCl and 1 ml of glacial acetic acid for complete solubilization of the lignin extract. After centrifugation (10,000 \times *g*, 5 min), the absorbance of the supernatant was measured at 280 nm. A standard curve was generated with alkali lignin (Aldrich 37, 096-7).

Lignin monomeric composition was assessed using alkaline nitrobenzene oxidation as described in (Moreira-Vilar *et al.*, 2014). 50 mg of protein-free cell wall fraction was sealed in a Pyrex® ampule containing 0.9 ml of 2 M NaOH and 0.1 ml of nitrobenzene and heated to 170 °C for 150 min. The sample was then cooled to room temperature, washed twice with chloroform, acidified to pH 3 with 5 M HCl and extracted twice with chloroform. The organic extracts were combined, dried, resuspended in 1 ml of methanol. All of the samples were filtered through a 0.45- μ m filter and analysed by HPLC. The mobile phase was methanol/acetic acid 4% (20:80, *v/v*), with a flow rate of 1.2 ml min⁻¹ for an isocratic run. Quantification of vanillin and syringaldehyde released by the nitrobenzene oxidation was performed at 290 nm using the corresponding standards.

Cell wall characterization by two-dimensional NMR

The whole-cell walls of maize tissues were characterized using two-dimensional heteronuclear single-quantum coherence NMR (2D-HSQC-NMR) at solution state as previously described (Kim *et al.*, 2008; Rencoret *et al.*, 2009). Dried samples (~500 mg) were successively extracted with acetone (8 h) and water (3 h) in Soxhlet apparatus. The extractive-free samples were finely ball-milled in a Restch PM-100 planetary mill (Retsch, Haan, Germany) equipped with a 50 ml agate jar and agate balls (10 \times 10 mm), at 600 rpm, during 2 h (alternating 10 min of pause every 20 min of milling). Next, 70 mg of extractives-free sample were swelled in 0.7 ml of DMSO-*d*₆. 2D HSQC-NMR spectra were recorded at 25 °C on a Bruker AVANCE III 500 MHz instrument equipped with a cryogenically-cooled 5 mm TCI gradient probe with inverse geometry, at the NMR facilities of the General Research Services of the University of Seville (SGI-CITIUS). The HSQC experiments were carried out using the Bruker standard pulse program “hsqcetgpsisp2.2” and the following parameters: spectra were acquired from 10 to 0 ppm in F2 (¹H) using 1000 data points for an acquisition time of 100 ms,

an interscan delay of 1 s, and from 200 to 0 ppm in F1 (^{13}C) using 256 increments of 32 scan, for a total experiment time of 2 h 34 min. The $^1J_{\text{CH}}$ used was 145 Hz. Processing used typical matched Gaussian apodization in ^1H and a squared cosine bell in ^{13}C . The central solvent peak was used as an internal reference ($\delta_{\text{C}}/\delta_{\text{H}}$ 39.5/2.49). 2D-NMR cross-signals were assigned by literature comparison (Fornalé *et al.*, 2017; Kim *et al.*, 2017). A semi-quantitative analysis of the volume integrals of the HSQC correlation peaks was performed using Bruker's Topspin 3.5 processing software. In the aromatic/unsaturated region, the signals used to quantitate the relative abundances of the aromatic units were S_{2,6}, G₂, T₆, FA₂, pCA_{2,6}; as signals S_{2,6} and pCA_{2,6} involve two proton-carbon pairs, their volume integrals were halved.

References

- Fornalé, S., Rencoret, J., García-Calvo, L., Encina, A., Rigau, J., Gutiérrez, A., del Río, J.C. & Caparrós-Ruiz, D. (2017) Changes in cell wall polymers and degradability in maize mutants lacking 3'- and 5'-O-methyltransferases involved in lignin biosynthesis. *Plant and Cell Physiology*, 58(2), 240-255.
- Foster, C.E., Martin, T.M. & Pauly, M. (2010). Comprehensive compositional analysis of plant cell walls (lignocellulosic biomass) part II: carbohydrates. *Journal of Visualized Experiments* (37), 1837.
- Goubet, F., Barton, C.J., Mortimer, J.C., Yu, X., Zhang, Z., Miles, G.P., Richens, J., Liepman, A.H., Seffen, K. & Dupree, P. (2009) Cell wall glucomannan in Arabidopsis is synthesised by CSLA glycosyltransferases, and influences the progression of embryogenesis. *Plant Journal*, 60(3), 527-538.
- Goubet, F., Jackson, P., Deery, M.J. & Dupree, P. (2002) Polysaccharide analysis using carbohydrate gel electrophoresis: a method to study plant cell wall polysaccharides and polysaccharide hydrolases. *Analytical Biochemistry*, 300(1), 53-68.
- Hodges, D. M., DeLong, J. M., Forney, C. F., & Prange, R. K. (1999). Improving the thiobarbituric acid-reactive-substances assay for estimating lipid peroxidation in plant tissues containing anthocyanin and other interfering compounds. *Planta*, 207(4), 604-611.
- Končítiková, R., Vigouroux, A., Kopečná, M., Andree, T., Bartos, J., Sebela, M., Morera, S. & Kopečný, D. (2015) Role and structural characterization of plant aldehyde dehydrogenases from family 2 and family 7. *Biochemical Journal*, 468, 109-123.
- Kim, H., Padmakshan, D., Li, Y., Rencoret, J., Hatfield, R.D. & Ralph, J. (2017) Characterization and elimination of undesirable protein residues in plant cell wall materials for enhancing lignin analysis by solution-state Nuclear Magnetic Resonance spectroscopy. *Biomacromolecules*, 18(12), 4184-4195.
- Kim, H., Ralph, J. & Akiyama, T. (2008) Solution-state 2D NMR of ball-milled plant cell wall gels in DMSO- d_6 . *Bioenergy Research*, 1, 56-66.
- Moreira-Vilar, F.C., Siqueira-Soares, R.d.C., Finger-Teixeira, A., de Oliveira, D.M., Ferro, A.P., da Rocha, G.J., Ferrarese, M.L.L., dos Santos, W.D. & Ferrarese-Filho, O. (2014) The acetyl bromide method is faster, simpler and presents best recovery of lignin in different herbaceous tissues than klason and thioglycolic acid methods. *PLOS ONE*, 9(10), e110000.
- Oliveira, D.M., Mota, T.R., Grandis, A., de Morais, G.R., de Lucas, R.C., Polizeli, M.L.T.M., Marchiosi, R., Buckeridge, M.S., Ferrarese-Filho, O. & dos Santos, W.D. (2020) Lignin plays a key role in determining biomass recalcitrance in forage grasses. *Renewable Energy*, 147, 2206-2217.
- Rencoret, J., Marques, G., Gutiérrez, A., Nieto, L., Santos, J.I., Jiménez-Barbero, J., Martínez, Á.T. & del Río, J.C. (2009) HSQC-NMR analysis of lignin in woody (*Eucalyptus globulus* and *Picea abies*) and non-woody (*Agave sisalana*) ball-milled plant materials at the gel state. *Holzforschung*, 63, 691-698.

ADDENDUM

Ten Simple Rules for Developing a Successful Research Proposal in Brazil

Dyoni M. Oliveira¹, Marcos S. Buckeridge², Wanderley D. dos Santos^{1*}

¹ Department of Biochemistry, State University of Maringá, PR, Brazil

² Department of Botany, Institute of Bioscience, University of São Paulo, São Paulo, São Paulo, Brazil

* Corresponding author

Wanderley D. dos Santos

E-mail: wdsantos@uem.br

Type of chapter:	Editorial
Journal:	PLoS Computational Biology
Impact factor:	4.428
Volume/issue, pages:	13(2), e1005289
Date of publication:	February 2017
DOI:	10.1371/journal.pcbi.1005289

Introduction

Writing well is fundamental to publishing and having a successful scientific career [1], and being able to write a good research proposal is critical for obtaining financial support [2]. In emerging economies, such as Brazil, it is necessary to confront drawbacks not encountered in high-income countries [3]. The developing world has growing investments in science, technology, and innovation in many areas [4–6], including computational biology [7]. These investments have produced positive results in scientific quality in developing countries [8]. Although this is remarkably positive, the emergence of high-level research groups creates a highly competitive environment. We suggest a roadmap of ten simple rules for writing a consistent and convincing research project, which may be useful for researchers in Brazil and other emerging economies. There are several funding agencies in Brazil, and two of them – the National Council for Research Development (CNPq) and the São Paulo Research Foundation (FAPESP) – are used as examples of how proposals can be better adjusted in order to be successful. The latter represents the state funding agencies. Our ten rules will consider these agencies as the generic targets of proposals. When describing the ten rules below, we consider applications for research grant proposals and for MSc and PhD fellowships.

Rule 1: Define the problem clearly

In general, the most important part of a research project is to precisely define the problem to be investigated. If you wish to ask for financial support for your research, it is imperative to attest that your interest is in line with research supported by the funding calls available. Some calls are generic and flexible, such as the Universal Call from the CNPq in Brazil. It is not essential to fit into specific calls, but it is certainly easier to swim downstream whenever possible. The relevance and originality of your research targets and, of course, internal coherence (between targets and methods) have a significant impact on the value of the project. An extensive and updated review of the relevant literature can guarantee the originality of your targets, averting as much as possible the risk of your findings being published by another group while your project is still ongoing. In this case, the risk is producing good results without relevance to your field. Although the originality and relevance of a proposal can be ensured, the relevance of your findings is unpredictable.

Originality is usually inversely proportional to risk. When an idea is proposed, the level of novelty may lead a reviewer to find the project too risky. When preparing your proposal, it is therefore important to describe the risks very clearly. Brazilian reviewers tend to be quite conservative, and even a low risk level can be considered too much risk. When reviewers of

FAPESP, for example, are completing the review form, there are boxes at the end that have to be ticked. If a box like “Very Good with Minor Deficiencies” is ticked, the coordinator (the level above a reviewer) who will make the final decision may hesitate to approve the proposal. Authors thus have to be very careful and clearly explain the risks related to the project in order to minimize the possibility of the reviewer ticking the boxes that point out deficiencies. Because this is a cultural problem related to the reviewers rather than to the applicants, it is very important that the applicant display preliminary results that clearly and elegantly show the reviewer that the risks are manageable. This is difficult and demands a hard and careful thinking, but it is the only way to change the conservative culture of Brazilians into one that incorporates a more open and braver view of the work in science.

Rule 2: Formulate falsifiable hypotheses and include preliminary data

Sometimes, you can summarize your research as a precise and complete survey of data; however, when studying complex systems (such as living beings), measuring everything might not be feasible or convenient. It can therefore be useful to formulate a hypothesis that you can test with a number of experiments. You must formulate the hypothesis as an affirmative, clear, and concise sentence (e.g., “The volume of the liquid water is directly proportional to the temperature”). This statement must express an up-to-date possibility based on a systematic review of scientific knowledge on the defined theme; however, you cannot know beforehand whether your hypothesis is really correct (as in the example above, which we currently know to be wrong). The important thing here is to ensure that your hypothesis is testable under the actual conditions you have or have access to (physical, financial, and human resources) so that you can develop plausible experiments to test it. In low-income countries, being creative in the proposition of accessible methodologies for testing a hypothesis is especially critical, as we discuss in Rule 5.

Often, the hypothesis of a research project arises as a result of previous observations, and presenting the preliminary data might provide crucial support for your hypothesis. The preliminary data will also help you to effectively convince a reviewer that you have the technical and scientific expertise to carry out the work as proposed [2].

Again, try to prepare the text so that the reviewer concludes, after reading the project, that what you want to do is indeed science and that it is more than that: it is good science that advances knowledge.

Rule 3: Establish clear objectives

After formulating your hypothesis (or hypotheses), you should establish a clear and explicit goal, the necessity of which is exemplified in the excerpt below:

Finding herself lost in Wonderland, Alice asked to the Cheshire Cat: "Would you tell me, please, which way I ought to go from here?" "That depends a good deal on where you want to get to," the cat replied. "I don't much care where—" said Alice. "Then it doesn't much matter which way you go," said the cat [9].

You can find much by chance or serendipity; however, what you discover by chance will not necessarily be the same thing you were looking for. In a project, you want to convince others to trust your goals and that you are competent. A clear goal will guide the choice of the methodologies that you will use to get there. Objectives underlie an experimental design and can serve as a basis for performance evaluation and a change of strategy, when necessary. During the execution of the research, you will probably have to divide your attention across many tasks: classes, paperwork, other projects, supervisions, and so on. A clear statement of the objectives will remind you and your collaborators of where are you going and how you intend to get there.

Most reviewers are busy scientists, and they have to perform a great deal of administration along with their scientific work. In some cases, they will read the objectives (and the title and abstract) more carefully than other parts of the project. Therefore, be absolutely sure that you are describing your objectives in a simple way.

Rule 4: Estimate the duration and requirements of experimental procedures carefully

If your goals define the specific procedures you will follow during the research, the reverse is also true. The design of your experimental approach will also help you define the goals of your proposal. To reach specific goals, it is important to gain access to the necessary in-house facilities or invite external collaborators, as previously discussed in Ten Simple Rules [10]. If you have no expertise, this can be crucial. Talk to experienced researchers about the techniques you have in mind. Ask how long procedures specifically require, and be careful about laconic answers—especially from your mentor! They can reflect optimistic expectations or the desire to obtain results without thinking deeply about realistic deadlines. Be sure that the time required to carry out experimental procedures is compatible with the maximum period established by the funding call. It is important to know as much as possible about experimental

methodologies in order to avoid a design that is impracticable within the timeframe and with the resources available. Calculate the required time, allotting sufficient time for replanning. Bear in mind that scientific research is full of unpredictable mishaps (but also serendipity), and thus, it is important to evaluate the possible risks of things that do not go well. By identifying these risks, you can attempt to avoid them when managing your research. The funding agencies and especially private funders expect you to fulfil what you promised in the proposal, even after the deadline (and in this case, without additional resources!), and thus, it is always wise to promise the minimum necessary to achieve your goals. In Brazilian science, this is the most important failing point in proposals. Reviewers are usually not aware of those failures, however. Proposals in Brazil rarely include a schedule showing clearly when each milestone of the project should be reached, by whom it will be produced, and how the different tasks are associated with the objective of the project. However, this is one of the most important parts of the project because it gives the reviewer a clearer idea about the feasibility of the proposal. Your project may be original, the objectives may be clear, and the methodology choices may be appropriate, but if you do not construct a framework of tasks and resources (people and money) that are clearly coordinated, the reviewer will not be able to evaluate the feasibility of your project. Brazilian funding agencies usually fund a relatively small percentage of the proposals submitted. Final decisions are also made in a comparative review, in which a board of reviewers may decide together who will be approved. If your competitors have a more detailed schedule, they will thus have an advantage, and your proposal is more likely to be turned down.

Rule 5: Explain the methodologies for the goal, to demonstrate that you can carry out the research

Provide methodological descriptions that best fit your needs, your knowledge, and your financial reality. Take special care not to write methodologies that are incomplete or inapplicable to your particular case. It is common to find inconsistencies in proposals due to the “copying and pasting” of methodologies from other proposals. A zealous reviewer may require correction, and you may find yourself in a difficult situation or be asked to correct your work, particularly if you have to defend your proposal in public. Remember that there are two kinds of knowledge: tacit and explicit. Written methodologies usually hide important details that belong to the domain of tacit knowledge. You learn the tricks of the trade only by practicing and training with an experienced researcher. If you only have access to explicit knowledge to perform an experiment, you will probably make mistakes. The person evaluating your proposal, who is usually specialized in the field, might consider this restriction by consulting your

curriculum vitae. You can lessen the potentially negative impact of this problem through careful planning, which allows a surplus of time for establishing a protocol [11].

Some scientists and reviewers think that the methodology is the most important part of a proposal, so be certain that you are using (1) the right methods for the purpose of each experiment and (2) a currently accepted methodology. This does not always mean that you should only use the most advanced technology. Reviewers usually base their evaluation on the basis of a trade-off between the novelty of the method and the adequacy of using it, especially in light of how much money you are going to spend to perform the experiments.

Rule 6: Clearly define the tasks, people in charge, and costs in your research proposal

In order to answer a scientific question, it may be necessary to complete a series of goals and perform a series of experiments. It is thus useful to clearly define the following points for each goal: (1) What are the dates for initiating and finishing the experiment? (2) Who will carry out the experiment (in the case of a group)? (3) How much will the experiment cost? (4) How will you assess the research progress? (5) What are the critical risks? (6) How might you deal with severe problems? Even with good maintenance, equipment might fail, or a technician become unavailable. Try not to underestimate the deadline required for a crucial task, and, if possible, identify spare facilities/specialists to whom you can resort, if necessary.

Rule 7: Preventing the unpredictable: establish a flexible schedule

The result of one goal may be essential for the start of another. It is thus advisable for you to outline the best order in which each task must be executed. Nonetheless, remember that the schedule works as a possible way to execute all necessary tasks in your proposal. Not everything you plan must happen exactly as you originally conceived it, and it is natural for the schedule to undergo changes throughout the project development. As such, a good schedule must be flexible enough to accommodate the unpredictable obstacles you will face.

If you have a well-constructed schedule, this could be where the reviewer will look very carefully to find inconsistencies and point them out as a deficiency. If the percentage of approval is low, the probability is that reviewers will start reading your proposal by looking for deficiencies. When they find something, they will consider this as an inconsistency in contrast with a top-level ideal proposal. You should thus expect to be penalized for every small mistake found in your proposal, and a complex schedule is somewhere a reviewer may find many problems, thus turning down your proposal.

Rule 8: Justify the benefits your research will provide

An exhaustive survey of the relevant literature will help you introduce the field and convince reviewers why the problem you chose deserves attention. If you are sure your research program is unique and relevant, prove it to the experts who will judge your proposal, presenting a complete state-of-the-art picture. Be parsimonious, however, with words, and do not lose focus. Before writing, establish a briefing with the necessary information. Organize the ideas as an inverted pyramid, from general information about the field to the specific area that your work will address. This will make it easy for the reader to follow your reasoning and to understand the focus of your research.

After the introductory context, it is important to stress to the reader why your work is important. Emphasize the practical advantages (technological) that may result from your research and the importance that these results may have in overcoming the knowledge gaps mentioned in the introduction. This is the time to provide a convincing support for the relevance and importance of your research project. A list of scenarios resulting from your research can facilitate appreciation by the reader of the possible impact of your proposal as a whole.

Currently, there is a clear trend for applications to note the societal implications of the proposed research, so it is quite important to explain the main connections between the results you will produce and the benefits they will bring to society. This issue is more important to the higher-level members of the funding agency – scientists who design and maintain the general policies of science for the country – than to the reviewer. If your proposal is considered excellent in all the items above, but your explanation of the benefits to the country or region is not clear, your proposal might be turned down if competition is tight.

Rule 9: Write a good title and abstract

The title must inform the reader about the scope of the project. It is common in scientific literature to have the title briefly describe the issue addressed in the work (article or project). Avoid the use of adverbs and scientific nomenclature, which are not strictly necessary. Remember that scientists are attracted by intelligence. A creative title can arouse empathy in the reviewer.

An abstract is optional; however, it facilitates reading and understanding the general idea of the proposal. Although you must avoid prolixity at all costs, depending on the complexity of the theme, the introduction may become long and complex. This may mislead the reader if you do not properly formalize the focus of the work in an abstract. Together, the title and the abstract are good opportunities to put forward your idea. Most reviewers will make

their initial decisions about whether to approve a proposal or not immediately after carefully reading the title and abstract, so do not underestimate them.

Again, many busy reviewers will read your title and abstract more carefully. Because scientists are quite busy, there is a tendency to use fast thinking rather than a slow and thoughtful analysis of projects [12]. Usually, after reading the title and the abstract, the reviewer will have already made a decision about whether his or her thumb will be up or down for the proposal. If your title and abstract are well designed, the reviewer will continue reading and will give you several other opportunities to sell your work. Check your title and abstract many times if necessary, and never leave spelling mistakes in them. Spelling mistakes and/or inadequate language at the beginning score much higher in the negativity scale of the reviewer than such mistakes in the middle of the text.

Rule 10: Organize a logical structure and make the text more readable

Your proposal should be concise and impart as much information as possible in the least number of words. After ensuring that your research has precise and feasible objectives, is well contextualized and justified, has a consistent schedule, and is convincingly introduced, it is time to review the text. In addition to the items outlined here (Title, Abstract, Introduction, and so on), you can add other items you find appropriate. Check for a model provided by the funding institution. If no such model is available, take a careful look at successful projects. Try not to be too creative in the way you organize your proposal. You do not need to be a copy machine, but try to respect practices already consolidated. Organize the text in order to make it enjoyable, educational, and accurate [11].

Review your text to find small mistakes that are easy to spot. An excess of easily detectable mistakes suggests laziness. Be careful with the bibliography, which is tedious to organize, because it is very easy to leave mistakes there. The accuracy of references is extremely important because a reader (reviewer) may at any time become curious and check one of them. Give preference to software that automatically organizes references, but also remember that you require a good word processing software program.

Language and semiotics have to be carefully adjusted by many people in the world, and Brazilians are not an exception. Brazilians do not like informal language, so the use of the words “I” or “we” in the text should be avoided. Although Brazilians are not usually direct when speaking, Portuguese has to be transformed into the English style for science texts, using short phrases and sparse punctuation. Discrete humility is important in the text. It is important to find the right balance regarding how you value your work.

Acknowledgments

The style for this article was inspired by the “Ten Simple Rules...” papers published by Philip E. Bourne in *PLOS Computational Biology*. This work was inspired by the discipline BIB0306 offered to the undergraduate students of the Department of Botany of the Institute of Biosciences of the University of São Paulo.

Competing Interests

The authors have declared that no competing interests exist.

References

- [1]. Zhang W (2014) Ten simple rules for writing research papers. *PLoS Comput Biol* 10(1): e1003453.
- [2]. Bourne PE, Chalupa LM (2006) Ten simple rules for getting grants. *PLoS Comput Biol* 2(2): e12.
- [3]. Moreno E, Gutiérrez J-M (2008) Ten simple rules for aspiring scientists in a low-income country. *PLoS Comput Biol* 4(5): e1000024.
- [4]. Noorden RV (2014) The impact gap: South America by the numbers. *Nature* 510(7504): 202-203.
- [5]. Catanzaro M, Miranda G, Palmer L, Bajak A (2014) South American science: big players. *Nature* 510 (12): 204-206.
- [6]. Regalado A (2010). Science in Brazil. Brazilian science: riding a gusher. *Science* 330(6009): 1306-1312.
- [7]. Neshich G (2007) Computational Biology in Brazil. *PLoS Comput Biol* 3(10): e185.
- [8]. Thomaz SM, Mormul RP (2014) Misinterpretation of 'slow science' and 'academic productivism' may obstruct science in developing countries. *Braz J Biol* 74(3): S1-S2.
- [9]. Dodgson CL (1865). *Alice's Adventures in Wonderland*. New York, D. Appleton and Co., p. 227.
- [10]. Vicens Q, Bourne PE (2007) Ten simple rules for a successful collaboration. *PLoS Comput Biol* 3(3):e44.
- [11]. Davies MB (2007) *Doing a successful research project. Using qualitative and quantitative methods*. London, Palgrave Macmillan, p. 25-26.
- [12]. Kahneman D. (2011) *Thinking, fast and slow*. Farrar, Straus and Giroux, 499p.

APPENDIX

Additional articles published or under review as author and coauthor during the PhD period (2016 to 2020). * indicates corresponding author(s).

1. Mota, T.R.*, de Souza, W.R., **Oliveira, D.M.**, Martins, P.K., Sampaio, B.L., Vinecky, F., Ribeiro, A.P., Duarte, K.E., Pacheco, T.F., Monteiro, N.K.V., Campanha, R.B., Marchiosi, R., Vieira, D.S., Kobayashi, A.K., Molinari, P.A.O., Ferrarese-Filho, O., Mitchell, R.A.C., Molinari, H.B.C.*, dos Santos, W.D. Suppression of a BAHD acyltransferase decreases *p*-coumaroyl on arabinoxylan and improves biomass digestibility in the model grass *Setaria viridis*. Under review in **Plant Journal**.
Impact factor: 5.726
2. Marchiosi, R., dos Santos, W.D., Constantin, R.P., Lima, R.B., Soares, A.R., Finger-Teixeira, A., Mota, T.R., **Oliveira, D.M.**, Foletto-Felipe, M.P., Abrahao, J., Ferrarese-Filho, O.* 2020. Biosynthesis and metabolic actions of simple phenolic acids in plants. Under review in **Phytochemistry Reviews**.
Impact factor: 4.257
3. **Oliveira, D.M.***, Mota, T.R., Grandis, A., Morais, G.R., de Lucas, R.C., Polizeli, M.L.T.M., Marchiosi, R., Buckeridge, M.S., Ferrarese-Filho, O., dos Santos, W.D.* 2020. Lignin plays a key role in determining biomass recalcitrance in forage grasses. **Renewable Energy**, 147(1), 2206-2217. DOI: 10.1016/j.renene.2019.10.020.
Impact factor: 5.439
4. Mota, T.R.*, **Oliveira, D.M.**, Morais, G.R., Buckeridge, M.S., Ferrarese-Filho, O., dos Santos, W.D.* 2019. Hydrogen peroxide-acetic acid pretreatment increases the saccharification and enzyme adsorption on lignocellulose. **Industrial Crops and Products**, 140, 111657. DOI: 10.1016/j.indcrop.2019.111657.
Impact factor: 4.191
5. Bevilaqua, J.M., Finger-Teixeira, A., Marchiosi, R., **Oliveira, D.M.**, Joia, B.M., Ferro, A.P., Parizotto, A.V., dos Santos, W.D., Ferrarese-Filho, O.* 2019. Exogenous application of rosmarinic acid improves saccharification without affecting growth and lignification of maize. **Plant Physiology and Biochemistry**, 142, 275-282. DOI: 10.1016/j.plaphy.2019.07.015.
Impact factor: 3.404

6. Ferro, A.P., Júnior, R.F., Finger-Teixeira, A., Parizotto, A.V., Bevilaqua, J.M., **Oliveira, D.M.**, Molinari, H.B.C., Marchiosi, R., dos Santos, W.D., Seixas, F.A.V., Ferrarese-Filho, O.* 2019. Inhibition of *Zea mays* coniferyl aldehyde dehydrogenase by daidzin: A potential approach for the investigation of lignocellulose recalcitrance. **Process Biochemistry**, 90, 131-138. DOI: 10.1016/j.procbio.2019.11.024.
Impact factor: 2.883

7. Falcioni, R., Moriwaki, T., **Oliveira, D.M.**, Andreotti, G.C., Souza, L.A., dos Santos, W.D., Bonato, C.M., Antunes, W.C.* 2018. Increased in gibberellins and light levels promotes cell wall thickness and enhance lignin deposition in xylem fibers. **Frontiers in Plant Science**, 9:1391. DOI: 10.3389/fpls.2018.01391.
Impact factor: 4.106

8. Lopes, T.L.C., Siqueira-Soares, R.C., Almeida, G.H.G., Melo, G.S.R., Barreto, G.E., **Oliveira, D.M.**, dos Santos, W.D., Ferrarese-Filho, O., Marchiosi, R.* 2018. Lignin-induced growth inhibition in soybean exposed to iron oxide nanoparticles. **Chemosphere**, 211, 226-234. DOI: 10.1016/j.chemosphere.2018.07.143.
Impact factor: 5.108

9. Mota, T.R.* , **Oliveira, D.M.**, Marchiosi, R., Ferrarese-Filho, O., dos Santos, W.D. 2018. Plant cell wall composition and enzymatic deconstruction. **AIMS Bioengineering**, 5 (1), 63-77. DOI: 10.3934/bioeng.2018.1.63.

10. Segato, F., Dias, B., Berto, G. L., **Oliveira, D. M.**, De Souza, F. H. M., Citadini, A. P., Murakami, M. T., Damásio, A. R. L., Squina, F. M., Polikarpov, I.* 2017. Cloning, heterologous expression and biochemical characterization of a non-specific endoglucanase family 12 from *Aspergillus terreus* NIH2624. **Biochimica et Biophysica Acta (BBA) - Proteins and Proteomics**, 1865 (4), 395-403. DOI: 10.1016/j.bbapap.2017.01.003.
Impact factor: 2.54

11. **Oliveira, D. M.***, Salvador, V. H., Mota, T. M., Finger-Teixeira, A., de Almeida, R. F., Paixão, D. A. A., De Souza, A. P., Buckeridge, M. S., Marchiosi, R., Ferrarese-Filho, O., Squina, F. M., dos Santos, W. D. 2016. Feruloyl esterase from *Aspergillus clavatus* improves xylan hydrolysis of sugarcane bagasse. **AIMS Bioengineering**, 4 (1), 1-11. DOI: 10.3934/bioeng.2017.1.1.